Modulation of NMDA Receptor Currents in Rat Substantia Nigra

Rumaitha Nasser Ali Al-Hosni

Submitted for the degree of:
Doctor of Philosophy

Department of Neuroscience, Physiology, and Pharmacology

University College London

I, Rumaitha Nasser Ali Al-hosni, confirm that the work presented in this thesis is my own. Where information has been derived from other sources, I confirm that this has been indicated in the thesis and due dedication given.

Signed: …….

Acknowledgements

There are many to acknowledge and thank, but my deepest gratitude goes to Prof. Alasdair Gibb for the time, knowledge and guidance he provided throughout my MSc and PhD. This has been a long and demanding journey, but he always assured me it would be one worthwhile. In that time, I have come to appreciate the complexities within neuropharmacology and importantly, electrophysiology. His constant support is unparalleled, and I will always be grateful. I would also like to thank Federica Cherchi, Xioachun Cai and Wanyu Lei (visiting students to the lab) for their contributions to my research on A2A receptors.

I would like to thank UCL for the endless opportunities it provided to allow me to grow and realise my potential. To the many in NPP, thank you for making me feel welcome, share laughs and cake.

My parents, without whom, my dreams would stand no chance. You always had a different vision for me but knew I would flourish where my mind saw fit and believed in me. The moral and financial support you provided will forever inspire me to do great things in this world.

To Rawiya, the sister who took this journey with me, I will forever be indebted to you for the love and support you offered and wish you all the greatness in this world. You stood by me at my worst and reassured me that I still had a standing chance to achieve all that I have in the last four years.

To the rest of my family and friends, thank you for your support and believing in me. This journey wouldn't haven't been the same without you.

Publications and Training courses

Publications:

Europhysiology 2016 (Dublin): "Absence of dopamine D2-receptor modulation of NMDA responses in neonatal rat substantia nigra dopaminergic neurones."

Society for Neuroscience, 2017 (Washington, DC): "Adenosine A2A - D2 dopamine receptor modulation of NMDA responses in rat substantia nigra dopaminergic neurones."

Europhysiology 2018 (London): "Adenosine A2A - D2 dopamine receptor modulation of NMDA responses in rat substantia nigra dopaminergic neurones." [Updated research].

Training:

Home office training (15th March 2016): completed accredited training for personnel working under the Animals (Scientific Procedures) Act 1986. Modules 1-3.

Lab Techniques in Mammalian Cell Biology (2016)

Understanding statistical concepts in research (Nov 2016)

Microelectrode Techniques for Cell Physiology (Plymouth): completed in September 2017.

UCL Arena One Gateway Workshop (2018)

UCL Arena One Teaching Associate program (leading to associate fellowship for Higher education): Completed Dec 2018.

Associate Fellowship for Higher Education (Awarded Dec 2019)

Abstract

Dopamine receptor signalling is essential for normal basal ganglia function but in Parkinson's Disease (PD) substantia nigra (SNc) dopaminergic (DAergic) neurons degenerate with consequent loss of dopamine signalling. SNc DAergic neurons express D2 autoreceptors (D2Rs) that have been shown to mediate inhibition of NMDA responses in both hippocampus and striatum while $G_{\alpha s}$-coupled adenosine A2A receptors (A2ARs) have the potential to counteract the action of $G_{\alpha\iota}$ -coupled D2Rs. Here I tested whether D2R activation with ropinirole, a D2 receptor agonist currently used in PD therapy, modulates DAergic neuron NMDA responses in the SNc along with other proteins in the cell.

Whole-cell patch clamp recordings were made from DAergic neurons in the SNc of acute midbrain slices from young (P7, P21 and P28) rats. DAergic neurons were identified by the presence of a prominent hyperpolarisation-activated inward current (in P7 rats, amplitude, 178 ± 5 pA; activation time constant, 797 ± 77 ms; mean ± SEM, N = 19) in response to a voltage step from -60 to -120 mV. In P7 and P28 rats, upon application of 200 nM ropinirole, the steady state NMDA current was not significantly changed suggesting D2-R activation may not modulate NMDARs in neonatal rat SNc. In addition, an A2AR agonist, CGS-21680, and an A2AR antagonist, SCH-58621 were applied in the presence and absence of ropinirole to test for any A2AR – D2R interaction. Upon A2A-R activation, the NMDA-R current increased (P = 0.002, N = 16). Furthermore, to establish the effects of PKA on NMDA-R responses, 2.5μM Forskolin was introduced. It produced a statistically significant increase in NMDA-R current (NMDA: 419 ± 78pA; NMDA+ Forskolin: 515 ± 54pA, N=13). To determine whether the lack of effect of the D2-R agonist on NMDA-R response might be due to a low resting concentration of cAMP in the cell, forskolin was introduced to increase the levels of cAMP prior to introducing ropinirole. However, following addition of D2-R agonist after forskolin treatment, the NMDA-R current changed by only 11% (N=12). Intracellular tyrosine kinases, Src and Fyn have shown modulatory potential on NMDA-Receptors (NMDA-R) that is governed by the

balance between kinase and phosphatase activity. Inhibiting Src kinase activity with PP2 and Src-I1 decreased the NMDA-R inward current however no such effect was seen in the presence of the interfering peptides suggesting a lack of direct interaction between Src/Fyn kinase and NMDA-Rs. Furthermore, ERK1/2 inhibitor, Ulixertinib, decreased the NMDA-R current suggesting an involvement in receptor modulation. Similar results were obtained in the presence of a CaMKII inhibitor CN21.

Impact statement

The deterioration of dopaminergic neurons of the substantia nigra is a key feature in the pathophysiology associated with Parkinson's disease. Understanding what might modulate this neuronal cell death is vital in determining therapeutic targets. NMDA receptors are a potential contributor to calcium-dependent neuronal cell death and thus the receptor is of interest in my thesis. The combined use of *in vitro* electrophysiology and pharmacology on brain slices is an ideal method to understand the actions of drugs in real-time and produces results that are easily repeatable when experiments are done correctly. My research highlights the diversity in modulation of neuronal NMDA-Receptor responses in the brain and highlights the necessity for a fine-tuned therapeutic approach when targeting D2 and NMDA-receptors in the basal ganglia.

The potential importance of receptor interactions between Adenosine-2A and Dopamine-D2 receptors investigated in my research is of interest in understanding the actions of dopamine receptor agonists used to treat Parkinson's Disease. In addition, use of interfering peptides targeting protein kinases with success in research, shows the potential of this method as a tool to investigate signalling in dopaminergic neurons in acute brain slices. The TAT-motif introduced to my kinase peptides is a cell-penetrating peptide that has the ability to cross the cell membrane and transport protein sequences with limited toxicity and great specificity to intracellular sites of action and could be delivered *in vivo* by virus.

Studying modulation of NMDA receptors on dopaminergic neurons of the substantia nigra provides new insights into NMDA receptor physiology and potentially new ideas that could be used in the treatment of Parkinson's disease.

Table of Contents

List of Figures

Chapter 1

Chapter 2

Chapter 3

Chapter 4

Chapter 5

Chapter 6

List of Tables

Abbreviations

5-HT: 5-hydroxytryptamine

7-Cl-K: 7-Chlorokynurenic acid

α-2aR: Alpha-2 non-adrenergic receptors

ABD: Agonist binding domain

AC: Adenylyl cyclase

ALS: Amyotrophic lateral sclerosis

AMPA: Amino-3-hydroxy-5-methyl-4isoxazolepropionic acid

AP: Action potentials

AP5: DL-2-Amino-5-Phosphonovaleric acid

BAC: Bacterial artificial chromosome

CaMKII: Ca^{2+}/Calmodulin-dependent protein kinase II

cAMP: cyclic Adenosine monophosphate

CaN: Calcineurin

CB: Calbindin

CNBD: Cyclic nucleotide-binding domain

CNG: Cyclic nucleotide gated channel

CNS: Central Nervous System

CPu: Caudate Putamen

CREB: cAMP-response element binding protein

Csk: C-terminus Src-Kinase

D1-R: Dopamine D1-Receptor

D2-R: Dopamine D2-Receptor

DA: Dopamine

DAergic: Dopaminergic

DAPK1: Death-associated protein kinase-1

DNQX: 6,7-Dinitroquinoxaline-2,3-dione

EDTA: Ethylenediaminetetraacetic acid

ePAS: excitatory Paired associative stimulation

EPSCs: Excitatory postsynaptic currents

ER: Endoplasmic reticulum

ERK: Extracellular regulated protein kinase

FRET: Fluorescence resonance energy transfer

GABA: gamma-Aminobutyric acid

GDNF: Glial cell-derived neurotrophic factor

GIRK: G-protein inwardly, rectifying K^+ channels

GPCR: G-protein coupled receptor

GPe: external segment of Globus pallidus

GPi: internal segment of Globus pallidus

GRK: G-protein receptor kinase

HCN: Hyperpolarization-activated, Nucleotide-gated channels

iGluRs: ionotropic glutamate receptors

Ih: Inwardly rectifying cation current

Kir: Inward rectifying K^+ channels

L-dopa: Levodopa

LGP: Lateral globus pallidus

LTD: Long term depression

LTP: Long term potentiation

MAO: Monoamine Oxidase

MAPK: Mitogen-activated protein kinase

MGP: Medial globus pallidus

MOPr: μ-opioid receptor

MSN: Medium Spiny Neurons

mtPTP: Mitochondrial permeability transition pore

NAc: Nucleus Accumbens

ND2: NADH dehydrogenase subunit 2

NMDA: N-Methyl-D-Aspartate

NTD: N-terminal binding domain

PACAP38: Pituitary adenylate cyclase activated peptide 38

PCD: programmed cell death

PD: Parkinson's disease

PDGF-R: Platelet derived growth factor receptor

PFC: Pre-frontal cortex

PKA: Protein Kinase A

PKC: Protein kinase C

PLC: Phospholipase C

PPN: pedunculopontine nuclei

PTKs: Protein tyrosine kinases

PTP: Protein tyrosine phosphatase

RACK-1: Receptor for activated kinase-1

RDI: Receptor desensitization and internalisation

ROS: Reactive oxygen species

SFKs: Src family kinases

SH: Src homology

Shh: Sonic hedgehog

SNc: Substantia nigra Pars Compacta

SNr: Substantia nigra reticulata

Src-I1: Src Inhibitor-1

STEP: Striatal enriched protein tyrosine phosphatase

STN: Subthalamic nucleus

TAT: Transactivator or transcription

tDCS: Transcranial direct current stimulation

TDP-43: TAR DNA binding protein-43

TGF-β: Transforming growth factor-beta

TH: Tyrosine hydroxylase

VTA: Ventral Tegmental Area

Chapter 1

Introduction

1.1 Dopaminergic neurons in the midbrain:

Dopaminergic neurons are essential to many brain functions such as the control of voluntary movement, decision making, recognition of reward or aversion and a broad influence on attention, mood and motivation (Hu, 2016). Dopamine plays a vital role in mental health and neurological disorders. The neurotransmitter is released most abundantly by dopaminergic neurons (DAergic) which constitute about 3-5% of the total number of neurons in the midbrain, ventral tegmental area (VTA) and the substantia nigra (Chinta and Andersen, 2005a). During development, the brain experiences a regression in the dopaminergic neuron population in order to establish a "functional brain, neurotransmission network" (Oppenheim, 1991; Fricker *et al.*, 2018). DAergic neurons form heterogeneous groups of cells with varying electrical properties as well as functional properties, particularly, being responsible for functions associated with motor behaviour, motivation and working memory. The neurons form clusters around the CNS that have different anatomical positions crucial to the roles instilled by their projections to other parts of the brain (Figure 1.1).

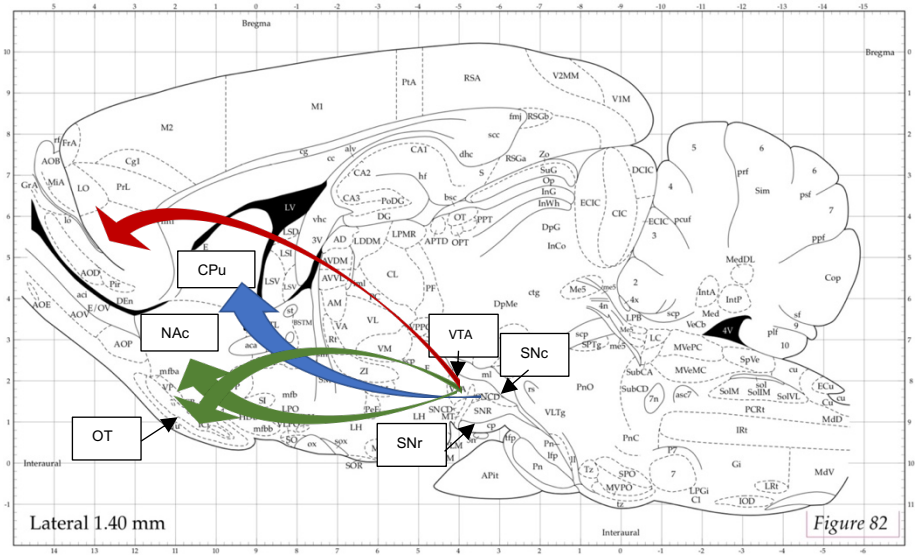

Figure 1.1 A schematic diagram showing the rat brain dopaminergic neuron populations *in the Substantia nigra (SNc), Ventral tegmental area (VTA) and Retrorubral field (RRF), and the axonal projections to the caudate/ putamen (CPu), Nucleus accumbens (NAc) and olfactory tubercle (OT). (Adapted from Luo and Huang, 2016) (Paxinos and Watson, 2013)*

The ventral part of the mescencephalon contains 90% of brain DAergic neurons, a brain region that can further be subdivided. The nigrostriatal pathway originates in the zona compacta of the substantia nigra (SNc: A9 nucleus) and projects to the dorsal striatum (Figure 1.1). This pathway is critical in controlling voluntary movement via modulating the cortico-striatal transmission to medium spiny neurons (MSN) expressing dopamine D1-receptors (D1-R) and D2-receptors (D2-R), leading to either movement facilitation or inhibition, respectively (Kravitz *et al.*, 2010; Tritsch and Sabatini, 2012; Calabresi *et al.*, 2014) . A second major dopaminergic system, the mesocorticolimbic system, involves projections of DAergic neurons from the ventral tegmental area (VTA: A10 nucleus) to the nucleus accumbens (NAc) (Figure 1.1). These DAergic neurons also innervate the septum, amygdala and the hippocampus (Wise, 2004). A third major DAergic nucleus is the Retrorubral field (A8 nuclei group) (Björklund and Dunnett, 2007).

In the dorsal and ventral striatum, the substantia nigra dopaminergic input regulates voluntary movement and is important in goal directed behaviours and habit learning (Bromberg-Martin, et al., 2010). Whereas, the VTA and retrorubral field influence will, reward and memory and regulate other cognitive functions including emotion, motivation, and addictive behaviours (Luo and Huang, 2016). Perturbations in these systems, contribute to several psychiatric disorders such as schizophrenia, depression, anxiety and addiction (Krashia *et al.*, 2016) and degeneration of substantia nigra DAergic neurons is the defining feature of Parkinson's disease (Hornykiewicz, 2001).

The number of DAergic neurons differ widely between different species. For instance, the rat midbrain system contains about 45,000 DAergic neurons, whereas monkeys have about 165,000 DAergic neurons. Humans over the age of 40 (German and Manaye, 1993) are estimated to have about 590,000 DAergic neurons in the brain. However, over the age of 60 there is a significant decrease in the number of DAergic neurons, reaching as low as 350,000 cells (Bogerts, *et al.*, 2017). Although dopamine is essential for many brain functions, the number of DAergic neurons is a tiny fraction of the total number of neurons in a mature human brain (≈100 billion).

Electrophysiological studies have shown distinct characteristics between populations of DAergic neurons. SNc DAergic neurons show long duration action potentials, slow spontaneous pacemaker like firing activity, as well as a pronounced voltage and time-dependent depolarizing component observed during membrane hyperpolarization. This is mediated by a hyperpolarization activated inwardly rectifying cation current (Ih). DAergic neurons that are positive for tyrosine hydroxylase (a rate-limiting enzyme in dopamine synthesis) have local somatodendritic dopamine release which can in turn be inhibited by dopamine and dopamine D2-receptor agonists (Grace and Bunney, 1984; Lacey, *et al*., 1988; Ungless and Grace, 2012). In the VTA, DAergic neurons show similar characteristics, however, there still remains great diversity among these neurons. For instance, in the VTA, the characteristic Ih current varies from cell to cell (Margolis, *et al.*, 2006), indicating its variable contribution in pace-making (Neuhoff *et al.*, 2002a; Khaliq and Bean, 2010).

Krashia et al. 2016 showed a lateral gradient in DAergic neurons from the SNc to VTA in terms of their spontaneous firing frequency (lateral ~2.5 Hz, medial ~1.5 Hz). Neurons in the lateral part of the SNc fire action potentials (AP) significantly faster than in the neighbouring medial SNc; illustrating the heterogeneity in spontaneous firing activity that exists not only among DAergic neurons in general, but specifically DAergic neurons of the SNc. However, despite the differences, the cells in the SNc have been found to have similar membrane properties irrespective of brain sub-region (Nicola, *et al*., 2000).

1.1.1 Dopaminergic neuron maturation and programmed cell death:

Perinatal and early post-natal stages are the defining stages in DAergic neuron development where extensive cell growth and maturation are observed. This is shown by the extensive neurite growth, synaptogenesis and the development of unique rhythmic firing properties (Lee and Tepper, 2009; Pearlstein *et al*, 2015). The rhythmic firing properties of SNc DAergic neurons are determined by the integration of synaptic inputs generated from different regions of the brain (Watabe-Uchida *et al.*, 2012). There is ample evidence to suggest that factors such as sonic hedgehog (Shh), Wnts, GDNF and TGF-β may modulate both the

maturation and synaptic connectivity of DAergic neurons in postnatal life (Bourque and Trudeau, 2000; Tiklová *et al.*, 2019).

During neurogenesis, the number of dopaminergic neurons in rats progressively increases from P0 to P14 when it reaches its maximum, during which some neurons undergo programmed cell death (PCD). Rats experience two waves of PCD activity in DAergic neurons with most of the PCD occurring between P0 and P4 and much less detected at P14 (Jackson-Lewis *et al.*, 2000). It has been proposed that the driver of DAergic neuron PCD could be competition for neurotrophic supports (Massagué and Chen, 2000; Schmierer and Hill, 2007).

1.2 Dopamine receptors:

Dopamine (DA) exerts its effects by binding to dopamine receptors. Once released from presynaptic terminals, DA activates G-protein coupled receptors (GPCRs) that are subdivided into five different receptors (D1, D2, D3, D4, D5) based on their amino-acid sequence, pharmacological and biochemical properties. These receptors provide opportunities to modulate DAergic transmission and its subsequent functions (Andersen *et al.*, 1990; Tiberi *et al.*, 1991; Missale *et al.*, 1998).

These five receptors can be grouped into two classes, namely, D1 class (comprises D1 & D5) and D2 class (D2, D3 & D4). Both classes exhibit high homology in their transmembrane domains where DA binds and thus have similar pharmacological properties. The D1 class of receptors activate the $G\alpha_{s/olf}$ family of G-proteins ultimately stimulating cyclic AMP (cAMP) production. They are found on post-synaptic densities on DA-receptive cells such as GABAergic MSNs in the striatum. The D2 class of receptors are coupled to $G\alpha_{i/o}$ decreasing the production of cAMP. They are expressed on both presynaptic (DAergic neurons) and postsynaptic (DA target cells) densities (Sokoloff *et al*. 2006; Rondou *et al.* 2010; Rankin *et al*, 2010). Activating D2-R in the DAergic neuron cell bodies, enhances K^+ conductance, namely the G-protein-coupled inwardly-rectifying K^+ channels (GIRK). This in turn, reduces the action potential firing of the neuron (Lacey, *et al*., 1987a; Gallo, 2019). However activation of D2-R in

the terminals that contact the striatum inhibits ion channels such as Ca^{2+} channels and activates inward-rectifying (Kir) channels, resulting in a decrease in DA release (Phillips and Stamford, 2000; Martel *et al.*, 2011; Borin *et al.*, 2014; Gallo, 2019).

DA receptors have a broad expression pattern in the brain. DA D1-Receptors are expressed at high levels in areas such as the striatum, NAc, SNc, olfactory bulb, amygdala and the prefrontal cortex (PFC) among others. The D5-R, however, show a much more restricted expression pattern appearing at very low levels in the aforementioned brain regions. The D2-R expression levels are highest in the striatum, NAc, SNc, hypothalamus, cortical areas and the hippocampus (Missale *et al.*, 1998; Gerfen, 2000; Seeman, 2006; Sokoloff *et al.*, 2006; Gerfen and Surmeier, 2011). A bacterial artificial chromosome (BAC) transgenic mouse model was used to determine the spatial arrangement of D1 and D2 -R containing MSN in the striatum and NAc (Shuen *et al.*, 2008; Valjent *et al.*, 2009). The study confirmed the presence of two different subgroups of MSN based on their projection sites and the proteins they express (Figure 1.2). The direct striato-nigral pathway contains MSNs that project to the medial globus pallidus (MGP) and SN reticulata (SNr) and selectively express D1-R. Whereas the D2-R are found on cells of the indirect pathway where MSNs project to the lateral globus pallidus (LGP) however indirectly reaching the SNc/r through synaptic relays in the LGP and subthalamic nucleus (Valjent *et al.*, 2009). D3 receptors, on the other hand, have more limited distribution pattern, with high levels of expression in the limbic regions (Sokoloff *et al.*, 2006) and lowest in the striatum, SNc, VTA and hippocampus. Lastly, D4-R have the lowest expression levels in the brain, localised in the frontal cortex, amygdala, hippocampus, hypothalamus and SNr (Missale *et al*. 1998; Rondou *et al*. 2010).

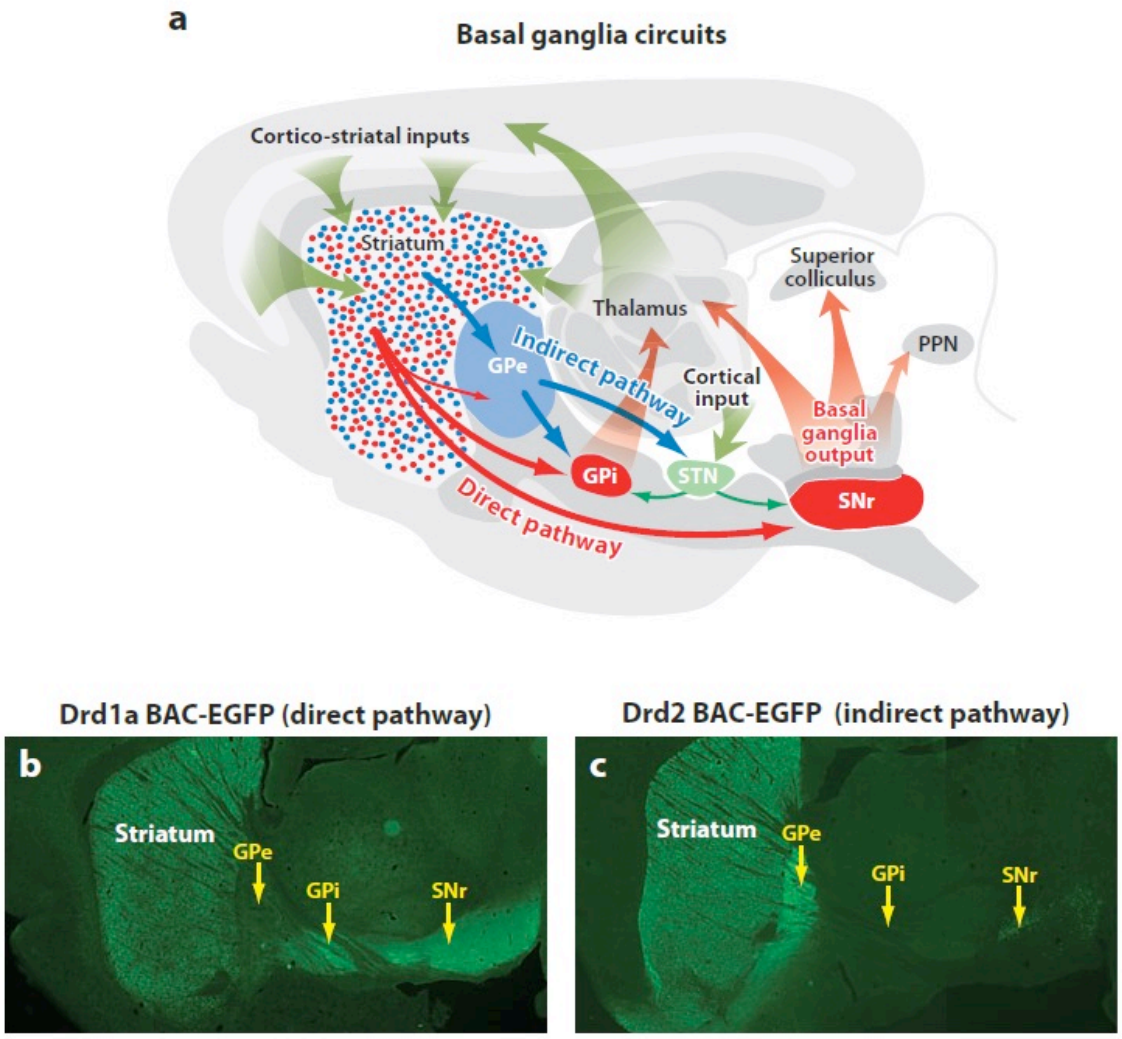

Figure 1.2 Illustration of the Basal Ganglia circuits. *A) Drd1a expressing cells (red) project to the internal segment of the Globus pallidus (GPi) and to the SNr via the direct pathway. Drd2 expressing spiny neurons (blue) project only to the external segment of the globus pallidus (GPe), which projects to the subthalamic nucleus (STN) via the indirect pathway. B) Fluorescence imaging to sagittal mouse brain section expressing EGFP, regulated by Drd1a promoter. Shows axons projecting from striatum to the GPe, GPi and SNr. C) EGFP expression under Drd2 promoter, showing cells projecting only to GPe and not GPi and SNr. Image from (Gerfen and Surmeier, 2011)*

Dopamine is involved in a number of physiological processes. There is substantial evidence showing that D1, D2 and D3-Rs control locomotor activity (Missale *et al*. 1998; Sibley 1999). D1-R are found on postsynaptic striatal medium spiny neurons of the direct pathway, whereas D2 and D3-R are found on both pre and post-synaptic locations of the indirect pathway (Missale *et al.*, 1998; Sibley, 1999; Gerfen and Surmeier, 2011)(Figure 1.2). Presynaptic D2 autoreceptors are responsible for modulating nerve terminal DA synthesis and

release in response to extracellular DA levels (Usiello *et al.*, 2000; De Mei *et al.*, 2009). Furthermore, D2 receptors are found post-synaptically, where they function to inhibit LTD at midbrain excitatory synapses along with controlling pacemaker activity and resting potential (Wolf and Roth, 1990; Misale *et al.*, 1998; Sibley, 1999; Hopf *et al.*, 2005). The activation of D2-autoreceptors and subsequent decrease in DA release results in a decrease in locomotor activity. Higher DA agonist concentrations result in increased locomotion, whereas, lower concentrations result in dampened activity levels. D3-autoreceptors exert moderate inhibitory action on locomotion via the activation of autoreceptors or through the involvement of postsynaptic signalling (Sibley, 1999; Joseph *et al.*, 2002). D4 and D5-Rs show a limited expression pattern in the brain and therefore have minimal effect on locomotor activity (Missale *et al*. 1998; Sibley 1999; Rondou *et al*. 2010).

Other functions that are controlled to various degrees by the D1 and D2-Rs are reward and reinforcement mechanisms. Therefore, any pharmacological and genetic perturbations in DA-R function may have direct implications for reward and addiction (Missale *et al*. 1998; Hyman *et al*. 2006; Sokoloff *et al*. 2006). D1 and D2-R are also critical for learning and memory mechanisms such as working memory (Goldman-Rakic *et al.*, 2004) while D3, D4, and D5-R have minimal modulatory influences on cognitive function.

1.2.1 Cell calcium and dopaminergic neuron cell death:

Increased calcium levels could induce apoptotic signals that could drive the cell to programmed cell death (Skeberdis *et al.*, 2006; Hardingham and Bading, 2010). This influx of calcium into dopaminergic neurons is partly dependent on voltage-sensitive Ca^{2+} channels and partly mediated by the presence of N-Methyl-D-Aspartate (NMDA) receptors on the cell surface (Blythe *et al.*, 2009; Sulzer and Surmeier, 2013a).

Dopamine-activated D2 receptors trigger reduced synthesis of cAMP, and a consequent decrease in Protein Kinase A (PKA) activity, which (among many targets) normally phosphorylates the NMDA receptor (Murphy *et al*., 2014). In

the absence of PKA, NMDA receptors get dephosphorylated, causing them to internalise, thus potentially decreasing calcium influx (Higley and Sabatini, 2010).

Enhancing excitability could lead to long-term changes such as Long-Term Potentiation (LTP) of synaptic transmission that could contribute to several symptoms experienced by Parkinson's patients, mainly dyskinesia. Determining the effects of D2 activation by dopamine or dopamine agonists on NMDA receptors will help to understand changes that can occur during dopamine agonist therapy. Similarly to the effects of dopamine agonists previously seen on hippocampal cells (Cepeda *et al.*, 1998), I investigated whether the activation of dopamine receptors with Ropinirole, a D2 receptor agonist (Shill and Stacy, 2009), will modulate the NMDA receptor (NMDA-R) currents in substantia nigra DAergic neurons.

1.2.2 Dopaminergic neurons and Parkinson's disease

DAergic neurons of the substantia nigra pars compacta (SNc) primarily project to neurones in the corpus striatum. This nigro-striatal pathway is of great importance in the control of voluntary movement. Release of dopamine occurs from both the terminal domain in the striatum and in the substantia nigra. The release of dopamine is self-regulated acting via D2 autoreceptors to inhibit the further release of dopamine (Lacey, *et al*., 1987b). Upon ionophoretic application of DA, *in vivo*, electrophysiological studies have demonstrated a decrease in firing capacity in the SNc (Bunney, *et al.*, 1973). This phenomenon tends to prevent spontaneous action potential firing.

DAergic neurons are also known for their potential to induce oxidative stress in themselves (Liss *et al.*, 2005; Sulzer and Surmeier, 2013b; Duda, *et al*., 2016). Their high rate of oxygen metabolism that can generate toxic reactive oxygen species (ROS) by an enzyme-catalysed reaction involving Monoamine Oxidase (MAO), which can oxidise dopamine producing toxic species such as hydrogen peroxide and oxygen free radicals (Schiemann *et al.*, 2012). MAO-inhibitors

have thus been used to treat symptoms of PD such as akinesia and motor fluctuations (Riederer and Laux, 2011).

Degeneration of dopaminergic neurons of the SNc is one of the key features of Parkinson's Disease (PD) which affects about 1.5% of the population over the age of 65 years (Hornykiewicz, 2001). The loss of dopaminergic neurons in the brain leads to the characteristic clinical symptoms of resting tremor, bradykinesia and rigidity. The main treatment is dopamine replacement therapy provided in the form of L-Dopa, supplemented in some patients with dopamine receptor agonists such as pramipexole or ropinirole (Constantinescu, 2008). Although the cause of PD is not known for most patients, many experimental investigations are currently directed towards investigating calcium signalling and the role of mitochondrial dysfunction in dopaminergic neurone degeneration (Sulzer and Surmeier, 2013a). In addition, DA neurons spontaneously generate action potentials and their membrane potential is relatively depolarized, where NMDA receptors will be partially relieved of their magnesium block, creating a potential source of extrasynaptic calcium that may contribute to excitotoxicity mechanisms in PD (Sulzer and Surmeier, 2013a). In this project, I investigated the possibility that activation of D2-class dopamine receptors in dopaminergic neurons may modulate NMDA receptors and so could indicate a new avenue to influence dopaminergic neurone cell death.

Pramipexole and ropinirole are both agonists at dopamine D2/3 receptors and although they are effective treatments for Parkinson's disease (PD), they can trigger impulse control disorders including gambling disorder (Dodd *et al.*, 2005). These changes in behaviour could involve NMDA receptor-mediated synaptic plasticity which is a second reason for investigating possible modulation of NMDA receptor responses by dopamine agonists.

1.2.*3* Parkinson's Disease Pathology:

Parkinson's disease is among a number of Parkinsonian disorders that share similar clinical features. The underlying factor of Parkinson's disease is loss of DAergic neurons in the substantia nigra that project to the putamen. PD is a

progressive degenerative neurological disease with clinical features such as bradykinesia, rigidity and tremors. Degenerative Parkinsonian disorders can be separated into two molecular divisions- tauopathies and α-synucleinopathies. α–synucleinopathies are characterised by an accumulation of α-synuclein in vulnerable neurons. This is observed in PD patients where they develop neuronal inclusions composed of α-synuclein. These inclusions are known as Lewy bodies that extend beyond the nigra (Jellinger, 1991; Dickson *et al.*, 2009; Dickson, 2012). Furthermore, macropathology associated with PD includes mild frontal atrophy and loss of the dark pigment in the brainstem. This is indicative of loss of DAergic neurons in the nigra and locus coeruleus (where nor-adrenergic neurons reside).

PD pathology begins in the dorsal motor nucleus of the vagus in the medulla and in the olfactory bulb. Disease progression is described as neuronal loss in the locus coeruleus neurons in the pons and DAergic neurons of the substantia nigra. In later disease stages, pathology is observed in the basal forebrain, amygdala and medial temporal lobe structures. In the final stages of PD, a progressive neuronal loss in the convexity cortical areas is observed (Braak *et al.*, 2004; Dickson, 2012).

1.2.4 Involvement of D2-receptors of dopaminergic neurons in Parkinson's disease*:*

Dopamine receptors can be divided into two classes: D1-like receptors that include D1 and D5; and D2-like receptors, (D2, D3 and D4 receptors) (Misale *et al.*, 1998). D2 class receptors are one focus of this project. D2 receptors are coupled to the Gαoi and Gαi proteins that cause respectively activation of inward rectifying K^+ channels and inhibition of cAMP production upon ligand binding by decreasing adenylate cyclase (AC) activity (figure 1.3). This then causes a reduction in PKA activity in the cell (Hisahara and Shimohama, 2011) (Panesar, 2015).

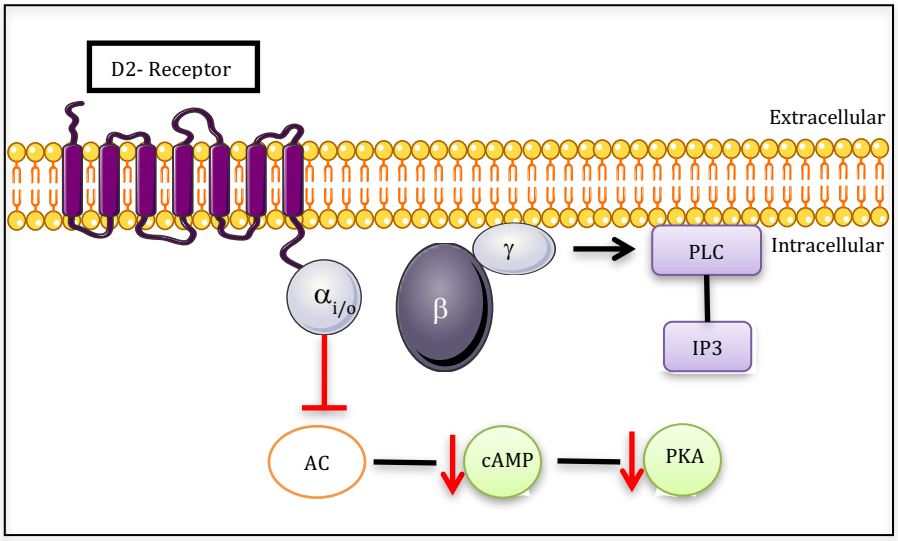

Figure 1.3 D2- Receptor activation. *AC-Adenyl cyclase, cAMP-cyclicAMP, PLC- Phospholipase C, IP3- Inositol triphosphate, PKA- Protein Kinase A*

Although dopamine receptors overlap in terms of their anatomical distribution, they are present in different numbers in different regions of the brain (Chinta and Andersen, 2005b). DAergic neuron D2-Rs act primarily to decrease the release of dopamine from the somato-dendritic region of midbrain DAergic neurons and dopaminergic nerve terminals (Ford, 2014). In rodents, the administration of low concentrations of dopamine agonist, quinpirole, suppresses motor activity by inhibiting the release of dopamine in the striatum. Although both D2-Rs and D3-Rs are found on midbrain DAergic neurons, studies have shown that D2-Rs specifically are involved as "somatodendritic, impulse-regulating autoreceptors on dopamine neurons" (Centonze *et al.*, 2002).

In Parkinson's disease, the loss of DAergic neurons in the substantia nigra are usually evident in DAergic projections that terminate in the striatum. In the striatum, D2-R density is altered due to the loss of DAergic neurons in PD patients and is dependent on the stage of the disease (Figure 1.4).

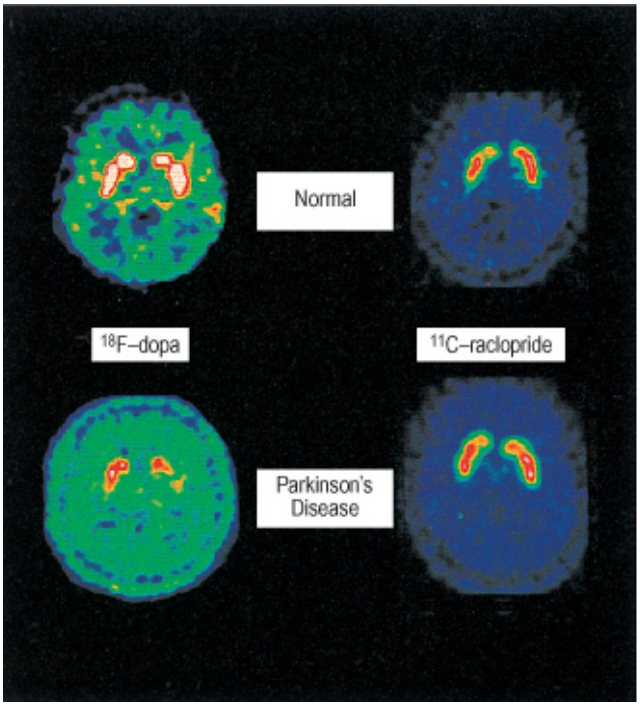

Figure 1.4: PET scan comparing normal and PD affected brains*. The top scans are from a normal individual while those on the bottom belong to someone with Parkinson's disease. On the left scans were made using [^{18}F]-dopa. This is taken up by the intact dopaminergic neuron nerve terminals and so tests the amount of dopamine store in terminals in the striatum. The scans on the right use the tracer [^{11}C] raclopride (a D2-R antagonist). This binds to the D2 dopamine receptors on striatal neurons demonstrating that the D2 receptors remain intact or even increase in Parkinson's disease* (Crossman, and Neary, 2005).

When the DAergic neurons begin to die, D2-Rs present on the nerve terminals are lost. However, as the disease progresses, the number of D2-R increases in the striatal regions (Figure 1.4). This increase could be due to the up-regulation of post-synaptic D2-R. D2-R coupling to the inhibitory G protein, $G\alpha_{i/o}$, could be enhanced, making the neurons supersensitive to DA agonist binding (Panesar, 2015). An increase in the number of D2-R present on the surface of DAergic neurons correlates with development of DA-R super sensitivity (Hisahara and Shimohama, 2011). In the 1970's and 1980's, several reports demonstrated that both D1-R and D2-R are overexpressed in untreated patients with PD. These levels are then thought to return to normal when L-dopa is administered (Hisahara and Shimohama, 2011). However, it has been suggested that treatment regimens involving L-dopa should contain periods where treatment is stopped to allow the DAergic receptors to rehypersensitize (known as a L-dopa

holiday) and therefore enhance their sensitivity to dopamine agonists (and to dopamine) (Panesar, 2015).

1.2.5 D2 receptor modulation of potassium channels:

Inward rectifying K^+ (Kir) channels are a subset of K^+ selective ion channels that are found as homo- or heterooligomers. They have a greater tendency to transport K^+ ions (current) in the inward direction compared to the outward direction. This phenomenon of inward rectification is a result of a high affinity block by intracellular Mg^{2+} ions blocking the channel pore at potentials positive to the K^+ reversal potential (Lopatin, *et al*., 1995). They play an important role in regulating neuronal activity, by stabilizing the resting membrane potential of the cell. They are also involved in synaptic inhibition, manipulating the neuronal firing rate and lastly, K^+ homeostasis.

GIRK channels are G-protein regulated, inwardly rectifying potassium channels. Those specifically localised in the substantia nigra are Kir3.0 subfamily channels that are subject to G-protein activation (Karschin *et al.*, 1996). Karschin et al. (1996) showed that only a single type of GIRK channel- GIRK2 (Kir3.2) was present at very high levels in the SNc however not in the reticulata. With the highest composition of neurons in the SNc comprising of DAergic neurons, it is safe to suggest that these GIRK channels are present on such neurons (Paxinos, and Franklin, 2012). Mutations of GIRK2 that produced the weaver mouse mutation were shown to cause neuroinflammation-mediated degeneration of the DAergic neurons. These mice had deficits in motor coordination (Peng *et al.*, 2006). The D2-R, the GPCR of interest in my research, highly regulates potassium conductance in DA neurons upon activation (Lacey, *et al*., 1987)(Figure 1.2).

1.2.6 D2 receptor modulation of cyclic nucleotide gated channels (I_h):

DAergic neurons are characterised electrophysiologically by the presence of membrane hyperpolarization-activated, cyclic nucleotide-gated channels (HCN channels)(Chu and Zhen, 2010). In my research, this was shown by introducing

a membrane potential step from -60 mV to -120 mV and back to -60mV. Under physiological conditions, HCN channels activate with slow kinetics between -70mV to -140mV. The four different HCN subunits (HCN1-4) show specific localization in different regions of the brain corresponding to their different biophysical properties. The HCN1 subunit, found in the hippocampal pyramidal neurons, shows the fastest kinetics with minimal sensitivity to cAMP. HCN2 subunits found dispersed throughout the brain and HCN4 subunits found mainly in the thalamus, SNc DAergic neurons and the olfactory bulb, show the slowest kinetics (Santoro *et al.*, 2000). They, on the other hand, are very sensitive to cAMP modulation (Wang, et al., 2001). Using qualitative single-cell RT-PCR, Santoro B, et al (2000) only detected HCN2-4 in SNc DAergic neurons with activation time constants of I*h* = 0.5-5 s*,* significantly slower than those in hippocampal pyramidal neurons (50 – 500 ms).

HCN subunits are each composed of 6 transmembrane domains, including a pore region, and cytosolic NH_2 and COOH termini. The COOH segment of the channel is subject to cAMP modulation. This occurs when cAMP binds to an intracellular cyclic nucleotide-binding domain (CNBD). Upon intracellular cAMP binding to this region, the voltage dependence of the channel is shifted to less hyperpolarized potentials. This induces channel opening after repolarization of the action potential, ultimately, helping the channel exert its pace-making functions (Wang, *et al.*, 2001).

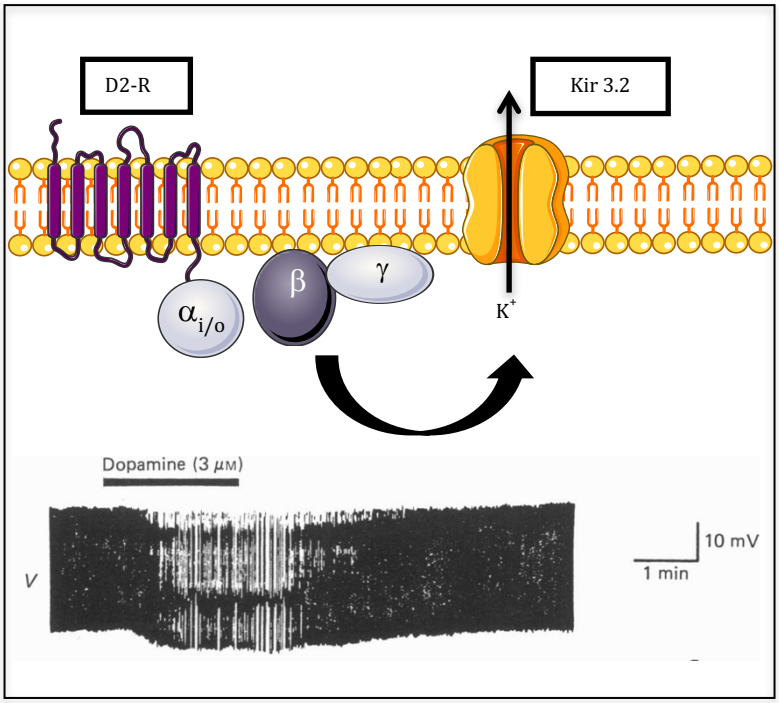

Figure 1.5 Effect of D2-R activation on K^+ conductance and action potential firing in dopaminergic neurons. *The cell is firing spontaneous action potentials until DA (3μM) is added. This reduces the firing rate (Lacey, et al., 1987a).*

Upon D2-R activation via dopamine binding in SNc DAergic neurons, the $G\alpha_{i/o}$ is activated. This inhibits adenyl cyclase activity, and thus reduces the production of cAMP. cAMP acts as an agonist at HCN channels, binding to each subunit of the channel from the inside of the cell and causing channel P_{open} to increase (Wang, Chen and Siegelbaum, 2001). As mentioned earlier, HCN2-4 have high sensitivity to cAMP. If cAMP is reduced, HCN channel activation will be reduced. The decrease would in turn reduce entry of sodium, potassium and calcium ions into the neuron via HCN channels. This was shown in a previous study by Wainger *et al*., (2001) where a truncated CNBD similarly shifted the activation curve of HCN1 and HCN2 in the depolarizing direction as seen in the presence of cAMP; this demonstrated CNBD's role in inhibiting the core transmembrane domain. The inhibition was relieved in the presence of cAMP, reinstating its modulatory role in HCN1 and HCN2 channels (Wainger *et al.*, 2001).

1.2.7 Dopamine receptor pharmacology:

D2-like agonists are used in the treatment of many neurological diseases. Despite the myriad of receptor agonists that exist, their exact receptor subtype affinity profiles show varying degrees of selectivity (Table 1). These are effective in the treatment of Parkinson's disease and restless legs syndrome among others (Jenner, 2003). They also play a vital role in targeting drug addiction as partial D2-R agonists and antagonists- most commonly used to treat cocaine and nicotine abuse (Pilla *et al.*, 1999; Di Ciano, *et al.*, 2014; J. D. Lowe *et al.*, 2015; Keck *et al.*, 2015; Butini *et al.*, 2016).

Table 1 Agonist affinities (pK_i values) for different DA receptor subtypes

	D1-R	D2-R	D3-R	D4-R	D5-R
DA	4.3-5.6 (Tiberis *et al.*, 1994)	4.7-7.2 (Zhao *et al.*, 1996)	6.4-7.3 (Burris *et al.*, 1995)	7.6 (Van Tol *et al.*, 1991)	6.6 (Sunahara *et al.*, 1991)
Pergolide	5.9-6.5 (Millan *et al.*, 2002)	7.5 (Millan *et al.*, 2002)	8.3 (Millan *et al.*, 2002)	7.2 (Millan *et al.*, 2002)	6.0-7.5 (Millan *et al.*, 2002)
Ropinirole		8.1 (Richard F. Heier *et al.*, 1997)	7.7 (Richard F. Heier *et al.*, 1997)		
Quinpirole		5.2 (Burris *et al.*, 1995)	6.4 (Burris *et al.*, 1995)	7.5 (Millan *et al.*, 2002)	
Pramipexole		5.1 (Mierau *et al.*, 1995)	8.4 (Mierau *et al.*, 1995)		
Lisuride					8.5 (Millan *et al.*, 2002)

Regardless of its initial potency in the treatment of PD, L-dopa shows a gradual decline in clinical efficacy during prolonged use (over several years), and the introduction of severe side effects such as motor fluctuations (wearing off or sudden on and off movement), dyskinesias, and dystonia (Jenner, 2003). Therefore dopamine agonists can be given to Parkinson's patients to delay the use of L-dopa and thus delay the onset of treatment-induced motor complications (Webster, 2001; Jenner, 2003). Long-acting dopamine agonists bind directly to D2-Rs and have far more advantages than the short-acting drugs that result in a pulsatile D2-R stimulation such as L-dopa. Continuous DAergic stimulation reduces the involuntary movements associated with pulsatile stimulation. Studies by Jenner's lab have confirmed that continuous DAergic stimulation with ropinirole produced significantly less dyskinesia relative to L-

dopa administration in experimental rats treated with 6-OHDA (Jenner, 2003). Furthermore, metabolites of these agonists do not produce free radicals and therefore are not deemed harmful to DAergic neurons (Hisahara and Shimohama, 2011).

Initially, D2-R agonists were developed to override the short-lived effects of L-dopa, which caused the patients to suffer from response fluctuation and motor complications. In 1989, a highly potent drug, Pergolide was introduced as a D1/D2-R agonist for PD treatment. It exhibited long acting characteristics in early stage disease and when it was used in adjunctive therapy, it showed enhanced efficacy in patients with advanced PD (Olanow *et al.*, 1994). Dopamine receptor agonists including pergolide and ropinirole (that will be used in this study) have several advantages over L-dopa. The major one being the three-fold decrease in motor complications (dyskinesia) caused after prolonged use (Jenner, 2003).

Ropinirole is a non-ergoline D2-R agonist that has a high affinity and is strongly active at D2 and D3-R however has a negligible effect on D1-R. It also binds to DAergic D2-autoreceptors to reduce release of dopamine. This may reduce continuous oxidation of dopamine via monoamine oxidase (MAO), and reduce ROS production, which could contribute to damage of nigrostriatal tissue (Parvez *et al.*, 2010).

Ergoline derivatives on the other hand, have a widespread pharmacological profile, targeting different DA-R subtypes to different extents as well as other GPCRs. They are effective in the treatment of disease such as, restless legs syndrome, acromegalia and hyperprolactinemia. Examples of such drugs include, bromocriptine and cabergoline. They possess approximately equal affinities for D2, D3 and D4-Rs of nanomolar concentrations (Gerlach *et al.*, 2003).

1.3 NMDA Receptors

N-Methyl-D-Aspartate (NMDA) receptors are ionotropic glutamate receptors that contribute to and regulate synaptic function. They convert specific patterns of neuronal activity to initiating long term changes in synaptic strength (Bliss and Collingridge, 1993; Esmenjaud *et al.*, 2018). They are unique in that they are activated by both glycine (or D-serine) and glutamate (Forsythe, Westbrook and Mayer, 1988; Westbrook, *et al*., 1988). These receptors have been targets of therapeutic interest as perturbations in their functionality have been associated with a number of neuropathological conditions such as, schizophrenia and depression. However, despite many efforts to target NMDA receptors, most NMDA-based therapeutics proposed for clinical use have shown poor side-effect profiles (Hackos and Hanson, 2017).

These glutamate receptors are tetrameric membrane proteins composed of three subunit types -GluN1, GluN2 and GluN3, that combine to produce an array of heteromeric NMDA-R compositions that localise at both synaptic and extra-synaptic sites. GluN1 and GluN3 subunits bind glycine while GluN2 subunits bind glutamate (Yi *et al.*, 2018). These receptors are formed in the endoplasmic reticulum (ER) where their pharmacological properties and patterns of synaptic targeting are determined (Lau and Zukin, 2007). Synaptic NMDA-R channels are permeable to Ca^{2+} and blocked by Mg^{2+} (MacDermott *et al.*, 1986; Westbrook, *et al*., 1988) and are co-activated by glycine or D-Serine (Johnson and Ascher, 1987; Westbrook, *et al*., 1988; Forsythe, Westbrook and Mayer, 1988; Thomson, *et al*., 1989; Panatier *et al.*, 2006). Glia-derived D-serine controls NMDA receptor activity and synaptic memory (Singh *et al.*, 2006) which is essential for experience-dependent synaptic remodelling, and induced plasticity in the form of LTP and LTD; which have both been linked to the development of memory and learning (Bliss and Collingridge, 1993). The ability of the receptors to induce such long-term changes, involves the phosphorylation state and subunit composition of α-amino-3-hydroxy-5-methyl-4isoxazolepropionic acid (AMPA) receptors. The Mg^{2+} block present on NMDA-Rs is a detector of pre- and postsynaptic firing. Presynaptic firing releases glutamate from the nerve

terminal, while post-synaptic firing gives depolarization. LTP or LTD are induced when an NMDA-R is activated, coincident with depolarisation. This relieves the Mg^{2+} block, causing an NMDA-mediated rise in Ca^{2+} concentration in the cell which goes on to activate a number of kinases (Lau and Zukin, 2007; Mavrikaki *et al.*, 2014). NMDA-R mediated Ca^{2+} influx also contributes to excitotoxicity cell death (Choi, *et al*., 1988).

1.3.1 Presence of diheteromeric and triheteromeric NMDA-Rs in the brain

NMDA-Rs are composed of two GluN1 and two GluN2 subunits (sometimes one of these is replaced by a GluN3 subunit) (Hansen *et al.*, 2018). The GluN2 subunits are coded by four different genes producing four different isoforms (A-D). Such a broad molecular heterogeneity is responsible for the multiple receptor subtypes present in the nervous system, producing a combination of diheteromers (containing 2 GluN1 and 2 identical GluN2 subunits) or triheteromers (containing 2 GluN1 and 2 different GluN2 or possibly a GluN3 subunit). They all have distinct biophysical, pharmacological and signalling properties (Wang *et al.*, 2011; Paoletti, *et al.*, 2013; Sanz-Clemente, *et al.*, 2013; Hansen *et al.*, 2018; Yi *et al.*, 2019). The different NMDA-R compositions are expressed at different developmental stages and in different brain regions, owing to gene expression changing at different stages in brain development (Watanabe *et al.*, 1993; Akazawa *et al.*, 1994; Monyer *et al.*, 1994a). This reflects the tailored role of different neuron subpopulations in the neural circuitry in the brain.

There is evidence to suggest subunit specific localisation of NMDA-Rs on individual neurons. For example, GluN2A containing receptors are found enriched at the synapse, whereas, GluN2B containing receptors are predominantly found extrasynaptically (Stocca and Vicini, 1998; Groc *et al.*, 2007; Rauner and Köhr, 2011). Due to differences in downstream signalling cascades coupled to GluN2A and GluN2B subunits, subunit composition may determine NMDA-Rs contributions to excitotoxic cell death in different disease models (Lynch and Guttmann, 2002; Hardingham and Bading, 2010). NMDA-R

subunit composition is dependent on subunit availability, hence the range in receptor subtypes at different developmental stages and in different brain regions will vary depending on gene expression (Watanabe *et al.*, 1993; Sans *et al.*, 2003).

Triheteromers are widespread in the CNS and possibly make up the majority of native NMDA-Rs (Sheng *et al.*, 1994; Rauner and Köhr, 2011; Paoletti, *et al*., 2013; Tovar, *et al.*, 2013; Bhattacharya *et al*., 2018; Yi *et al.*, 2019). Their presence in the brain was confirmed after multiple biochemical co-immunoprecipitation studies on brain tissue. In rodent forebrains, both GluN2A and 2B showed evidence of co-immunoprecipitation, indicating the presence of both subtypes in a single NMDA-R, thus forming GluN1, GluN2A/B ternary complexes (Sheng *et al.*, 1994; Chazot and Stephenson, 2002). Other ternary complexes comprising GluN1, GluN2A/C or B/D are found in the cerebellum, thalamus and midbrain (Dunah *et al.*, 1998; Bhattacharya *et al.*, 2018; Stroebel, *et al.*, 2018). Functional studies on brain slices and isolated cells indicated the presence of different subtypes of NMDA-Rs co-existing, composed of both diheteromers and triheteromers (France *et al.*, 2017). Strong electrophysiology studies have shown GluN1/2A/2B triheteromers localised in the hippocampus, making up majority of receptors at the CA3-CA1 synapses (Rauner *et al*., 2011) while 2A/2C triheteromers are found in cerebellum (Bhattacharya *et al*., 2018). These receptors have different gating properties, sensitivity to agonists and deactivation kinetics relative to diheteromers. These differences confer unique charge transfer capacities and signalling properties. They are also known to deactivate much faster than GluN1/2B but nearly as fast as GluN1/2A diheteromers (Hansen *et al.*, 2014).

GluN3A and B can also co-assemble with other GluN2 subunits, to produce populations of triheteromers (Perez-Otano *et al.*, 2001). This assembly of subunits produces NMDA-Rs contributing to synaptic maturation during brain development (Pérez-Otaño, *et al.*, 2016). Despite the extensive studies performed on these receptors, not much is known with regards to receptors in ternary complexes comprising GluN2C/D or GluN3 subunits. GluN1/2A/2C receptors display fast deactivating kinetics and low Mg^{2+} block (Bhattacharya *et*

al., 2018). GluN2D containing triheteromers have shown to contribute to synaptic transmission in the substantia nigra and hippocampus (Brothwell *et al.*, 2008a; Harney, *et al.*, 2008; Yi *et al.*, 2019). During postnatal development, synaptic inputs into the SNc DAergic neurons have shown similar characteristics to NMDA-Rs containing GluN1/2B and 2D subunits (Brothwell *et al.*, 2008a).

1.3.2 NMDA-R mediated synaptic currents follow a postnatal developmental sequence

The level of dopamine release from neuron terminals are dependent on the firing rate and firing pattern of the SNc neurons (Gonon, 1988; Wise, 2004). The neuronal firing activity in turn is a result of interactions between intrinsic membrane conductance and afferent inputs (Grace and Bunney, 1983; Blythe *et al.*, 2009; Wang *et al.*, 2011). Dopamine release during pace-making is essential to maintain motor activity. Pace-making is vital in its role in delivering a constant basal level of dopamine to the striatum, enabling its function in controlling motivation (Wise, 2004). On the other hand, burst firing results in a significant increase in dopamine release which in turn induces cortico-striatal plasticity essential in habit learning (Gonon, 1988; Grillner and Mercuri, 2002). Glutamatergic afferents terminating on the SNc neurons, mainly originate in the subthalamic nucleus (STN) and pedunculopontine nuclei (PPN) (Hammond *et al.*, 1978; Sarah *et al.*, 2009; Ammari *et al.*, 2010; Pearlstein *et al.*, 2015). Activation of NMDA and AMPA receptors are responsible for generating transient high frequency activity in DAergic neurons. Therefore, any changes in the number, distribution and glutamate receptor composition, has the potential to affect excitatory synaptic integration in the DAergic neurons and further affect its activity pattern in adulthood. Pearlstein et al. (2015) sought to elucidate the postnatal development profile of AMPA and NMDA receptor mediated excitatory postsynaptic currents (EPSCs) in the SNc DAergic neurons in immature (P4-10) and adult (P30-50) TH-green fluorescent mice and determine how they influence the bursting of SNc neurons in response to STN stimulation. It was demonstrated that somatodendritic fields of SNc DAergic neurons are already mature in immature mice (P4-10) (Pearlstein et al., 2015). On the other hand, glutamatergic firing shows a developmental sequence, related to the NMDA-R

subunit composition. GluN2D-containing NMDA-Rs were found in SNc DAergic neurons in P4-10 mice in the postsynaptic densities, where they developmentally regulate the generation of large, frequent single spontaneous EPSCs and bursts. GluN2B-containing NMDA-Rs, however, are present in both immature and young adult DAergic neurons and are vital in the generation of NMDA sEPSCs. Due to the presence of both GluN2B and GluN2D-containing NMDA-Rs in the immature mice, NMDA EPSCs are larger and more frequent in neonatal compared to the younger adults. Thus, the decrease of GluN2D-containing NMDA-R induced sEPSC in young adult DAergic neurons are due to the disappearance of synaptic GluN2D-containing receptors (Pearlstein *et al.*, 2016). In contrast, in rat SNc, Brothwell *et al.*, (2008b) observed a maximum ifenprodil effect of about 60% block suggesting other receptors are contributing up to P21 days old.

1.3.3 The contribution & relevance of GluN2D-containing NMDA-Rs

NMDA-Rs are expressed at almost all mammalian excitatory synapses. They are activated by coincident detection of glutamate, glycine/serine and a depolarisation, which relieves the receptor of the Mg^{2+} block (Forsythe and Westbrook, 1988; Forsythe, Westbrook and Mayer, 1988; Traynelis *et al.*, 2010). As mentioned earlier, they are mainly comprised of two GluN1 subunits and two GluN2 subunits, that form heteromeric complexes. With that said, the GluN2 subunits are the main determinant of NMDA-R functional diversity (Hansen *et al.*, 2018), as they are coded by 4 different genes, producing at least four possible diheteromeric subunit subtypes, and additional triheteromeric variants (Hansen *et al.*, 2018). Furthermore, the distribution and availability of the GluN2 subunits follow a post-natal developmental regulation throughout the brain (Monyer *et al.*, 1994b; Hansen *et al.*, 2018). The GluN2B subunit is found at its highest at birth in the cortex and hippocampus, after which it experiences a slow decline in prevalence in adulthood (Akazawa *et al.*, 1994; Monyer *et al.*, 1994a). GluN2A, however, is present at low levels at birth, but gradually increases throughout development (Wenzel *et al.*, 1984; Monyer *et al.*, 1994). GluN2C subunits are expressed in the cerebellum and olfactory cortex later in development (Watanabe *et al.*, 1992; Monyer *et al.*, 1994b; Bhattacharya et al.,

2018; Morris, *et al*., 2018). Lastly, GluN2D subunits are prominent in the brainstem and diencephalon in neonates, however, decrease during postnatal development. In more mature neurons, GluN2D containing NMDA-Rs are found in the cerebellar nuclei, the striatum, SNc DAergic neurons, STN and hippocampal interneurons (Watanabe *et al.*, 1992; Monyer *et al.*, 1994b; Standaert *et al.*, 1994; Dunah *et al.*, 1998; Cull-Candy, et al., 2001a; Piña-Crespo and Gibb, 2002; Jones and Gibb, 2005; Brothwell *et al.*, 2008a; Yi *et al.*, 2019).

Morris *et al*. (2018) used Grin2D-null mice to study the contribution of GluN2D subunit containing receptors to synaptic and extrasynaptic NMDA-R responses in substantia nigra DAergic neurons. Their data showed that GluN2D subunits contribute to both synaptic and extrasynaptic NMDA-Rs in SNc DAergic neurons throughout postnatal development. This was demonstrated by looking at the overall expression of NMDA-Rs and AMPA-Rs in wild-type and GluN1D-null mice. In the presence of 50μM picrotoxin (GABA inhibitor) and 10μM glycine, GluN2D-null mice showed a significant reduction in NMDA-R and AMPA-R-induced EPSC amplitude relative to the control in P7 mice. However, in P21 mice, there was no difference in EPSC peak amplitude. Furthermore, it was previously shown that NMDA-R- EPSCs in rat SNc DAergic neurons are inhibited by a GluN2D inhibitor UBP141 up to P21 (Brothwell *et al.*, 2008a). This triggered a pharmacological approach to study the developmental contribution of GluN2D in synaptic plasticity (Harney, *et al*., 2008). Morris *et al.* (2018) introduced a more selective GluN2C/2D NMDA-R antagonist, 10μM DQP-1105 and compared the NMDA-EPSC current amplitude during baseline and in the presence of DQP-1105. In P7 mice, the wildtype (WT), showed a significant difference in peak amplitude, and no statistically significant difference was seen in the GluN2D-null mice. Similar results were observed in the P21 mouse.

1.3.4 Effects of dopamine receptor activation on NMDA-R

There is extensive evidence showing that dopamine receptors have modulatory effects on NMDA-R activity. In the prefrontal cortex, D1-R activation has been shown to enhance NMDA-R currents through a signal transduction pathway

involving PKA (Cepeda *et al.*, 1998). In the striatum, activation of D1-R leads to the activation of the adenylate cyclase pathway by activation of the coupled G_s-G-protein. This causes a subsequent rise in cAMP levels, which will allow for the phosphorylation by PKA of DARPP-32, the potent protein phosphatase-1 inhibitor. Phosphorylating DARPP-32 will enhance the NMDA-R phosphorylation and so enhance NMDA-R currents (Tong and Gibb, 2008).

Some research has shown a decrease in NMDA receptor function following DA receptor activation that does not involve G-protein signalling. NMDA-R modulation occurred either by direct protein-protein interactions between both receptors (Lee *et al.*, 2002; Liu *et al.*, 2006) or via an intracellular adaptor protein or via the activation of intracellular tyrosine kinase (Suhas *et al.*, 2002; Tong and Gibb, 2008). Tong, et al. (2008), suggested a developmental switch in D1-R modulation of NMDA-Rs which is driven by the change in NMDA-R subunit composition. Early in development, when GluN2B subunits predominate, D1-R activation down-regulates NMDA-Rs. In older animals, when there is a likely mix of GluN2A/B containing NMDA-Rs, D1-R activation maintains NMDA-Rs at the synapse.

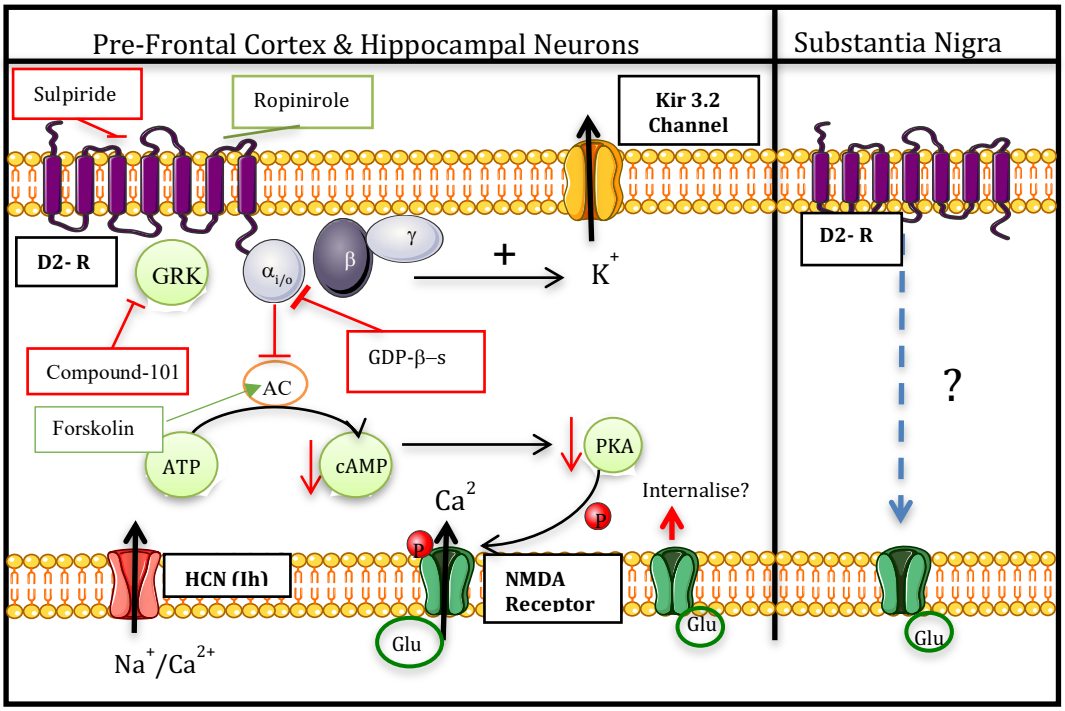

Figure 1.6 A diagram of possible intracellular pathways involved in NMDA-R modulation by PKA upon D2-R activation. *AC, adenyl cyclase; HCN ,Hyperpolarisation-activated cyclic nucleotide gated channel.*

1.4 Effects of adenosine 2A receptors (A2A-Rs)

1.4.1 A2A-R dependent effects in the cell

A2A-Rs are Gαs-protein coupled receptors that raise cAMP via the activation of adenyl cyclase (AC) (Chang *et al.*, 1997; Chen, *et al.*, 2014; Lai *et al.*, 2018b). The elevation in cAMP, in turn, leads to multiple downstream effects such as activation of cAMP-response element binding protein (CREB). The phosphorylation of CREB has been shown to promote neuronal plasticity and survival (Josselyn *et al.*, 2005). In the CNS, A2B receptors are found widespread in the brain, whereas, the A2A-R are localised in the striatum and other nuclei of the basal ganglia and olfactory bulb. They are found primarily in dopaminergic regions of the brain generally colocalised with D2-Rs (Rosin *et al.*, 2003; Cieślak, *et al.*, 2008). A2A-Rs are characterised by their high affinity for adenosine (EC_{50}= 0.7μM) (Fredholm *et al.*, 2001; Cieślak, *et al.*, 2008). Due to their localisation in the basal ganglia, A2A-Rs are a target for therapeutic intervention for a number of diseases including PD (Ferré *et al.*, 1994; Richardson, *et al.*, 1997); which may be related to their anatomical and

biochemical interaction with D2-Rs. The incidence of PD has been seen to decrease with increasing levels of caffeine intake (Gerlach *et al*., 1996; Ross *et al.*, 2000). Caffeine is a potent A2A antagonist ($K_i \approx 1$ μM). Blocking A2A-Rs may protect dopaminergic neurons against excitotoxicity and ischemic neuronal injury (Ongini *et al*. 1997; Chen *et al.* 2001). This was suggested in a study carried out by Chen et al. (2001), that elucidated the therapeutic effects of caffeine on the pathophysiological responses of DAergic neurons in PD mouse models. They determined that caffeine dose-dependently decreased the "MPTP-induced depletion of functional and anatomical markers of the nigrostriatal neurons targeted in PD."

1.4.2 D2-R and A2A-R heteromerization in the brain

Biophysical studies, such as FRET and mass spectrometry have helped elucidate the heteromerization potential of D2-R and A2A-Rs (figure 1.7) (Canals *et al.*, 2003; Fuxe *et al.*, 2010; Bonaventura *et al.*, 2015). D2-Rs can be found on striatopallidal indirect pathway medium spiny neurons (MSNs), coupled to $G\alpha_i$ proteins, whose activation results in reduced cAMP in the cell, whilst enhancing phospholipase C (PLC) activity and causing the release of calcium from internal stores (Missale *et al.*, 1998; Bonci *et al.*, 2005; Higley et al., 2010). A2A-Rs are also expressed on MSNs however, coupled to $G\alpha_s$-proteins, which results in raised cAMP levels. This could potentially counteract the effects of D2-R activation (Strömberg *et al.*, 2000; Schiffmann *et al.*, 2007). A2A-Rs play an important role in the regulation of DAergic transmission in the basal ganglia (Simola *et al.*, 2006), such that A2A-Rs are colocalised with D2-Rs post-synaptically in GABAergic striatopallidal enkephalinergic MSNs. It has been suggested that chronic striatal DA denervation results in increased interaction between A2A-Rs and D2-Rs (Ferré *et al.*, 1992; Strömberg *et al.*, 2000). Furthermore A2A-R stimulation, was shown to counteract the inhibitory modulatory role of D2-R stimulation, which is responsible for modulating calcium influx and neuronal firing (Azdad *et al.*, 2009; Higley and Sabatini, 2010). This dynamic is responsible for the locomotor depression and activation observed after the introduction of A2A-R agonists and antagonists, respectively (Armentero *et al.*, 2011). Therefore, considering both receptors simultaneously

provides a therapeutic approach in the treatment of diseases such as PD, based on the co-administration of D2-R agonists and A2A-Rs antagonists (Svenningsson *et al.*, 1999; Azdad *et al.*, 2009).

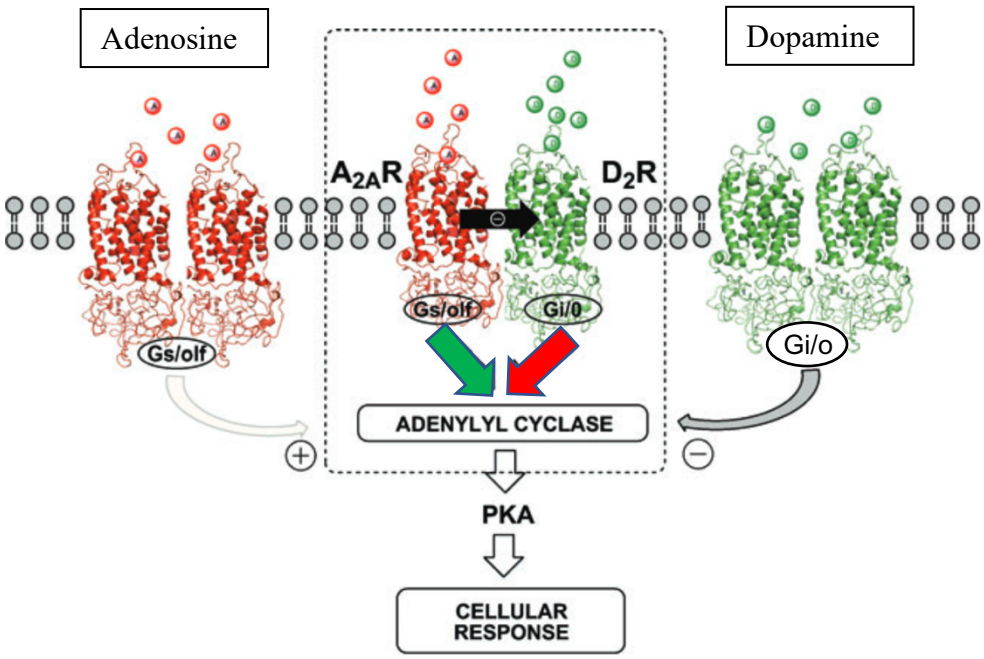

Figure 1.7 Receptor dimers: A schematic representation of both A2A-R and D2-R homodimers and the heterodimer in the centre. *Canonical pathway associated with A2A-R activation, is an increased activity of adenyl cyclase and PKA, and the contrary for D2-R activation of Gi/o (Fuxe et al., 2010).*

1.4.3 D2-R and A2A-R induced heterologous desensitization

Stimulating or blocking A2A-Rs can induce functional effects independent of D2-Rs as well as decrease the binding affinity of D2-R agonists. Strömberg *et al.*, (2000) showed that low, ineffective doses of A2A-R antagonists potentiated the electrophysiological effects of D2-R agonists in the striatum. In contrast, the application of an A2A-R agonist, attenuated the effects of the D2-R agonist binding thus affecting the overall striatal neuronal activity. A further study showed that at concentrations used for A2A-R agonist, CGS-21680 and antagonist, MSX-3, an electrophysiological response was not produced when present alone. However, they counteracted and potentiated, respectively, the effects of D2-R stimulation in the DA-denervated striatum. These results highlight the importance of D2-R & A2A-R antagonistic interactions and how A2A-Rs play a vital role in modulating D2-R responses in the striatum.

Furthermore, in a study by Lai *et al.*, (2018a), it was shown that binding of a D2-R agonist, quinpirole, reduced the therapeutic effects caused by A2A-R activation on amyotrophic lateral sclerosis (ALS). A2A-R activation may act by preventing ROS-induced TAR DNA Binding Protein-43 (TDP-43) mis-localisation and delays motor impairment. TDP-43 is an essential nuclear protein in the cells whereby any irregularities in cellular distribution, cleavage and inclusion formation in motor neurons of the spinal cord drives ALS pathophysiology (Neumann *et al.*, 2006; Chen-Plotkin, *et al*., 2010). D2-Rs have potential implications in ALS in the lumbar spinal cord as they are the most highly expressed receptors in the region (Zhu *et al.*, 2007; Lai *et al.*, 2018a). Therefore, elucidating D2-R role in the A2A-R modulation, is valuable in understanding any therapeutic intervention.

Another study by Bonaventura *et al.*, (2015) showed that both A2A-R agonists and antagonists have the ability to co-counteract the effects of D2-R agonist-induced modulation. The A2A-R agonist and antagonist produced a conformational change in the A2A-R/D2-R heteromers that reduced the binding affinity for the D2-R agonist. They tested their findings by introducing increasing concentrations of A2A-R antagonist, caffeine or SCH58261 in the presence of an A2A-R agonist (CGS21680) to test its ability to decrease the D2-R agonist binding affinity. It was noted that at lower concentrations, the A2A-R antagonist counteracted the effects of CGS21680, whereas a higher concentration, led to a decrease in the D2-R agonist binding (figure 1.8). These results strongly suggest that both A2A-R agonists and antagonists that bind competitively to orthosteric sites, produce the same allosteric modulation on D2-R agonist binding when applied alone. However, when co-administered, they cancel each other's effects. In addition, this data suggests the presence of two binding sites on the A2A-R homodimer which was later confirmed in the study using sheep striatal preparations.

Treatment	[^{3}H]Quinpirole-binding K_{DA1}, nM	[^{3}H]Raclopride-binding K_{DA1}, nM
Control	5 ± 2	1.8 ± 0.7
CGS 21680 (3 μM)	10 ± 2*	4.2 ± 0.7*
Caffeine (3 mM)	14 ± 3*	3.7 ± 0.7*

K_{DA1} is the equilibrium dissociation constant. Values are mean ± SEM from three to five different experiments. Statistical significance was calculated using the Student *t* test. *$P < 0.05$ compared with controls.

Figure 1.8 The effect of A2A-R ligands on [^{3}H]quinpirole and [^{3}H]raclopride affinity for D2Rs. *It is evident, although a small effect, that there is an allosteric interaction between A2A and D2 receptors. Data drawn from membrane preparations from sheep striatum (Bonaventura et al., 2015).*

1.4.4 PKA effects on NMDA-Receptor activity

PKA is essential to NMDA-R modulation as it phosphorylates multiple sites on GluN1 and GluN2 subunits (Leonard and Hell, 1997; Tingley *et al.*, 1997; Aman *et al.*, 2014) (Figure 1.10). PKA can potentially alter the synaptic NMDA-R calcium signal without affecting the EPSC (Rycroft and Gibb, 2002; Iacobucci and Popescu, 2018). On the other hand, there is evidence to suggest that PKA activity can increase the NMDA-R current amplitude (Skeberdis *et al.*, 2006) and prevent calcineurin induced decrease in EPSC amplitude (Raman, *et al*., 1996; Aman *et al.*, 2014). Furthermore, PKA was shown in one study to have differential effects on NMDA-Rs that are subunit specific. For instance, in GluN2A containing receptors, PKA inhibitor- H89, reduces calcium flux without affecting macroscopic NMDA-R currents. Whereas, in GluN2B containing NMDA-Rs, H89 decreases the NMDA-induced calcium flux and macroscopic current amplitude (Skeberdis *et al.*, 2006). The mechanisms for these effects have not been clarified.

A study by Aman *et al.*, (2014) using cultured HEK293 cells, looked into the extent to which PKA can modulate different aspects of NMDA-R induced currents. They recorded both single channel and macroscopic NMDA-R

currents to better understand ion flux modulation and receptor desensitization. They discovered that PKA could modulate gating via GluN2B subunit phosphorylation at Ser1166 and calcium permeability through GluN1 subunit phosphorylation at Ser897 of NMDA-Rs. β-adrenoceptor and dopamine D1/D5 receptor activation were both shown to induce Ser1166 phosphorylation and potentiation of NMDA currents (Murphy *et al.*, 2014). To further study the effects of PKA on NMDA-Rs, Aman et al., (2014), used PKI, a naturally occurring PKA inhibitor which exhibits high specificity. Along with (Skeberdis *et al.*, 2006), they showed a lack of effect on single channel gating and macroscopic current kinetics but PKI decreased calcium influx. On the contrary, Townsend, Liu and Constantine-Paton, (2004) found that PKA phosphorylation of NMDA-Rs lengthens the NMDA-R induced EPSCs suggesting that in neurons or at synapses other factors also influence kinetics such as CaM-receptor interactions (Rycroft and Gibb, 2002; Iacobucci and Popescu, 2018).

In addition to modulation of receptor gating and ion flux, PKA was also observed to modulate NMDA-R desensitization. PKA phosphorylation causes NMDA-R desensitization in hippocampal neurons by increasing the amplitude and Ca^{2+}-dependent desensitization induced current. When PKA is inhibited, phosphatases are recruited and rapidly dephosphorylate NMDA-Rs (Skeberdis *et al.*, 2006). To further investigate PKA involvement and in turn cAMP-dependent modulation of NMDA-Rs, adenyl cyclase (AC) was targeted. An AC inhibitor, SQ22536 (100μM), produced a steady-state decrease in NMDA-R current as well as decreased receptor desensitization (Skeberdis *et al.*, 2006). These results all suggest that enhanced PKA signalling increases NMDA currents while reduced PKA signalling will result in a decrease in the NMDA current.

1.5 Non-receptor tyrosine kinase modulation of GluN2B containing NMDA Receptors

Src family of protein tyrosine kinases (PTK) are comprised of 5 members that are found ubiquitously in the CNS: Src, Fyn, Yes, LCK and Lyn. They all appear to have a similar generic structure, with homologous regions such as Src

Homology 1 (SH), SH2 and SH3. The kinase is comprised of two prominent domains- SH1- the catalytic domain, contains the activation loop and is responsible for kinase activity. Within its structure, is a tyrosine residue (Y416) that regulates all kinase activity (Sadowski, *et al*., 1986; Salter and Kalia, 2004). The SH2 domain binds to peptide motifs that contain phosphorylated tyrosine (Moran *et al.*, 1990; Salter and Kalia, 2004). Lastly, despite only containing 60 amino acids, the SH3 domain is responsible for initiating protein-protein interactions (Ren *et al.*, 1993; Salter and Kalia, 2004). The final domain with the least homology is SH4. This domain is essential in anchoring the protein to the cell membrane. It contains a short sequence of amino acids at the N-terminus that contain signals for post translational lipid modifications (Resh, 1993; Liang *et al.*, 2004).

Src Family kinases (SFKs) are vital in the CNS as they are involved in modulating ion channel activity such as NMDA-R, K^+ and Ca^{2+} channels, and $GABA_A$ receptors (Wang and Salter, 1994a). Electrophysiological studies observed the relevance of SFKs in regulating the NMDA-R steady-state currents by introducing a fine balance between kinase and phosphatase activity, leading to the phosphorylation and dephosphorylation of the receptor, respectively. This was observed when introducing PTK inhibitors or introducing exogenous protein tyrosine phosphatase (PTP), caused a suppression in NMDA-R current (Yu Tian Wang, *et al*., 1996). In contrast, introducing Src kinases, enhanced the NMDA-R current (Wang and Salter, 1994a). Studies on excised membrane patches, suggest that PTK and PTP activity are closely connected to NMDA-Rs, thus regulating their function closely (Y T Wang, Yu and Salter, 1996). Furthermore, GluN2 subunit of NMDA-Rs are phosphorylated on tyrosine residues located within the C-terminal domain such as Y1472 or Y1070 (Trepanier *et al.*, 2011; Kalia and Salter, 2003; Poetschke *et al.*, 2015).

Wang and Salter, (1994) provided substantial evidence to suggest the close interaction and modulation between PTKs and NMDA-Rs. Whole cell perforated patch recordings were performed on spinal cord dorsal horn neurons. They used a highly recognised PTK, $pp60^{c\text{-}src}$ to test whether it would potentiate NMDA-Rs. The drug was applied directly to the cells via the intracellular pipette solution

and an increase in steady-state NMDA-R current was observed 10mins after the start of the recording. This indicates that PTK activity causes a potentiation of NMDA-R current. Aside from the dorsal horn, the drug was applied to hippocampal neurons to determine whether the effect was ubiquitous around the CNS. To confirm the effect was NMDA-R specific, 500μM Mg^{2+} was applied extracellularly. This caused a voltage-dependent blockade of current. Furthermore, a bath application of genistein (a PTK inhibitor) caused a progressive concentration dependent reduction in NMDA-R current. Once the drug was washed off, the current returned to baseline. A second inhibitor, Lavendustin A was used, and a similar effect was observed. An important consequence of stimulating NMDA-R currents is a rise in $[Ca^{2+}]_i$. Therefore, Wang and Salter, (1994) tested the effects of inhibiting PTKs on NMDA-R mediated calcium responses in neurons. Calcium was measured using Fura-2 whilst simultaneously recording whole cell currents. 100μM Genistein caused a reversible reduction in $[Ca^{2+}]_i$ signal, however, did not change the baseline. Lastly, a phosphatase inhibitor, orthovanadate (100 μM) was introduced to the cultured dorsal horn neurons. This potentiated the NMDA-R current 1.5 to 2-fold (Wang and Salter, 1994a).

1.5.1 Src and Fyn signalling and modulation of NMDA-Rs

Src and Fyn kinases are the first established regulators of NMDA-Rs and NMDA-R-dependent synaptic plasticity in the hippocampus (Yu *et al.*, 1997; Lu *et al.*, 1998; Huang *et al.*, 2001; David M Thal *et al.*, 2011; Scanlon *et al.*, 2017). Src became an integral protein from which all components of NMDA-R modulation stemmed from involving other intracellular cascades. Src kinase is composed of the highly homologous domains, SH1, SH2 and SH3, and the least homologous, SH4 (Xu, *et al.*, 1997). Anchoring of the Src kinase to the membrane is important for kinase phosphorylation of the GluN2 subunit of the NMDA-R, a mechanism carried out by the NADH dehydrogenase subunit 2 (ND2) (Figure 1.9). ND2 is a mitochondrial encoded core subunit of complex 1 (Efremov and Sazanov, 2011). Scanlon *et al.*, (2017) showed that ND2 anchors Src to NMDA-Rs in the hippocampus via post synaptic densities and the stability of this interaction is crucial as any disruption can de-anchor Src from the

receptor, thus leaving ND2 solely attached to the NMDA-R. This dissociation has implications in reducing pain hypersensitivity as Src is prevented from upregulating NMDA-R activity (Liu *et al.*, 2008).

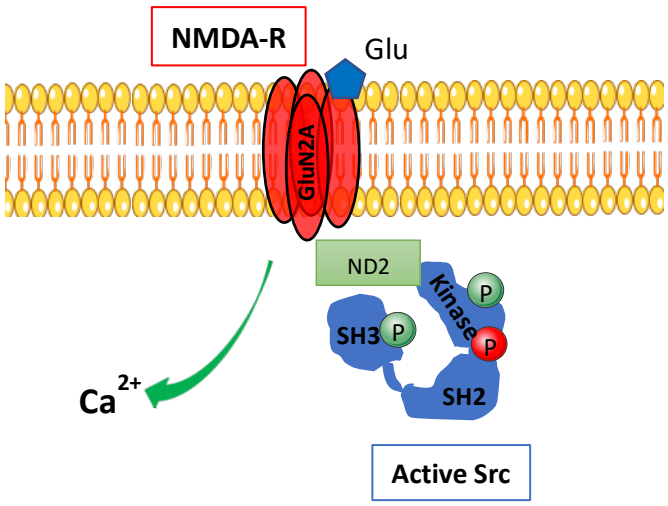

Figure 1.9 Representation of Src/Fyn activation and phosphorylation of NMDA-Rs*. Src binds to the GluN2A subunit of NMDA-Rs via NADH dehydrogenase subunit 2 (ND2) which allows for receptor phosphorylation. This triggers NMDA-R activation and* Ca^{2+} *influx.* (Green P: activating phosphorylation sites; Red P: de-activating phosphorylation sites.

As mentioned in section 1.5, receptor phosphorylation is dynamically balanced between kinase and phosphatase activity via neuronal cues that are essential in driving "activity-dependent synaptic plasticity without themselves changing synaptic efficacy" (Lu *et al.*, 1998; Salter and Kalia, 2004; Xu *et al.*, 2008). In CA1 synapses of hippocampal neurons, both Fyn and Src activity are required to drive LTP induction (Lu *et al.*, 1998; Huang *et al.*, 2001; Yang *et al.*, 2012a). Yang *et al.*, (2012) observed GluN2A containing NMDA-Rs responding to Src regulation of the receptor mediated currents on isolated hippocampal CA1 neurons. This regulation was inhibited when Src interfering peptide Src (40-58) was co-applied. Src-induced potentiation of NMDA-R current was sensitive to the GluN2A subunit specific inhibitor, NVP-AAM077 and not affected by the GluN2B inhibitor (Ro25-6981) (Neyton and Paoletti, 2006). Furthermore, GluN2B containing NMDA-Rs alone, were involved in Fyn regulated receptor mediated currents. Upon addition of a recombinant Fyn-kinase, they observed an increase in NMDA-R current which was inhibited by Ro 25-6981 (500 nM), a GluN2B selective inhibitor and not by a GluN2A selective inhibitor. By introducing a Fyn-interfering peptide, they observed a similar effect as with the Src-peptide, decreasing the enhanced current. To test GPCR involvement in NMDA-R modulation, they used rat hippocampal slices and observed a selective receptor phosphorylation pertaining to GluN2A and B subunits induced by Src and Fyn kinases,

respectively (Macdonald *et al.*, 2005). Previously identified pituitary adenyl cyclase activating peptide 38 (PACAP38) induced an increase in NMDA-R current which was driven by Src-kinase activity and not Fyn. In addition, there was an increase in tyrosine phosphorylation of GluN2A subunits relative to GluN2B. This enhancement in GluN2A-subunit phosphorylation was prevented by Tat-Src(40-58), further proving Src kinase involvement in the receptor phosphorylation and subsequent increase in current (MacDonald *et al.*, 2005).

Fyn kinase has been shown to phosphorylate both GluN2A and GluN2B subunits, however, the evidence shows selectivity towards GluN2B phosphorylation (Nakazawa *et al.*, 2001). Receptor phosphorylation occurs in the post-synaptic densities of rat forebrains (Cheung and Gurd, 2001). Tryptic mapping showed seven phosphorylation sites on the GluN2B subunit, three of which are identified as Fyn selective and prominent phosphorylation sites- Tyr1252, Tyr1336, and Tyr1472 (Nakazawa, *et al*., 2002) (Figure 1.10, Table 2). It has been established that the mechanism of modulation of NMDA-Rs by Fyn is governed around stabilizing the receptor in the surface membrane by preventing the interaction of the clatherin adaptor protein, AP2, with the YEKL motif on GluN2B, ultimately preventing receptor endocytosis (Trepanier *et al.*, 2012; Bonifacino and Traub, 2003). Fyn-induced phosphorylation of NMDA-Rs is also controlled by the receptor for activated kinase-1 (RACK-1), an inhibitory scaffolding protein. RACK1 binds to both Fyn and GluN2B, keeping them in close proximity, however, preventing receptor phosphorylation (Yaka *et al.*, 2002). When RACK-1 is released, after PKA activation, Fyn can proceed to phosphorylate GluN2B (Yaka *et al.*, 2003). This modulatory component keeps GluN2B phosphorylation to a minimum (Yaka *et al.*, 2002, 2003).

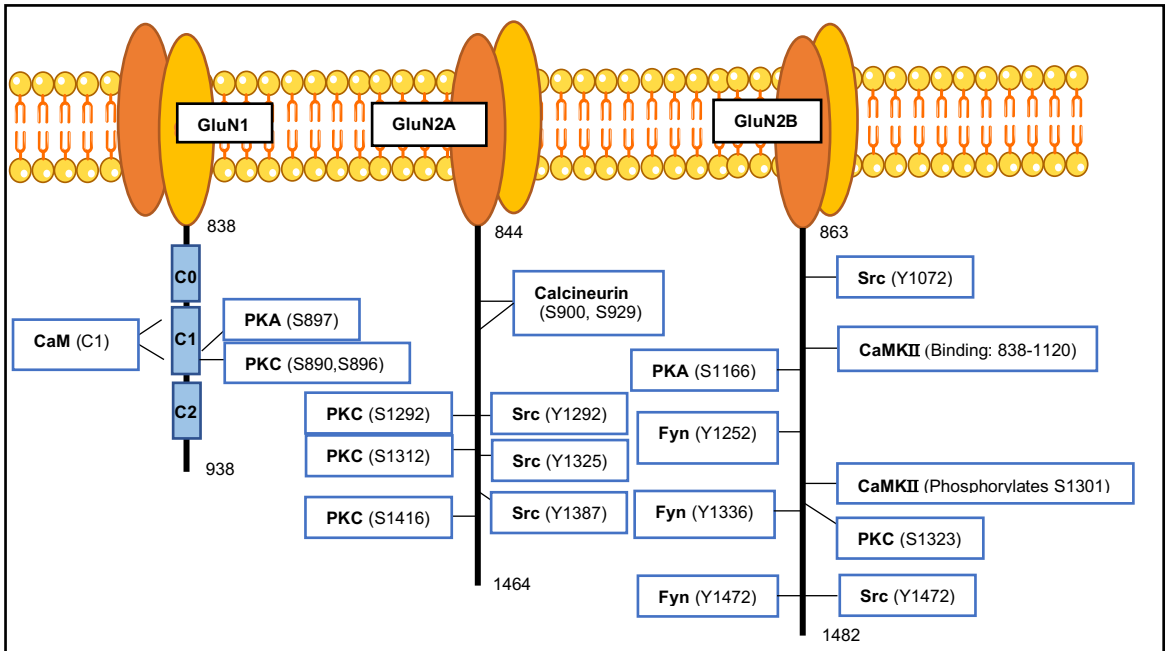

Figure 1.10 A diagram illustrating putative phosphorylation sites on NMDA-R subunits*. CaM (Calmodulin), CaMKII (Calmodulin-dependent protein kinase II). The GluN2B subunit has the longest C-terminal and include potential sites of Fyn and Src tyrosine phosphorylation.*

Table 2 A summary table of the putative phosphorylation sites of endogenous NMDA-R regulators.

Endogenous regulator	NMDA Binding site	Induced effect	References
PKA	GluN1: Ser897	Regulates Ca^{2+} permeability	(Murphy *et al.*, 2014)
	GluN2B: Ser1166	Modulates receptor gating	
PKC	GluN1: Ser890, Ser896	Promotes NMDA-R translocation to the cell membrane, increasing channel opening time and decreases voltage-gated Mg^{2+} block.	(Chen and Mae Huang, 1992; Lan *et al.*, 2001; Chen and Roche, 2007; Sanz-Clemente, et al, 2013)
	GuN2A: Ser1291, Ser1312, Ser1416		
	GluN2B: S1323		
CaMKII	GluN2B: 838-1120	Maintaining synaptic strength and inducing LTP.	(Coultrap and Bayer, 2012; Lisman, et al., 2012; Bayer and Schulman, 2019)
	Phosphorylates Ser1301		
Calcineurin (PP2B)	GluN2A: Ser900, Ser929	A protein phosphatase activated by Calmodulin and is required for LTD induction by triggering receptor desensitization.	(Krupp *et al.*, 2002; Rycroft and Gibb, 2004)
Calmodulin (CaM)	GluN1: C1 Cassette (875-898)	Induced NMDA-R inactivation by reducing receptor open rate and mean time.	(Ehlers *et al.*, 1996; Ataman *et al.*, 2007)
Src kinase	GluN2A: Tyr1292, 1325, 1387	Upregulates the activity of NMDA-Rs to induce LTP.	(Nakazawa *et al.*, 2001; Kalia and Salter, 2003; Yang *et al.*, 2012b; Poetschke *et al.*, 2015)
	GluN2B: Tyr1472,1072		
Fyn kinase	GluN2B: Tyr1252, 1336, 1 472	Responsible for the phosphorylation and trafficking of NMDA-Rs	(Ogawa *et al.*, 2002)
ND2	GluN1-M4 (transmembrane helix)	Essential for Src induced upregulation of NMDA-Rs	(Scanlon *et al.*, 2017)
RACK1	GluN2B	An inhibitory scaffolding protein that keeps Fyn kinase and GluN2B subunit of NMDA in close proximity whilst preventing receptor phosphorylation.	(Yaka *et al.*, 2002)

1.5.1.1 Csk inhibition of Src-kinase activity on NMDA-Rs

As mentioned in previous sections, Src family kinases (SFKs) are essential in regulating cell growth, proliferation and differentiation (Neet and Hunter, 1996; Bolen and Brugge, 1997; Yaqub *et al.*, 2003). Activating SFKs requires the phosphorylation and dephosphorylation of two tyrosine residues, Tyr^{416} and Tyr^{527}, that act on the activation loop of the catalytic subunit and the C-terminus, respectively (Okada, 2012; Roskoski, 2015). The C-terminus is regulated by the C-terminus Src-Kinase (Csk) which causes a down regulation of the SFK activity (Nada *et al.*, 1991; Bergman *et al.*, 1992). Any disruptions in the gene have shown to produce a deficit in the neural tube of the developing embryo. This leads to the overactivation of SFKs that ultimately lead to embryonic lethality (Imamoto and Soriano, 1993; Nada *et al.*, 1993; Yaqub *et al.*, 2003). Csk in mainly localised in the cytosol, however, they are lipid penetrable due to the interaction with the transmembrane adaptor molecule, Csk-binding protein. Csk-binding proteins are found exclusively in lipid rafts were the SFKs reside (Brdicka *et al.*, 2000).

Crystal structures have elucidated the structural similarities and differences between Csks and SFKs. The kinase domain is preserved in both kinases however, the distance between the SH2 and SH3 domains and the kinase domain differ between SFKs and Csks (Sicheri, *et al*., 1997; Xu, Harrison and Eck, 1997; Ogawa *et al.*, 2002; Yaqub *et al.*, 2003). There are mechanisms proposed for the regulation of phosphotransferase activity. The $G\beta\gamma$ subunit, via binding to the catalytic subunit of the Csk, upregulates its activity 2-fold (Lowry *et al.*, 2002). Csk can also be activated by covalent modifications (Vang *et al.*, 2001), whereby PKA phosphorylates Csk on the Ser^{364} residue, causing the 2 to 4-fold increase in Csk activity. Furthermore, the interaction between Csk and NMDA-Rs controls the Src-dependent regulation of NMDA-R activity. Xu *et al.*, (2008) showed that Csk associates with the NMDA-R signalling complex in the adult brain. This leads to the inhibition of Src-dependent potentiation of NMDA-RS in CA1 neurons, causing an alteration in Src-dependent LTP. Socodato *et al.*, (2017) showed that upon D1-R activation at glutamatergic synapses in retinal neurons, the subsequent activation of cAMP accumulation and the

increase in PKA activity, promotes Csk activity leading to the inhibition of Src activation. This then decreases its phosphorylation potential on GluN2B subunit containing NMDA-Rs causing a depression in the NMDA-R response. Research carried out by Xu *et al.*, (2008) elucidated the effect of introducing a recombinant Csk in acutely isolated CA1 neurons from young rats. They observed a decreased in NMDA-R current. This decrease was dependent on SFK activity as it was entirely abolished when a pharmacological approach using SFK inhibitors, PP2 and SU6656 was used. In addition, it was dependent solely on Src-kinase inhibition, as a Src-selective inhibitory peptide Src (40-58) blocked Src kinase activity. Lastly, they showed that Csk inhibited Src and Fyn kinase activity on GluN2A and GluN2B subunits, respectively.

1.5.2 A pharmacological approach to targeting Src and Fyn kinases

There are several approaches to targeting SFKs to study their involvement in NMDA-R modulation. Among them are PP1 & PP2, Lavendustin, Src inhibitor-1 (Src-I1), and interfering peptides Tat-Src (45-58) among other inhibitors. Pyrazolopyrimidine PP1 and PP2 have been widely used to test the proposed physiological roles of the Src family protein kinase. However, they are not specific inhibitors as they cannot discriminate between different members of the PK family (Hanke *et al.*, 1996; Liu *et al.*, 1999; Bain *et al.*, 2007). In assays by Bain *et al.*, (2007), PP1 and PP2 both inhibited Src and Lck kinases with IC_{50} values of 50nM. Src1-I was seemingly a potent inhibitor of Src, but it was not capable of inhibiting other members of the Src family.

Tong and Gibb (2008), used striatal medium spiny neurons of 7-day old rats to study the effect of D1-R activation on NMDA-Rs. They observed that D1-R stimulation, caused a decrease in NMDA-R steady state current, however this effect changes with age (Tong & Gibb, 2008). It was established that the effect was not G-protein dependent but instead was abolished when a Src inhibitor, PP2 was introduced. The D1-R agonist SFK-82958 caused a statistically significant decrease in NMDA-R current from 249 ± 36pA to 153 ± 31pA. Henceforth, to establish the mode of modulation, they initially introduced Lavendustin A, a non-selective inhibitor of non-receptor tyrosine kinase (Onoda

et al., 1989; Lu *et al.*, 1999; Tong and Gibb, 2008). When the drug was introduced intracellularly, it reduced the D1-R induced decrease in NMDA-R steady state current. Its analogue, Lavendustin B, did not. A Src-selective drug was then introduced, PP2 (10μM), in the presence of SFK-82958, a D1-R antagonist. They observed no statistically significant difference in the NMDA-R current in the control relative to the NMDA-R response in the presence of SK-82958 and spiperone, a D2-R antagonist. This suggests that tyrosine kinase is essential for D1-R induced inhibition of NMDA-R response.

Another study by Trepanier *et al.*, (2013) sought to investigate the effects mGluR2/3 activation had on NMDA-R evoked currents in CA1 neurons of the hippocampus. They hypothesised that the activation of group 2 mGluRs has varied activation tendencies of Gαq which in turn activates PKC and/or Src kinase. This then leads to the increase in NMDA-R current (Lu *et al.*, 1999; Macdonald *et al.*, 2005; Yang *et al.*, 2012a). To test their hypothesis, they used Src (40-58) peptide. This essentially mimics the unique domain of Src and prevents binding to NMDA-Rs. It does not however, inhibit the enzymatic activity of Src, but interferes with the binding of Src to the scaffolding protein NADH dehydrogenase subunit 2. This in turn prevents the localisation of Src to the vicinity of the receptor, preventing NMDA-R phosphorylation (Gingrich *et al.*, 2004a). Src (40-58) was then introduced to the pipette prior to the electrophysiological recording, and it prevented the enhancement of the NMDA-R current by the mGluR2/3 antagonist, LY379268 (10 nM). In addition, they looked at the potential involvement of Fyn kinase on the resulting NMDA-R current. Using a similar approach to Gingrich *et al.* (2004), they produced a Fyn (39-57) peptide and introduced it in the same manner. They previously showed that Fyn (39-57) alone blocks NMDA-R currents induced by recombinant Fyn kinase but not Src kinase (Yang *et al.*, 2012a). In this instance, the Fyn-interfering peptide failed to prevent the potentiation of NMDA-R current by LY379268. This suggests that LY379268 enhances Src activity and not Fyn in its regulation of NMDA-Rs.

The several successful studies done using Src kinase inhibitors encouraged me to implement some of these inhibitors in my research. As will be seen later in this thesis, PP2, Src-Inhibitor 1 and Src (40-58) & Fyn (39-57) were used to study modulation on NMDA-Rs via D2-R activation.

1.6 Understanding the effects of ERK signalling

Extracellular regulated protein kinase (ERK kinase) is a member of the MAPK pathway and is essential in regulating neuronal survival and cellular differentiation (Neve, *et al*., 2004). ERK 1 and 2 are 85% identical by sequence and their expression levels differ in all tissues where they are activated following a cascade of phosphorylation events (Geyer and Wittinghofer, 1997). As mentioned earlier, D2-R activation is known to decrease cAMP accumulation. In addition, it leads to the phosphorylation of ERK 1/2, PLC and subsequent receptor internalisation (Neve, *et al.*, 2004; Skinbjerg *et al.*, 2009; Beaulieu *et al.*, 2011). D2-R modulation of intracellular pathways can be altered by the heterodimerization of D2-Rs and A2A-Rs. In neuroblastoma cell lines, long-term exposure to D2 & A2A-R agonists can cause co-desensitization and receptor internalisation (Hillion *et al.*, 2002). To investigate whether D2-A2A-R heteromers can modulate ERK phosphorylation, Huang *et al.*, (2013) introduced an A2A-R antagonist, ZM241385. They observed an attenuation in D2-R-induced ERK phosphorylation, in a dose-dependent manner. This indicated the possible involvement of the heteromers in ERK phosphorylation. Furthermore, it was established that D2-R-induced activation of ERK involves Src kinase in a G-protein independent manner (Neve, *et al*., 2004; Kim *et al.*, 2004; Huang *et al.*, 2013). However, ERK activation may differ under various conditions. Therefore, to isolate the possibility of Src kinase activation of ERK following D2-R and A2A-R heteromers activation, a Src kinase inhibitor, PP2 was applied. This inhibited the quinpirole (D2-R agonist)-induced ERK phosphorylation, further supporting the involvement of Src kinase in modulating ERK phosphorylation.

Several phosphorylation events drive the activation of ERK1/2, these include GPCR and receptor tyrosine kinase activation which primarily leads to Ras (a

GTP-binding protein) activation. Ras then binds to and activates Raf (Geyer and Wittinghofer, 1997; Roux and Blenis, 2004). Raf in turn, binds to and activates MEK1 and 2, which ultimately leads to the phosphorylation of ERK1/2 (Chong, *et al.*, 2003). Hallberg, *et al.*, (1994) showed that only 5% of Ras molecules have the potential to fully activate ERK1/2 leading to their accumulation in the nucleus (Chen, *et al.*, 1992).

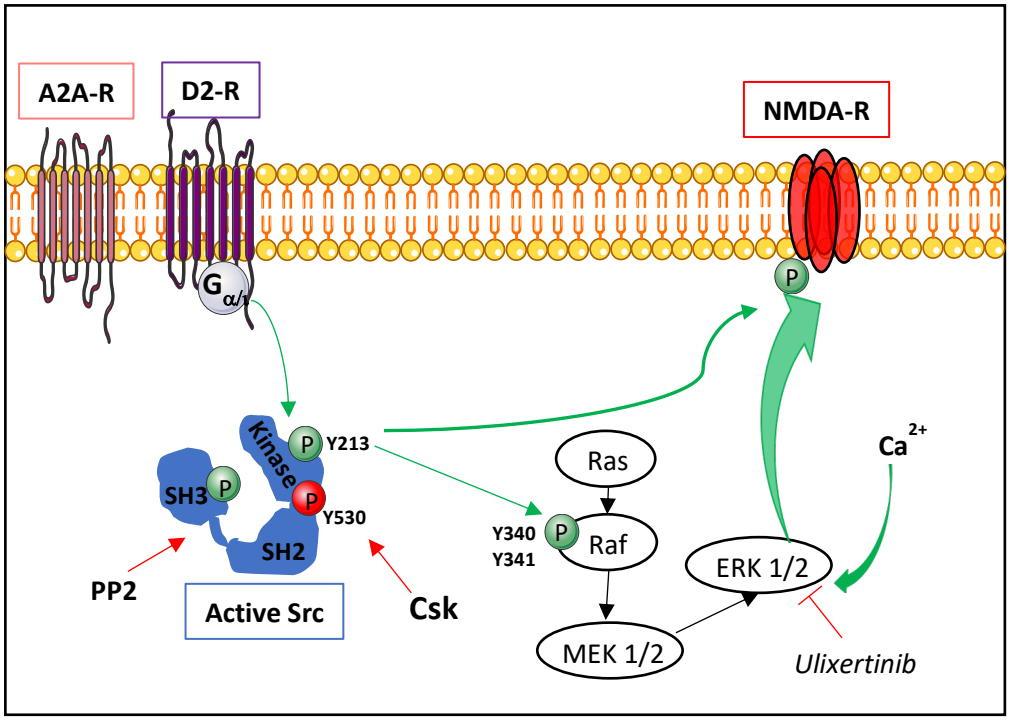

Figure 1.11 MAPK activation via Src kinase and subsequent activation of NMDA-R. *Activation of A2A-R inhibits D2-R activation of Src (G-protein dependent). Src in turn, activates ERK1/2. The kinase can activate transcription factors or trigger receptor phosphorylation, as in NMDA-Rs (Csk: C-terminal Src Kinase).*

The ERK pathway is also activated upon NMDA-R induced calcium entry into the cell, a process responsible for activating multiple signalling cascades alongside ERK (Sweatt, 2008). Downstream of ERK activation are multiple transcription factors that drive synaptic plasticity and AMPA receptor trafficking (Zhu *et al.*, 2002). Extracellular signals such as calcium entry are essential to drive ERK kinase activation and as stated above, this is known to involve GTP binding protein- Ras (Lida *et al.*, 2001). As ERK signalling is sensitive to internal calcium elevation, it is speculated to be spatially confined to the vicinity of NMDA-Rs (Hardingham, *et al.*, 2001). Payne *et al.*, (1991) studied ERK activity

using immunostaining with an antibody targeted at active, phosphorylated ERK kinase. A dominant negative form of RasGRF1 significantly attenuated NMDA-R induced ERK signalling, suggesting its critical involvement in signal transduction between NMDA-Rs and ERK activation (Krapivinsky *et al.*, 2003). RasGRF1 and SynGAP, are responsible for linking NMDA activation and subsequent Ca^{2+} entry with RAS and other signalling molecules such as ERK (Chen *et al.*, 1998). RasGRF1 is expressed in the CNS, enriched specifically at synapses (Sturani *et al.*, 1997). Furthermore, Krapivinsky *et al.*, (2003) determined the relevance of the GluN2B subunit of the NMDA-R in ERK activation. They demonstrated that RasGRF1 binds specifically to the GluN2B subunit which leads to ERK activation. Numerous studies have expressed the importance of GluN2B in neuronal plasticity; thus, understanding how ERK is modulated in the substantia nigra dopaminergic neurons may be important in determining its potential involvement in DAergic neuron development, survival and/or excitotoxicity.

As ERK1/2 signalling plays an important role in cellular proliferation and cell survival, ERK1/2 inhibitors have been investigated in clinical trials as anti-cancer treatment (Kidger, *et al.,* 2018). An example, is BVD-523 (also referred to as Ulixertinib), a reversible inhibitor of ERK1/2 (Ward *et al.*, 2015). In vitro studies showed that BVD treatment resulted in reduced proliferation and enhanced caspase activity in the BVD-523 sensitive cells (Germann *et al.*, 2017).

1.7 The role of CaMKII in maintaining synaptic strength

Synaptic plasticity and strength are governed by the combined functions of Ca^{2+}/Calmodulin-dependent protein kinase II (CaMKII) and the NMDA receptor. They are both necessary to drive learning, memory and cognition (Coultrap *et al.*, 2014). LTP induction has been associated with CaMKII, however Barcomb *et al.*, (2016) hypothesized its involvement in maintaining synaptic strength (Coultrap and Bayer, 2012; Lisman, *et al*., 2012; Hell, 2014; Bayer and Schulman, 2019). CaMKII activity is triggered upon Ca^{2+} influx through the NMDA-Rs leading to CaMKII autophosphorylation at the Tyr-286 reside. This phosphorylation is sufficient to induce CaMKII binding to the GluN2B subunit of

the NMDA-R (Bayer *et al.*, 2001; Coultrap and Bayer, 2012). This calcium-independent autonomous kinase activity is crucial to provide the molecular memory necessary for LTP induction (Giese *et al.*, 1998). Lee *et al.*, (2009) showed that kinase phosphorylation is reversed within 2 minutes of LTP induction, however its inhibition once LTP is triggered does not affect the maintenance of synaptic strength (Coultrap *et al.*, 2010). A CaMKII inhibitor tat-CN21 was shown to reduce synaptic strength but only at high concentrations (20μM). However, at such high concentration, off-target effects may happen. At lower concentrations (5μM) sufficient for kinase inhibition, a decrease in synaptic strength or a complete blockage of kinase activity and LTP induction would be expected (Coultrap *et al.*, 2010). Therefore, to distinguish between correlation and causality, Barcomb *et al.*, (2016) used a combined pharmacogenetic approach to separate the specific on-target effects to the specific off-target effects. This approach used a mouse with a mutant GluN2B subunit of the NMDA-R that is incompetent in CaMKII-binding (GluN2BΔ CaMKII) and introduced tat-CN21. Therefore, any effects that are GluN2B-CaMKII-specific should be abolished. Any remaining effects would be indicative of a non-specific, off-target effect.

Electrophysiological studies on mice showed similar results to those studies done on rat hippocampal slices. The effects of tat-CN21 were examined relative to the baseline synaptic strength. In WT mice, 20μM tat-CN21 significantly reduced both basal and potentiated signal transmission and exhibited a partial recovery (Lisman, *et al.*, 2012). A 30-minute treatment with tat-CN21 produced a 10% reduction is basal transmission relative to the baseline. After a washout period, LTP could be re-induced. On the other hand, when 20μM was applied to the GluN2BΔ CaMKII KI mice, there was an initial reduction in synaptic strength, however it did not recover to the baseline after a washout period of 1 hour. This response differed to the WT mice, as in this instance, the drug and washout phases were not different; however, they were significantly lower than the baseline. The loss of tat-CN21 effect in the KI (knock-in) mice was due to the disruption between GluN2B/CaMKII interaction introduced by the mutant

GluN2B subunit. This provides evidence that this interaction is required not only for the induction of LTP but maintenance of synaptic strength.

Following on, Goodell *et al.*, (2017) hypothesized that the localisation and binding of CaMKII to GluN2B during LTP is a mechanism that specifically favours LTP and that LTD is driven through an LTD-specific suppression of this binding. They went on to show that LTD is driven by the suppression of the synaptic CaMKII accumulation by Death-associated Protein kinase-1 (DAPK1) activation. This drives the DAPK1 mediated blockade of CaMKII - GluN2B interaction. During LTD, DAPK1 activity is triggered by Calcineurin (CaN), a Ca^{2+} - activated protein phosphatase, required for NMDA-R-dependent LTD (Mulkey *et al.*, 1994; Goodell *et al.*, 2017).

1.8 Aims

There is substantial evidence to suggest NMDA-R modulation via dopamine receptors. In hippocampal neurons, D2 agonists decrease PKA activity and cause a subsequent decrease in NMDA currents along with other forms of dopamine receptor- induced NMDA modulation. Therefore, my study aimed to investigate the different mechanisms associated with the modulation NMDA-R responses in the substantia nigra DAergic neurons.

Objective 1:

- Investigate age-related effects of D2-R activation on NMDA-R modulation.
- Investigate G-protein receptor kinase 2 and 3 (GRK2/3) in D2-R induced desensitization.

Objective 2:

- Study the role of D2-R and A2A-R interaction in NMDA-R modulation in dopaminergic neurons.

Objective 3:

Targeting intracellular pathways responsible for receptor phosphorylation.

- Understand the involvement of Src and Fyn, in NMDA-R modulation
- Investigate ERK signalling in NMDA-R modulation.
- Investigate the role CaMKII in NMDA receptor modulation.

Chapter 2

Methods

2.0 Overview:

NMDA receptor currents in DAergic neurons of the SNc were measured using whole cell patch clamp recordings from brain slices of P7, P21 and P28 rats. NMDA-Rs were activated with 20μM NMDA and 10μM glycine. The drugs used to activate and inhibit D2-Rs and A2A-Rs were applied in the bath solution as they bind to the extracellular surface of the receptors.

- D2-Rs were activated using ropinirole (200 nM and 20 μM) and inhibited with sulpiride (1 μM).
- A2A-Rs were activated with CGS21680 (1 μM and 10 μM) and inhibited with SCH58621 (200 nM and 1 μM).

Intracellular kinase stimulators and inhibitors were placed in the pipette solution to allow direct entry into the cell.

- 10 μM Compound-101 was used to inhibit GRK2/3.
- 1 μM PKI was used to inhibit PKA. Forskolin (0.5 μM and 2.5 μM) was used to target cAMP.
- Src and Fyn inhibitors, 10 μM PP2 (and its inactive analogue PP3), Src-I1 (10 μM and 100 μM) and interfering peptides at 10 μM were used.
- 1 μM Ulixertinib was used to inhibit ERK1/2.
- 20 μM CN21 was used to inhibit CAMKII.

2.1 Preparing Solutions:

2.1.1 Recording (Krebs) Solution (1L):

Recording solution was used to prepare the incubation chamber that holds the brain slices and served as a control when testing the effects of drugs on the dopamine cells. It contained 125 mM NaCl (VWR Chemicals BDH Prolabo, Belgium), 26 mM NaH_2CO_3 (VWR Chemicals BDH Prolabo, Belgium), 2.5 mM KCl (Sigma-Aldrich, USA), 1.26 mM $NaH_2PO_4 \bullet 2H_2O$ (Sigma- Life science,

USA), and 25 mM glucose (Fsher Scientific, UK) dissolved in 1L distilled water. It was then bubbled with 95% O_2 and 5% CO_2 medical gas mixture (BOC Medical, Manchester, UK) for approximately 15 minutes to aerate the mixture and set the pH=7.4. 1 mM $CaCl_2$ (Panreac AppliChem, ITW Companies, Spain) was then added along with 100 nM Tetrodotoxin (Hello Bio). Magnesium was excluded from the recording solution to prevent Mg^{2+} block of NMDA-Rs.

2.1.2 Slicing Solution (500ml)

Slicing solution was comprised of 75 mM NaCl, 25 mM $NaHCO_3$, 2.5 mM KCl, 1.25 mM $NaH_2PO_4 \bullet 2H_2O$, 0.25 mM kynurenic acid (Sigma Chemical Co., USA), 2 mM pyruvic acid (Fisher Scientific, Belgium), 0.1 mM ethylenediaminetetraacetic acid (EDTA) (Aldrich, Germany), 25 mM glucose, and 100 mM sucrose (VWR Chemical BDH Prolabo, Belgium) mixed with 500 ml of distilled water. The solution was then bubbled with 95% O_2 and 5% CO_2 medical gas mixture for approximately 15 minutes. 1 mM $CaCl_2$ and 4 mM $MgCl_2$ (Fluka Analytical, Switzerland) were then added to the bubbled mixture and cooled until ready to be use.

2.1.3 Intracellular Caesium Gluconate Pipette solution (100 ml)

Composed of 140 mM CsCl (Sigma Chemical, USA), 111 mM gluconolactone (Sigma Chemical, USA), 10 mM ethylene glycol tetraacetic acid (EGTA) (Sigma Chemical, USA), 10 mM HEPES (Sigma Chemical, USA), 1 mM magnesium ATP (Sigma Chemical, USA), and 0.5 mM sodium GTP (Sigma Chemical, USA). Both ATP and GTP were added to prevent rundown of whole cell current (Wild, Jones and Gibb, 2014).

2.1.4 Intracellular Solution Drug tools:

10 μM Compound-101 (Cmpd-101) (Hello Bio, UK) was added to the pipette solution in *Experiment 2* to block the G-protein Receptor Kinase 2/3 (GRK2/3), with the aim of blocking D2-R desensitization. This was done to test whether desensitization of D2-Rs was affecting modulation of NMDA receptor response upon D2-R activation.

2.1.5 NMDA Dose Response Curve:

An NMDA dose response curve was measured using 5, 10, 20, 50, 100 and 200 μM [NMDA] applications for 2 mins each on DAergic neurons of the SNc in P28 rats. They were introduced in succession, each followed by a wash off period of 5 mins (figure 2.1). The graph established an EC_{50}=56 μM. Therefore, to trigger an NMDA response in the DAergic neurons, I used 20 μM to prevent overactivation of the NMDA receptors.

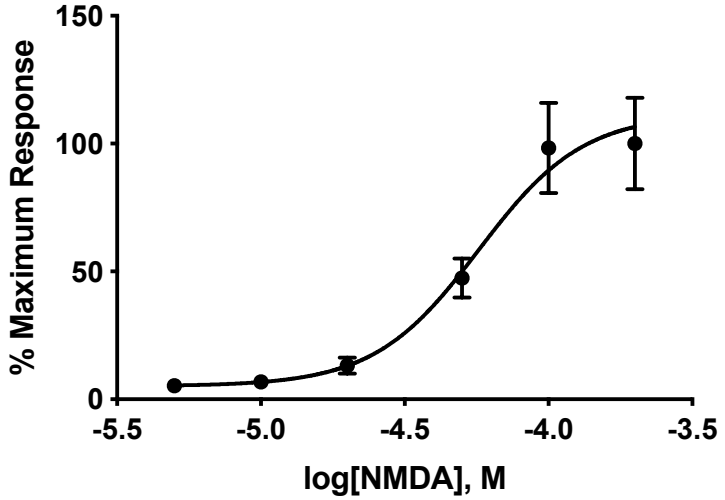

Figure 2.1 NMDA Dose-response curve. Each point represents mean ± SEM at the NMDA concentrations tested, from 5-200 μM (N = 13 cells from 3 rats). The EC_{50} was determined by fitting the data to the Hill equation. The half-maximal NMDA response was at [NMDA] = 57 μM. The maximum response was 1177 ± 211 pA.

2.2 Preparing Drugs

Drug solutions for all protocols, included a reservoir of recording solution, a second with NMDA control solution, and the rest were a duplicate of the NMDA solution with the addition of the drug of interest. As mentioned earlier, D2-R agonist and antagonist, along with the A2A-R-targeted drugs were applied to the bath solutions.

2.2.1 NMDA Control Experiment:

The solution contained 10 μM strychnine (Sigma Chemical Co., India), 10 μM picrotoxin (Sigma- Life Science, India), 10 μM glycine (TOCRIS, USA), and 20 μM NMDA (Cayman Chemical Co.).

2.2.2 Use of Compound-101

Compound-101 (Hello Bio) was introduced alongside the Cs-gluconate pipette solution. 10 μM Compound-101 was used as the ATP occupancy of the kinase can be estimated $P_{AR} = \frac{2000\ \mu M}{30\ \mu M + 2000\ \mu M} = 0.94$ as the [ATP] in the pipette solution is 2 mM. The IC_{50} for Compound-101 was estimated by Thal *et al*. to be 35 nM. The K_i for compound-101 can be estimated from $K_i = \frac{IC_{50}}{1+\frac{ATP}{K_M}} = \frac{35\ nM}{1+\frac{500\ \mu M}{30\ \mu M}} = 2\ nM$. ATP occupancy of the GRK in the presence of compound-101 and 2 mM ATP is therefore $P_{AR(B)} = \frac{2000\ \mu M}{30\ \mu M\left(1+\frac{10\ \mu M}{0.002\ \mu M}\right)+2000\ \mu M} = \frac{2000\ \mu M}{15000+2000} = \frac{2000}{17000} = 0.118$.

2.2.3 Use of Src kinase inhibitor: 100 μM Src-1Inhibitor

Test 28 was repeated at a higher concentration of Src-1I as it was calculated (using Gaddum equation of occupancy) to have 69% binding efficiency.

2.2.4 Use of ERK1/2 inhibitor: 1 μM Ulixertinib

Ulixertinib was dissolved in DMSO to produce a 10 mM stock which was then further diluted to produce 1 μM in 1ml pipette solution.

2.2.5 Fusion peptide inhibitors: P28

Fusion peptides were produced to target kinases that interact with NMDA-Rs. Peptide inhibitor sequences for Src 40-58 (Liu *et al.*, 2008) and Fyn 39-57 (Yang *et al.*, 2012a) were developed and provided by GenScript. Scrambled sequences were also developed to serve as controls for the experiments. All of the peptide inhibitors were introduced to 1 ml pipette solution separately, thus present throughout the recording. Control 20 μM NMDA recordings were

performed in the presence of the drug-infused pipette solutions. The peptide sequences used are as follows:

10 μM TAT- sSrc (scrambled):

- *Peptide sequence: DVASPHAPFPAGPAGANRA (generated by GenScript scramble library)*

10 μM TAT-Src:

- *Peptide sequence: PASADGHRGPNAAFVPPAA*

10 μM TAT-sFyn (scrambled):

- *Peptide sequence: SAGVGHIFNYTPNNAYFPS (generated by GenScript scramble library)*

10 μM TAT-Fyn:

- *Peptide sequence: YPSFGVTSIPNYNNFHAAG*

2.2.6 Use of CAMKII inhibitor peptide:

The protocol included a fusion peptide inhibitor targeting CAMKII, CN21 and its scrambled peptide. Both peptides were dissolved in DMSO. These peptides were produced by GenScript. The experiment was tested on P30 rats to determine if there was a more visible effect in older animals compared to P7. In addition, the cells were stained with neurobiotin (added to pipette solution) and fixed for histology, to determine whether location of neuron correlated to a particular response.

2.3 Preparing Brain slices:

2.3.1 P7/P21/P28 Rats:

Seven, 21 and 28-day-old Sprague-Dawley rats of both sexes were used to test for age-related effects of D2-R activation on NMDA receptor current. Animal procedures were carried out in accordance with the guidelines of the UK Animals (Scientific Procedures) Act, 1986, and European Directive 2010/63/EU and were approved by local ethical review. P21, P28 and P60 rats were anesthetized with an overdose of isoflurane prior to decapitation. The rats were decapitated by Prof Alasdair Gibb using a pair of large scissors (RS-6930, ROBOZ, Germany). Within 60 seconds of decapitation, the brain had to be

placed in a bath filled with ice-cold slicing solution. The portion of the brain cut was then lifted using a broad spatula and submerged in a bath filled with fresh ice-cold slicing solution. The slicing solution had to contain ice crystals and the cold temperature was maintained by resting the container on ice (Gibb & Edwards, 1994). This process was to occur within 60 seconds to preserve the health of the brain.

2.3.2 Producing brain slices:

Coronal midbrain slices were obtained using a vibrating blade microtome (Leica VT 1000S) (Figure 2.2) set to produce slices 300µm thick for P7 rats and 200 µm for P21 and P28 rat brains. This thickness would allow for adequate amount of oxygen to reach the cells as well as enhance microscopic visualisation of the neurons (Colbert, 2006). Once a slice had been produced, it was placed in an incubation chamber (or holding chamber) rested in a 32-34°C water bath for 45 mins to allow restoration of normal ionic balance (induced by the warm environment). The incubation chamber comprised of 50% slicing solution and 50% recording solution with a continuous supply of 95% O_2 and 5% CO_2. The individual slices were then transferred to the microscope in the same method.

Figure 2.2 VT 1000 Vibrating Blade Microtome used to perform brain slices 300 µm thick. *The image to the right is a close-up of the stage where the slices are produced (Leicabiosystems.com).*

2.4 Fabrication of Micropipettes:

Patch pipettes were prepared using Clark glass capillaries, sized at OD 1.5 mm, ID 0.86 mm and L 75 mm (Harvard Apparatus). Prior to forming the pipettes, their ends are heated using the alcohol flame of a burner to smooth the edges. This prevents damage to the rubber piece fitted in the pipette head stage. They were then placed in a Vertical glass electrode puller (Model PC-10, Narishige, Japan) to produce patch pipettes with a resistance of 5-8 MΩ. Prior to loading the pipettes onto the CV 201AU head stage (Axon Instruments, USA), they were filled with the pipette solution about 1cm from the shoulder towards the end of the pipette. The solution was inserted using a fabricated yellow pipette tip (Tip One. Star Lab Products), a 1 ml Luer (BD Plastipak, Spain) and a syringe driven filter unit (Millex-GS, MF-Millipore membrane, Tullagreen, Carrigtwohill Co. Cork, Ireland) to prevent any debris from blocking current flow through the patch pipette tip. Only the taper and a few millimetres of the shaft of the pipette shoulder were filled.

2.5 Setting up the Perfusion System:

The perfusion system was set up to limit delay between initial drug perfusion and exchange of solution in the recording chamber. The drug solutions were held in 50 ml solution reservoirs each connected to a 2.5 mm diameter tube that ran through a solenoid valve set to drive the solutions at a flow rate of 2 ml/min. The tubing was then connected to a narrower 1 mm tube. At this point all tubes connected to their corresponding solution reservoir converged into a manifold comprising of a set of 0.4 mm diameter tubes. This stage in the manifold produced the rate-limiting point which the solution would pass through. The manifold was then attached to a glass capillary tube (internal diameter 0.6 mm) with a volume of 0.1 ml that introduced solutions into the recording chamber. Prior to the initial recording, 5 ml of each solution was allowed to pass through the tubing to ensure it reached the tip of the capillary tube to minimise delay into the bath. The delay produced from initiation of perfusion to replacing the solution in the 0.3 - 0.5 ml bath is ~20 seconds (also the time at which an inward current is visible in response to the NMDA application).

2.6 Whole Cell Patch Clamp Recordings:

2.6.1 Setting up recording station:

I began by placing the brain slice on the stage of the microscope and identifying the substantia nigra. It is located on the slightly protruding edges on either side of the midbrain slice. Finally, I lowered the patch pipette into the recording chamber keeping it in focus. The recording solution runs continuously through the recording chamber (flow $\approx$ 2 ml/min). Recordings were made at room temperature (22 – 24ºC).

2.6.2 Identifying a Dopamine Cell:

Dopamine cells of the substantia nigra are usually seen as large cells in the SNc. Cells that are healthy enough to patch have a shiny and smooth appearance. The shinier the cell, the closer it is to the surface of the brain slice allowing for easier patching to take place. Cells that are deemed unhealthy

usually have a visible nucleus or an inward curvature and should thus be avoided.

2.6.3: Whole cell patch clamp procedure

I began by lowering the pipette tip until it touched the cell membrane. Contact with the cell membrane is confirmed by observing the trace produced on the two-channel oscilloscope. An increase in resistance resulting from the contact made will cause a decrease in the size of the t-pulse current pulse (generated by a 5 mV, 50 Hz rectangular voltage command produced by the amplifier). I gradually lowered the pipette to increase the resistance by 2-fold. Once a dimple was produced (Figure 2.3), negative pressure was applied to the pipette. A holding current of <10 pA confirmed a gigaohm seal (>5 GΩ) with the pipette voltage set at -60 mV using the holding command on the current amplifier (Axopatch 200A, Integrating patch clamp, Axon instruments, USA). To achieve the whole cell mode, a pulse of strong suction was applied to break into the cell. This can be confirmed by visualising the cell capacitance transient spikes produced in the trace in response to the 5 mV t-pulse.

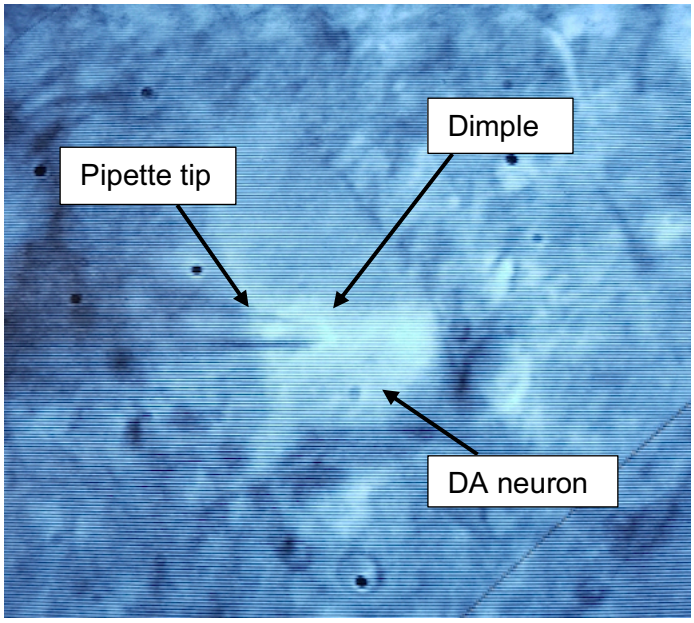

Figure 2.3 Figure showing dimple formation on the DA neuron during seal formation using patch-pipette.

The whole cell patch clamp procedure results in the interior of the pipette becoming continuous with the cell cytoplasm. This arrangement allows the measurement of electrical potentials and currents from the entire cell - thus, "Whole-cell" recording (Hamill *et al.*, 1981). Once in whole cell mode, I increased the output gain to 20x and turned on the whole-cell parameters. Using the whole cell capacitance and series resistance controls simultaneously, I minimized the capacity transients. The membrane capacitance and series resistance are then read off potentiometers on the Axopatch amplifier. In addition, I gradually increased the % Compensation to about 75-80%. Once satisfied with the trace produced, I turned on the external command and increased the offset range on the general-purpose amplifier to 10 Volts. Using the Strathclyde electrophysiology WinEDR data recorder V3.0.9 program, I began a recording approximately 30 seconds after establishing the whole-cell configuration. The current signal was low-pass filtered at 1 kHz (8-pole Bessel) and digitized at 10 kHz. The recording begins by producing a hyperpolarising voltage step from -60 mV to -120 mV for 1.8 seconds to activate the 'I_h' current (indicative of a dopamine cell; see Results, Figure 3.1)(Margolis, Lock, Chefer, *et al.*, 2006). Cells were deemed to be dopaminergic if the I_h current amplitude was greater than 50 pA with activation time constant in the range 0.2 – 2.0 seconds. The whole-cell capacitance, resistance and the % compensation were then recorded. Cells with series resistance greater than 25 MΩ or holding current greater than -250 pA were excluded from recordings and during recordings, if the series resistance increased by more than 20%, the recording was terminated.

2.6.3.1 Recording NMDA Currents:

Example Control experiment:

Once in whole-cell mode, the 20 μM NMDA solution runs through the recording chamber for 120 seconds and the resulting current recorded. The solution is then washed off by running recording solution through for 300 secs (recording the final depolarising current). This returns the response to baseline to which the second NMDA response will be measured against. A second dose of NMDA is applied to ensure the legitimacy of the initial response. The difference in

current expected is about 13% based on previous studies of Ca^{2+}-dependent inactivation and altered distribution of NMDA receptors on the dopamine cell membrane (Wild et al, 2014).

2.6.4 Electrophysiological data and Statistical analysis

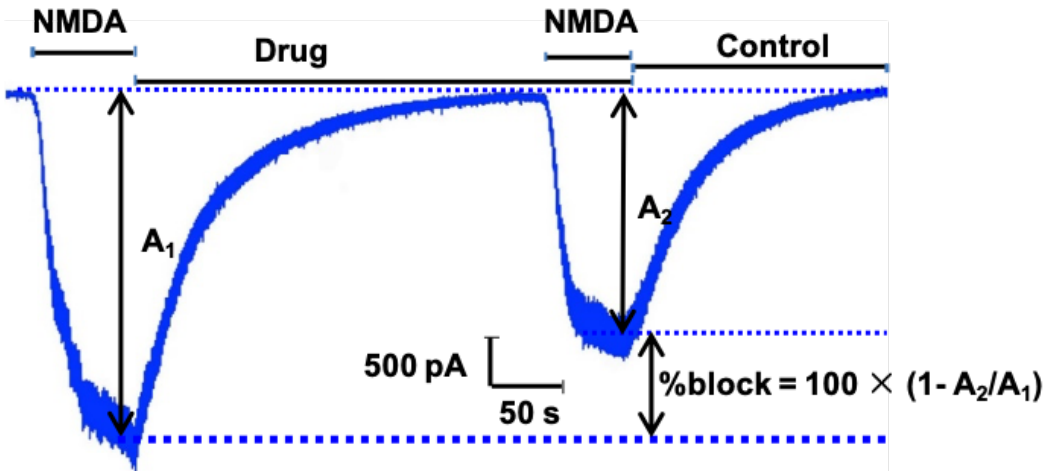

Figure 2.4 Example trace produced after two applications of NMDA *for 120 seconds, followed by a wash off period of 300 seconds. During wash off, the drug of interest was pre-applied simultaneously to allow receptors to equilibrate. % block is measured as indicated and dotted lines represent midway point in current through where measurement is taken.*

Once the data is compiled, the change in current produced after each application of NMDA (20 μM) or the experimental drug solutions, was quantified using the Strathclyde electrophysiology WinEDR data recorder V3.0.9. The current amplitude is measured from the immediately preceding baseline to the midpoint of the current during the NMDA response (Figure 2.4) subtracting the baseline current from the response. The % change and block is also determined and compared to the rest of the conditions as shown in figure 3.4. The amplitude, time constant and steady-state current produced in response to the initial and secondary Ih current were quantified using the WinWCP: Strathclyde Electrophysiology Software V4.4.1. To determine whether the change in peak current was statistically significant in each data set, a paired t-test was performed with a value of $P<0.05$ to be deemed significant (using Graphpad Prism Version 6). To compare data sets from different experiments, an unpaired t-test was carried out. When three or more groups of data were compared, a one-way ANOVA was performed along with a Bonferroni multiple comparisons test. Statistical power calculations were made for NMDA response data using

the University of British Columbia web site (Brant, R. Inference for Means: Comparing Two Independent Samples. University of British Columbia, Department of Statistics. https://www.stat.ubc.ca/~rollin/stats/ssize/n2.html). Data are recorded as means ± SEM, whereby N = number of cells recorded and used for the experiments. For a mean NMDA (20 μM) response of 959 ± 283 pA (mean + SD), to detect a 20% change in response with P = 0.05 and power = 0.8 would require n = 35 cells while a 30% change would require n = 16 cells.

2.6.5 The staining protocol:

Biocytin Hydrochloride (CF488A Biocytin) was added to the pipette solution in order to introduce the label into the cell. After the experimental protocol was completed, the slices were fixed with 4% Paraformaldehyde/4% sucrose solution overnight. The slices were then subject to 3 PBS washes for 20 minutes each on a shaker. They were then permeabilised for two hours in 0.5% Triton-X after which the slices underwent a second wash phase (consisting of 3 PBS washes for 20 minutes each). The slices were then placed on a shaker for two hours submerged in steptavatin-Alex488. A streptavidin-Alex488 conjugates stock solution at a concentration of 2 mg/ml was used from which 2 μl was added to 1 ml PBS to reach desired concentration. A final set of 3 PBS washes were performed, each for 20 minutes on a shaker. The slices finally underwent a series of increasing concentrations of alcohol washes to initiate the drying process. They were then mounted on glass slides. Two drops of prolong Gold antifade reagent were applied prior to placing the glass slip over the slice to complete the mounting process. The slides were allowed to dry overnight at 4 degrees Celsius.

Declaration:

The patch-clamp recordings made in this project were obtained in collaboration with my supervisor. P7, P21, P28 and P60 rats were killed by my supervisor, Prof Gibb and the brain slices made with the help of my supervisor. I made all other preparations for the experiments including slicing solution and recording solution, drug solutions, and making patch pipettes. Data analysis (WinEDR and WinWCP) was initially demonstrated by Prof Gibb and I subsequently made all the analysis, except for help from Professor Gibb with preparing the figures. Professor Gibb provided comments and suggestions on drafts of this thesis and I prepared the final thesis myself.

Chapter 3

Investigating the effect of D2-R activation on NMDA-R responses in dopaminergic neurons of the substantia nigra

3.1 Introduction

D2-Receptors are localised in various areas around the brain, including the VTA and the substantia nigra dopaminergic neurons (Sesack, *et al*., 1994; Gallo, 2019). They function as autoreceptors, whereby their activation induces a reduction in DA- neuron firing, dopamine production and release (Schmitz, *et al*., 2002; Gallo, 2019). There are various subcellular effects and downstream signalling changes associated with D2-R activation. Among those is the activation of $G\alpha_{i/o}$ coupled G-proteins. This triggers a canonical pathway involving the reduction of cAMP levels and reduced PKA activity. Such a decrease in kinase activity has been shown to decrease NMDA-R and voltage-dependent Ca^{2+} channel phosphorylation, thus decreasing overall cellular excitability and Ca^{2+} entry (Kotecha *et al.*, 2003; Trepanier *et al.*, 2013b). D2-R activation is also known to modulate various other ion channels via the $G\beta\gamma$ subunits coupled to the receptor (Beaulieu and Gainetdinov, 2011). D2-R activation triggers the activation of the G-protein inwardly rectifying K^+ channels (GIRKs) that work to reduce cellular firing (Lacey, *et al*., 1987a; Uchida, *et al.*, 2000; Gallo, 2019). In addition, in some cells D2-R activation activates the MAPK/ERK signalling pathway (Hutton *et al.*, 2017).

β–arrestins are involved in various cascades in the cell once activated by D2-Rs. Among them, is G-protein receptor desensitisation and subsequent internalisation (Kim *et al.*, 2001; Beaulieu and Gainetdinov, 2011; Gallo, 2019). Once receptor desensitisation is triggered, G-Protein coupled receptor kinases

(GRKs) are translocated to the membrane (Kelly, *et al*., 2008; Lowe *et al.*, 2015). GRK channels are involved in μ–opiod (MOPr) activated GIRK current desensitisation and have been studied using compound-101 (a GRK inhibitor) on LC neurons, which promoted my study of receptor desensitisation on dopaminergic neurons of the substantia nigra. It is understood that various mechanisms of ι(MOPr) desensitisation may be present in different areas in the brain but was not observed in hippocampal dentate gyrus brain slices (Terman *et al.*, 2004; Lowe *et al.*, 2015)

To further understand the canonical pathways triggered by D2-R activation and its potential to modulate cellular excitation via NMDA-Rs, the following experiments tested whether D2-R activation can modulate NMDA-R responses in P7 rats, followed by a brief study on older rats at age P21 and P28. Ropinirole and sulpiride were used as a D2-R agonist and antagonist, respectively. Compound-101 was used to inhibit potential dopamine receptor desensitisation.

3.2 Results

About 500 whole-cell patch-clamp recordings were collected under various conditions to investigate the effects of ropinirole- a D2-receptor agonist in dopaminergic (DA) and non-dopaminergic (non-DA) neurones of the rat substantia nigra. Sulpiride, a potent D2-R antagonist, was used to clarify that any effect of ropinirole was via D2 receptor activation, and finally compound-101, a GRK-2/3 inhibitor, was used to prevent D2-R desensitization. Cells were obtained from brain slices of P7, P21-23, and P28 Sprague-Dawley rats.

Identification of dopaminergic neurones:

Cells were distinguished as either DA or not, based on the amplitude and time constant of a hyperpolarisation-activated inward current induced in response to a 1.8 second voltage step from -60 mV to -120 mV (Figure 3.1 A). An exponential amplitude of >50pA and a time constant of 200 – 2000 ms were both taken as indicative of a DA cell as in SNc there is >90% correspondence

between presence of I_h and positive staining for tyrosine hydroxylase, the rate-limiting enzyme for biosynthesis of dopamine (Margolis *et al.*, 2006).

Drug treatment:

Cells were treated with different 20 μM NMDA and 10 μM Glycine-containing drug solutions, to which experimental drugs were added, to observe any effect on the NMDA current. Once recordings were obtained and analysed using the WinEDR and WinWCP programs, the average current produced was statistically analysed. All protocols involved an initial NMDA and glycine containing solution application devoid of experimental drugs, followed by a wash-off period for 300 secs. A second NMDA solution was applied for a further 120 secs containing the drug of interest. 10 μM Compound-101, however, was applied in the pipette (intracellular) solution to allow its entry into the cell during whole-cell recordings.

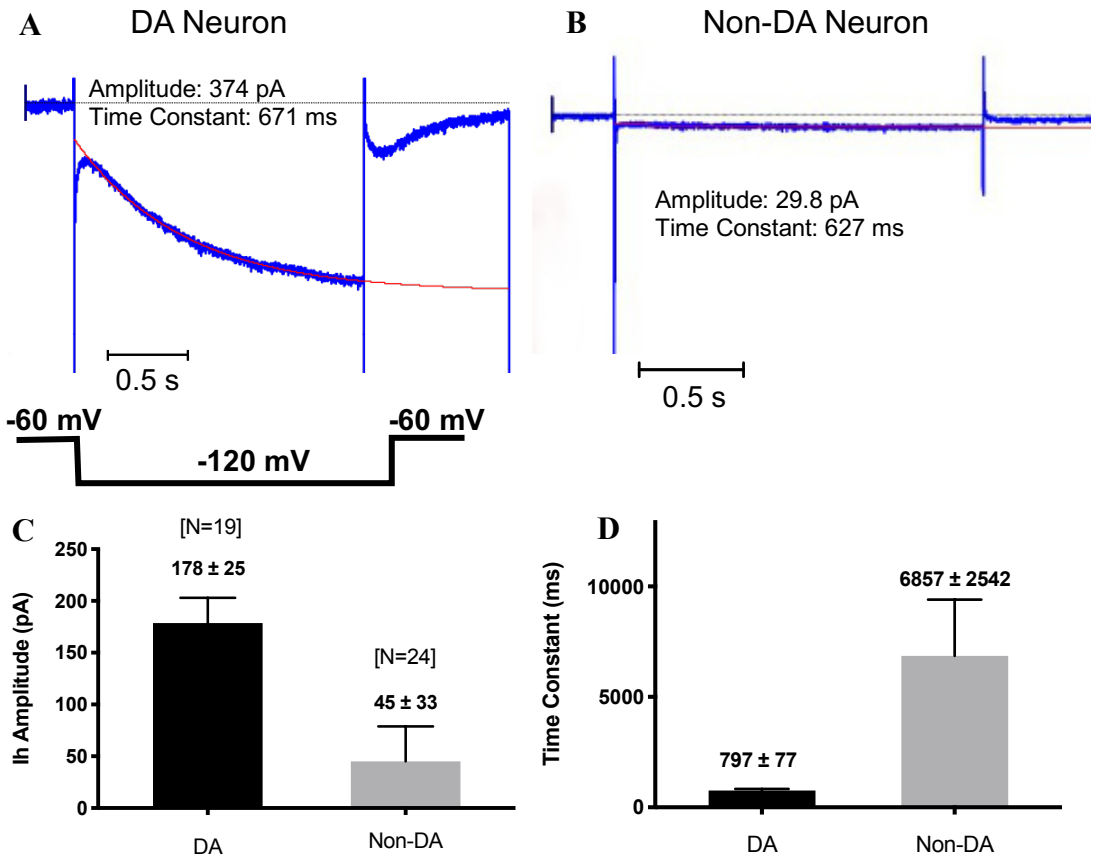

Figure 3.1 Hyperpolarization-activated inward current (I_h) in DA and Non-DA neurons from P7 rats. *A) I_h current indicative of a dopaminergic neuron (threshold used: Amp:>50 pA; Tau: 200-2000 ms). B) An absent I_h current expected for non-dopaminergic neurons. C) Corresponding mean amplitudes ± SEM for DA and non-DA neurons. D) Mean time constant ± SEM of Ih corresponding to DA and non-DA neurons.*

3.2.1 Steady-state whole-cell NMDA current is not changed by repeated 120 sec applications of NMDA to P7 rat DA and non-DA neurons

Control experiments involving two successive applications of 20 μM NMDA and 10 μM glycine were made to test the reproducibility of the NMDA response (figure 3.2). The NMDA drug solutions were run for 120 secs followed by 300 secs periods of wash-off with control solution to allow the membrane current to return to baseline. Prior to drug application the I_h current was evoked to characterise the neurons. In these recordings, DA neurons produced an average I_h amplitude of 178 ± 25 pA (mean± SEM) and a time constant (tau) of 797 ± 77 ms (mean ± SEM) (figure 3.1). Non-DA neurons, on the other hand, had a mean I_h amplitude of 45.10 ± 33 pA and a tau of 6857 ± 2542 ms.

NMDA (20 μM) evoked an obvious inward current in all DA neurons, with mean currents of 959 ± 65 pA and 912 ± 88 pA. There was no significant difference between the 1st and 2nd response (N = 19 cells from 8 rats, paired t-test, P = 0.35) during the 1st and 2nd applications of NMDA, respectively (figure 3.2 B). Small non-significant differences in the amplitude of the NMDA response were also observed in non-DA neurons that produced mean currents of 774 ± 128 pA and 716 ± 98 pA in response to two successive applications of 20 μM NMDA for 120 secs (N=12 cells from 8 rats, paired t-test, P = 0.23) (with 300 secs of wash off) (figure 3.2 C). Repeated applications of NMDA showed the relative extent to which such cells can respond to 20 μM NMDA.

3.2.2 Co-application of 20 μM Ropinirole did not decrease the steady-state NMDA current relative to the control in P7 rat DA neurons

Ropinirole, a D2-R agonist, was used to test whether D2-R activation would modulate the NMDA-R response. The protocol began with an initial control NMDA response in the presence of 20μM NMDA and 10μM glycine for 120 secs. This produced a mean NMDA current of 946 ± 89 pA (mean ± SEM, N=24 cells

from 11 rats). Followed, was a wash off period of 300 secs to allow the cells to recover. The second NMDA current was then measured for 120 secs in the presence of 20μM ropinirole. The NMDA current produced had a magnitude of 896 ± 75 pA (paired t-test, P = 0.514). The lack of a statistically significant difference indicated no effect of ropinirole on the NMDA-R current. This high concentration of ropinirole might have caused a desensitization of D2 receptors in the tissue and so obscured an effect. Therefore, the next set of experiments tests for an effect of ropinirole in the presence of compound-101 which has been shown to inhibit GPCR desensitization.

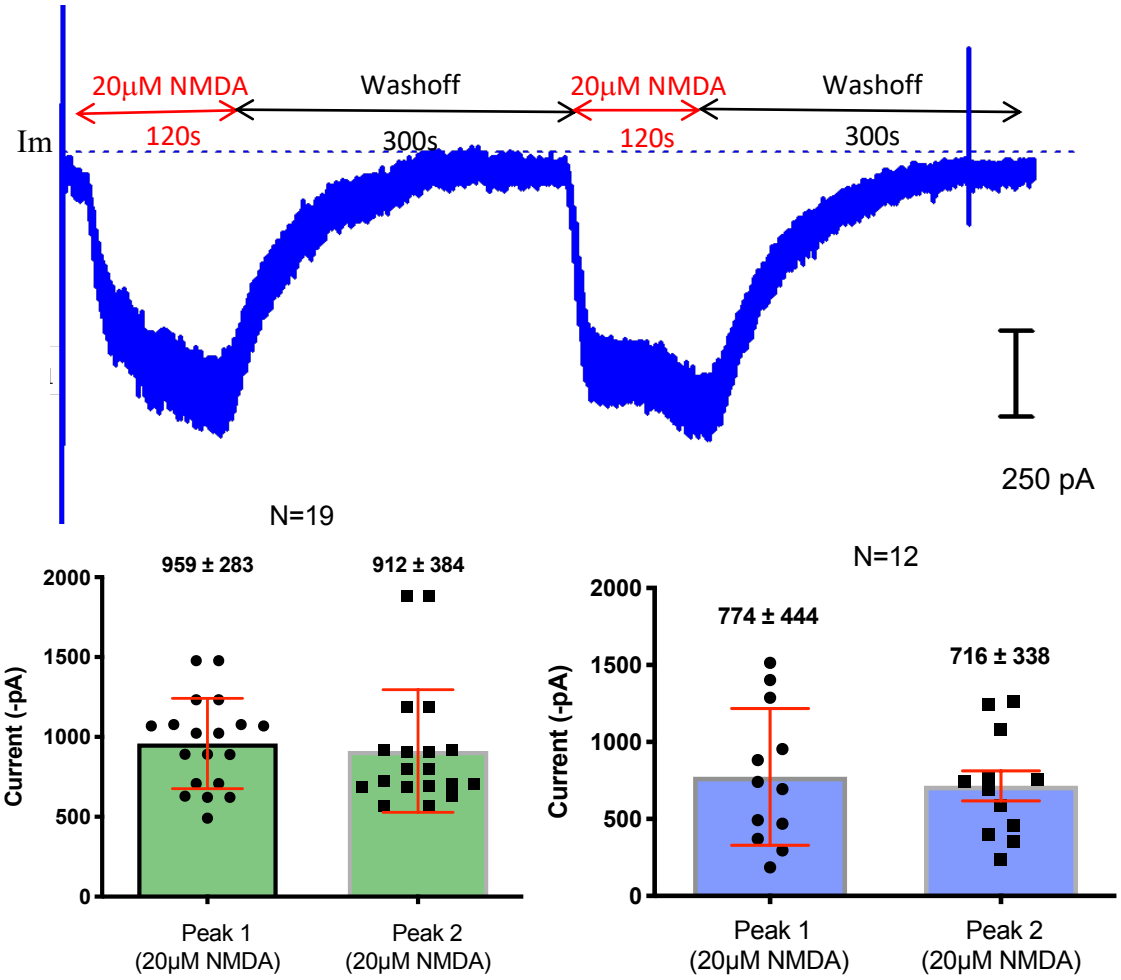

Figure 3.2 Steady-state NMDA current in response to two 120 s long applications of 20 μM NMDA in P7 rats. A) *Illustrates NMDA current produced by two consecutive applications of NMDA interrupted by a 300 sec period of wash off.* ***B)*** *A graphical representation of the overall response to two repeated applications of NMDA in DA neurons and* ***C)*** *in non-DA neurons (Mean ± SD).*

3.2.3 Compound-101 does not affect steady-state NMDA current relative to previous control experiments in P7 rat DA neurons

Compound-101 (Cmpd-101, 10 μM) was used to inhibit intracellular G-protein coupled Receptor Kinase (GRK-2/3) proteins, which could be responsible for D2-R desensitization, thus preventing ropinirole exerting an effect. A control experiment was performed to determine whether Cmpd-101 had any effect on the NMDA-R current in absence of exogenous D2-R activation. The protocol consisted of 2 repeated applications of 20 μM NMDA, each followed by a receptor recovery period for 300 secs (figure 3.3 A). 10 μM Cmpd-101 was added to the pipette intracellular solution to gain access into the cell's cytoplasm immediately after the whole-cell state was achieved. Prior to the NMDA applications, Ih currents were tested to determine cell characterization. DA neurons produced I_h currents with amplitude and tau of 140 ± 35 pA and 1311 ± 144 ms, respectively (figure 3.3 B-C). Non-DA neurons produced I_h currents with amplitudes and tau or 44 ± 11 pA and 1736 ± 419 ms, respectively. The two repeated NMDA applications that followed produced currents of 980 ± 168 pA (N=11 cells from 4 rats) and 979 ± 127 pA (N=11 cells from 4 rats, paired t-test, P = 0.992), respectively (figure 3.3 D). When these values were compared to previous control experiments in absence of Cmpd-101, these NMDA responses were not significantly different in the presence of Cmpd-101 compared to previous control responses (ANOVA, P=0.97) and the difference between the first and second peak showed no statistically significant difference (peak 1, unpaired t-test P = 0.754; peak 2, unpaired t-test, P = 0.570, N = 11). Non-DA cells similarly showed no difference in NMDA-R current, with values of 808 ± 116 pA and 887 ± 136 (N=10, unpaired-test P = 0.345) after repeated applications of 20 μM NMDA in the presence of 10 μM Cmpd-101 (figure 3.3 E).

3.2.4 Preventing desensitization of D2-Rs did not change the steady-state NMDA current in the presence of 20 μM Ropinirole in P7 rat DA neurons

Once the effects of cmpd-101 and ropinirole had been analysed independently of each other, the two drugs were combined in the following protocol. Cmpd-101 was present throughout the recording as it was added to the intracellular solution (refer to figure 3.4A). 20 μM NMDA was first applied for 120 secs, producing a current of 418 ± 101 pA (N=9 cells, from 5 rats) (figure 3.4 B). The cells were then allowed to recover from NMDA application for 300 secs in the presence of 20 μM ropinirole to equilibrate the receptors should D2-Rs show tonic activity. A second application of NMDA was then added in the presence of ropinirole producing a mean current of 620 ± 77 pA (N=9, paired t-test, P = 0.193). Attempting to prevent desensitization of D2-Rs did not seem to alter the lack of effect of ropinirole on NMDA-R current in DA neurons.

A different effect was seen in non-DA neurons that produced currents of 418 ± 71 pA and 587 ± 70 pA (N=30, from 11 rats, paired t-test, P = 0.012) in response to NMDA alone and NMDA in the presence of ropinirole, respectively (figure 3.4 C). The statistically significant increase in NMDA current was unexpected. However, note the small size of the 1st response, compared to previous control NMDA current (980pA). I_h currents induced to distinguish cell type had an amplitude of 116 ± 16 pA and -33 ± 13 pA in DA and non-DA neurons respectively. The corresponding time constants were 931 ± 248 ms and 883 ± 241 ms in DA and non-DA, respectively (figure 3.4 D-E).

3.2.5 Decreasing the concentration of Ropinirole had no effect on the NMDA current produced in the presence of 10 μM Compound-101 in P7 rats

The concentration of ropinirole was decreased to 200 nM to determine whether a lower concentration would prevent possible off-target effects. A similar protocol was run with the lowered concentration of ropinirole (figure 3.5 A). The

two NMDA currents produced in DA neurons were 706 ± 112 pA and 893 ± 116 pA (mean ± SEM, N=11 cells from 6 rats, paired t-test, P = 0.12) in the presence of 20 μM NMDA alone and in the presence of 200 nM ropinirole respectively (figure 3.5 B). Non-DA neurons produced an NMDA current of 403 ± 71 pA in the presence of 20 μM NMDA and 10 μM glycine, and 512 ± 50 pA (N= 15 cells from 5 rats, paired t-test, P = 0.168) in the presence of 20 μM NMDA and 200 nM ropinirole (figure 3.5 C). DA neurons produced I_h currents with an amplitude and time constant of 200 ± 58 pA and 1247 ± 210 ms, respectively (figure 3.5 D-E). Non-DA neurons on the other hand produced I_h currents with values 22 ± 4 pA and 3387.2 ± 1219 ms.

Figure 3.3 *(Below)* ***Effects of 10 μM Compound-101 on NMDA-R steady state current in P7 rats.*** *A) Trace illustrating Control NMDA currents in the presence of 2 repeated applications of 20 μM NMDA in the presence of 10 μM Cmpd-101. B) Mean amplitude of Ih currents in DA and Non-DA neurons. C) Mean Time constant of Ih currents in DA and Non-DA neurons. D) Graphical representation of repeated measures of 20 μM NMDA and 10 μM Cmpd-101 in DA neurons and E) in non-DA neurons. F) Overall there was no significant difference betweenf 1st and 2nd peak currents in both control experiments (with and without 10 μM cmpd-101) (ANOVA, P=0.96).*

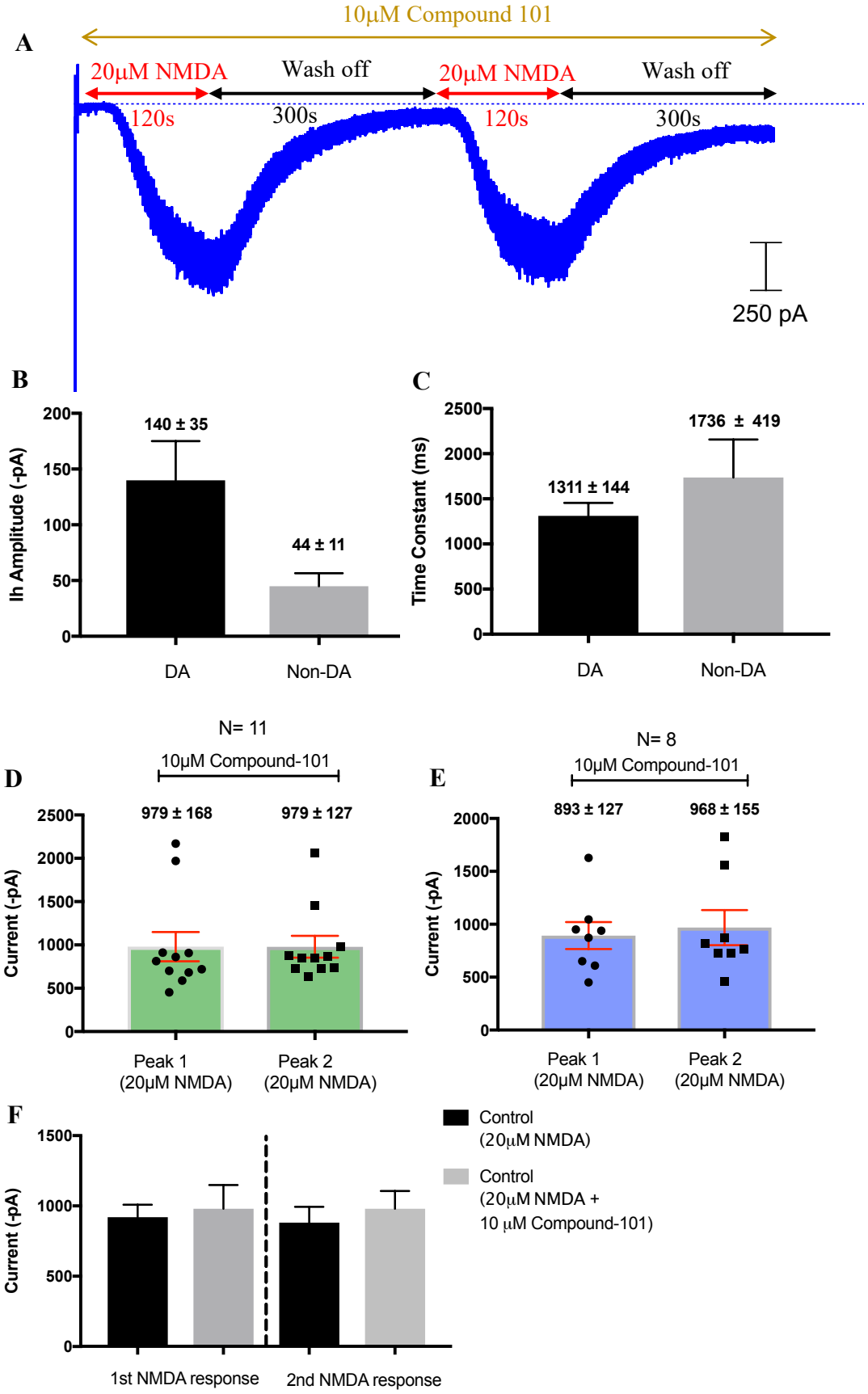
A
10μM Compound 101
20μM NMDA
Wash off
20μM NMDA
Wash off
120s
300s
120s
300s
250 pA
B
Ih Amplitude (-pA)
140 ± 35
44 ± 11
DA
Non-DA
C
Time Constant (ms)
1311 ± 144
1736 ± 419
DA
Non-DA
D
N= 11
10μM Compound-101
Current (-pA)
979 ± 168
979 ± 127
Peak 1
(20μM NMDA)
Peak 2
(20μM NMDA)
E
N= 8
10μM Compound-101
Current (-pA)
893 ± 127
968 ± 155
Peak 1
(20μM NMDA)
Peak 2
(20μM NMDA)
F
Current (-pA)
1st NMDA response
2nd NMDA response
Control
(20μM NMDA)
Control
(20μM NMDA +
10 μM Compound-101)

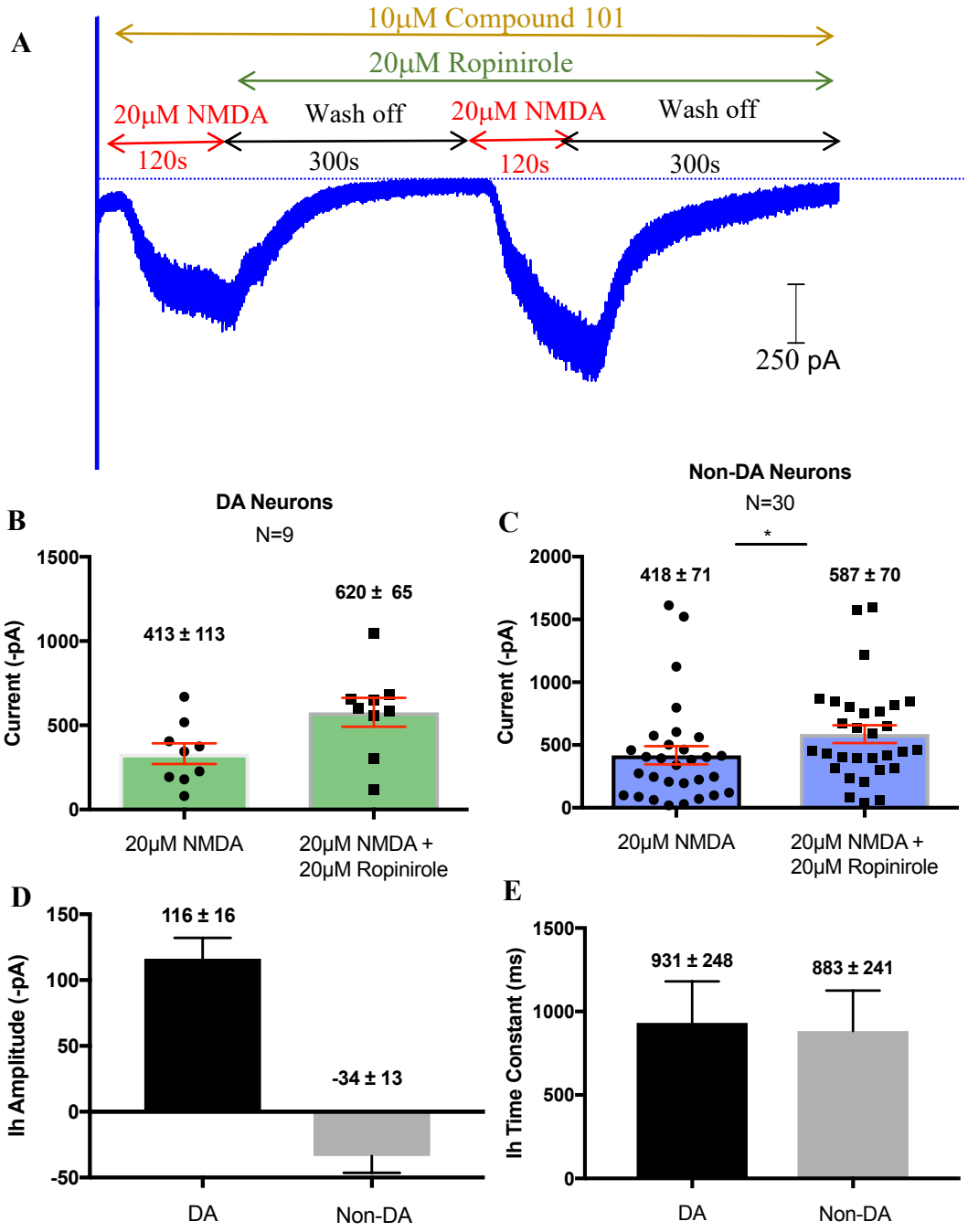

Figure 3.4 Recordings in presence of 10 µM Compound-101and 20 µM ropinirole in P7 rats. *A) Example trace produced in response to two 20 µM NMDA applications in the presence and absence of 20 µM Ropinirole. B) Overall mean currents produced in response to different drug profusions in DA neurons, and C) likewise in non-DA neurons (P=0.012). D) Corresponding amplitude and E) time constant of I_h was in DA and Non-DA neurons.*

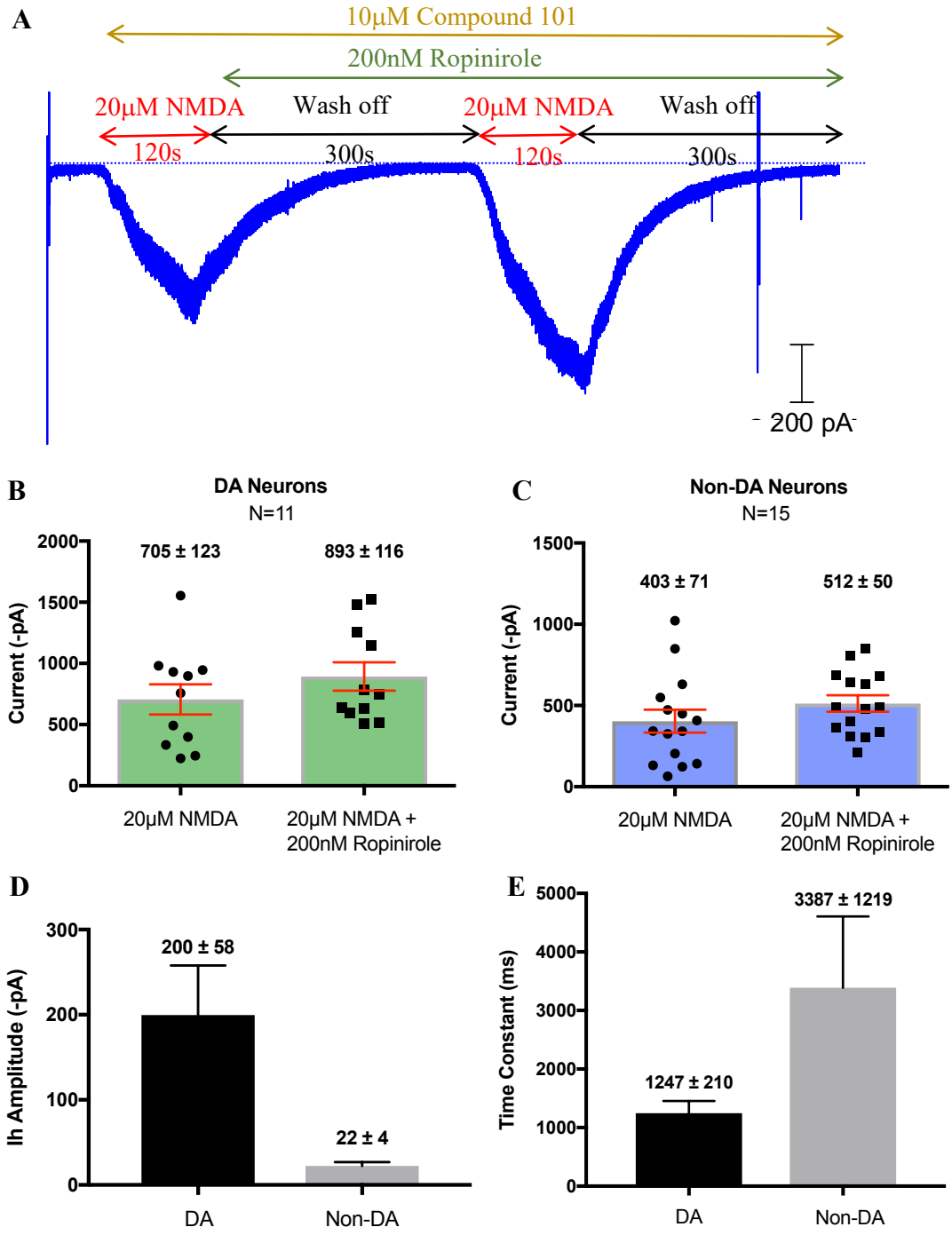

Figure 3.5 Recordings in the presence of 10 µM Cmpd-101 and 200 nM ropinirole. *A) A trace depicting steady-state NMDA current from P7 rats in the presence of 200 nM ropinirole and 10 µM compound-101. B) Graphical representation of the two NMDA currents in the presence and absence of 200 nM ropinirole in DA neurons, C) and in non-DA neurons. D) Corresponding Amplitude and E) Time constant prodcued upon I_h current induction in DA and Non-DA neurons.*

3.2.6 Steady-state whole cell NMDA current stays the same after three repeated applications of 20 μM NMDA in P21 rat DA neurons

P21-23 rats were used to determine whether the absence of effects seen in P7 rats would change with development. A control protocol was run that included three applications of 20 μM NMDA interrupted by 300 secs wash periods to allow the cells to recover (figure 3.6 A). The currents produced in response to the three NMDA applications were 432 ± 72 pA, 527 ± 71 pA, and lastly 564 ± 73 pA (mean ± SEM, N=11/9 cells from 2 rats, One-way ANOVA, P = 0.4295) (figure 3.6 B). The I_h current in these cells had a mean amplitude and time constant of 229 ± 26 pA and 1129 ± 163 ms, respectively.

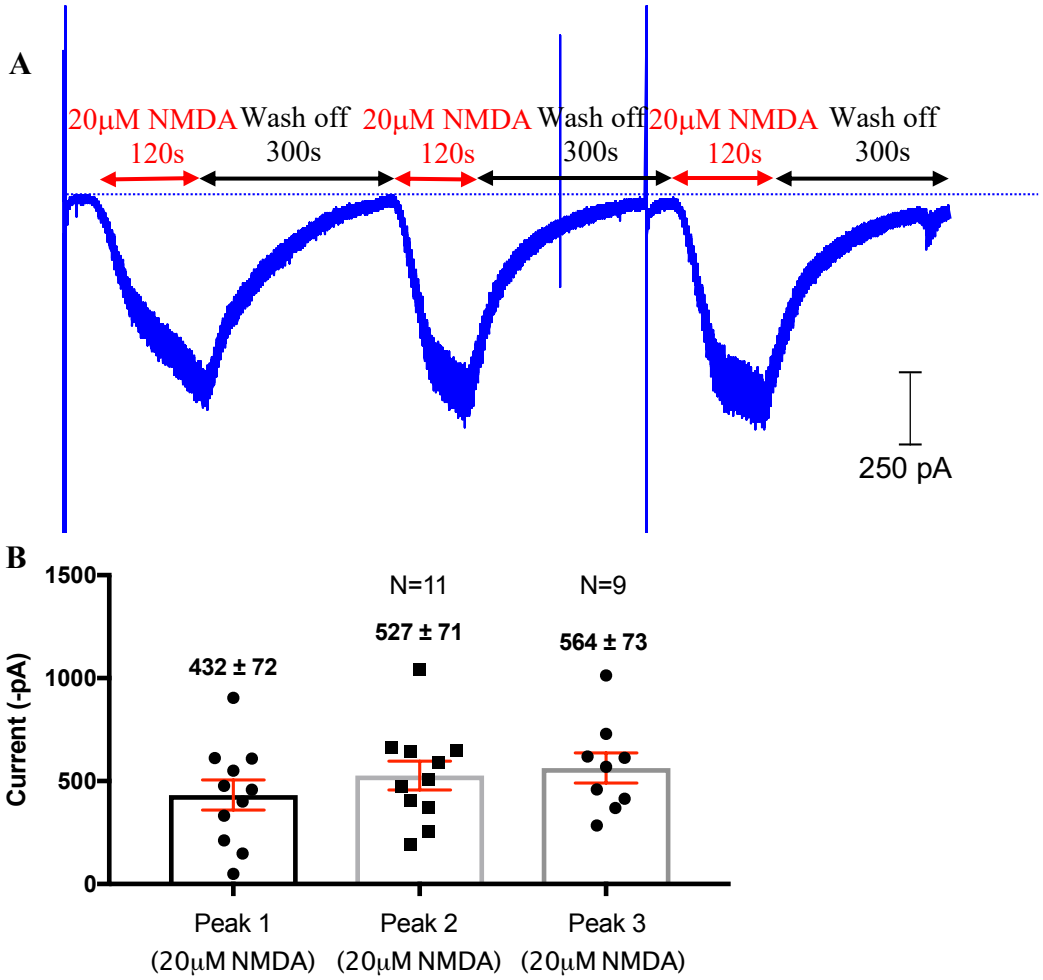

Figure 3.6 Control NMDA responses from P21 rat dopaminergic neurons. ***A)*** *A trace depicting a steady-state NMDA current in response to 3 applications of 20 μM NMDA for 120 secs each. Each NMDA application is followed by a 300 secs receptor recovery period.* ***B)*** *A graphical representation of the 3 NMDA currents produced.*

3.2.7 200 nM Ropinirole increased the steady-state NMDA-R current in P23 rat DA neurons

After establishing the consistency in NMDA currents in the control experiment, I then investigated whether 200 nM ropinirole would influence the NMDA-R current. Ropinirole was pre-applied for 300 secs in the control solution prior to the second NMDA application (figure 3.7 A). During the first application of 20 μM NMDA for 120 s, a mean current of 591 ± 78 pA (mean ± SEM) was produced (figure 3.7 B). During the second application in the presence of 200 nM ropinirole, a mean current of 828 ± 77 pA was produced (N=12 cells from 2 rats, paired t-test $P < 0.001$). The increase in current between the two responses was statistically significant. The I_h current produced a mean amplitude of 252 ± 43 pA and a mean time constant of 1009 ± 130 ms.

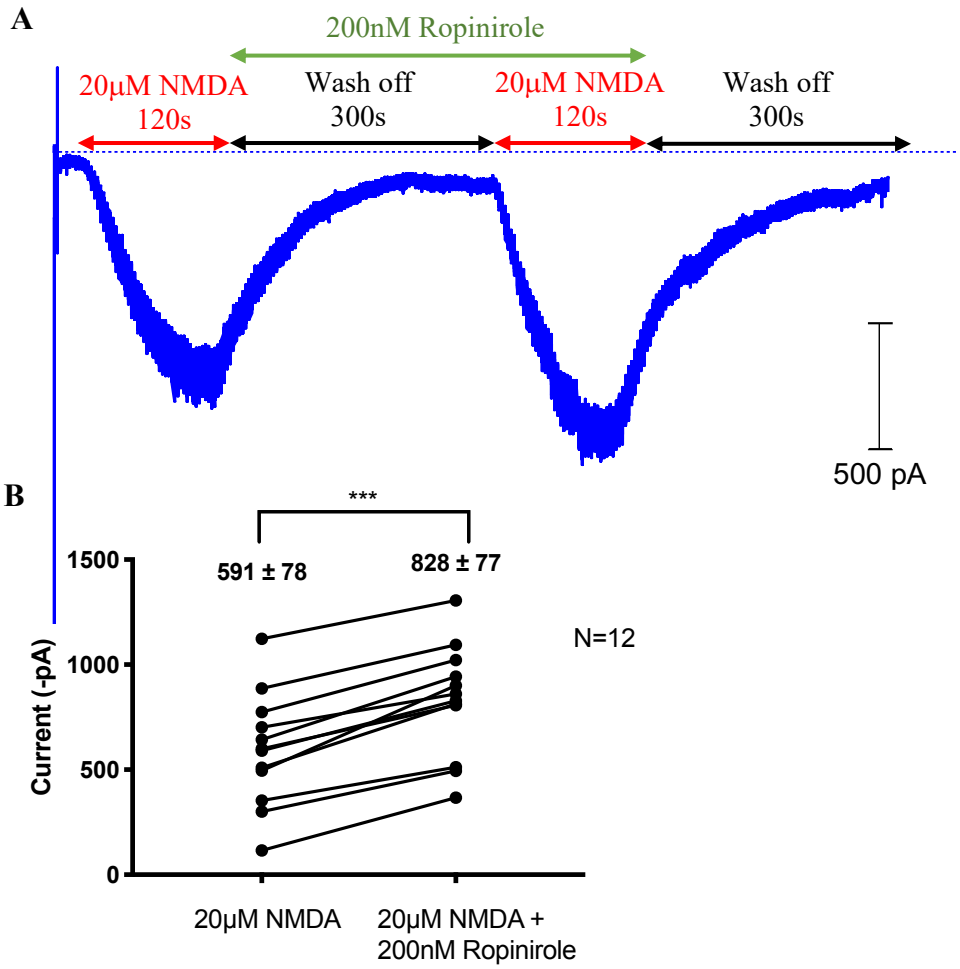

***Figure 3.7 Testing 200nM Ropinirole on NMDA responses from P23 rats**. **A)** 20 µM NMDA was added for 120 s. This was followed by 300 secs of receptor recovery and a pre-application of 200 nM ropinirole. Following, was a second application of NMDA in the presence of ropinirole for a further 120 secs. **B)** A graphic representation of the 2 NMDA currents in the absence and presence of ropinirole (Paired T-test, P=0.001).*

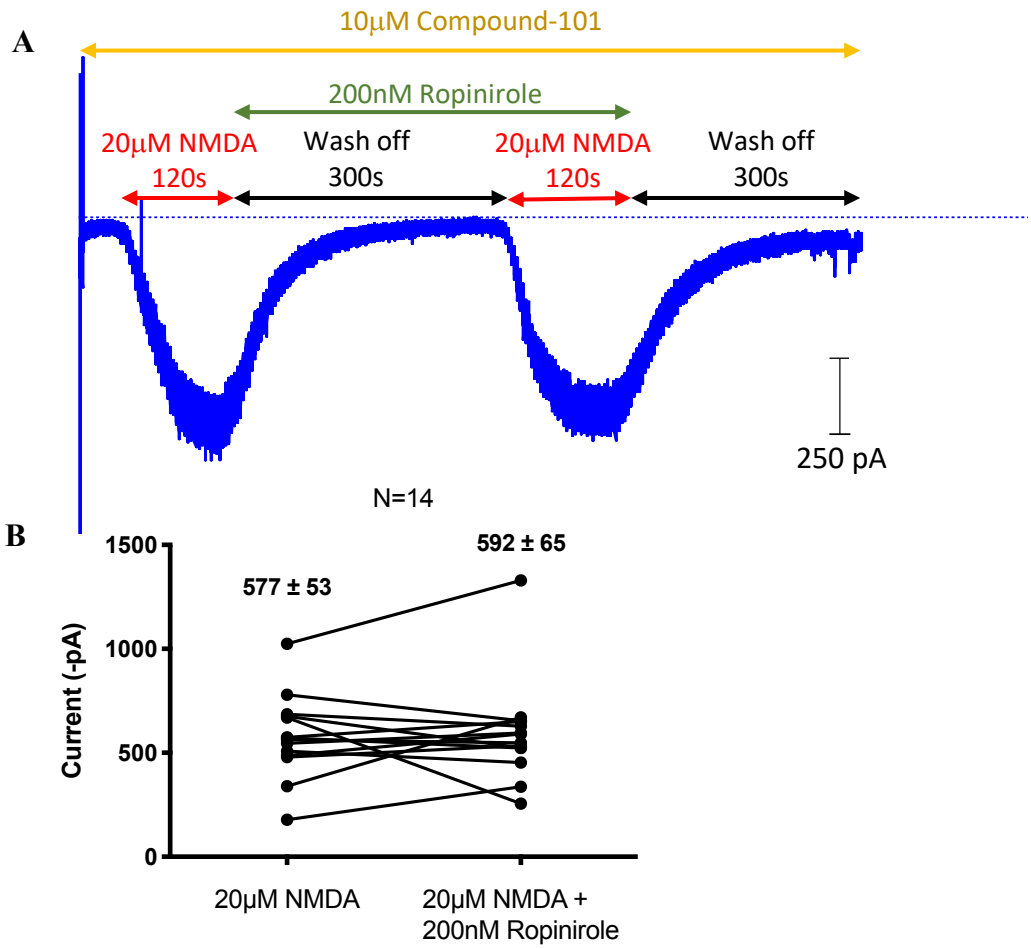

Figure 3.8 Recordings in presence of 10 µM Cmpd-101 and 200 nM ropinirole in P21 rats. ***A)*** *Two repeated 20 µM NMDA applications in the absence and presence of ropinirole (200 nM) in P21 rat DA neurons. Compound-101 was present throughout the protocol as it was added to the pipette solution.* ***B)*** *A graphical representation of the DA neuron currents in both drug conditions.*

3.2.8 Compound-101 did not have any effect on D2-R activation in P21 rat DA neurons

10 µM cmpd-101 did not change the overall NMDA current in the presence of 200 nM ropinirole (figure 3.8 A). The initial application of 20 µM NMDA in the presence of cmpd-101 for 120 secs produce a current of 577 ± 53 pA, and the second current produced in the presence of ropinirole and cmpd-101 was 593 ± 65 pA (N=14 cells from 3 rats, paired t-test, P = 0.767) (figure 3.8 B). The slight increase in NMDA-R current was not statistically significant. At the beginning of the protocol the cells were tested to determine their characteristics.

The I_h produced in these DA cells had mean amplitude and time constant of 238 ± 24 pA and 1066 ± 132 ms, respectively.

3.2.9 Repeated applications of 20 μM NMDA did not change the steady-state whole cell NMDA current in P28 rat DA neurons

Inward-rectifying hyperpolarizing currents induced by a voltage step from -60 to -120 mV were used to identify dopaminergic neurons. In P28 rats, the average Ih amplitude produced was 184 ± 38 pA (mean ± SEM) and time constant, 990 ± 150 msecs. Repeated applications of NMDA were performed to test the reproducibility of NMDA response in P28 rat dopaminergic neurons. 20 μM NMDA and 10 μM Glycine was applied three times for 120 seconds with a 300 seconds period of wash off between each application (figure 3.9 A). After the first application of NMDA, an average inward current of 687 ± 114 pA was produced. There were no significant differences in average NMDA-R responses (720 ± 94 pA, second application and 726 ± 95 pA, third application; N=12, cells from 5 rats, one-way ANOVA P= 0.647) (figure 3.9 B).

Figure 3.9 C compares the first two mean ± SD NMDA-R responses in control recordings between P7, P21 and P28 rats. Furthermore, there is a statistically significant difference in the first NMDA receptor responses in all three age groups (One-way ANOVA, P=0.0003). However, the NMDA-R currents are similar within each age group.

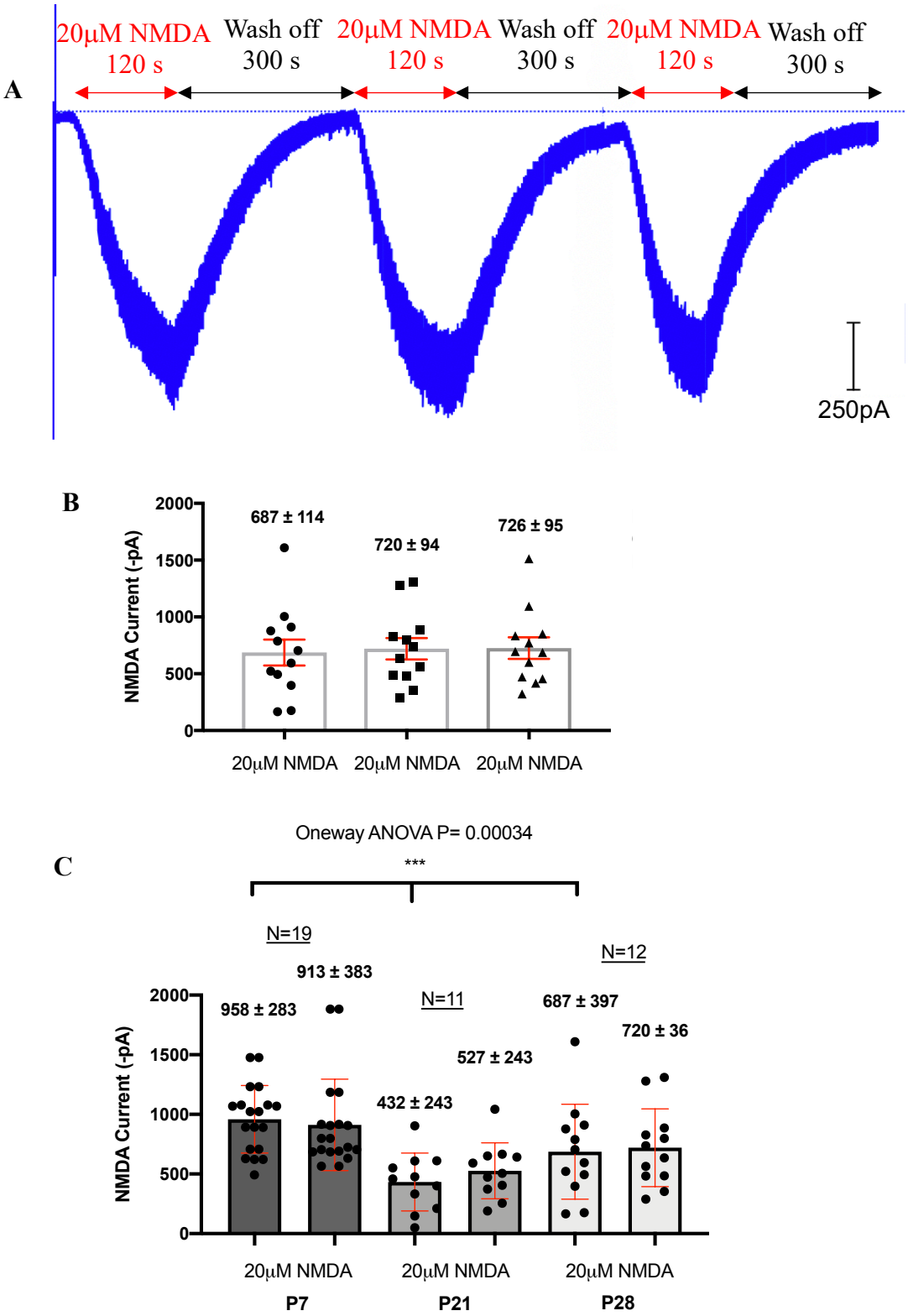

Figure 3.9 This figure illustrates a control experiment performed on P28 rats. *A) a trace showing three repeated applications of 20 μM NMDA for 120 seconds, each followed by wash off periods of 300 seconds B) A quantitative analysis of the three NMDA responses. (N=12 cells, 5 rats). C) Comparison of two repeated 20 μM NMDA responses (mean ± SD) in P7, P21 and P28 rats.*

3.2.10 200 nM Ropinirole does not change the NMDA-R response at ages from one to four weeks

After the first application of NMDA, 200 nM Ropinirole was pre-applied to allow the receptors to equilibrate for five minutes prior to second application of NMDA in the presence of ropinirole (figure 3.10 A). The initial application of NMDA produced an average NMDA-R current of 635 ± 132 pA followed by an average inward current of 611 ± 81 pA in the presence of 200 nM Ropinirole (figure 3.10 B). Despite the slight decrease in average current, the reduction was not statistically significant indicating no effect on NMDA-Rs (N=15 cells from 5 rats, paired T-test, P=0.736). An analysis was then carried out to compare the effect of ropinirole at different levels of brain maturity (P7, P21 and P28 rats). Over this age range, there was a marginally significant difference in the mean NMDA-R response (One-way Anova, P=0.0427). In the P7 rats, D2-R activation increased the overall NMDA-R current by 26 ± 22% (N=11 cells from 6 rats) (figure 3.10 C). In P21 rats, the mean percentage increase in NMDA-R current increased by only 10 ± 11% (N=14) with a smaller difference in P28 rats where the current decreased by 7.4 ± 7.3%.

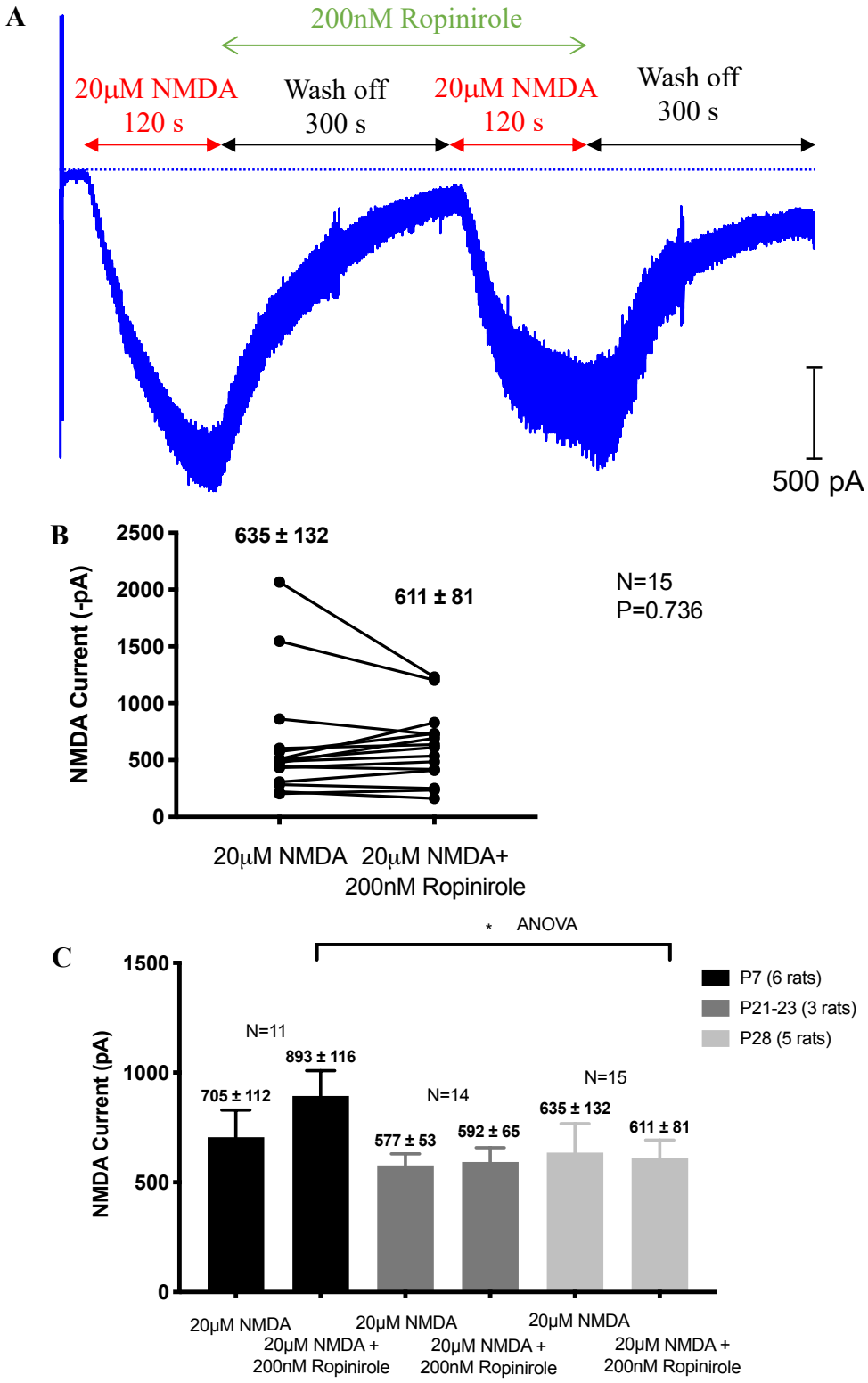

Figure 3.10 Ropinirole, a D2-R agonist does not change the NMDA-R current in P28 rats. *A) A trace showing the protocol used. 200 nM Ropinirole was pre-applied for 300 secs before the 2nd NMDA response. B) A quantitative analysis showing the effect of Ropinirole on the average NMDA-R response (N=15 cells, 5 rats). C) A comparison demonstrating the absence of age-related effects of ropinirole on NMDA-Rs.*

3.2.11 In the presence of Compound-101, repeated application of 20μM NMDA gave consistent responses in P28 rat substantia nigra

In the presence of ropinirole alone, there was a statistically significant increase in the NMDA current. To reduce possibility of D2-receptor desensitization once activated, a GRK2/3 inhibitor-(Compound-101) was included in the pipette solution. After running a control protocol in the presence of 20 μM NMDA alone, to determine whether cmpd-101 can potentially modulate the NMDA currents, average currents of 419 ± 114 pA, 460 ± 95 pA and 503 ± 140 pA were produced after the first, second and third application of 20 μM NMDA, respectively (N=11 cells from 3 rats, ANOVA, P=0.8798) (figure 3.11B). 10 μM Compound-101 had no effect on the overall NMDA current of P28 DAergic neurons of the substantia nigra. The overall currents were no different to P28 control experiments with 20 μM NMDA alone. The I_h currents produced were indicative of DAergic neurons

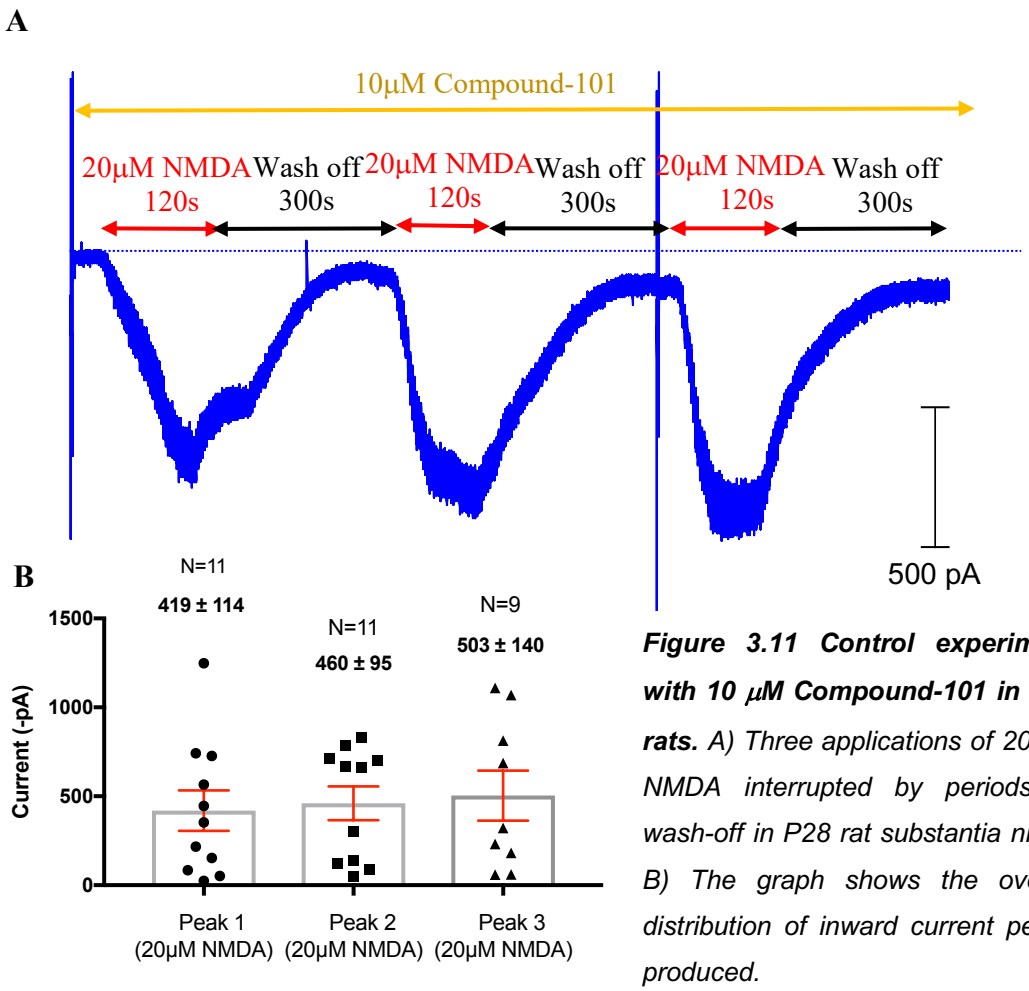

Figure 3.11 Control experiment with 10 μM Compound-101 in P28 rats. *A) Three applications of 20 μM NMDA interrupted by periods of wash-off in P28 rat substantia nigra. B) The graph shows the overall distribution of inward current peaks produced.*

and had an average amplitude and time constant of 250 ± 86 pA and 997 ± 144 ms, respectively.

3.2.12 Compound-101 did not change the absence of effect of D2-Receptor activation in P28 DAergic neurons of the substantia nigra

10 μM cmpd-101 was introduced via the intracellular pipette solution therefore present throughout the recording. The protocol began with a control NMDA response that produced an average inward current of 665 ± 159 pA, followed by a wash off period while simultaneously pre-applying 200 nM ropinirole. This was then followed by a second NMDA current, now in the presence of both ropinirole and cmpd-101. The peaks had an average inward current of 784 ± 164 pA (figure 3.12). However, the small increase in mean current in the presence of ropinirole was not statistically significant (N=10, from 4 rats; paired t-test, P=0.2782). The hyperpolarisation-activated inward current produced in all 10

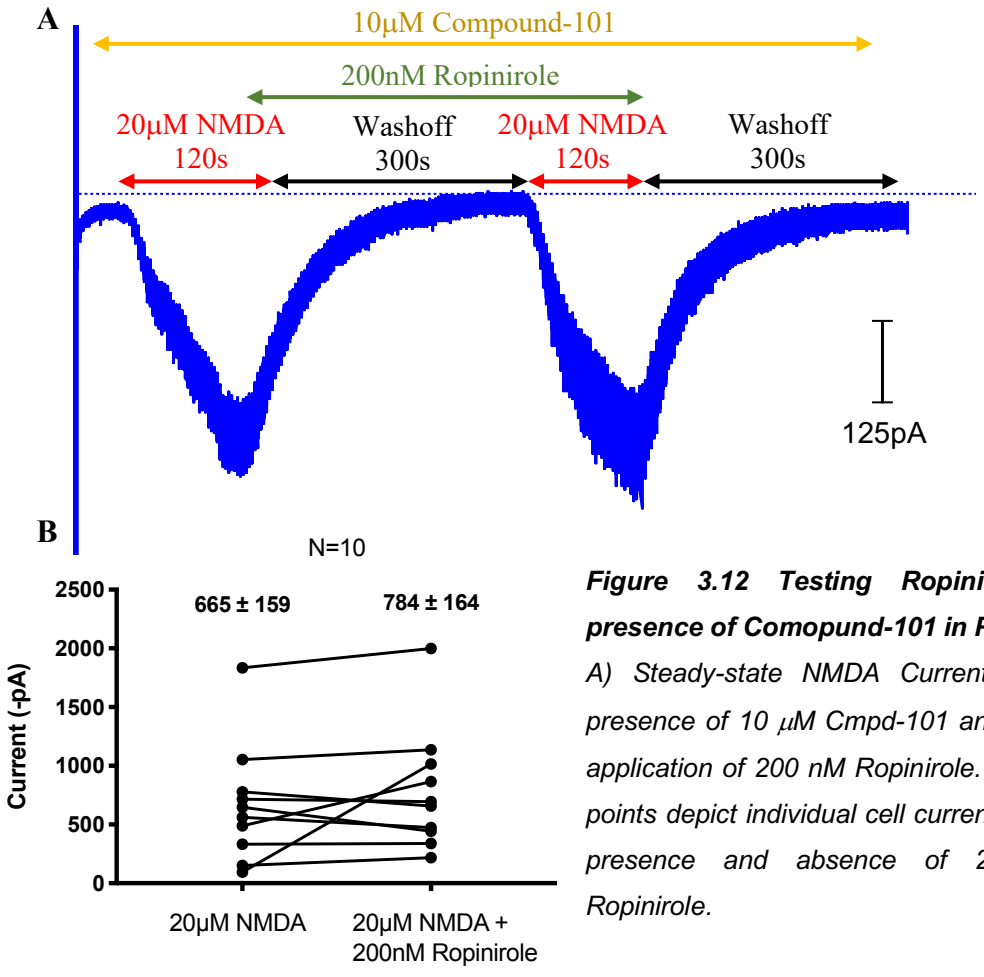

Figure 3.12 Testing Ropinirole in presence of Comopund-101 in P28 rats. *A) Steady-state NMDA Current in the presence of 10 μM Cmpd-101 and a pre-application of 200 nM Ropinirole. B) Data points depict individual cell currents in the presence and absence of 200 nM Ropinirole.*

cells had a mean amplitude and time constant of 175 ± 28 pA and 859 ± 117 ms.

3.3 Results Summary

Table 3 Summary of experiments studying the effect of D2-R activation and desensitization on NMDA-R current in P7 DAergic neurons of the substantia nigra.

Experiment	Result	Statistical analysis
20 μM NMDA Control	Repeated applications of NMDA produced similar responses.	Paired T-test: P=0.35; N=19, 9 Rats
Does activating D2-Rs decrease NMDA-R current?		
20 μM Ropinirole (D2-R Agonist)	No effect on NMDA-R current.	Paired T-test: P=0.514; N=24, 11 Rats
10 μM Compound-101 (GRK2/3 Inhibitor)	No effect on NMDA current	Paired T-test: P=0.992; N=11, 4 Rats
Does inhibiting GPCR receptor desensitization allow D2-R to affect NMDA-R current?		
10 μM Compound-101 + 20 μM Ropinirole	Did not alter NMDA-R response.	Paired T-test: P=0.193; N=9, 5 Rats
10 μM Compound-101 + 200 nM Ropinirole	Decreasing the concentration of ropinirole did not affect NMDA response.	Paired T-test: P-0.12, N=11, 6 Rats

Table 4 Summary of experiments investigating the effect of D2-R activation and desensitization in P21 DAergic neurons of the substantia nigra.

Experiment	Result	Statistical analysis
20 μM NMDA Control	Repeated applications of NMDA produced three similar responses.	Paired T-test: P=0.429; N=11/9, 2 Rats
Does activating D2-Rs and preventing receptor desensitisation decrease NMDA-R current?		
200 nM Ropinirole (D2-R Agonist)	Statistically significant increase in NMDA-R current.	Paired T-test: P=0.001; N=12, 2 Rats
10 μM Compound-101 (GRK2/3 Inhibitor)	No effect on NMDA current	Paired T-test: P=0.767; N=14, 3 Rats

Table 5 Summary of experiments studying the effect of D2-R activation and desensitization on NMDA-R current in P28 DAergic neurons of the substantia nigra.

Experiment	Result	Statistical analysis
20 μM NMDA Control	No change in NMDA current following three applications of NMDA.	Paired T-test: P=0.647; N=12, 5 Rats
200 nM Ropinirole (D2-R Agonist)	No significant effect on NMDA-R current.	Paired T-test: P=0.736; N=15, 5 Rats
10 μM Compound-101 (GRK2/3 Inhibitor)	No effect on NMDA current	Paired T-test: P=0.879; N=11, 3 Rats
10 μM Compound-101 + 200 nM Ropinirole	No effect on NMDA-R current	Paired T-test: P=0.278; N=10, 4 Rats

3.4 Discussion

NMDA-receptor dysregulation has been associated with several neurological disorders including PD and schizophrenia (Paoletti, *et al*., 2013). Therefore, understanding NMDA receptor modulation is paramount. D2-R activation is known to follow a canonical pathway involving the accumulation of cAMP and activation of PKA activity, respectively, which ultimately leads to NMDA-R phosphorylation, receptor trafficking to the membrane, increase in receptor response and calcium entry (Lau and Zukin, 2007). The experiments described in this chapter focused on P7, P21 and P28 rats to test for receptor modulation by D2-R activation and whether the NMDA responses change with age or in presence of Cmpd-101.

Whole cell patch clamp recordings were initially carried out on P7 dopaminergic neurons of the substantia nigra. A control experiment with two repeated applications of 20 μM NMDA showed no differences in inward current between applications. In addition, when 20 μM Ropinirole, a D2-R agonist was introduced, there was no difference in inward current between control and ropinirole treated responses. It was postulated that at this concentration of ropinirole, off-target effects may have occurred. Ropinirole, at higher concentrations is known to activate D1-like receptors, 5-hydroxytryptamine (5-HT) and Alpha-2 noradrenergic receptors (α2aR) (Sibley, 1999). The concentration of ropinirole was then reduced to 200 nM. Nonetheless, the observed lack of NMDA-R effect was similar in the presence of ropinirole. A

likely phenomenon which could happen in these experiments, receptor desensitization, is not uncommon and as Guo *et al.*, (2010) demonstrated, occurs within minutes of agonist exposure causing D2 receptors to internalise (Skinbjerg *et al.*, 2010). GPCR-desensitization is the physical uncoupling of the G-protein from the receptor rendering it non-functional, a process driven by GRKs (Evron, *et al*., 2012). GRKs are responsible for phosphorylating many GPCRs which leads to binding of arrestins and adapter proteins ultimately leading to the reduction in G-protein signalling (Lefkowitz and Shenoy, 2005). In the experiment described in this chapter, compound-101, a GRK2/3 inhibitor was introduced into the pipette solution in the presence of 200 nM ropinirole. Relative to the experiments with NMDA or ropinirole alone, there was no difference in the NMDA-R responses. Thus, in neurons from P7 rats ropinirole did not modulate the NMDA-R response (figure 3.4 and 3.5).

To determine whether ropinirole has any effect in older animals, similar protocols were performed on P21 rats. Relative to the control experiment with three repeated applications of 20 μM NMDA, 200 nM ropinirole increased the NMDA-R response (figure 3.6 and 3.7 paired t-test, P=0.001). The potentiation was not expected considering the known effects of activating a $G\alpha_{i/o}$ proteins on NMDA-Rs, i.e. an expected decrease in current following inhibitory D2-R acitvation. 10 μM Compound-101 was then introduced. This levelled the NMDA-R responses suggesting the possible inhibition of D2-R desensitization. Lastly, similar experiments on P28 rats showed no difference in NMDA-R response in the presence of 200 nM ropinirole, suggesting a potential developmental change in D2-R activation-induced modulation. After the application of the GRK2/3 inhibitor, there was no change in NMDA-R activation, suggesting no involvement of D2-R desensitization upon G-Protein activation in older rats.

In retrospect, I would consider experiments on larger age intervals, i.e. P7, P28 and P60 rats as such age differences would test for more obvious developmental differences in receptor activation and modulation and reduce the number of rats used in the process. As in some experiments the NMDA response did not seem to reach a steady-state (perhaps due to slow diffusion

of NMDA into the slice) it would be useful to test longer agonist applications (Suarez et al., 2010). Furthermore, as ropinirole is known to have off-target effects at concentrations above 10 μM, lower drug concentrations would be used throughout the age groups (Newman-Tancredi *et al.*, 2002).

Chapter 4:

Elucidating the modulatory role of D2 and A2A receptors on NMDA receptor response in P28 rat dopaminergic neurons of the substantia nigra

4.1 Introduction

Experiments mentioned in chapter 3, on P7 rats, showed minimal response to different drug applications. This could be due to the still developing neuronal networks in the brain. At P21, the number of NMDA-Rs present on the cell surface seem to have decreased suggested by the smaller NMDA responses relative to P7 control experiments (figure 3.6B) (Suárez *et al.*, 2010). In addition, NMDA-R desensitisation appeared to increase with age. A developmental change in NMDA-R subunit composition and distribution pattern has been observed at a cellular and synaptic level, especially involving GluN2A and GluN2B containing receptors (Hestrin, *et al,* 1990; Flint *et al.*, 1997). They differ in glutamate sensitivity and deactivation kinetics (Monyer *et al.*, 1994b; Cull-Candy, *et al.*, 2001b). In immature brains, GluN2B-containing NMDA-Rs predominate and exhibit slow kinetics relative to GluN2A (three to four fold slower kinetics) (Monyer *et al.*, 1994b; Stocca and Vicini, 1998; Traynelis *et al.*, 2010; Hansen *et al.*, 2017). This developmentally visible speeding up of receptor kinetics in early development is due to the delayed expression of GluN2A containing receptors. These then become the predominant receptor subunit present in mature brains (Akazawa *et al.*, 1994). The inconsistency in receptor subtypes throughout the brain (Watanabe *et al.*, 1993) directed further studies in older, more mature rats, providing a better understanding of NMDA receptors in young rats.

As mentioned in section 1.4.3, GPCR receptor heteromers are becoming an important target in drug development, for instance, potentially involving D2 and A2A receptors in the treatment of PD (Guidolin *et al.*, 2015). The biochemical properties of these GPCR heteromers are partly owed to their allosteric interaction suggesting both a functional and pharmacological significance (Fuxe *et al.*, 2010). The next set of experiments in this thesis aim to investigate possible heteromeric effects of targeting D2 and A2A receptors on NMDA-R response in P28 rats. Ropinirole and Sulpiride will be used to activate and inhibit D2-Rs, respectively. Whereas, CGS-21690 and SCH56821 will be used to activate and inhibit A2A-Rs, respectively.

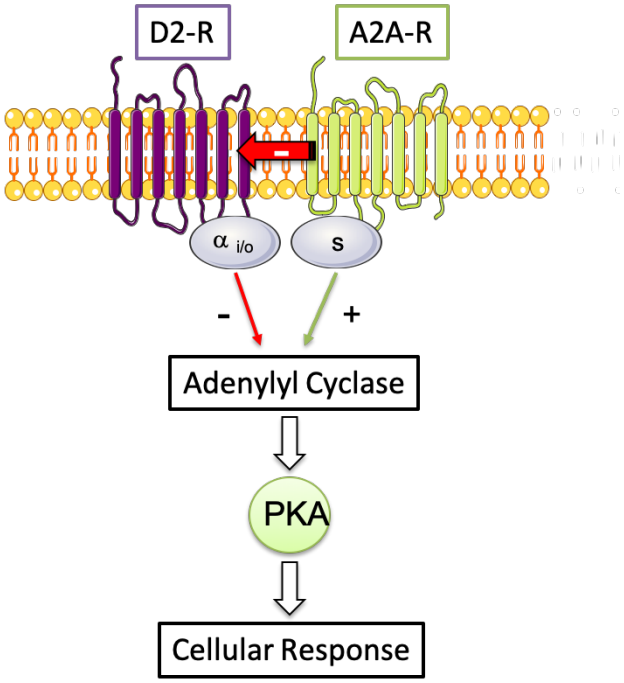

Figure 4.0 A schematic illustration of the potential D2-R and A2A-R heteromerization and resulting effects on cellular response. *(Adapted from Fuxe et al., 2010)*

4.2 Results

4.2.1 Blocking D2-Receptors demonstrated a potential increase in steady-state NMDA-R current in P28 rat substantia nigra dopaminergic neurons

Sulpiride was used to test the effect of blocking D2-Rs on the resulting steady-state NMDA-R current. After the first control response, where 20 μM NMDA was applied for 120 secs, a mean current of 587 ± 109 pA was produced. 1 μM sulpiride was then pre-applied for 300 secs, prior to the second application of NMDA in the presence of sulpiride (figure 4.1A). This gave an apparent increase in the average steady-state current by 35% (649 ± 89 pA, mean ± SEM) however this was not statistically significant (Paired T-test, P=0.354) (figure 4.1B). After

a 300s period of wash off, 20 μM NMDA was added a final time to determine whether any effects of sulpiride were potentially reversible. As seen in figure 4.3B, the mean current was not significantly different to that of the control.

4.2.2 Blocking Adenosine 2A-Receptors with 200 nM SCH58621 did not change the NMDA-R response

20 μM NMDA was first applied as a control producing an average steady-state NMDA-R current of 596 ± 50 pA (mean ± SEM, N=13 cells, 3 rats). 200 nM SCH58621 was then pre-applied during the wash off phase for about 300 secs (figure 4.2A). The A2A-R antagonist was then added in the presence of 20 μM NMDA and 10 μM glycine. There was no statistically significant change in inward current relative to the control, with a mean current of 658 ± 30 pA (Paired T-test, P=0.16) (figure 4.2B). The antagonist and NMDA were then washed off for 300 sec prior to a final application of 20 μM NMDA. The average steady-state NMDA-R current increased to 796 ± 40 pA (N=10). Overall a low concentration of the A2A-R antagonist, SCH58621 showed a minimal modulation in NMDA-R response suggesting there could be some adenosine-dependent tonic modulation of NMDA receptors.

4.2.3 Increasing the concentration of SCH58621 to 1 μM produced a similar absence of effect on the NMDA-R response

200 nM concentration of the A2A-R antagonist did not show a significant effect on NMDA-R response. The concentration was then increased to 1 μM to determine whether a higher concentration would be sufficient to produce a heightened modulation on NMDA-R current. After the first application of NMDA the average inward NMDA-R current was 535 ± 67 pA (mean ± SEM, N=14 cells from 3 rats). In the presence of 1 μM SCH58621, the NMDA-R current was 652 ± 56 pA (paired t-test P=0.08, N=14) (figure 4.3B). Increasing the concentration of A2A-R antagonist did not significantly increase in NMDA-R current. 200 nM

SCH58621 produced an 18 ± 8% increase, whereas 1 μM SCH58621 showed a 43 ± 19% increase in NMDA-R inward current.

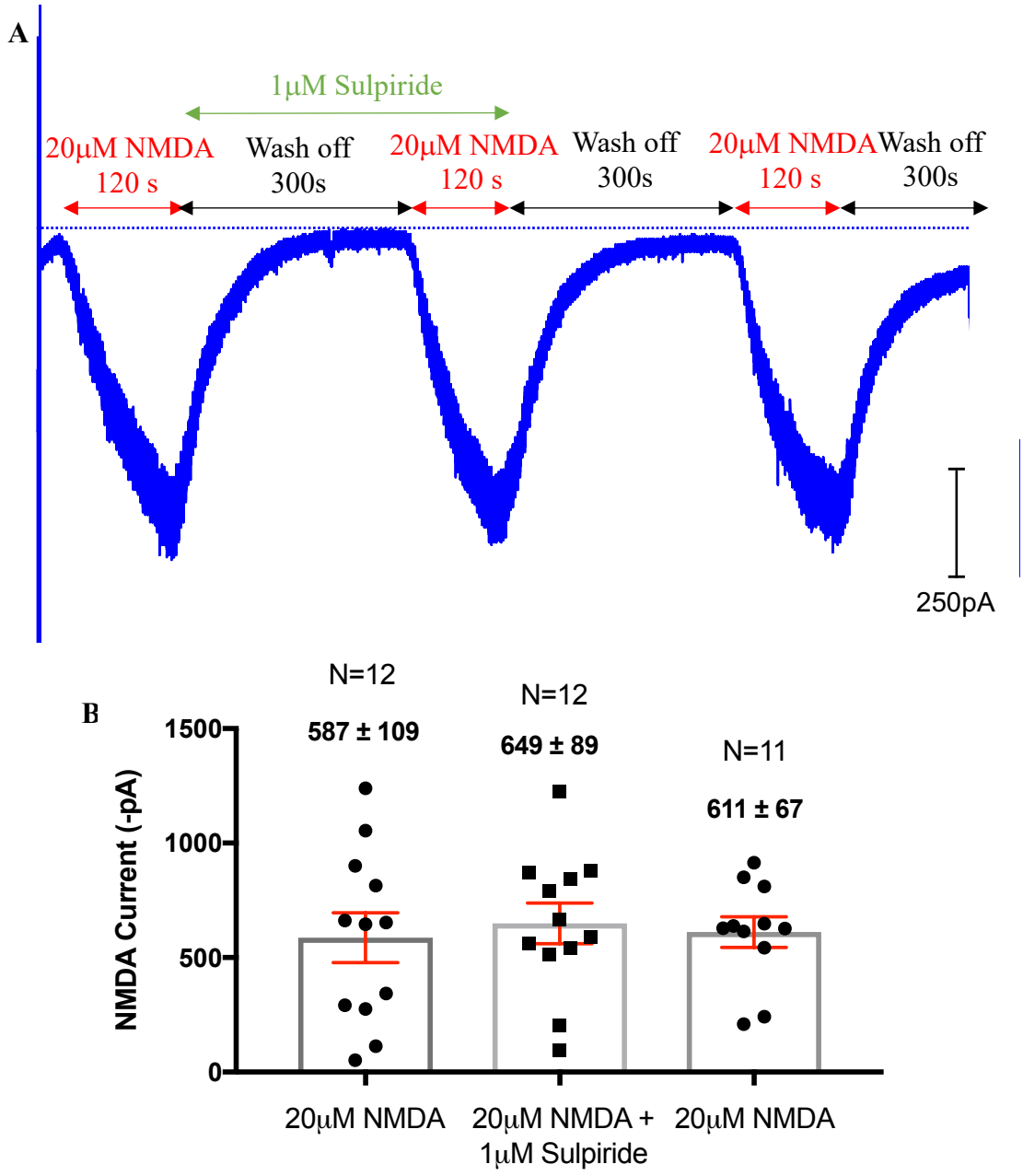

Figure 4.1 Sulpiride, a D2-R antagonist, shows no significant effect on average NMDA-R response in P28 rats*. A) A trace illustrating the experimental protocol. Three applications of 20 μM NMDA and 10 μM glycine were performed interrupted by five minutes of wash off with recording solution after each. 1 μM Sulpiride was pre-applied for 5 mins. B) A graph showing the mean steady-state NMDA-R current in presence of 1 μM sulpiride.*

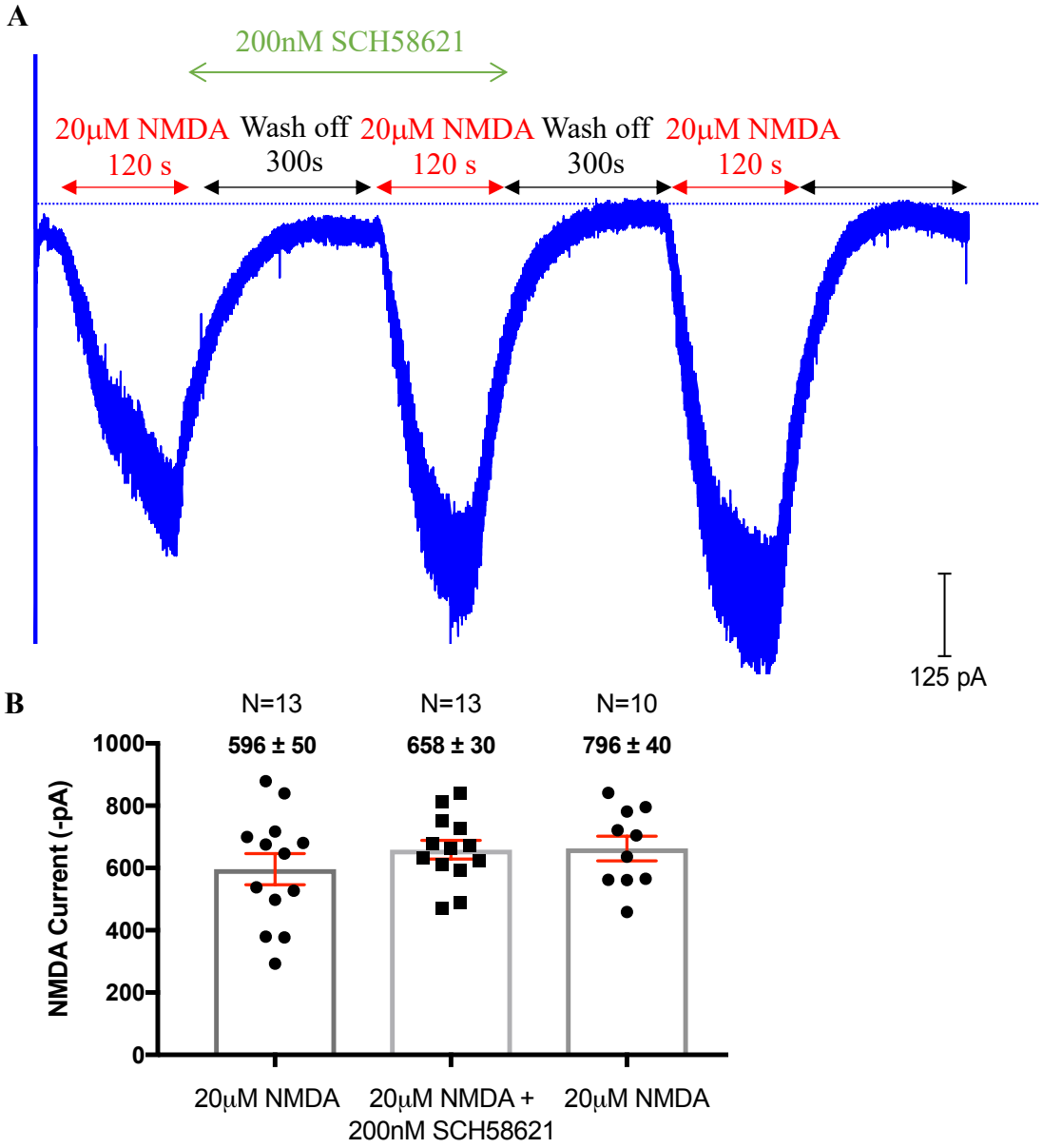

Figure 4.2 200 nM SCH58621, an A2A-R antagonist did not change the NMDA-R current. *A) The trace demonstrates he pre-application protocol of 200 nM SCH58621 for 300 s. It was then introduced in the presence of 20 μM NMDA. B) The graph shows the scatter of responses in the presence of 20 μM NMDA alone and in the presence of 200 nM SCH58621 (N=13 cells, 3 rats).*

4.2.4 Activating Adenosine 2A-Receptors potentiates the NMDA-receptor steady state current in dopaminergic neurons

1 μM CGS21680 was used to activate A2A-Rs on dopaminergic neurons to determine whether they could potentially demonstrate the endogenous effects of A2A-R activation on NMDA-R modulation. The control protocol produced a steady-state inward current of 584 ± 80 pA (mean ± SEM, N=12 cells from 7 rats). In comparison to the control application of 20 μM NMDA, the second response, in the presence of 1 μM CGS21680, produced a statistically significant increase in NMDA-R response with a mean current of 818 ± 134 pA (paired T-test, P=0.05; N=12) (figure 4.4A & B). CGS21680 was finally washed off and a third application of NMDA was performed to determine the reversibility potential of A2A-R activation via CGS21680. Despite the absence of the agonist, the steady-state NMDA-R inward current continued to increase, however at a much lower rate. 1 μM CGS21680 produced a 46 ± 16% increase in NMDA-R current relative to the control, and when washed off, the following NMDA-R current only produced a 12% increase in mean current. At 10 μM, CGS21680 did not significantly increase the NMDA-R response from 796 ± 134 pA to 869 ± 113 pA (paired T-test, P=0.36; N=13 from 5 rats) (figure 4.5A &B). When 10 μM CGS21680 was washed off, a third application of NMDA on its own, produced a decreased response that was trending towards statistical significance. Figure 4.5C compares the immediate effects of CGS21680 at 1 μM and 10 μM. As mentioned above, 1 μM CGS21680 produced a 46 ± 16% increase in mean current compared to much lower effect at 10 μM (18 ± 9%).

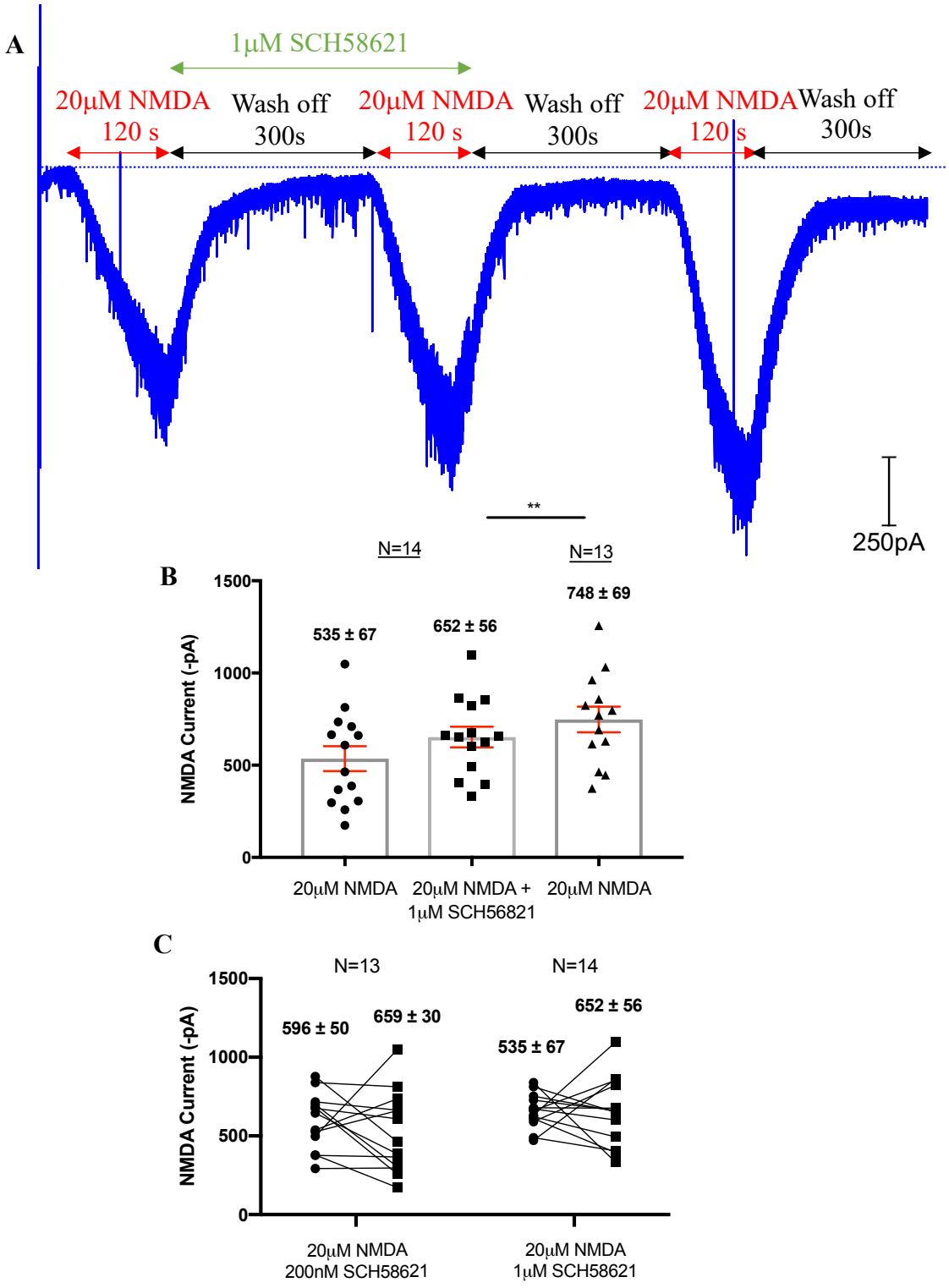

Figure 4.3 The effect of the adenosine A2A receptor antagonist, SCH58621 (1 μM) on NMDA-R currents. *A) A trace demonstrating the protocol performed and resulting inward currents. B) A graph highlighting the increasing trend in NMDA-R response in the presence of 1 μM SCH58621 and 20 μM NMDA. C) A comparison of the effects between 200 nM (as in Figure 4.2B) and 1 μM SCH58621 on NMDA-R steady state current.*

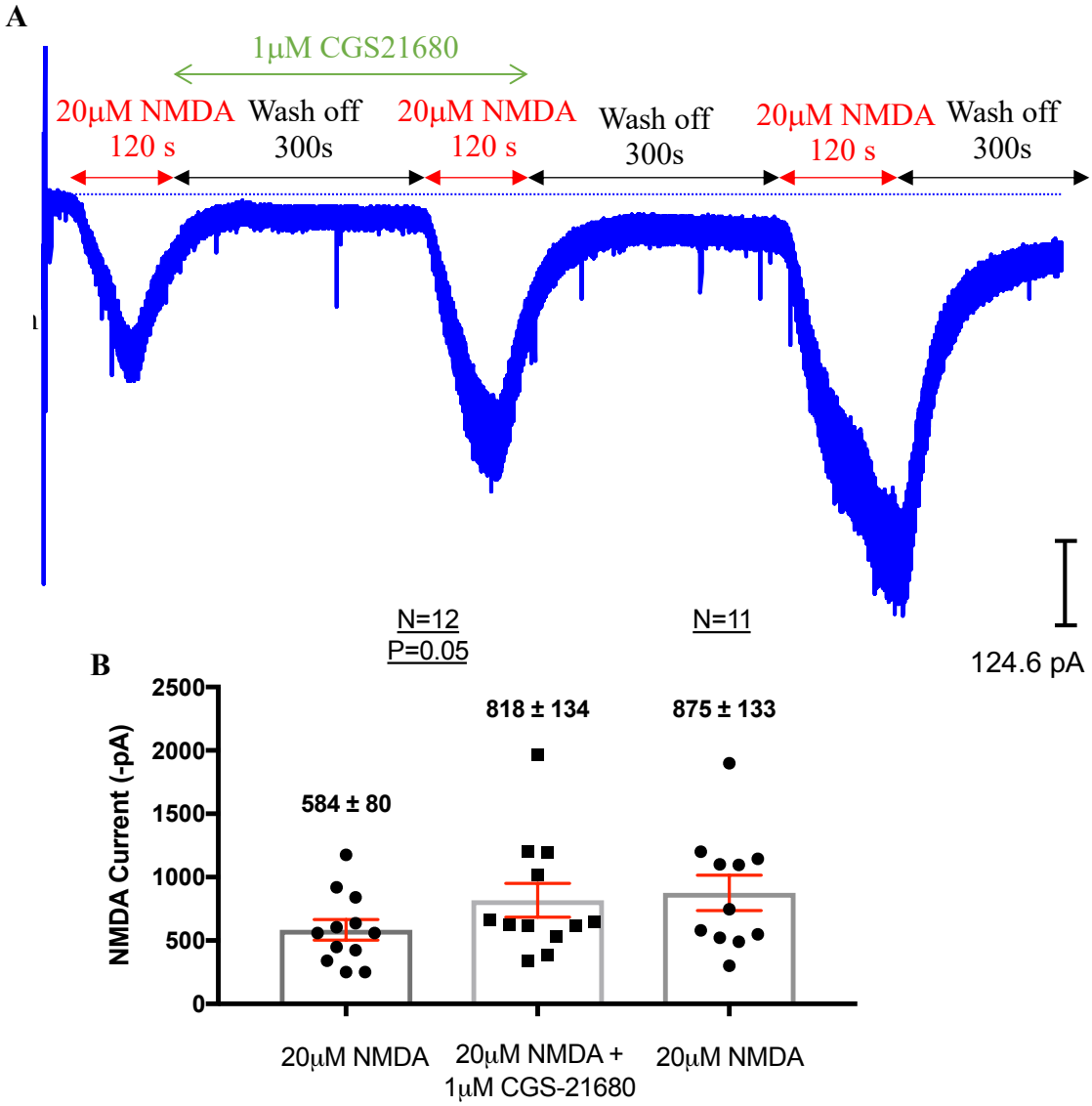

Figure 4.4 A2A-R agonist, CGS21680 was used to test for an effect of A2A-R activation on NMDA-R response. *A) Three repeated measures of NMDA were carried out. 1 μM CGS21680 was pre-applied before being introduced in the presence of 20 μM NMDA for 120 secs. B) A quantitative analysis of the mean NMDA-R inward current (mean ± SEM, N=12 cells from 7 rats).*

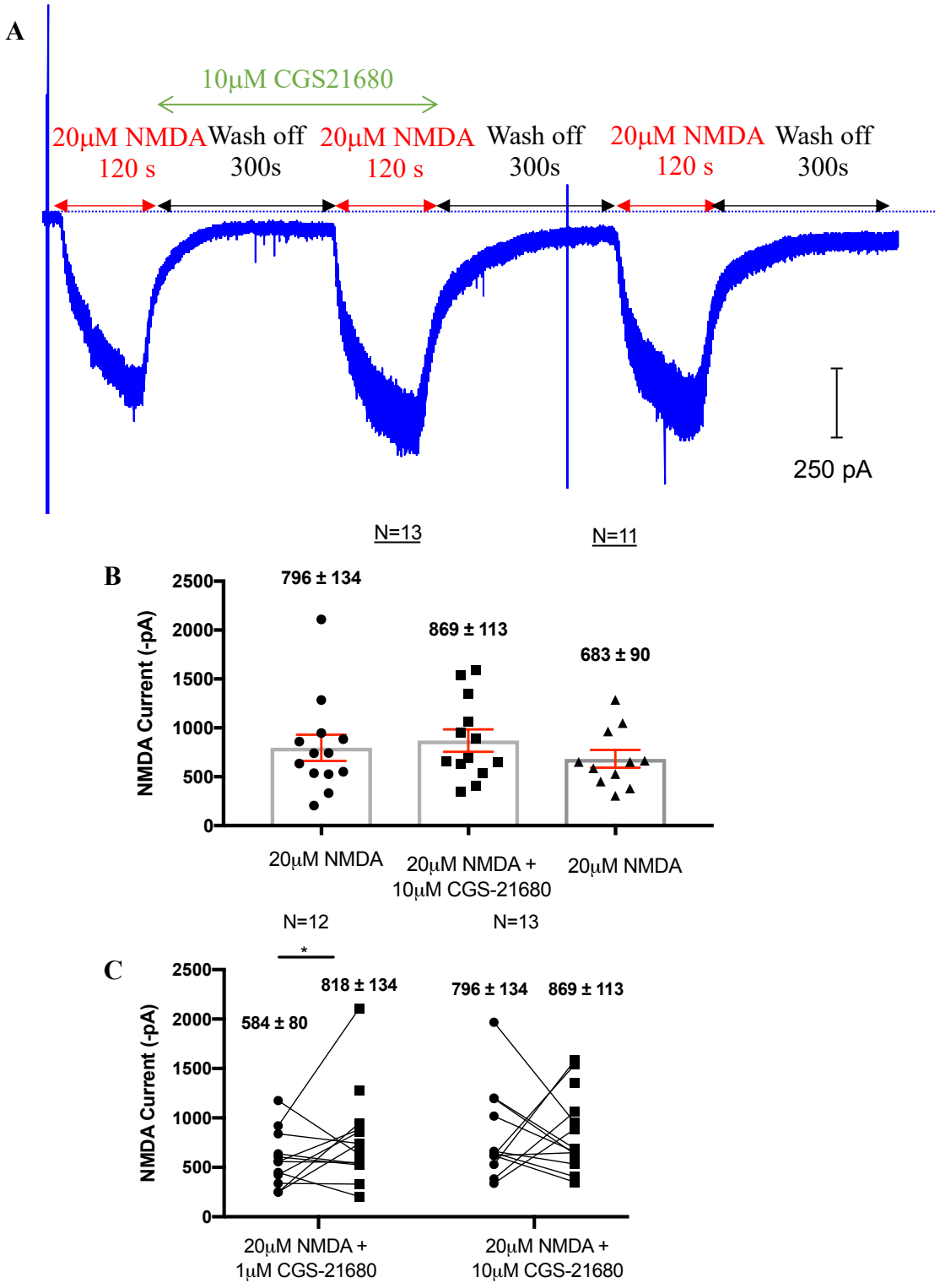

Figure 4.5 The effect of increasing the concentration of CGS21680 on NMDA-R response. *A) Trace highlighting the pre-application of 10 μM CGS21680. B) Graph showing the mean NMDA inward current produced in absence and presence of CGS21680. C) A comparison of the effects of different concentrations of CGS21680 on NMDA-R steady state current (1st column in each grouped data is 20μM Control followed by CGS-21680 data).*

4.2.5 Blocking A2A-Rs in the presence of a D2-R agonist, did not increase the NMDA-R current

After studying the effects of D2-R and A2A-R agonist and antagonist, respectively, they were examined simultaneously to determine potential effects of activating the hypothesized heterodimer. After the first application of NMDA an inward current of 636 ± 123 pA was produced. 200 nM Ropinirole (D2-R agonist), and 200 nM SCH58621 (A2A-R antagonist) were pre-applied for 5 mins prior to activating the NMDA-Rs (figure 4.6A). The second NMDA-R response in the presence of both drugs of interest produced a mean steady-state inward current of 704 ± 94 pA (figure 4.6B) (P=0.4; N=11 cells from 6 rats). When ropinirole and SCH58621 were washed off, the following NMDA-R current did not change relative to the initial control current.

4.2.6 Blocking both D2-Rs and A2A-Rs increased the NMDA receptor response

Sulpiride, the D2-R antagonist was used to block the receptors in the presence of the A2A-R antagonist, SCH58621 to determine the potential and extent to which tonic activation of the receptors may be involved in NMDA-R modulation. After the first control application of 20 μM NMDA for 120 secs, there was an increase in inward current by 562 ± 86 pA (mean ± SEM; N=14 cells from 6 rats) relative to the baseline (figure 4.7 A& B). The NMDA was then washed out with simultaneous pre-application of 1 μM Sulpiride and 200 nM SCH58621. When NMDA was applied a second time, in the presence of both drugs of interest, there was a statistically significant increase in the steady-state NMDA current. The corresponding response showed a 75 ± 24% increase in current to 830 ± 83 pA (N=14, paired T-Test- P=0.001) (figure 4.7B). Figure 4.7C, highlights the differences between D2-Rs activation (with ropinirole) and inhibition (with sulpiride) in the presence of an A2A-R blocker. Evidently, D2-Rs seem to have a potential role in the modulation of NMDA-Rs when A2A-Rs are blocked.

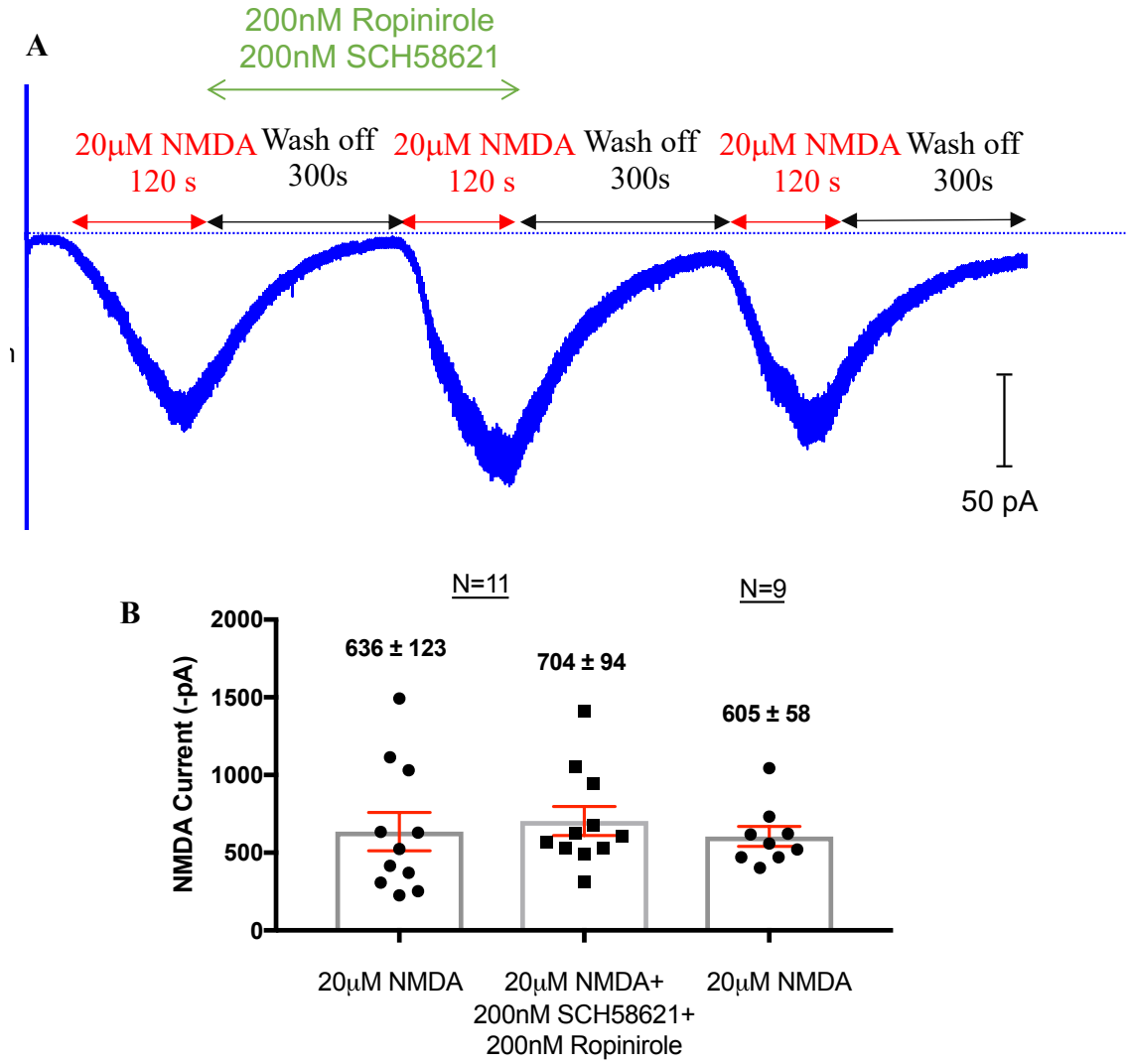

Figure 4.6 Test of hypothesized D2-A2A receptor heterodimer interaction via the inhibition of A2A-R and simultaneous activation of D2-R*. A) A trace showing the application method of the drugs of interest. B) the quantitative analysis of NMDA-R response before and after the simultaneous activation and inhibition of D2-R and A2A-R, respectively.*

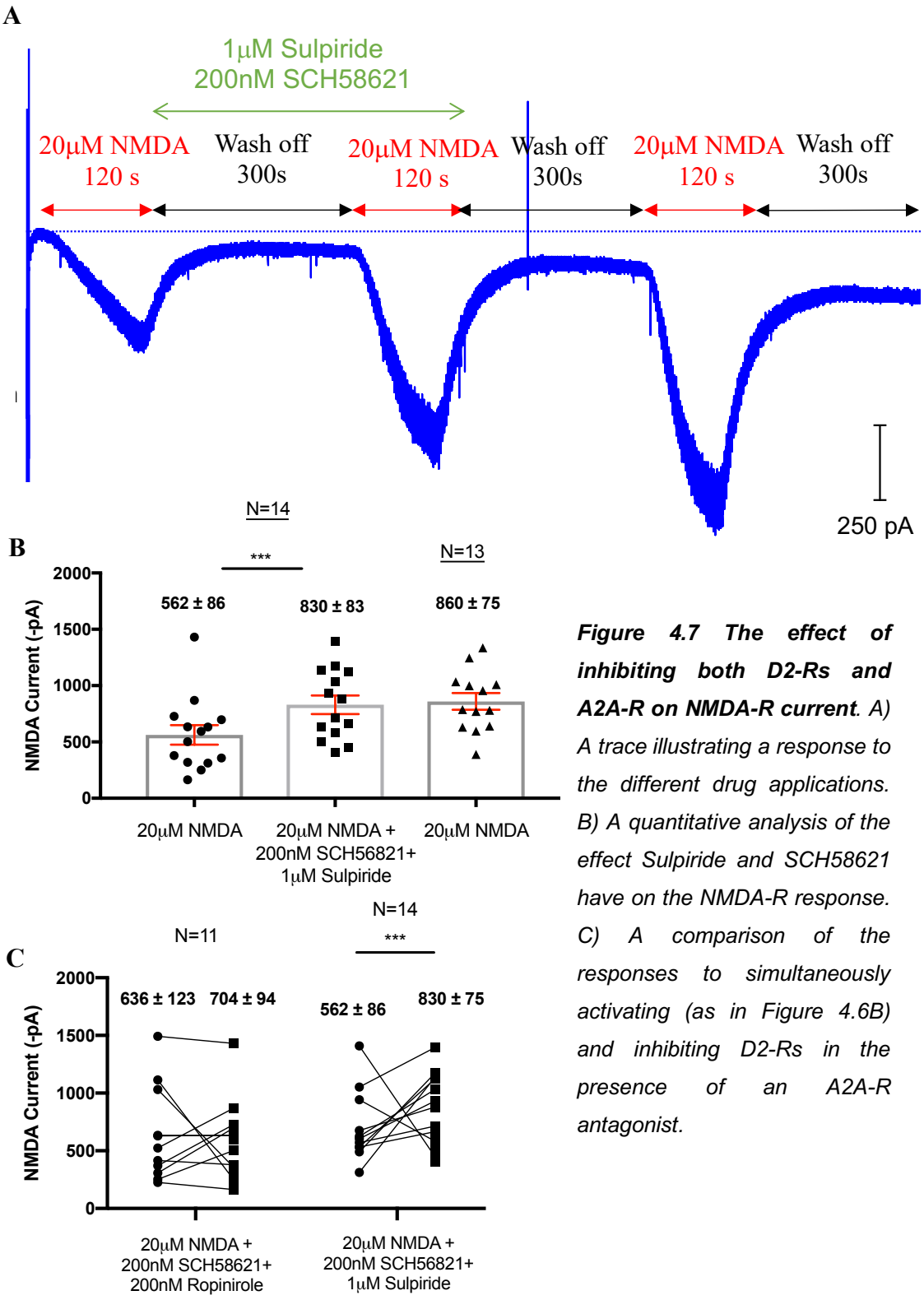

Figure 4.7 The effect of inhibiting both D2-Rs and A2A-R on NMDA-R current*. A) A trace illustrating a response to the different drug applications. B) A quantitative analysis of the effect Sulpiride and SCH58621 have on the NMDA-R response. C) A comparison of the responses to simultaneously activating (as in Figure 4.6B) and inhibiting D2-Rs in the presence of an A2A-R antagonist.*

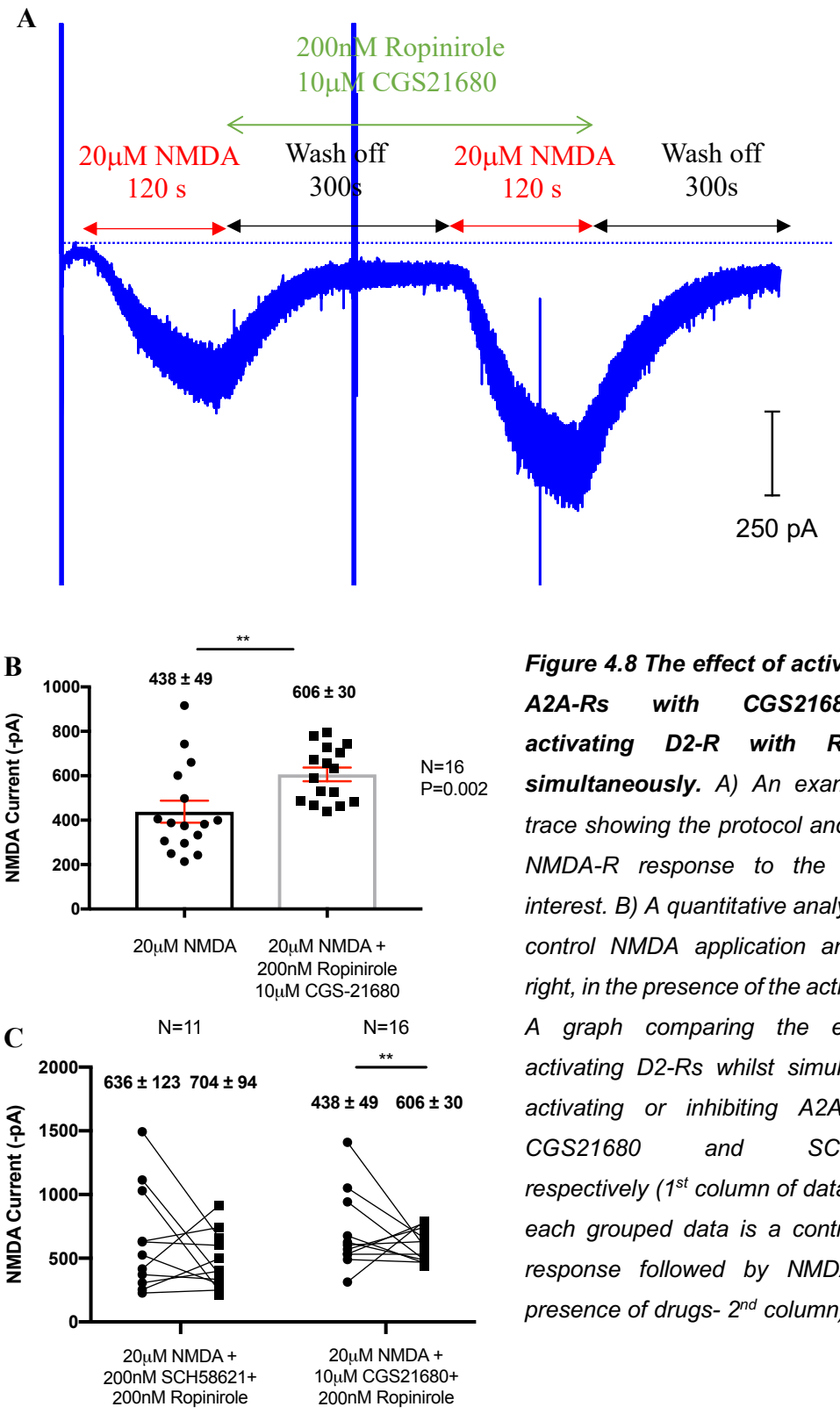

Figure 4.8 The effect of activating the A2A-Rs with CGS21680 and activating D2-R with Ropinirole simultaneously. *A) An example of a trace showing the protocol and average NMDA-R response to the drugs of interest. B) A quantitative analysis of the control NMDA application and to the right, in the presence of the activators. C) A graph comparing the effects of activating D2-Rs whilst simultaneously activating or inhibiting A2A-Rs with CGS21680 and SCH586212, respectively (1st column of data points in each grouped data is a control NMDA response followed by NMDA in the presence of drugs- 2nd column).*

4.2.7 Combined activation of D2-Rs and A2A-Rs significantly increased the NMDA-R response

As shown in section 4.2.5, blocking the A2A-R possibly allowed the D2-R to exert some effect, which might be pronounced had there been prolonged exposure to the drug. To determine whether the A2A-R was vital in modulating the NMDA-R response, 200 nM ropinirole was introduced in the presence of an A2A-R agonist, CGS21680 at 10 μM. Figure 4.8 A shows the preincubation of the receptors for 300 secs with ropinirole and CGS21680 and the effect on NMDA-R responses. The first control application of 20 μM NMDA on its own, produced a steady state current of 438 ± 49 pA (mean ± SEM, N=16). After washing off NMDA followed by pre-incubation with ropinirole and CGS-21680, a second application of NMDA was performed. This produced a statistically significant increase in inward current to 606 ± 30 pA (N=16; Paired T-Test, P=0.002), a 27 ± 7% increase. Relative to the controls of each experiment, activating the hypothesized heteroreceptor showed to have a greater impact on the NMDA-R response (figure 4.8 C).

4.2.8 Inhibiting D2-Rs with 1 μM sulpiride and activating the A2A-R with CGS21680, modulated the NMDA-R

The first application of 20 μM NMDA was applied for 120 secs and an inward current of 831 ± 99 pA (mean ± SEM; N=18) was achieved (figure 4.9 A & B). NMDA was then washed off for 300 secs whereby sulpiride and CGS21680 were pre-applied to allow the D2 and A2A receptors to equilibrate. This brought the current close to baseline. NMDA was then applied in the presence of sulpiride and CGS21680 and produced a statistically significant increase in NMDA-R response relative to the control. The corresponding current was 990 ± 93 pA (N=18; Paired T-test, P=0.04) (figure 4.9 A & B). The drugs were then washed off for a period of 300 secs prior to a final application of NMDA. This produced an even greater response of 1054 ± 92 pA (N=15), however the response was not statistically different to the second NMDA application. It is

evident that activating the A2A-R, regardless of the compound bound to D2-R, will significantly modulate NMDA-Rs (figure 4.9 C).

4.2.9 Applying equimolar concentrations of an A2A-R agonist and antagonist favours an increase in NMDA steady-state current

Both A2A-R agonist and antagonist were applied simultaneously at equimolar concentrations with approximately equal binding (estimated 98% receptor occupancy). After the first control application of 20 μM NMDA, a steady-state inward current of 489 ± 72 pA (mean ± SEM, N=16 cells from 3 rats) was produced. NMDA was then washed off for 300 secs whilst 1 μM SCH58621 and 1 μM CGS21680 were pre-applied simultaneously (figure 4.10). 20 μM NMDA was then applied in the presence of the A2A-R agonist and antagonist producing an NMDA inward current of 602 ± 54 pA. The increase was of statistical significance relative to the control (N=16; Paired T-test, P=0.03) (figure 4.10 B) producing a 20 ± 8% increase in current. The third NMDA-R current did not change relative to the previous drug application, 644 ± 60 pA (N=14).

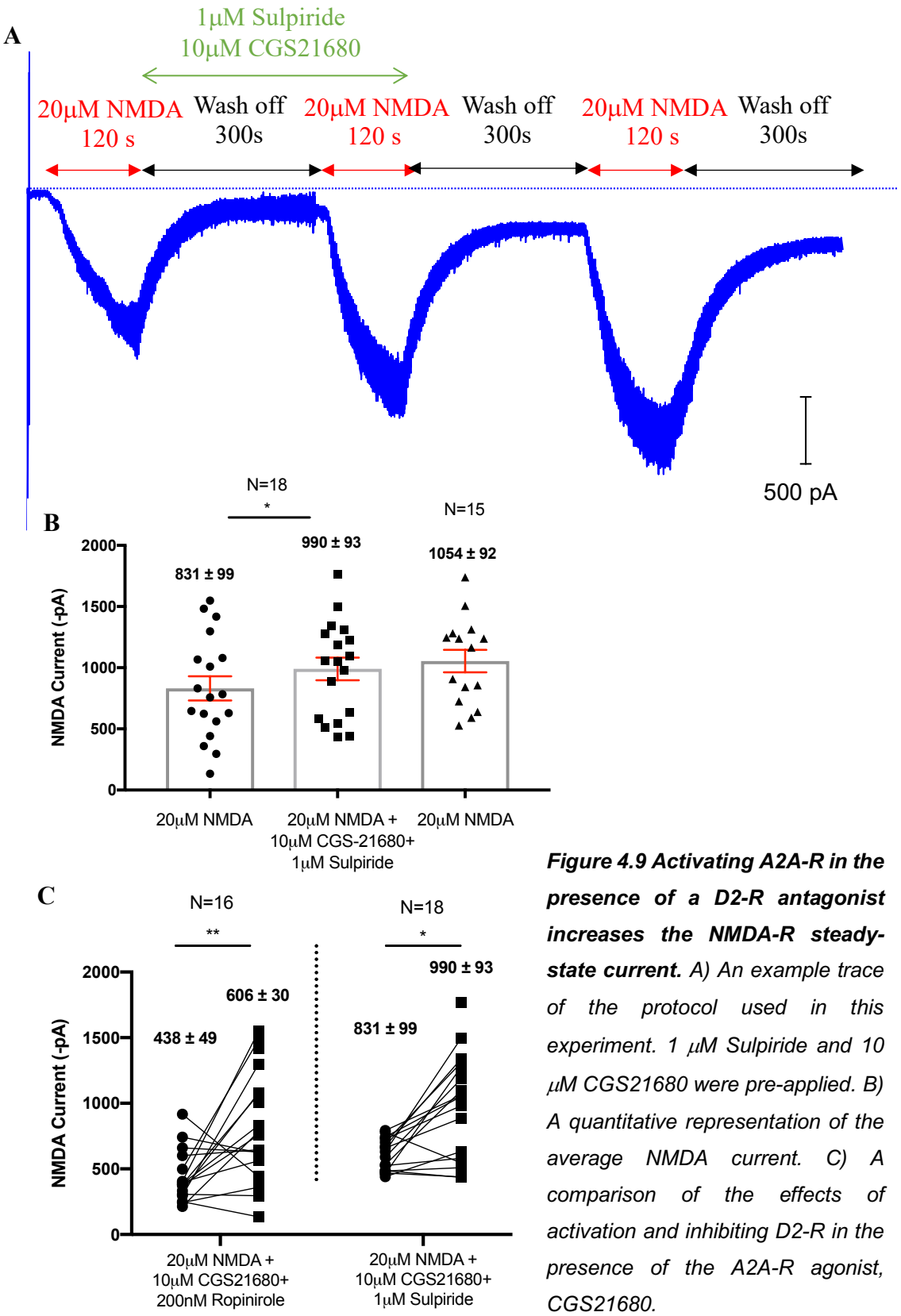

Figure 4.9 Activating A2A-R in the presence of a D2-R antagonist increases the NMDA-R steady-state current. *A) An example trace of the protocol used in this experiment. 1 μM Sulpiride and 10 μM CGS21680 were pre-applied. B) A quantitative representation of the average NMDA current. C) A comparison of the effects of activation and inhibiting D2-R in the presence of the A2A-R agonist, CGS21680.*

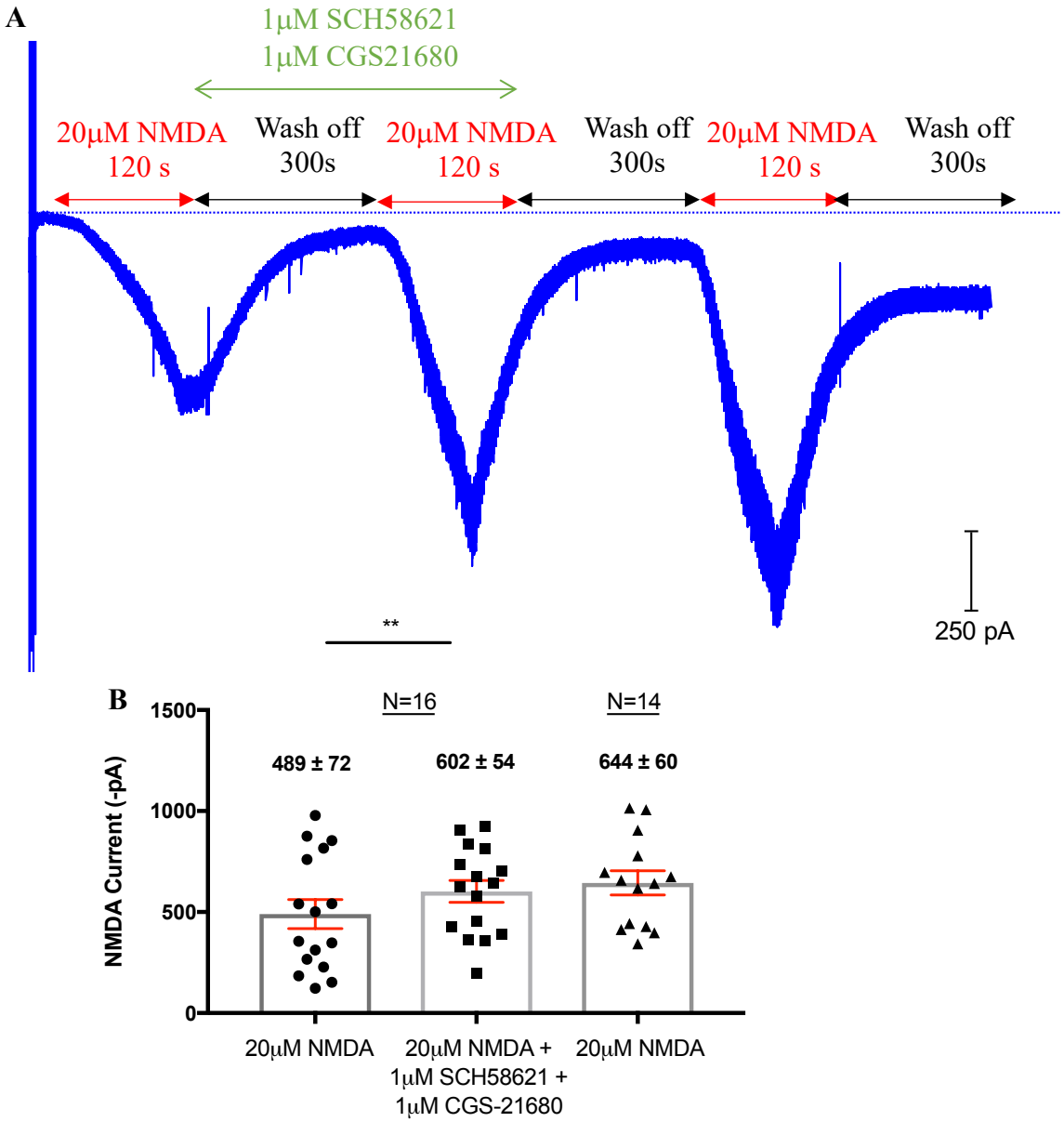

Figure 4.10 A test to determine the effect of applying an A2A-R agonist and antagonist simultaneously on NMDA-R current in substantia nigra dopaminergic neurons. *A) An example trace depicting the protocol used in the experiment. B) A graph showing the spread and averaged data obtained with 3 applications of NMDA.*

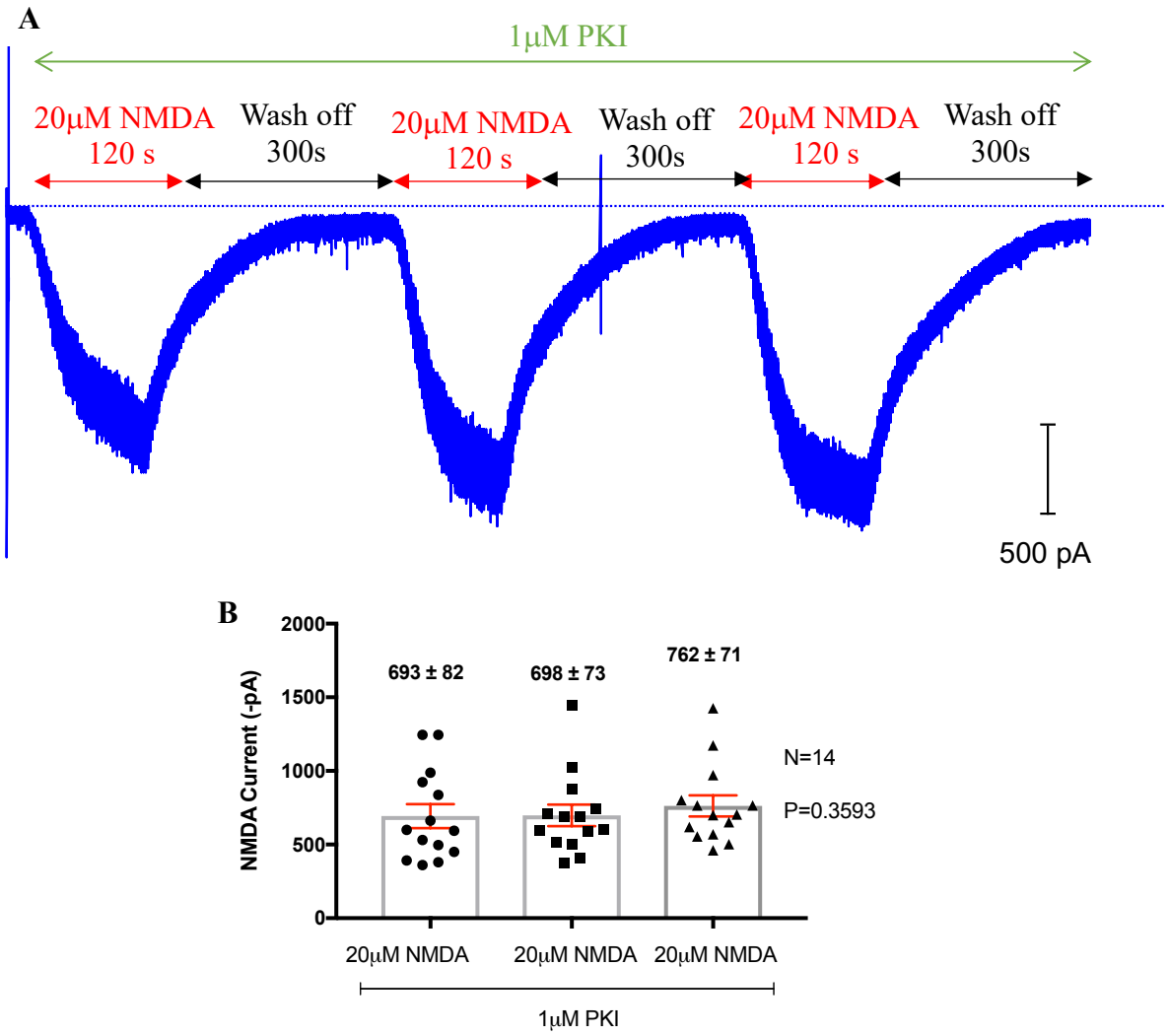

Figure 4.11 Inhibiting part of the 2nd messenger system by introducing a PKA inhibitor, 1 μM PKI directly into the dopamine cell of the substantia nigra*. A) A trace depicting NMDA responses in presence of PKI throughout the experiment. B) A quantitative analysis of repeated applications of NMDA in the presence of 1 μM PKI (One-way ANOVA).*

4.2.10 Inhibiting the production of cyclic AMP did not seem to modulate NMDA-R response during 3 applications of 20 μM NMDA

PKI was introduced into the pipette solution to determine whether NMDA-R modulation was dependent on PKA in P28 dopaminergic neurons of the substantia nigra. It was added to the pipette solution therefore granting it direct access to the cytoplasm and was thus present throughout the experiment (figure 4.11 A). The three applications of NMDA for 120 secs were each followed by a 300 sec period of wash off. The first application of NMDA produced an inward current of 693 ± 82 pA (mean ± SEM, N=14 cells from 3 rats), 698 ± 73 pA after the second, and 762 ± 71 pA after the final application of NMDA in the presence of PKI. The differences between the currents were not statistically significant (One-way ANOVA, P=0.3593) (figure 4.11 B). These findings were compared to the equivalent control experiments in the absence of PKI (Figure 3.9B) and there were no significant effects of time of NMDA application (1^{st}, 2^{nd} or 3^{rd}) or differences in NMDA-R current in presence of PKI (2-way ANOVA, P=0.93).

4.2.11 D2-R agonist, Ropinirole decreases the NMDA-R current in the presence of raised cAMP concentration in the cell

Forskolin was introduced to increase the intracellular concentration of cAMP to possibly allow ropinirole to exert any effect. Due to the partially invasive method of accessing the internal environment of the cell, $[cAMP]_i$ could have decreased relative to normal. Therefore, increasing its concentration could potentially have an effect on NMDA-R current in the presence of the D2-R agonist. A control study was performed to determine whether increasing the cAMP would in turn increase the NMDA-R response. The first control application of 20 μM NMDA gave a mean inward current of 500 ± 83 pA (mean ± SEM). 0.5 μM Forskolin was then pre-applied to allow it time to penetrate the cell membrane (figure 4.12 A). When 20 μM NMDA was then applied in presence of Forskolin, the mean steady-state inward current increased significantly to 688 ± 73 pA (paired T-test, P=0.01, N=14 cells, from 4 rats) (figure 4.12 B). The two compounds were then washed off for 300 secs and a third application of NMDA was performed to

determine whether there was any residual effect of the Forskolin. The mean inward current produced was 822 ± 92 pA. The continued increase in NMDA response was statistically significant relative to the previous application of NMDA and Forskolin (Paired T-test, P=0.02, N=14). A One-way ANOVA for the whole experiment produced a P value of 0.0312, indicating a significant trend towards elevating the NMDA-R current in the presence of 0.5 μM Forskolin.

After performing the control experiment with 0.5 μM Forskolin, 200 nM ropinirole (D2-R agonist) was then introduced to determine whether its effect on NMDA-R current could be elucidated. Initially, 20 μM NMDA was applied as a control for reference, producing a mean steady-state inward current of 461 ± 80 pA (mean ± SEM). 0.5 μM Forskolin was then pre-applied for 300 secs (figure 4.13 A). Thereafter, Forskolin was applied in the presence of NMDA for 120 secs, producing a mean current of 597 ± 74 pA. The increase as seen in section 4.13, was of statistical significance (paired T-test, P=0.03, N=13 cells from 5 rats). Forskolin and NMDA were then washed off. Meanwhile 200 nM ropinirole was introduced to allow the D2-Rs to equilibrate (figure 4.13 A). 200 nM ropinirole was then applied with 20 μM NMDA producing a mean inward current of 580 ± 60 pA. Although the current difference was not statistically different, a declining trend was evident. This decline continued into the second application of NMDA in the presence of ropinirole (512 ± 68 pA) (figure 4.13 B). Overall, despite no significant difference in current (One-way ANOVA, P=0.5512), there is an obvious decreasing trend in NMDA-R current in the presence of ropinirole, possibly owing to the sufficient presence of cAMP induced by Forskolin.

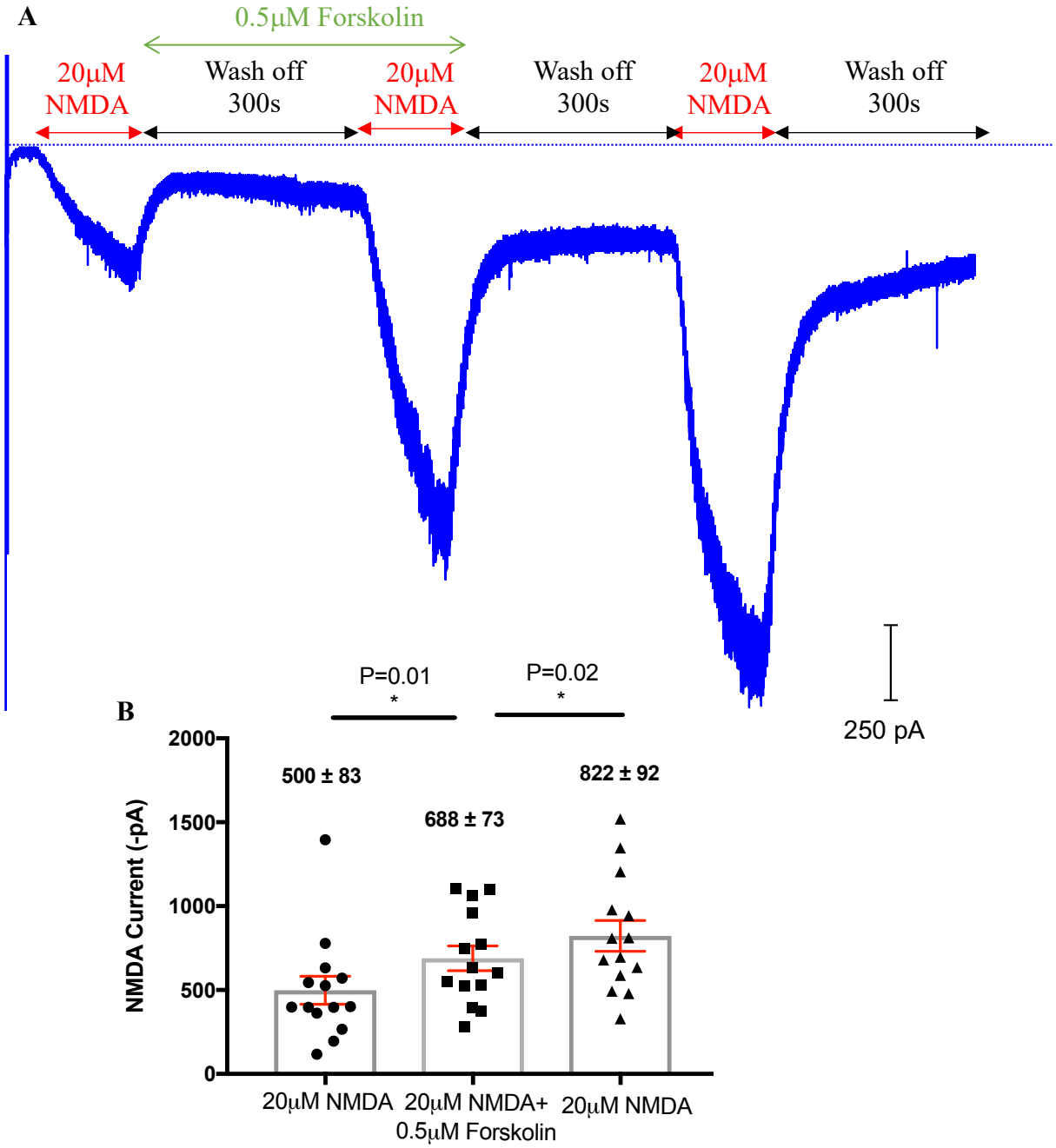

Figure 4.12 The impact of Forskolin treatment to increase cAMP concentration in the cell on NMDA-R inward current. *A) An example trace showing forskolin's application in the experiment. B) A quantitative representation of the repeated applications of NMDA in the absence (control) and presence of 0.5 μM forskolin.*

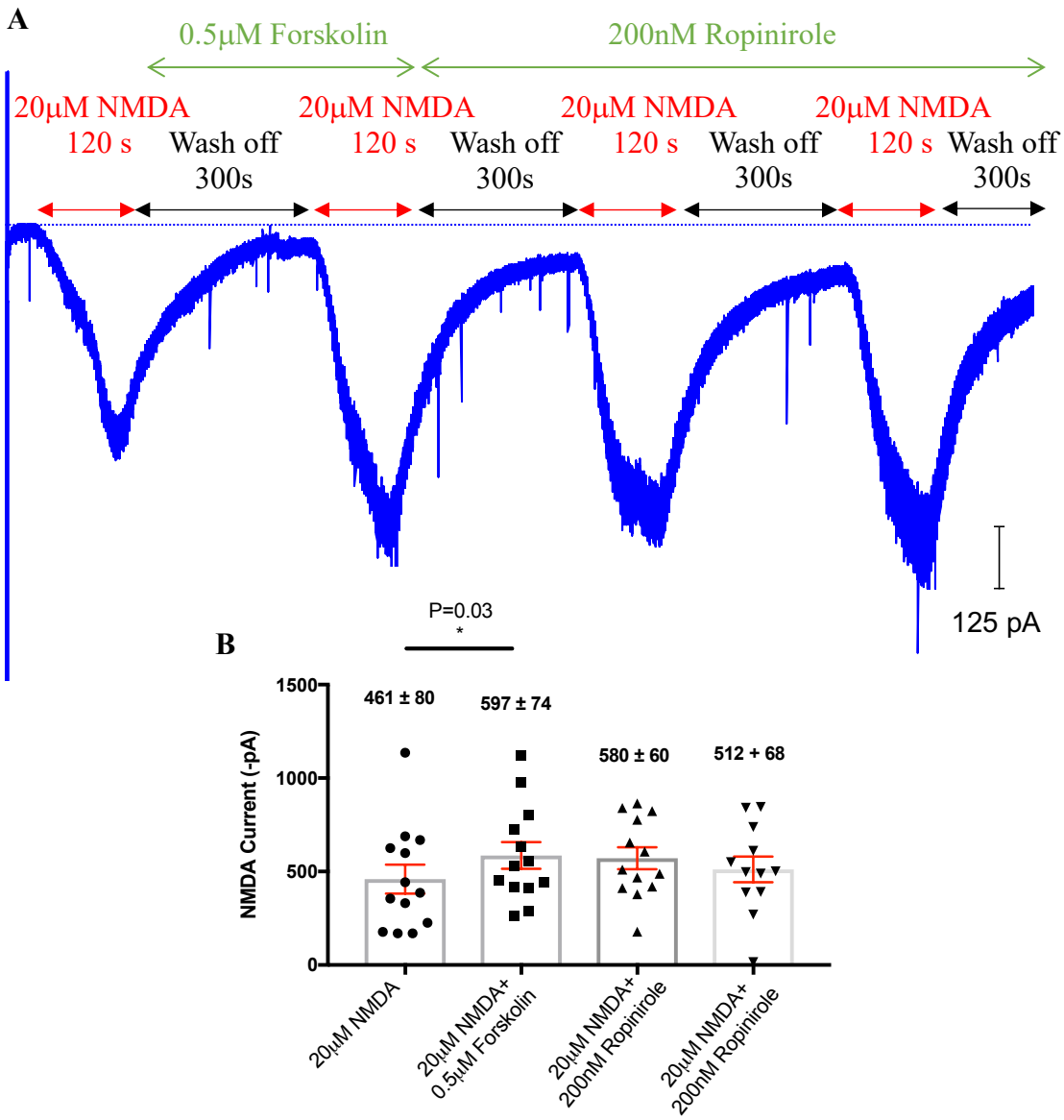

Figure 4.13 Ropinirole may occlude run up effect of forskolin. *A) A trace representing the experimental protocol. Both drugs (indicated in green) were pre-applied for 300 secs. B) A graphical representation of mean currents produced in the presence of 20 µM NMDA.*

4.2.12 Increasing the concentration of Forskolin to 2.5 μM did not increase the effect on NMDA-R response any more than 0.5 μM, nor did this further translate into an enhanced effect upon addition of a D2-R agonist

The concentration of forskolin was increased to 2.5 μM to determine whether possibly increasing the accumulation of cAMP would in turn increase the effect on NMDA-R inward current even further. After the first application of 20 μM NMDA, a mean steady-state inward current of 419 ± 78 pA (mean ± SEM) was achieved. As in figure 4.12, forskolin was pre-applied for 300 secs before introducing NMDA. Upon NMDA application in the presence of forskolin, the average inward current produced a statistically significant increase at 551 ± 54 pA (paired T-test, P=0.03, N=13). Forskolin and NMDA were then washed off. NMDA was finally applied to determine whether there was any residual forskolin effect on the NMDA-R response. The current continued to increase in its absence (596 ± 57 pA), however the increase was not statistically significant (N=11) (figure 4.14 B). Figure 4.16 C highlights the difference in NMDA-R response upon increasing concentrations of forksolin. It is evident that as the concentration of forksolin increases, a saturation level is met whereby the possible increase in cAMP levels do not increase NMDA-R response any further.

To mimic the previous experiment at a lower concentration of forskolin, 200 nM ropinirole was added. The first application of NMDA produced a mean current of 393 ± 63 pA. Forksolin was then pre-applied to allow it sufficient time to penetrate the cell membrane and take effect. 300 secs later, NMDA was introduced alongside forskolin for 120 secs. This increased the current significantly at 515 ± 54 pA (paired T-test, P=0.02, N=12) (figure 4.14 D). The two drugs were then washed off, as ropinirole was pre-applied. Upon NMDA application alongside ropinirole, the mean NMDA-R inward current began to decrease gradually at 459 ± 85 pA. However, the decrease in current was short-lived, as a final application of NMDA and ropinirole increased the overall NMDA-R current (624 ± 60 pA, N=11) (figure 4.14 D).

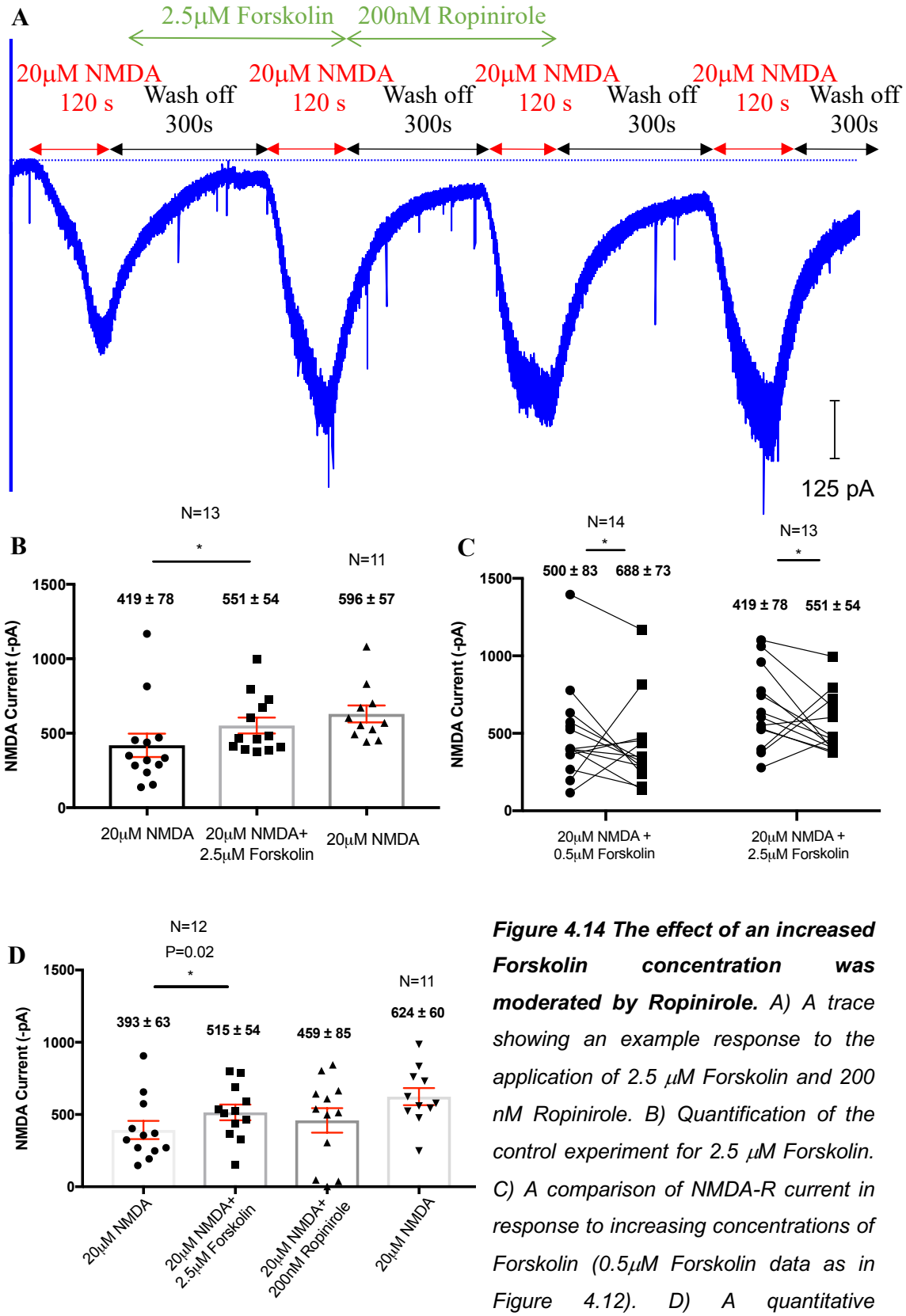

Figure 4.14 The effect of an increased Forskolin concentration was moderated by Ropinirole. *A) A trace showing an example response to the application of 2.5 µM Forskolin and 200 nM Ropinirole. B) Quantification of the control experiment for 2.5 µM Forskolin. C) A comparison of NMDA-R current in response to increasing concentrations of Forskolin (0.5µM Forskolin data as in Figure 4.12). D) A quantitative representation of activating D2-Rs at a*

4.2.13 Activating A2A-Rs and a simultaneous stimulation of cAMP production does not significantly increase the resulting NMDA-R response

Both CGS-21680 and Forskolin alone, have shown to increase the mean NMDA-R response significantly. In this experiment they were introduced simultaneously to determine whether or not they would demonstrate a summative effect on the resulting NMDA-R current. After the first application of 20 μM NMDA for 120 secs, an average current of 563 ± 63 pA (mean ± SEM) was produced. 2.5 μM Forskolin and 1 μM CGS-21680 were then pre-applied to allow cell penetration and receptor equilibration, respectively (figure 4.15 A). When NMDA was applied in their presence, a mean inward current of 662 ± 50 pA was produced (figure 4.15 B). The drugs were then washed off prior to a final application of NMDA alone. This produced an inward current of 801 ± 65 pA. Despite the trend to increase in current, the differences were not statistically significant (one-way ANOVA, P=0.15, N=11 cells from 3 rats).

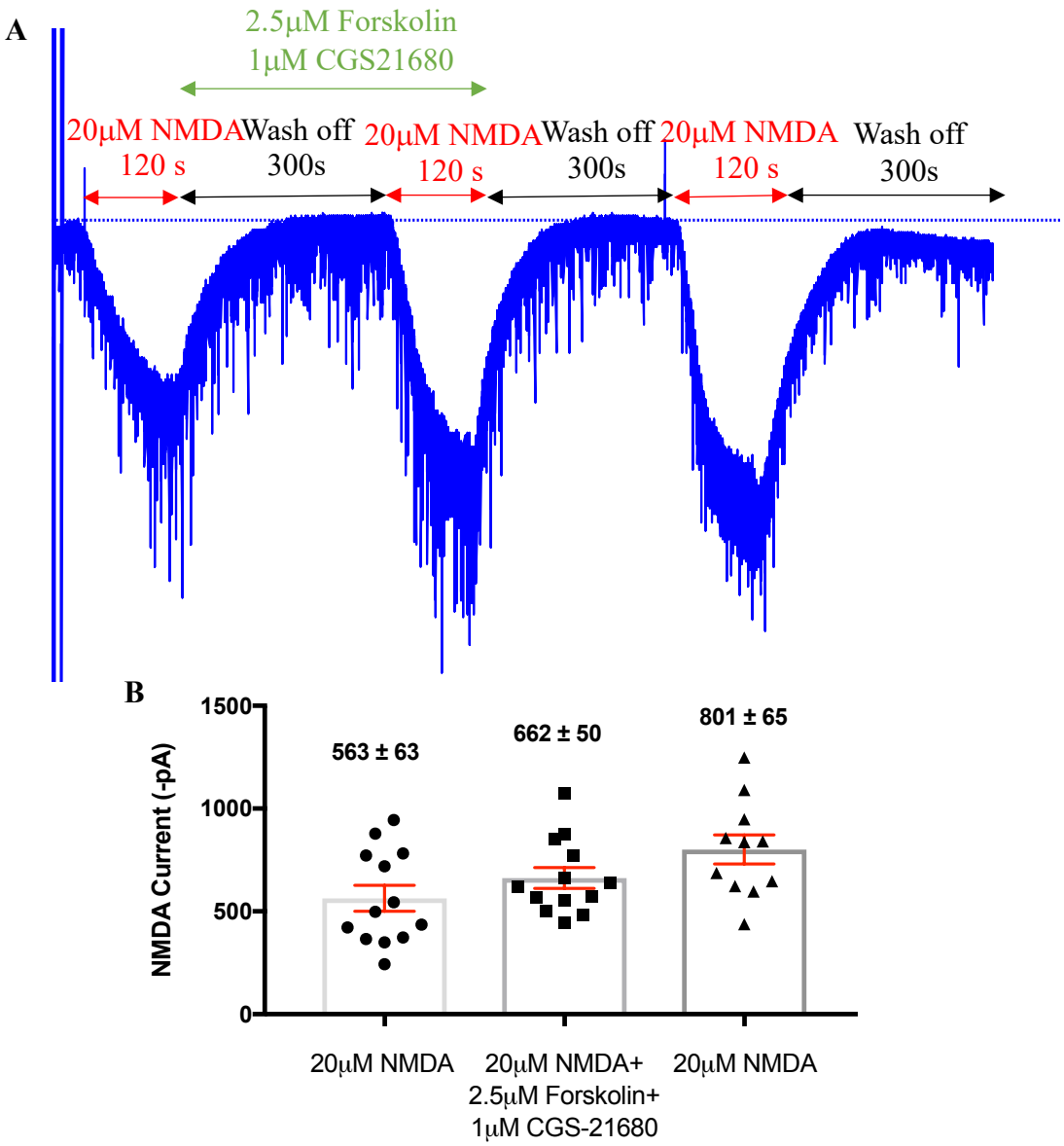

Figure 4.15 Activating A2A-Rs with simultaneous stimulation of cAMP production. *A) A trace showing the time of drug application during the whole-cell recording. B) Quantification of the average NMDA currents in response to addition of 2.5 μM Forskolin and 1 μM CGS-21680 simultaneously.*

4.2.14 Inhibiting PKA activity in the presence of forskolin, did not alter the effect of forskolin initially observed

1 μM PKI was introduced in the presence of forskolin to determine whether PKI required an increased concentration of cAMP in order to visualise any effect on NMDA-R response. As in section 4.12, PKI was introduced via the pipette solution to grant it direct access to the cell cytoplasm- thus, present throughout the recording (figure 4.16A). A control experiment with 20 μM NMDA produced a mean NMDA inward current of 412 ± 35 pA (mean ± SEM) (figure 4.16 B). 2.5 μM forskolin was then pre-applied for 300 secs after which NMDA was introduced producing a mean current of 604 ± 53 pA. The increase in current was statistically significant as observed previously in the absence of PKI (paired T-test, P=0.005, N=14). The two drugs were then washed off for 300 secs, prior to a final application of NMDA to elucidate a residual effect of forskolin. The steady-state NMDA current continued to increase to 689 ± 68 pA (N=11). Figure 4.18 C compares the effect of Forskolin alone, and in the presence of PKI. What is evident, is that in both cases, the increase in steady-state NMDA current is significant regardless of the addition of 1 μM PKI. In the absence of PKI, the current increases by 70 ± 30% when Forskolin is added. In the presence of PKI, the current increases by just 60%. Despite the current potentiation in both instances, there is a trend towards to a smaller increase as PKI is applied.

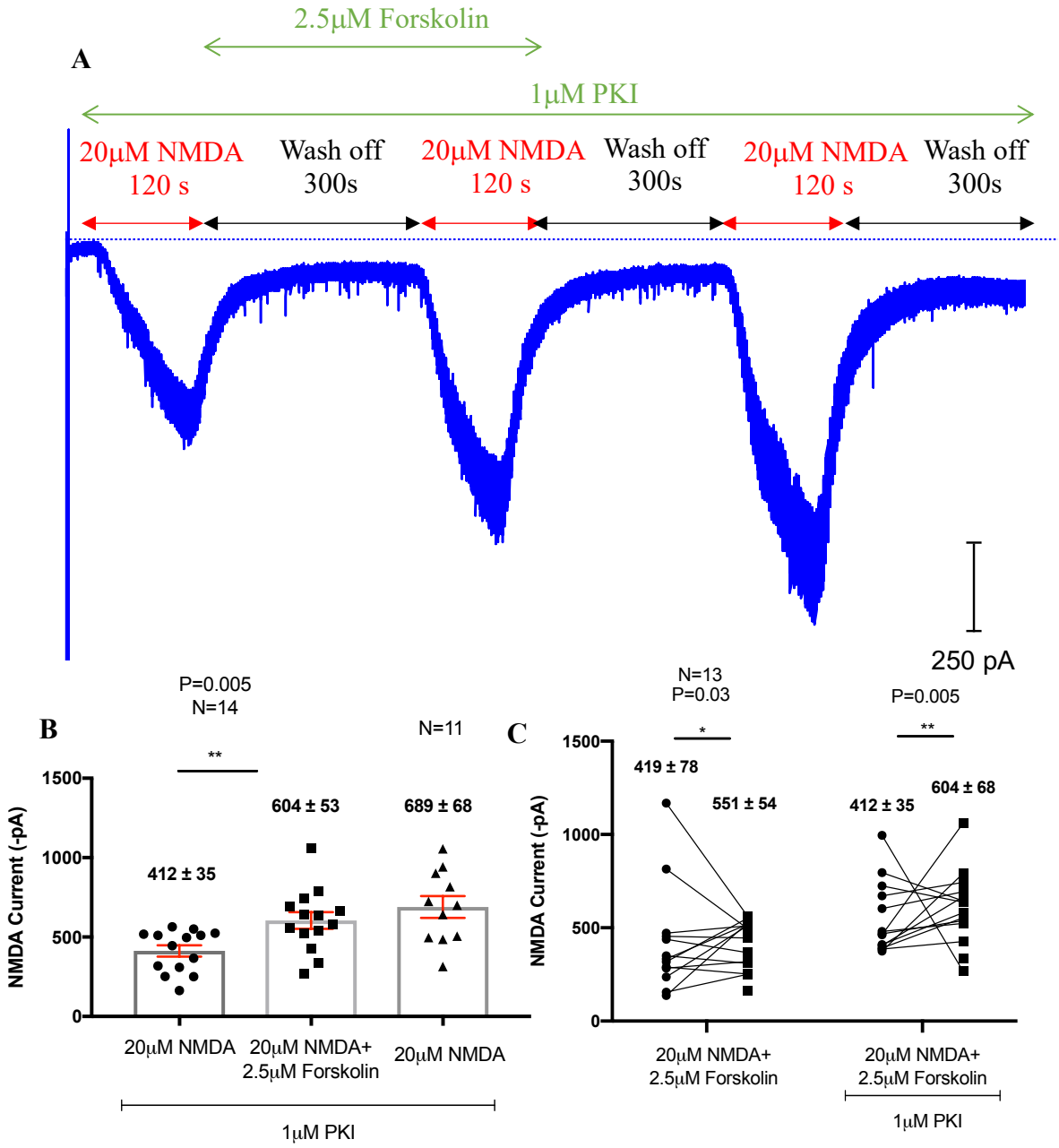

Figure 4.16 Experiment to inhibit PKA activity with PKI in the presence of 2.5 μM Forskolin. *A) A trace of a whole-cell recording. PKI was added to the pipette solution therefore present throughout the recording. Forskolin was pre-applied for 300 secs prior to the application of 20 μM NMDA. B) Quantification of the whole cell currents. C) A comparison of the effects of forksolin, in the absence and presence of PKI.*

4.3 Results Summary

Table 6 Summary of experiments investigating effect of hypothesized A2A-R and D2-R heteromers on NMDA-R response in P28 DAergic neurons of the substantia nigra

Experiment	Result	Statistical analysis
200 nM Ropinirole (D2-R agonist)	No significant effect on NMDA-R current.	Paired T-test: P=0.736; N=15, 5 Rats
Could inhibiting D2-Rs increase NMDA-R current?		
1 μM Sulpiride (D2-R antagonist)	No significant effect on NMDA-R current.	Paired T-test: P=0.354; N=12, 2 Rats
Does activating A2A-Rs enhance NMDA-R current?		
1 μM CGS 21690 (A2A-R agonist)	Produced a statistically significant increase in NMDA-R current.	Paired T-test: P=0.05; N=12, 7 Rats
200 nM SCH58621 (A2A-R antagonist)	Did not alter NMDA-R response.	Paired T-test: P=0.16; N=13, 3 Rats
1 μM SCH58621	Increasing trend in NMDA-R current	Paired T-test: P-0.08, N=14, 3 Rats
Does inhibiting both A2A-R and D2-R increase NMDA-R current?		
200 nM SCH58621 + 1 μM Sulpiride	Enhanced the NMDA-R current.	Paired T-test: P=0.001; N=14, 6 Rats
Will inhibiting A2A-Rs and activating D2-R decrease the NMDA-R response?		
200 nM SCH58621 + 200 nM Ropinirole	Slight increase in NMDA-R current (not statistically significant).	Paired T-test: P=0.4; N=11, 6 Rats
1μM SCH58621 + 1μM CGS-21680	Produced a statistically significant increase in steady-state NMDA-R current.	Paired T-test: P=0.03; N=16, 3 Rats
Does increasing cAMP, increase NMDA-R current?		
0.5μM Forskolin (cAMP activator)	Increased NMDA-R current.	Paired T-Test: P=0.01, N=14, 4 Rats
200nM Ropinirole + 0.5μM Forskolin	Decreasing trend in NMDA-R current, however the change in current was not statistically significant.	One-way ANOVA: P=0.5512; N=13, 5 Rats

1 μM PKI (PKA inhibitor)	No significant effect on NMDA-R current.	One-Way ANOVA P=0.3593, N=14, 3 Rats

4.4 Discussion

There is some evidence to suggest the oligomerization potential of A2A-Rs and DA-Rs in the brain (Ferré *et al.*, 2008). In addition, it has been shown that chronic striatal DA denervation may cause increased interaction between these two receptors, thus the experiments mentioned in this chapter aimed to elucidate their effects on NMDA-Rs (Svenningsson *et al.*, 1999; Strömberg *et al.*, 2000). Studying the dynamics between these receptors and their involvement in NMDA-R modulation might thus provide a window into a therapeutic approach for the treatment of neurodegenerative diseases such as PD.

A2A-Rs are coupled to $G\alpha_s$ -protein thus increase cAMP levels in the cell and PKA levels, resulting in receptor phosphorylation. SCH-58621, an A2A-R antagonist was thus used to elucidate the effects on NMDA-R response in the presence of ropinirole (D2-R agonist) and sulpiride (D2-R antagonist). An A2A-R agonist, CGS-21680 was used to test whether it would block the effects of D2-R activation. In the presence of CGS-21680, the NMDA-R current increased even in the presence of ropinirole and sulpiride, suggesting a possible advantage over D2-R activation. Furthermore, a comparable result was observed in the presence of SCH-58621 (and similarly in CA1 hippocampal neurons- refer to appendix). However, it was not until SCH-58621 was introduced, that sulpiride managed to increase the NMDA-R current (refer table 4). On its own, it did not seem to change the NMDA-R response. This suggests that, by blocking the A2A-Rs, there is an increase in binding potential for D2-R ligands to the receptors.

It was apparent that the control 20 μM NMDA applications in experiments with two concentrations of CGS21680 experiments were different (figure 4.9C). This may have been due to the general-randomised selection of DAergic neurons within the substantia nigra. There is evidence to suggest a heterogenous

population of DAergic cells that differ in excitability, depending on their localisation within the substantia nigra (C. J. Wilson and Callaway, 2000).

Table 7 Summary table indicating effect on NMDA-R current in the presence of different drug combinations (+, Potentiation; -, No effect)

	Sulpiride (D2 Inhibitor)	Ropinirole (D2 Activator)	SCH58621 (A2A Inhibitor)	CGS21680 (A2A Activator)
Sulpiride	-	-	+++	+
Ropinirole	-	-	-	++
SCH58621	+++	-	+	++
CGS21680	+	++	++	++

It was evident that A2A-R interaction with D2-Rs and the corresponding modulation of NMDA-R response is PKA dependent, as the introduction of Forskolin increased the NMDA-R current in a concentration-dependent manner. With the subsequent increase in cAMP concentration in the cell, the application of ropinirole after the fact, tended to occlude the effect of forksolin thus, reducing the NMDA-R current. This suggests that the endogenous levels of cAMP may not have been high enough in previous experiments to elicit an obvious response.

Chapter 5

Investigating intracellular kinases involved in NMDA receptor modulation in P28 rats

5.1 Introduction

Src and Fyn kinases are among a group of intracellular protein tyrosine kinases. In the CNS they modulate ion channel activity (Wang and Salter, 1994b; Groveman *et al.*, 2011; Salter and Pitcher, 2012a), for instance, the phosphorylation of NMDA-Rs where they have been shown to enhance the NMDA-R currents, as well as K^+ and Ca^{2+} channels (Y T Wang, Yu and Salter, 1996; Yang *et al.*, 2012b). Electrophysiological studies have provided evidence to suggest currents are regulated via the cooperative activity of protein kinases and phosphatases (Wang, *et al*., 1996; Salter and Pitcher, 2012a). Both Src and Fyn have shown differential preference for NMDA-receptor subunits. As shown by Yang *et al.*, (2012) on isolated neurons of the hippocampal CA1, Src regulation was only observed on GluN2A-containing NMDA-Rs, where an interfering peptide was introduced. Whereas Fyn kinases have shown greater selectivity towards GluN2B-containing NMDA-R phosphorylation (Nakazawa *et al.*, 2001; Chen and Roche, 2007). The experiments in this chapter used a Src/Fyn-selective inhibitor, PP2 as well as the introduction of interfering peptides (Src 40-58 and Fyn 39-57), that interfere with the binding of Src or Fyn to the scaffolding protein NADH dehydrogenase subunit 2 (ND2), which ultimately prevents the Src localisation in the NMDA-R vicinity, preventing receptor phosphorylation (Gingrich *et al.*, 2004b).

Following studies on the hypothesized contribution of Src and Fyn kinases to NMDA-R modulation in substantia nigra dopaminergic neurons, ERK signalling was investigated as ERK kinases play a vital role in neuronal survival and cellular differentiation (Neve, *et al.,* 2004). Furthermore, they in turn, can be modulated by D2-R activation, via the enhancement of Src kinase activity in a

G-protein-dependent manner (Neve, *et al.*, 2004). This further developed the incentive to study the final component of the MAPK pathway, ERK as it would link D2 receptors to NMDA receptors. Ulixertinib was used to inhibit ERK signalling and the resulting NMDA response was investigated.

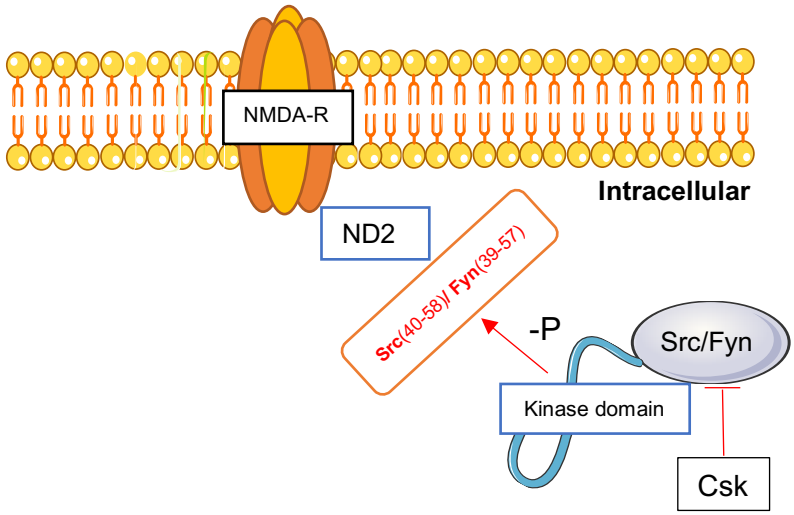

Figure 5.0 A schematic diagram illustrating kinase inhibition of NMDA-Rs via interfering peptides- Tat-Src/Fyn*. They prevent the binding of Src to NMDA-Rs, but do not interfere with the enzymatic activity of the kinase. ND2, NADH dehydrogenase 2.*

Lastly, an intracellular component with substantial involvement in the NMDA-R-driven LTP and LTD is CaMKII, which is necessary to drive learning, memory and cognition (Coultrap *et al.*, 2014). Furthermore, its involvement in synaptic plasticity is well established (Barcomb *et al.*, 2016; Bayer and Schulman, 2019). Such kinase activity is driven via Ca^{2+} influx through the NMDA-Rs leading to CaMKII autophosphorylation. This is sufficient to trigger its binding to the GluN2B subunit of the NMDA-Rs (Bayer *et al.*, 2001). The tool used to test this kinase in dopaminergic neurons was an interfering peptide tat-CN21. It has previously been shown to disrupt the interaction between the GluN2B of NMDA-Rs and CaMKII (Barcomb *et al.*, 2016).

5.2 Results

5.2.1 Targeting Src and Fyn protein kinases with PP2 decreased NMDA-R amplitude in dopaminergic neurons of the substantia nigra

Src and Fyn kinases are responsible for phosphorylating and modulating NMDA-R, thus regulating NMDA-R-dependent synaptic plasticity in most of the CNS (Grant *et al.*, 1992; Salter and Kalia, 2004). For this reason, I sought to determine whether this modulation was present in dopaminergic neurons of the substantia nigra. 10 μM PP3 is an inactive compound of PP2 and was used as a control. It was applied to the pipette solution to allow direct entry into the cell. Three repeated applications of 20 μM NMDA were performed. The first application produced a mean steady-state inward current of 274 ± 50 pA (mean ± SEM) (figure 5.1B). This was followed by a second application that produced an average current of 416 ± 49 pA. The final application produced an inward current of 475 ± 62 pA. The gradual increase throughout the whole-cell recording was statistically significant (One-way ANOVA, P= 0.00345, N=15 from 3 rats). However, there was a suppression of the currents relative to the control experiment with 20 μM NMDA alone (One-way ANOVA, P= 0.0001). For this reason, the following experiment with the active Src inhibitor was compared to the inactive analogue- PP3, as well as the control NMDA experiment to better interpret the results. 10 μM PP2 was used to target and block Src kinase activity. It was applied via the pipette solution and thus present throughout the recording (figure 5.1 A). The whole cell recording involved three repeated applications of 20 μM NMDA each followed by a wash off period of 300 secs (figure 5.1). The three NMDA responses produced mean NMDA steady-state inward currents of, 369 ± 48 pA, followed by 514 ± 46 pA and finally 579 ± 49 pA. The increase in current was statistically significant throughout the recording (One-way ANOVA, P=0.0089, N=27 cells from 6 rats). Relative to PP3, PP2 showed a statistically significant increase in current (One-way ANOVA, P=0.0014). However, when compared to NMDA alone, there was an overall suppression in the NMDA-R current (One-way ANOVA, P= 0.0185). Thus, these experiments show a

significantly decreasing NMDA response in presence of PP3 and PP2 relative to control.

5.2.2 Targeting Src kinase via the application of 10 μM and 100 μM Src-Inhibitor-1 (Src-I1) decreased the NMDA-R current in the dopaminergic neurons of the substantia nigra

Both PP3 and PP2 suppressed the NMDA-R current. To further confirm the effect of Src kinase inhibition, I decided to use a different Src kinase inhibitor with greater specificity for Src kinase. Two different concentrations of Src-I1 were used to investigate the differential effect on NMDA-R modulation. The inhibitor was applied directly in the pipette solution as with the previous kinase inhibitor. The first application of 20 μM NMDA produced an inward current of 312 ± 65 pA (mean ± SEM) in the presence of 10 μM Src-I1 (figure 5.2 A & B). The second application of NMDA produced a mean current of 494 ± 65 pA. This increase was statistically significant and was also seen following the final application of NMDA with a mean current of 607 ± 80 pA (One-way ANOVA, P=0.0055, N=12, from 3 rats). The first NMDA response in the presence of the Src-I1, showed a decrease relative to the control experiment in its absence (unpaired T-Test, P=0.0058). However, the final response was similar to that in the control experiment (unpaired T-test, P=0.3077). 2-Way ANOVA comparing control NMDA responses with NMDA responses recorded with Src-1 (10 μM) in the pipette shows a significant main effect of Src-1 to reduce the NMDA current (P = 0.0012). The concentration of Src-I1 was then increased to 100 μM to determine whether this would facilitate a more pronounced effect (figure 5.3 A). After the first application of NMDA, the mean inward current was 481 ± 63 pA. NMDA was then washed off for 300 secs and followed by a second application of 20 μM NMDA (figure 5.3 A). This produced an average current of 577 ± 56 pA. The increase in current was statistically significant, however after a third application, the current increased just slightly to 607 ± 80 pA. Overall, despite the initial increase in current the overall statistics suggests a change that is not statistically significant (One-way ANOVA, P=0.39, N=16, from 3 rats) as the data began to plateau the longer the cell was exposed to the inhibitor. In addition, the

first NMDA responses in the presence of 100 μM Src-I1 were similar to that of the control (One-way ANOVA, P=0.2417). 2-Way ANOVA comparing control NMDA responses with NMDA responses recorded with Src-1 (100 μM) in the pipette gave a significant main effect of Src-1 to reduce the NMDA current (P = 0.0235).

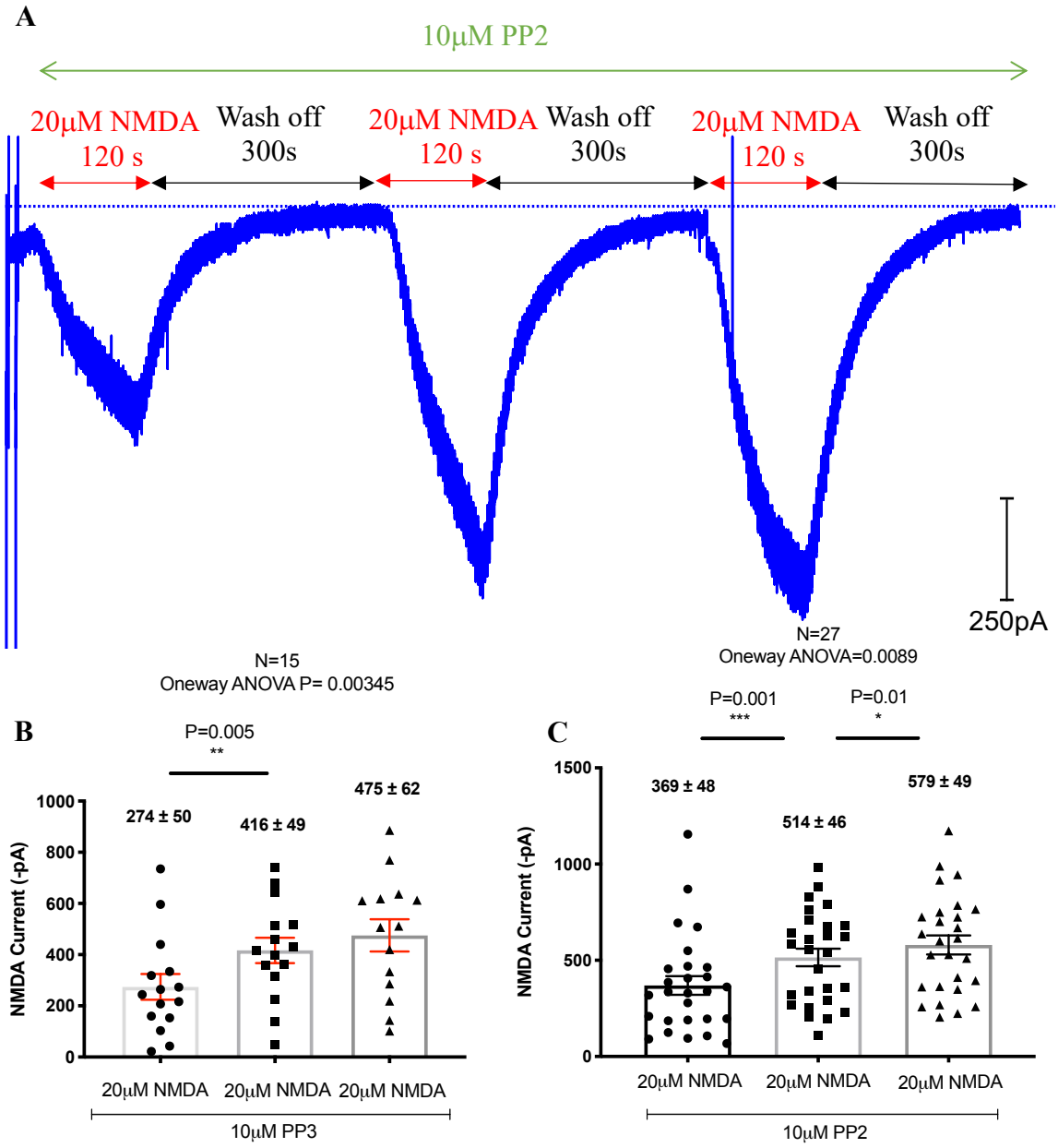

Figure 5.1 Targeting Src and Fyn protein kinases to elucidate their modulatory role on NMDA-R in P28 rat dopaminergic neurones. *A) A whole-cell recording trace showing the three repeated applications of NMDA in the presence of PP2 (and PP3- inactive isoform). B & C) A quantitative analysis of the mean NMDA-R current in the presence of an inactive and active isoform of PP2, respectively.*

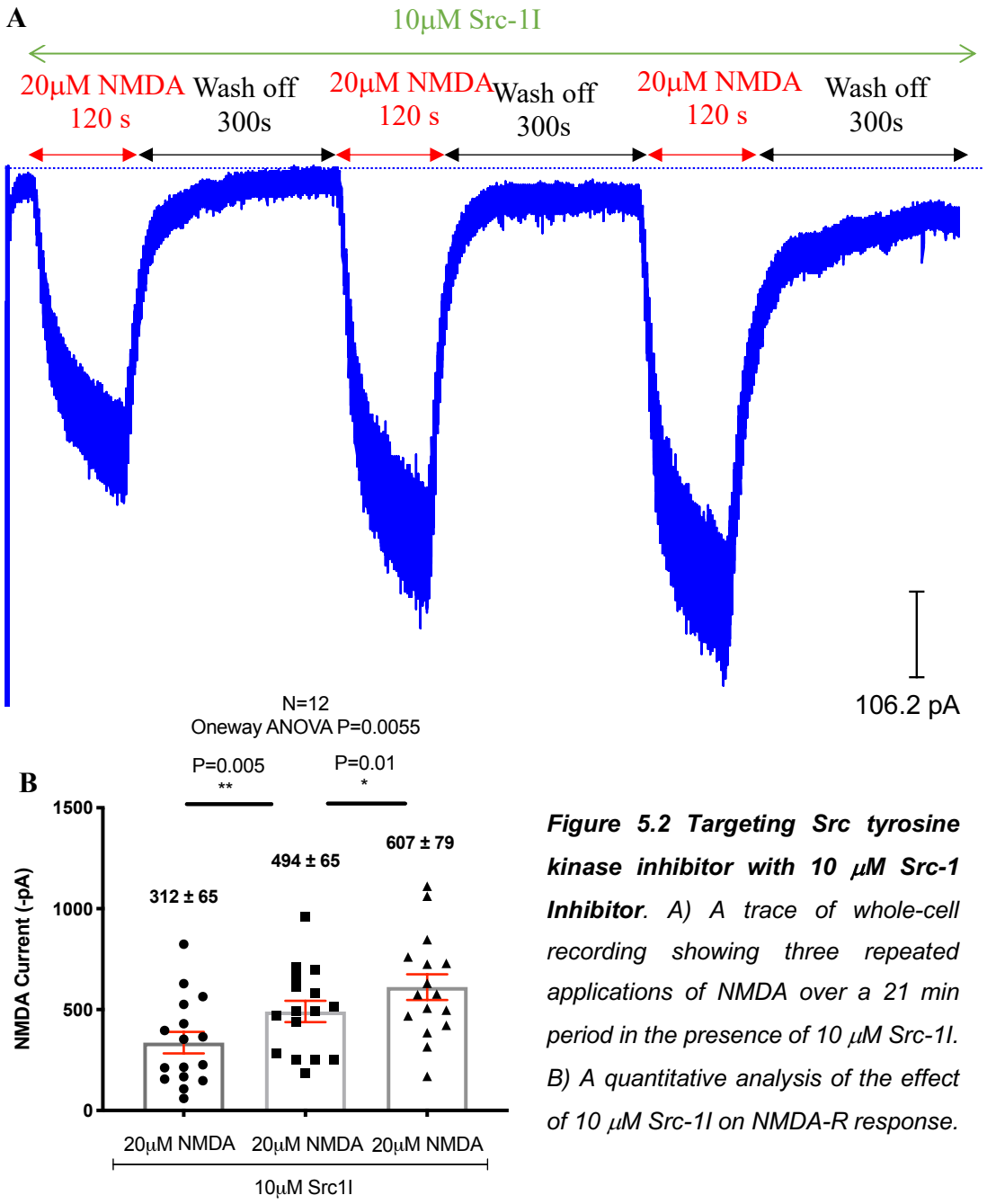

Figure 5.2 Targeting Src tyrosine kinase inhibitor with 10 μM Src-1 Inhibitor*. A) A trace of whole-cell recording showing three repeated applications of NMDA over a 21 min period in the presence of 10 μM Src-1I. B) A quantitative analysis of the effect of 10 μM Src-1I on NMDA-R response.*

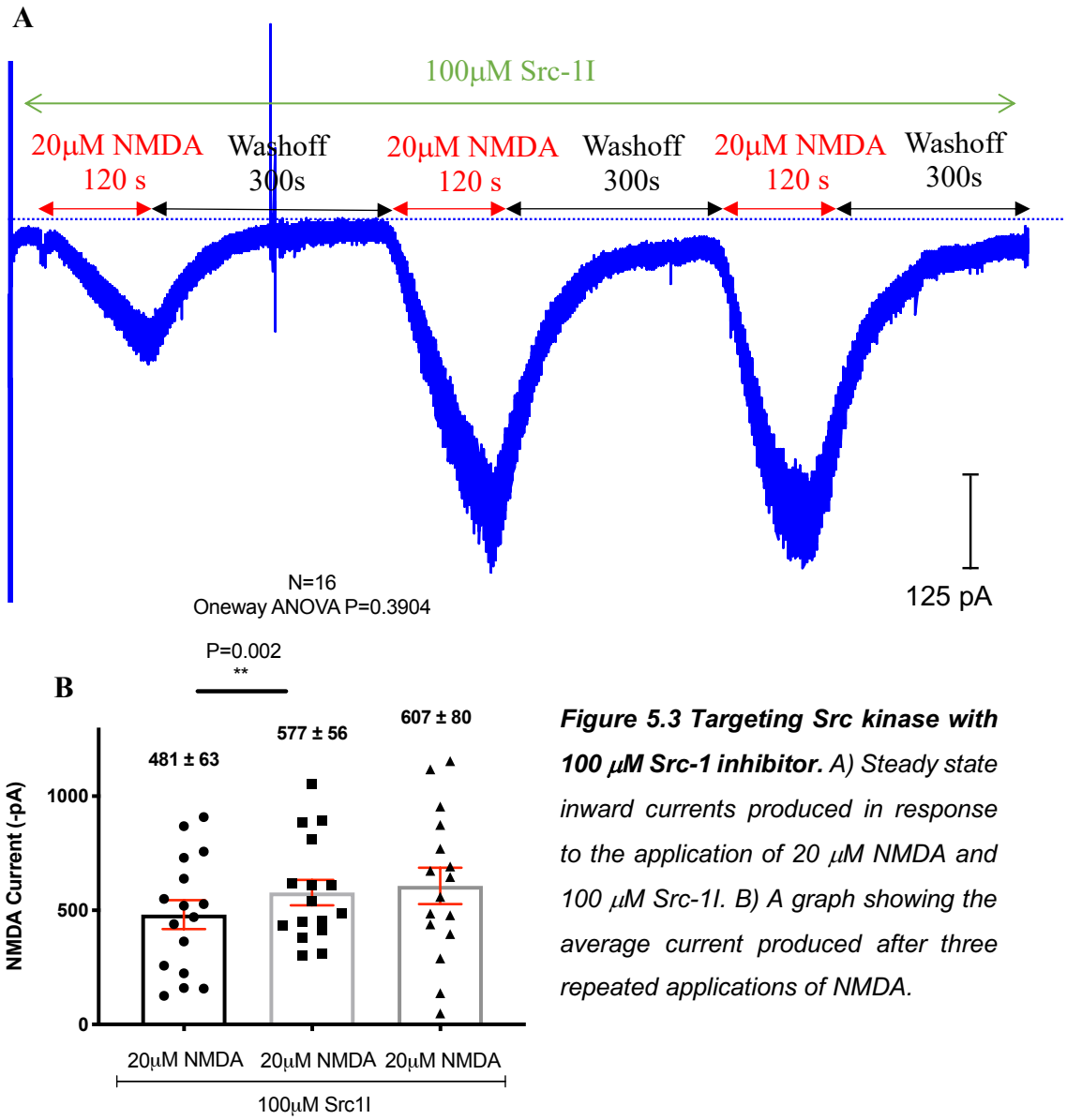

Figure 5.3 Targeting Src kinase with 100 µM Src-1 inhibitor. *A) Steady state inward currents produced in response to the application of 20 µM NMDA and 100 µM Src-1I. B) A graph showing the average current produced after three repeated applications of NMDA.*

5.2.3 Inhibiting Src kinase with inhibitor peptide, prevents further increase of NMDA-R phosphorylation

Interfering peptides were introduced because of their ability to selectively interact directly with molecules and prevent phosphorylation by other kinases. The Src peptide, ligated to cell permeable Tat motif -Tat-Src (40-58) was previously shown to block the interaction of Src with NMDA-Rs (Gingrich *et al.*, 2004a; Salter and Pitcher, 2012b). In this experiment, the Tat-Src peptide was introduced via the pipette solution to allow direct access to the cytosol. A control experiment was initially performed to rule out any possible interference the peptide may have in the resulting NMDA-R response, be it active or not. The control peptide involved a scrambled sequence of the Tat-Src peptide. In the presence of 10 μM scrambled peptide (Tat-sSrc), three applications of 20 μM NMDA were applied, each followed by wash off periods of 300 secs (figure 5.4 A). The first application produced a mean inward current of 311 ± 43 pA (mean ± SEM). The second application produced a statistically significant increase in NMDA-R response at 459 ± 63 pA (paired t-test, P=0.0003, N=16, from 6 rats) (figure 5.4 B), after which the NMDA-R inward current continued to increase slightly into the third application of 20 μM NMDA (480 ± 73 pA, N=14). Overall, the responses showed a depression in NMDA-R current relative to the control in the absence of the peptide (One-way ANOVA, P=0.0007). 2-Way ANOVA comparing control NMDA responses with NMDA responses recorded with scrambled Src peptide (10 μM) in the pipette shows a significant main effect of to reduce the NMDA current ($P < 0.001$).

The active interfering Src peptide was then introduced (figure 5.4 C). Following three applications of 20 μM NMDA, the presence of 10 μM Tat-Src, did not change the mean NMDA-R inward current throughout the experiment. The three mean NMDA-R currents produced were 803 ± 111 pA (N=15), 887 ± 76 pA (N=15), and 895 ± 78 pA (N=14, from 2 rats), respectively (figure 5.4 D). The overall currents were much higher than that in the control experiment in presence of the scrambled protein. However, they were similar to the control experiment (as in Figure 3.9B) in the absence of the Src peptide. 2-Way ANOVA

comparing control NMDA responses with NMDA responses recorded with Src-interfering peptide (10 μM) in the pipette shows no significant effect of Src-peptide on the NMDA current (P = 0.06).

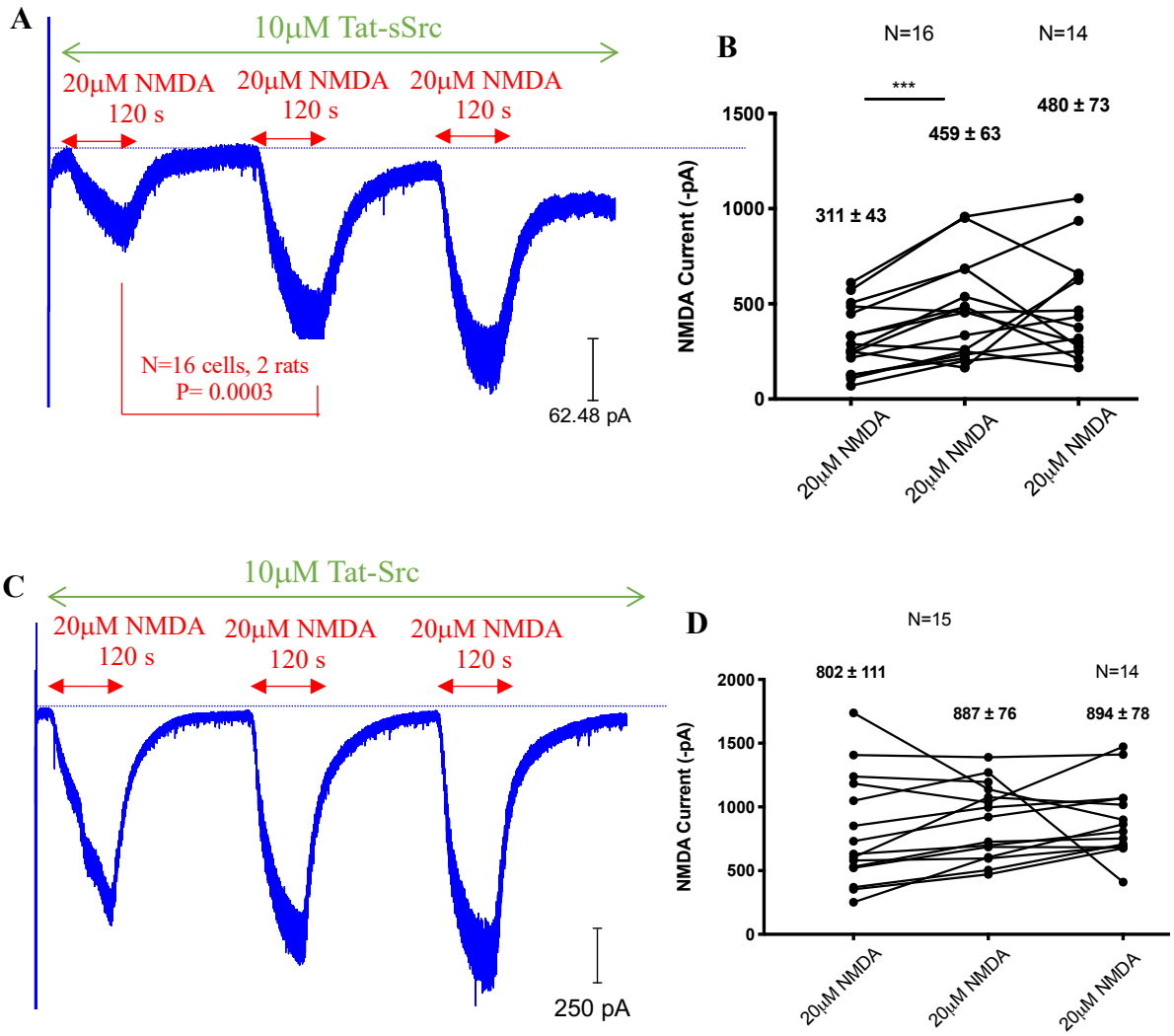

Figure 5.4 The effect of 10 μM Src kinase interfering peptide (Tat-Src) on NMDA-R current. *A) A trace showing the whole-cell recording produced in response to 3 applications of 20 μM NMDA for 120 secs each (indicated by trough amplitudes) in the presence of a scrambled Tat-sSrc peptide. Paired T-test (P= 0.0003). B) A quantitative analysis of the controlled mean amplitudes (Tat-sSrc). C) A trace showing the resulting NMDA-R currents in the presence of 10 μM Tat-Src peptide. D) A graph showing the mean NMDA inward currents in the presence of 10 μM Tat-Src.*

5.2.4 Blocking Fyn kinase activity with interfering peptides, enhanced NMDA-R responses

Following the experiment where the effect of Src kinase inhibition was in question, Fyn kinase was targeted via the introduction of a Fyn-interfering peptide- 10 μM Tat-Fyn (39-57) (Xu *et al.*, 2008). A scrambled version was used as a control (Tat-sFyn). During the control experiment, the interfering peptide was introduced via the pipette solution as in the previous experiment, thus present throughout the whole-cell recording (figure 5.5 A). The resulting mean NMDA-R current after each application, each followed by wash off periods of 300 secs, increased significantly from one to the next (figure 5.5 B). The first application of NMDA produced an average steady-state inward current of 327 ± 44 pA (mean ± SEM), followed by a second mean current of 457 ± 56 pA. The mean NMDA current continued to increase into the third application of 20 μM NMDA, 572 ± 70 pA (One-way ANOVA, P=0.0003, N=12, from 5 rats). The overall currents exhibited a supressed response when compared to the control experiment in the absence of the peptide (One-way ANOVA, P=0.0042). There was a significant increase observed when the active Fyn-peptide was tested relative to its scrambled peptide (figure 5.5 C). The first application of 20 μM NMDA produced a mean inward current of 707 ± 116 pA. This was followed by a mean current of 971 ± 123 pA (figure 5.5 D). The increase in current between the first two applications of NMDA, was statistically significant (paired T-test, P=0.003, N=16 from 2 rats). The current continued to increase into the third application of NMDA in the presence of Tat-Fyn peptide, producing a mean current of 1255 ± 213 pA (N=12). The application of the peptide to the pipette solution allowed for direct entry into the cell and potentially immediate effect on NMDA-R response. For this reason, the results obtained in the presence of the Fyn peptide were then compared to the control experiment in their absence (as in Figure 3.9B). There was a statically significant increase in NMDA-R response in the presence of the Fyn peptide relative to the control (One-way ANOVA, P=0.0218).

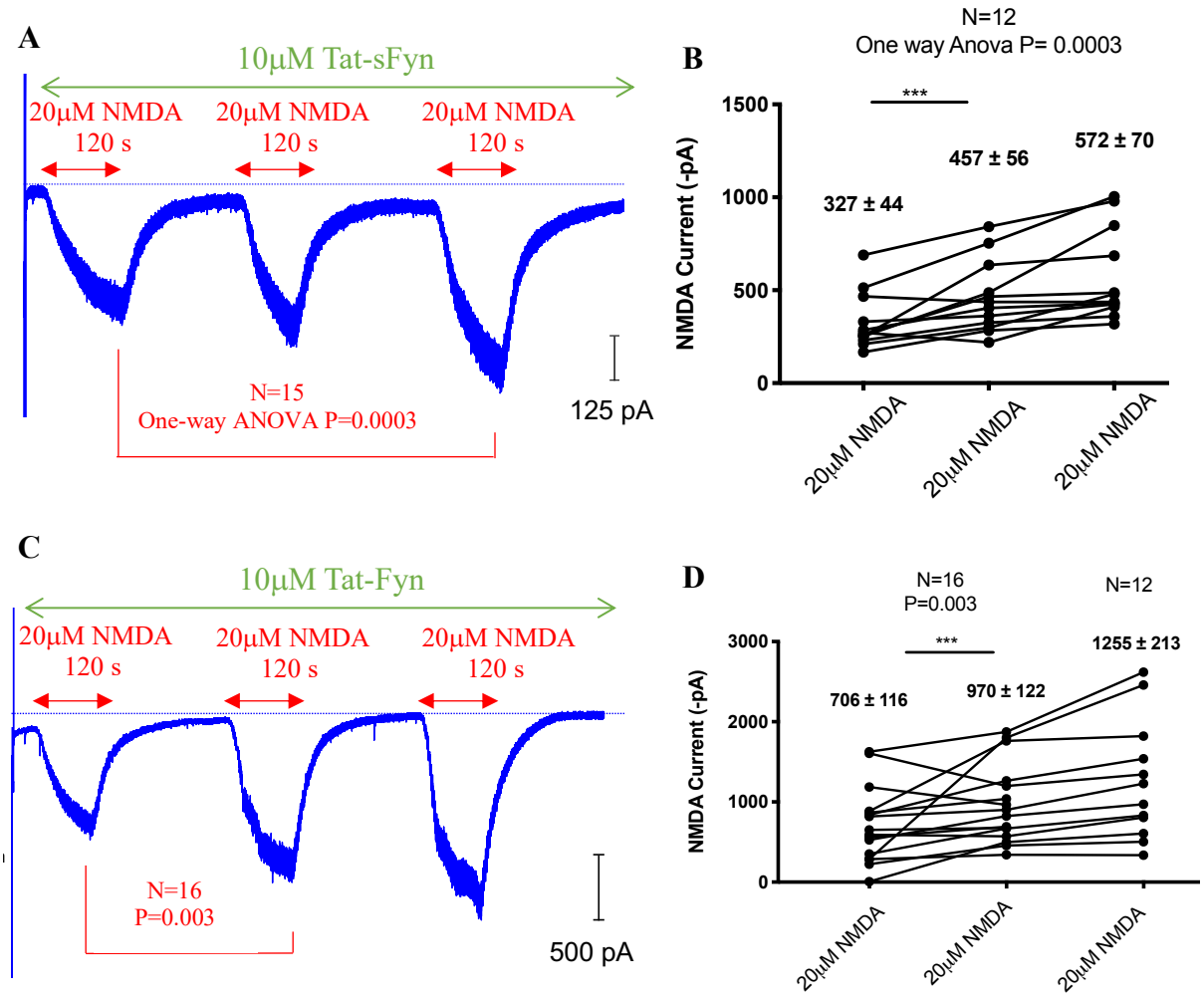

Figure 5.5 The effect of inhibiting Fyn-kinase with interfering peptides*. A) A trace of a whole-cell recording showing three inward currents in response to 20 μM NMDA in the presence of 10 μM Tat-sFyn. B) A graphical representation of the mean NMDA-R currents when scrambled Tat-sFyn is applied. C) A trace showing the NMDA inward currents in the presence of 20 μM NMDA and 10 μM Tat-Fyn. D) A quantitative analysis of the mean NMDA-R responses in the presence of 10 μM Tat-Fyn.*

5.2.5 Introducing 10 μM Tat-Src and 10 μM Tat-Fyn simultaneously, did not change the NMDA-R current

After testing the effects of both interfering peptides on NMDA-R modulation alone, they were both introduced simultaneously to determine whether their effects would summate or mask the other. They were both applied to the pipette solution and allowed direct access to the cell cytosol and present throughout the experimental protocol (figure 5.6 A). The first application of 20 μM NMDA produced a mean inward current of 696 ± 85 pA (mean ± SEM) (figure 5.6 B). The second NMDA application produced an inward current of 772 ± 86 pA. This was then followed by a final application of NMDA producing a mean current of 839 ± 74 pA. Despite the gradual increase in NMDA-R inward current, the difference was of no statistical significance (One-way ANOVA, P=0.279, N=15 cells from 4 rats). The lack of change was also observed when compared to the control experiment in the absence of the peptides (One-way ANOVA, P=0.1325).

5.2.6 1 μM Ulixertinib (ERK1/2 inhibitor) rapidly decreased NMDA steady state current

Targeting the MAPK pathway was suggested due to ERK's involvement in the NMDA-R signal transduction pathway (Krapivinsky *et al.*, 2003). ERK1/2 was targeted using Ulixertinib, an ATP competitive inhibitor of ERK1. 1 μM Ulixertinib was introduced via the pipette solution, therefore present throughout the recording (figure 5.7 A). The first mean NMDA steady-state current produced was 453 ± 74 pA (mean ±SEM) (figure 5.7 B). This was followed by a second application of 20 μM NMDA that produced a mean inward current of 653 ± 95 pA. The final inward current produced increased to 839 ± 66 pA. Despite the increase in NMDA-R current throughout the experiment (One-way ANOVA, P<0.0001, N=15 cells from 3 rats), when compared to the control experiment, the overall difference in responses were smaller (Oneway ANOVA P=0.0340).

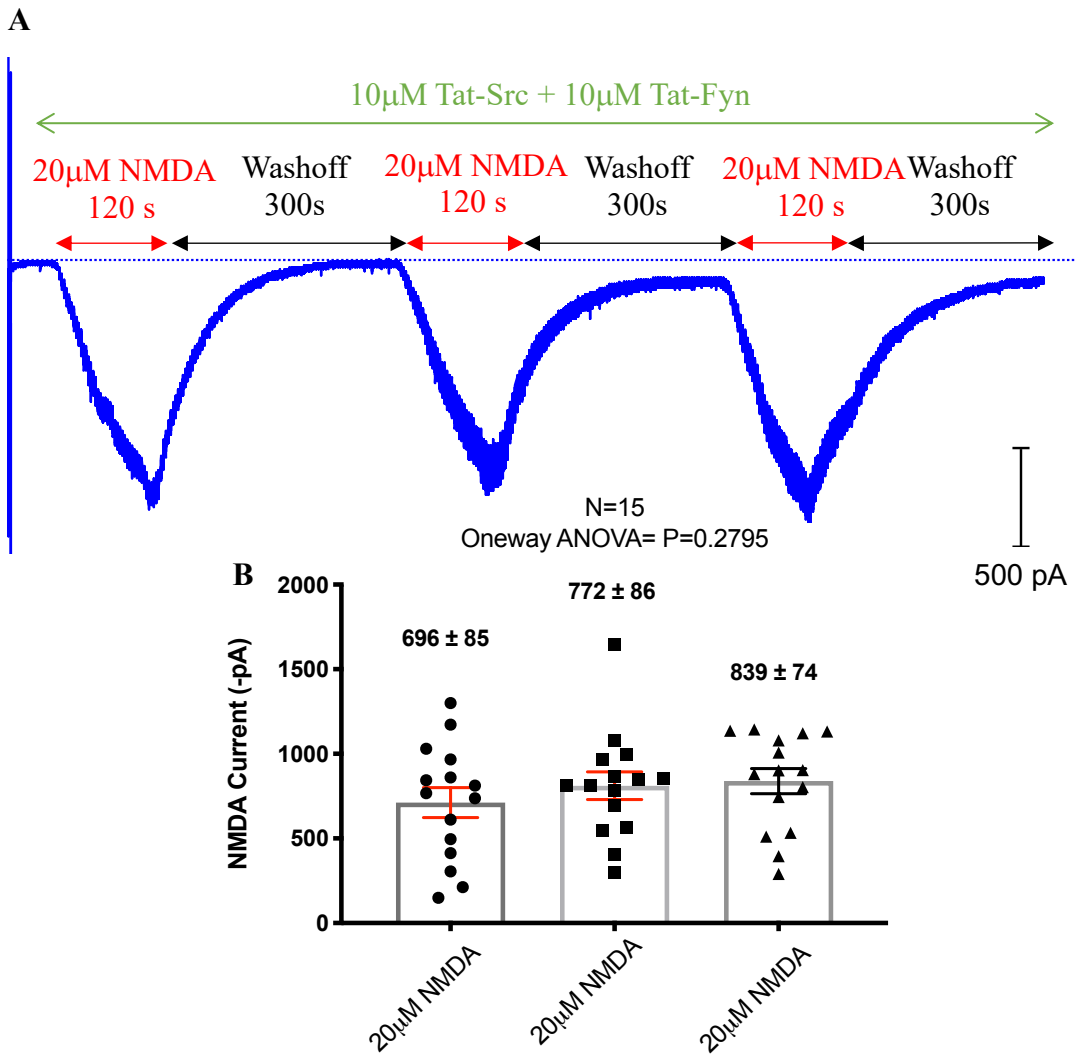

Figure 5.6 The simultaneous targeting of Src and Fyn kinase using interfering peptides. *A) A trace of a whole-cell recording showing repeated applications of NMDA in the presence of both 10 μM Tat-Src and 10 μM Tat-Fyn. B) A quantitative analysis showing the mean ± SEM NMDA current after three applications in the presence of the kinase interfering peptides.*

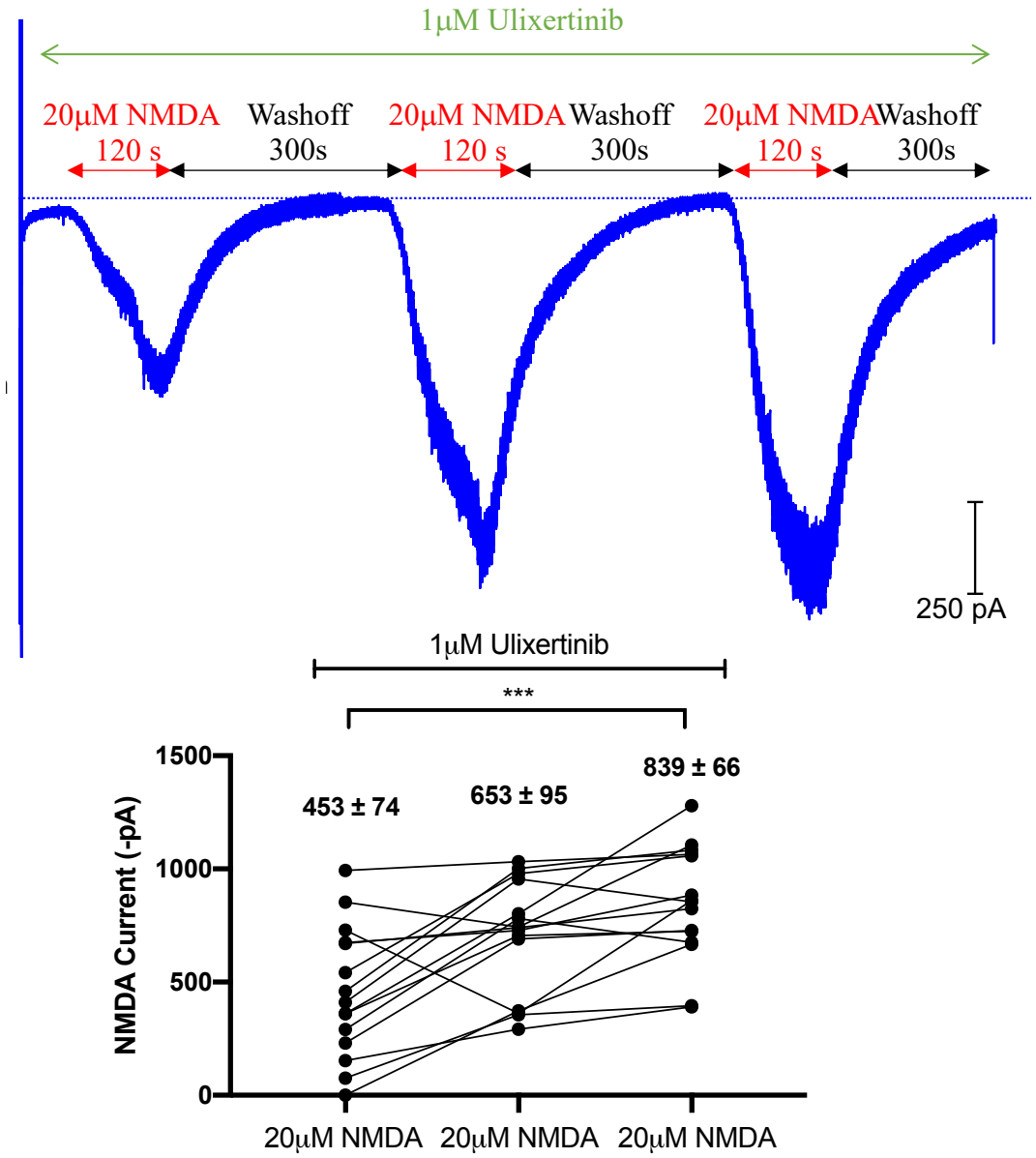

Figure 5.7 The effect of inhibiting ERK 1/2 phosphorylation on NMDA-R current with 1 μM Ulixertinib. *A) A whole-cell recording showing repeated applications of NMDA. B) A graph comparing mean NMDA-R currents in the control experiment and in presence of 1 μM Ulixertinib.*

5.2.7 Inhibiting CaMKII in dopaminergic neurons of the substantia nigra in P30 rats did not change the NMDA-R response during repeated applications of NMDA.

20 μM Tat-CN21 was used to inhibit CaMKII to reduce synaptic strength highlighted by a change in NMDA-R current. A control experiment was performed using a scramble version of the interfering peptide (figure 5.8 A). The same protocol as in the other peptides was carried out, where three applications of NMDA for 120 secs were each followed by 300 secs of wash off, all in the presence of the interfering peptide. After the first application of 20 μM NMDA in the presence of 20 μM Tat-scrambled CN21, the resulting inward current was 224 ± 60 pA (mean ± SEM) (figure 5.8 B). The current gradually increased to 437 ± 57 pA after the second application, which was followed by a mean steady-state current of 423 ± 55 pA. The gradual increase in NMDA-R current was statistically significant (One-way ANOVA, P=0.018, N=7 cells from 4 rats). It is evident that the NMDA currents in the presence of the scrambled peptide were supressed relative to the control experiment in their absence (One-way ANOVA, P=0.0038). The control experiment was then followed by the introduction of an active Tat-CN21 peptide at 20 μM (figure 5.8 C & D). The three resulting mean NMDA-R steady-state inward currents were 294 ± 45 pA, followed by 307 ± 55 pA and 341 ± 55 pA. Although there was a steady increase in inward current, the mean differences were of no statistical significance, and the lack of change was also observed when compared to the scrambled peptide (One-Way ANOVA, P=0.204, N=14 cells from 6 rats). However, the overall currents were significantly reduced compared to the control experiment where NMDA was applied alone (One-way ANOVA, P=0.0001).

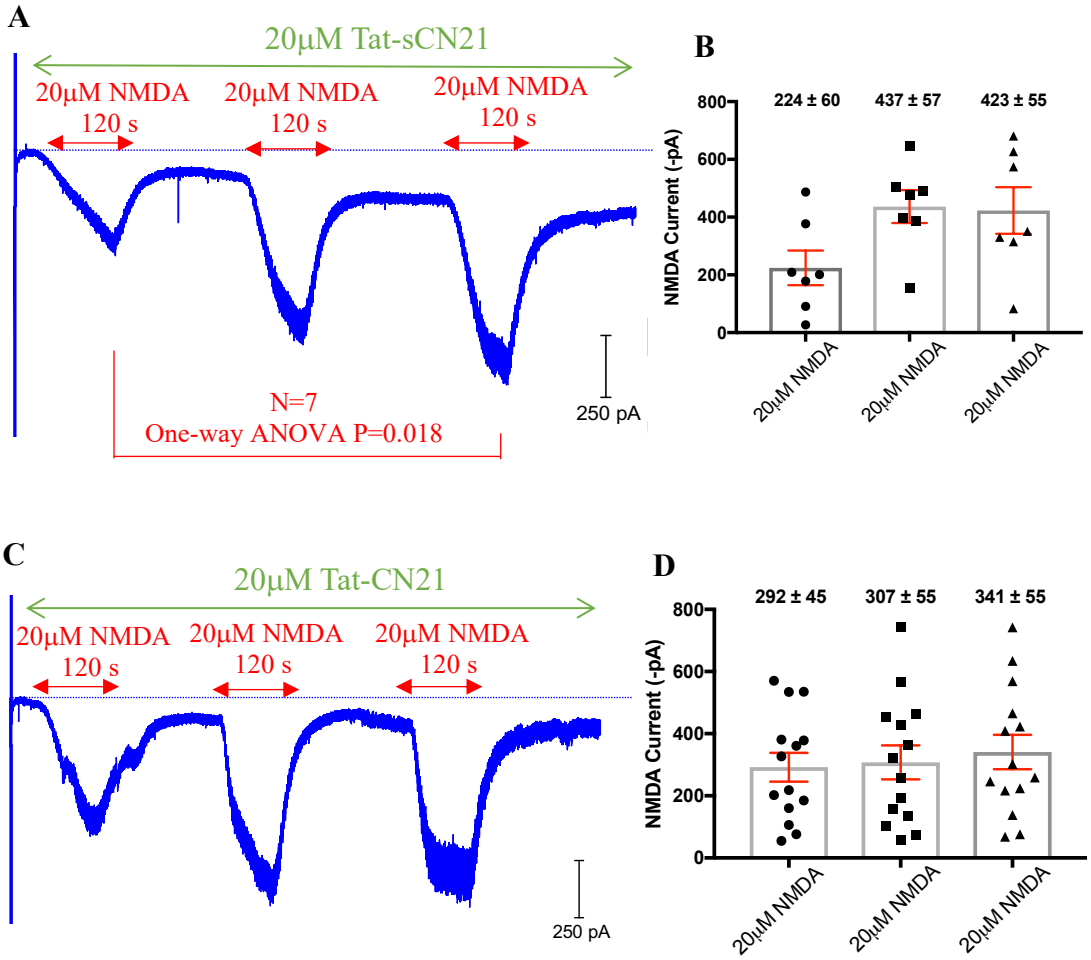

Figure 5.8 (P25-30) The effect of blocking CaMKII activity via the addition of 20 μM Tat-CN21 interfering peptide. *A) A trace of a whole-cell recording showing the resulting NMDA currents after three repeated applications of 20 μM NMDA (peaks from baseline) in the presence of 20 μM Tat-sCN21. B) A quantitative analysis of the controlled experiment showing the mean NMDA-R responses in the presence of a scrambled Tat-sCN21 peptide. C) A trace showing the peak currents produced after three applications of 20 μM followed by periods of wash off for 300 secs in the presence of 20 μM Tat-CN21.*

5.2.8 Cells closer to the lateral portion of the Substantia nigra, showed homogenous response to 20 μM Tat-sCN21

Biocytin hydrochloride was introduced in the experiments described in section 5.2.7 and figure 5.8 to tag and localise the cells patched and their corresponding response in the presence of 20 μM Tat-sCN21. It is evident that the cells closer to the lateral position of the substantia nigra are more homogenous in activity in response to 20μM NMDA in the presence of 20 μM Tat-sCN21 (repeated applications of NMDA produce similar responses in different cells) and progressively more different as the cells approach the medial position. The mean NMDA-R responses in the bridging region between medial and lateral show a pronounced reduction in NMDA-R inward current relative to the more lateral or more medially located dopaminergic neurons of the substantia nigra.

A

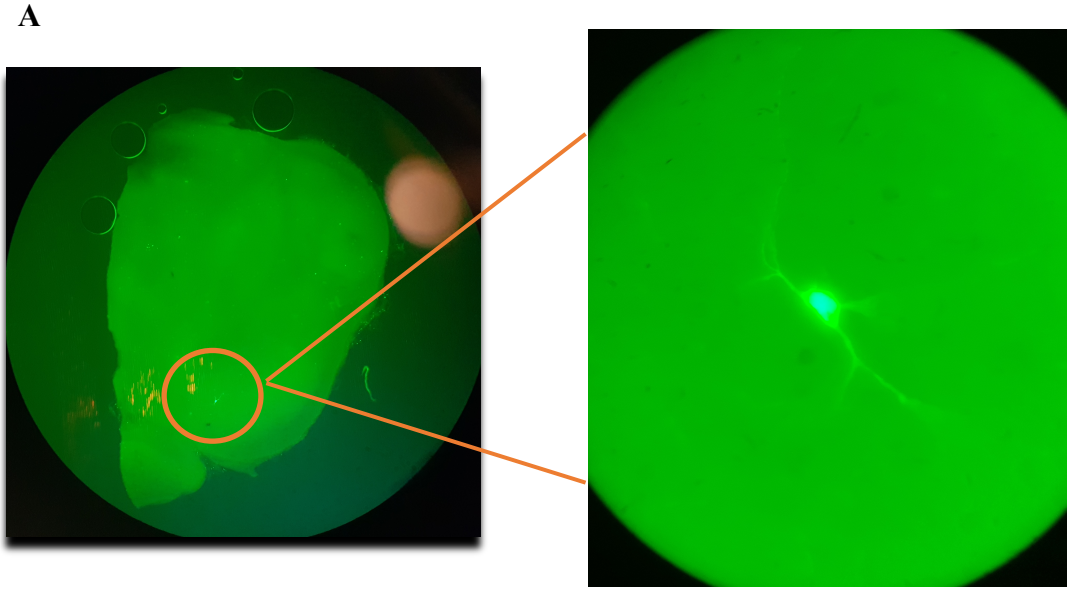

B

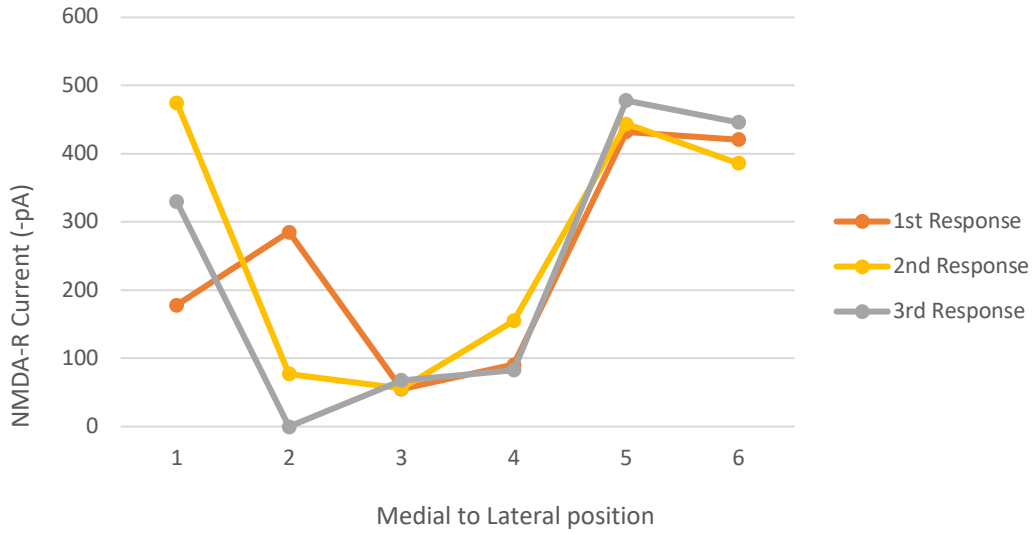

Figure 5.9 Heterogeneity of DAergic neurons in the SNc. *A) Fluorescent images of P28 rat coronal brain slice (left) and Neurobiotin stained DAergic neuron of the SNc (right). B) NMDA-R response corresponding to the location of the dopaminergic cell in the substantia nigra in the presence of 20μM Tat-sCN21 in P30. rats.*

5.3 Results Summary

Table 8 Summary of experiments investigating the effect of intracellular kinases on NMDA-receptor response in DAergic neurons of P28 rats.

Experiment	Result	Statistical analysis
Will inhibiting Src and Fyn kinase decrease NMDA-R phosphorylation, thus decrease NMDA-R current?		
10 μM PP2 (Src/Fyn inhibitor)	Statistically significant decrease in NMDA-R current compared to control.	Oneway ANOVA: P=0.0089; N=27, 5 Rats
10 μM Src-1I	Statistically significant decrease in NMDA-R current relative to control.	Oneway ANOVA: P=0.0055; N=12, 3 Rats
100 μM Src-1I	A higher concentration did not produce a statistically significant NMDA response.	Oneway ANOVA: P=0.39; N=16, 3 Rats
10 μM Tat-sSrc (40-58)	Statistically significant increase in NMDA current between first 2 applications of NMDA.	Paired T-test: P=0.0003; N=16/14, 6 Rats
10 μM Tat-Src (40-58)	NMDA current did not change following three applications of NMDA.	Paired T-test: P-0.08, N=15/14, 2 Rats
10 μM Tat-sFyn (39-57)	Enhanced the NMDA-R current.	Oneway ANOVA: P=0.0003; N=12, 5 Rats
10 μM Tat-Fyn (39-57)	Statistically significant increase in NMDA-R current after first two applications of NMDA	Paired T-test: P=0.003; N=16/12, 2 Rats
10 μM Tat-Fyn (39-57) + 10 μM Tat-Src (40-58)	No change in NMDA-R response.	Oneway ANOVA: P=0.297; N=15, 4 Rats
Will inhibiting ERK1/2 decrease NMDA-R current?		
1 μM Ulixertinib (ERK1/2 Inhibitor)	Decreased NMDA-R current reversibly (NMDA-R current began to increase to baseline).	Oneway ANOVA: P=0.0001, N=15, 3 Rats
Will inhibiting CaMKII suppress NMDA-R current?		
20 μM Tat-sCN21 (CaMKII Inhibitor)	Increased the NMDA current.	One-way ANOVA: P=0.018; N=7, 4 Rats
20 μM Tat-CN21 (CaMKII Inhibitor	Decreased NMDA-R current relative to control	One-Way ANOVA P=0.0001, N=14, 6 Rats

	with gradual increase to baseline.	

5.4 Discussion

Non-receptor tyrosine kinase inhibitors were applied to rule out their involvement in NMDA-R modulation. However, the data suggests a time-dependent effect of Src and Fyn kinase inhibitors on NMDA-Rs. When PP2, a Src and Fyn inhibitor was introduced, there was a robust and rapid decrease in current relative to control in the absence of NMDA. This decrease suggests a decrease in NMDA-R phosphorylation by either Src of Fyn kinase as would be expected based on what is already known of these non-tyrosine kinases (Trepanier *et al.*, 2011; Yu and Salter, 1999; Mao and Wang, 2015). The gradual increase in NMDA-R current seems to highlight a time-dependent effect and reversible nature of the kinase inhibitor as the effect wears off. The increase in NMDA-R current persists for a few minutes as it returns to a level that is statistically not significantly different to the control- "baseline" (Mao and Wang, 2016). To determine whether the effect on NMDA-R response was a Src-specific effect, a potent Src inhibitor, Src-I1 was used. This rapidly decreased the NMDA-R current relative to control followed by a gradual increase towards "baseline" over a 20 minute-period, suggesting the drug's transient decrease in NMDA -R current and reversible nature. The overall effects were similar to that in the presence of PP2. However, highlighting the specific effect of Src kinase phosphorylation on NMDA-R modulation.

Interfering peptides were then used to determine whether the known src and fyn kinase domains, Src(40-58) (Jiang *et al.*, 2008) and Fyn(39-57) (Yang *et al.*, 2012b) were responsible for NMDA-R phosphorylation and subsequent modulation. The results relative to their scrambled counterparts were not as expected. The scrambled peptides displayed similar effects to that of previous src inhibitors, used in my research where the NMDA-R currents were significantly reduced. On the other hand, active interfering Src peptide - Src(40-58) did not change the NMDA-R response relative to the control (in the absence on NMDA). The peptides used don't interfere with the enzymatic activity of Src

and Fyn kinase but prevent the physical interaction with NMDA-Rs. My data thus suggests Src and Fyn may not physically interact with NMDA-Rs in order to modulate the receptor phosphorylation and subsequent current.

Ulixertinib, an ERK2/3 inhibitor was used to elucidate the importance of the MAPK pathway on NMDA-R modulation, suggesting an alternative mode of modulation alongside the D2-R-$\alpha_{i/o}$ and A2A-R method proposed by the data in my experiments. The data shows a possible involvement as there was an overall decrease (One-way ANOVA, P=0.034) in the NMDA-R current following three applications of 20 μM NMDA. The initial reduction in NMDA current was slowly reversed over a 20 minute-period as the NMDA-R current showed a transient but significant increase in current to baseline owing to potential receptor phosphorylation. To determine other factors and proteins involved in NMDA-R modulation in substantia nigra dopaminergic neurons, CaMKII inhibitor CN21 was used. Interfering with CaMKII activity produced a rapid decrease in the NMDA-R currents relative to control (in the absence of the peptide) (One-way ANOVA, P= 0.0001) which persisted over a 20-minute period. To further test out the involvement of CaMKII on NMDA-R modulation, residue S1303 could be disrupted as shown previously to determine any effects on NMDA-Rs (Chen and Roche, 2009; Won and Roche, 2020). All in all, NMDA-R modulation in substantia nigra dopaminergic neurons seems to be driven by Src and/or Fyn kinase activity, ERK1/2 activation and CaMKII.

Chapter 6:
Discussion

Understanding the interaction and modulation of NMDA receptors is an essential aspect of understanding their implications in the treatment of neurological disorders. In this thesis, NMDA receptor modulation was investigated in dopaminergic neurons of the substantia nigra. I have shown that D2-R activation potentially affects NMDA-R current when cAMP signalling is stimulated, and its modulation, to some extent, is A2A-R dependent. Furthermore, intracellular kinases, particularly Src kinase and ERK1, are able to modulate NMDA-R responses in DAergic neurons of the substantia nigra. These mechanisms were investigated over rat developmental stages from 7 days to 28 days old.

In the prefrontal cortex, Banks *et al.*, (2015) showed that D2-R activation in the hippocampal-prefrontal projections caused lasting depression of NMDA receptor current, thus leading to a marked disruption of synaptic transmission. NMDA receptor activation has predominantly been associated with synaptic plasticity and synaptogenesis, allowing for long term changes such as LTP. This is partly driven by post-synaptic calcium influx and second messengers that control and activate kinases involved in the signalling cascade such as PKC, PKA and CaMKII. In striatum PKA and DARPP-32 result in enhanced phosphorylation of NMDA-Rs thus potentially modulating post-synaptic current. When de-phosphorylated, NMDA-Rs internalise, decreasing current flowing into the cell (Higley and Sabatini, 2010). However, a dysregulated NMDA-R mediated calcium influx can have detrimental effects to the cell, affecting apoptotic homeostasis by inducing apoptotic signals, that could drive the cell into programmed cell death (Hardingham and Bading, 2010) . Several studies have shown the effects of D2-R activation on NMDA-R modulation in hippocampal and pre-frontal cortex dopaminergic neurons, however not much is known of D2-R effects on NMDA-Rs in the substantia nigra, where a major population of the dopaminergic neurons reside (Skeberdis *et al.*, 2006). The canonical pathway associated with D2-R activation has driven the hypothesis

that its activation by a dopamine D2-R agonist, ropinirole, should decrease the NMDA steady state current in dopaminergic neurons of the substantia nigra. In this thesis, my initial study involved the use of the D2 agonist ropinirole, sulpiride- a D2-R antagonist and compound-101- a GRK2/3 inhibitor, used to prevent receptor GPCR desensitization. Classically, D2 receptors couple to the $G_{i/o}$ G-protein and so following on from this work, this thesis also investigated modulation by adenosine A2A receptors, a G_s G-protein coupled receptor to understand their role in potentially affecting the D2-R modulation on NMDA-Rs.

6.1 D2-R modulation in P7 rats

In the initial protocol, 20 μM ropinirole was used to determine its effects on NMDA-R steady-state current. A high concentration of ropinirole was selected in order to give a rapid effect and maximal receptor activation in the slice. The pronounced potentiation of NMDA-R after 20 μM NMDA alone and in the presence of 200 nM ropinirole was not expected having briefly mentioned the canonical effects of D2-R activation. This was also seen in experiments by Cepeda *et al.*, (1998) that looked at dopaminergic modulation of NMDA whole cell currents in medium-sized neostriatal neurons. When D2-Rs were activated with ropinirole in the presence of NMDA, they saw inconsistent effects on NMDA-R current, either increasing, decreasing or showing no modulation at all of the steady state current.

The uncertainty in the responses obtained with in vitro ropinirole may be complicated by the fact that ropinirole might scavenge reactive oxygen species (ROS) released by oxidative dopamine inactivation and so alter mitochondrial physiology and energy supply; thus hypothesised to potentially prevent damage to nigrostriatal tissue (Carter and Müller, 1991). However, in addition, ropinirole is a tertiary amine of highly lipophilic nature which previously suggested its ability to penetrate cell membranes and interact with the mitochondrial permeability transition pore (mtPTP) (Luzardo-Alvarez, et al, 2001). This hypothesis lead several research groups to investigate the effects of ropinirole on mitochondrial release of apoptotic factors such as cytochrome c, that drive

the cell to programmed cell death. Parvez *et al.*, (2010) investigated the possible effects of ropinirole on the desensitization of brain mtPTP. Patch clamp recordings in the presence of 30 nM to 10 μM ropinirole inhibited the opening of the mtPTP, thus preventing the release of cytochrome c and other normally impermeable constituents in the mitochondria. However, the effect of ropinirole was also antagonised by the presence of P_i. Furthermore, it is concentration dependent. In the presence of 1 mM P_i, the inhibitory effects of ropinirole on the mtPTP were significantly reduced (Parvez *et al.*, 2010). This attenuation fits with the current understanding of the effects of P_i as a mPTP inducer (Green and Kroemer, 2005). In my protocols, 1.5 mM of ATP and 0.75 mM of GTP was placed in the pipette solution. This may have triggered the activation of mtPTP, but whether this could indirectly affect NMDA responses is unknown. There are several postulates to explain this, one being that P_i could in fact decrease the effective concentration of ropinirole in the cell. Therefore, increased calcium release from the mitochondria could potentially enhance Ca^{2+}-dependent inhibition of the resulting NMDA current (Rosenmund, *et al.*, 1995; Rycroft and Gibb, 2004; Iacobucci and Popescu, 2017). However, to fully understand this, calcium signalling experiments would need to be done upon D2-R activation to determine if a change in $[Ca^{2+}]_I$ was occurred after D2-R activation with ropinirole.

Although several mechanisms might underlie a possible effect of ropinirole on NMDA currents, the concentration range tested may be important. This was brought to my attention when 20 μM ropinirole used to stimulate D2-Rs, showed no visible effect. Likewise in the presence of 200 nM ropinirole, having potentially blocked desensitization via a GRK2/3 inhibition, there was no effect of ropinirole on the NMDA current in SNc cells from P7 rats. Monte-Silva *et al.*, (2009) showed in humans using trans-cranial direct current stimulation (tDCS) that not only did D1-like stimulation via receptor agonists exert an inverted U-shape response, but D2-like activation with ropinirole did too. Too little or too much D2-stimulation via ropinirole suggested to be sub-optimal, impairing non-focal plasticity induced tDCS and excitatory paired associative stimulation (ePAS)-generated plasticity. The narrow dose-range used from 0.125 mg to 1.0

mg of ropinirole shows the importance of obtaining an optimal concentration for D2-R activation. Furthermore, Fukuzaki, et al., (2000) showed a positive outcome at a dose of 2 mg cabergoline (D2-R agonist) where it enhanced practice-dependent plasticity. On the other hand, Breitenstein *et al.*, (2006) showed that a dose of 0.1 mg, pergolide- another D2-R agonist impaired verbal associative learning. In addition, ropinirole at concentrations higher than 10 μM are known to have off-target effects, including 5-HT receptors, and α2A-adrenergic receptors that are known to inhibit AC activity (Kvernmo, Houben and Sylte, 2008). All in all, these findings indicate complicated dosage-dependent effects of D2-like activity in the brain. For this reason, future experiments on older animals were carried out at 200 nM to decrease chances of off-target effects.

D2 and D3 receptor agonist induced activation, has been shown to precede its desensitization making the receptors functionally inactive. This D2-receptor desensitization and internalisation (RDI) has been demonstrated *in vivo* (Guo *et al.*, 2010b) and is a phenomenon that occurs within minutes of agonist exposure, which may cause receptors to internalise for a prolonged period (Skinbjerg *et al.*, 2010). RDI occurs when specific residues on the C terminal domain of the receptor are phosphorylated by GRK2/3. This phosphorylation elicits the recruitment of β–arrestins that then trigger receptor desensitization and internalization (Beaulieu and Gainetdinov, 2011). However, ropinirole is an unbiased ligand that solely activates the $G_{\alpha i}$ protein therefore a GRK2/3 inhibitor, compound-101 was used as a tool in my protocols to prevent tonic D2-R desensitization. 10 μM compound-101, a GRK2/3 inhibitor was used, as it's known to bind with great specificity to the ATP binding domain of GRK2/3. In the paper by Thal *et al.*, (2011), inhibition of GRK2 is investigated. The K_m for ATP is estimated to be approximately 30 μM and the K_i for compound-101 = 2 nM (Table 2 of Thal *et al.*, 2011). Therefore, we expected 10 μM Compound-101 would reduce the GRK activity by 87.5 % (see Methods). However, the presence of compound-101 did not change the NMDA-R response either in the presence or absence of ropinirole suggesting D2-R desensitization via GRK is not obscuring an effect of ropinirole in substantia nigra dopaminergic neurons

further demonstrating ropinirole's unbiased binding ability. This was seen in both P7 and P21 rat brain slices suggesting D2-R desensitization is not the reason there was a lack of D2 modulation of NMDA responses in early post-natal development.

6.2 Developmental differences in D2-Receptor modulation of NMDA-Receptors

Understanding the developmental changes that take place, primarily in NMDA-Rs, directed the remaining of the pharmacological experiments on older rats. The distribution pattern on NMDA-R subunits observed at both a cellular and synaptic level have significant effects on the overall kinetics of the NMDA-Rs (Pearlstein *et al.*, 2016). Therefore, to understand mechanisms associated with the modulation of NMDA-Rs, it is important to test the dopaminergic neurons at different stages of development (P7, P21, and P28). When the control NMDA-R responses were compared between all three stages of development, it was obvious that there is decreased NMDA receptor responses at later ages compared to P7 rats where responses neared 900pA. As previous pharmacology has suggested receptor subtypes are not changing during development (Brothwell *et al.*, 2008a; Suárez *et al.*, 2010), it is likely there is a decrease in the number of receptors available on the surface of the cell. The overall inward current significantly decreased (P=0.006). 200 nM ropinirole was then introduced to P21 and P28 rats, as done in P7 rats to determine whether activating the D2-Rs could affect the NMDA-R response in older animals. D2-R activation on P21 rats increased the NMDA-R inward current. This may coincide with a change in receptor subunit composition thus change in kinase phosphorylation of the NMDA-Rs. Furthermore, when D2-Rs were activated with simultaneous inhibition of GRK2/3 (responsible for receptor desensitisation), the current reduced to baseline (as in the P21 control experiment) relative to D2-R activation alone (Unpaired t-test, P=0.0265). This suggests a change in tonic D2-R receptor desensitization in 21 days post-natal development. However, it was evident that as the rats aged, there was no visible change in the effect of ropinirole as seen in P28 rats.

Upon D2-R activation P7 rats showed a change in NMDA inward current of 55 ± 22% relative to the control. P21 rats exhibited a smaller change in NMDA-R response at 10 ± 11% relative to its control, followed by P28 rat dopaminergic neurons, that showed a 7.4 ± 7.3% decrease in NMDA-R current. These small variations in response could be due to changes in proportions of GluN2B and GluN2D subunits present with age as suggested in Brothwell *et al.*, (2008) (see also Watanabe *et al.*, 1993; Morris, et al., 2018) as well as number of receptors embedded on the membrane.

6.3 A2A and D2-Receptor heteromerization in P28 dopaminergic neurons

The allosteric interaction of D2-Rs and A2A-Rs is a potential target in drug development in the treatment of Parkinson's disease (Fuxe *et al.*, 2010). There is substantial evidence to suggest the heteromerization of these two receptors in various parts of the brain. BRET and FRET experiments carried out *in vitro* to study the oligomerization potential of GPCRs, showed that A2A-Rs are inclined to decrease D2-R recognition and activation in the striato-pallidal GABA pathway (Canals *et al.*, 2003; Fuxe *et al.*, 2010). Considering the canonical binding and subsequent activation of A2A-Rs to $G\alpha_s$ protein (increasing cAMP and PKA activity), an increase in NMDA-R phosphorylation would occur, thus an enhancement in NMDA current (Rebola *et al.*, 2008). In the experiments carried out in this study, inhibiting A2A-Rs with SCH58621, did not change the NMDA-R current. This was observed at both 200 nM and 1 μM concentrations. Assuming the presence of minimally present endogenous dopamine, the D2-R activity should be completely masked by SCH58621 preventing any activation and subsequent $G\alpha_{i/o}$ stimulation of the GPCR secondary pathway, which should decrease NMDA-R phosphorylation and resulting current. This suggests any tonic inhibition of A2A-Rs is not sufficient to modulation NMDA-Rs current. A comparable result was observed in the presence of 200 nM Ropinirole (D2-R agonist) in the presence of 200 nM SCH58621 (A2A-R antagonist). This experiment was done to determine whether the binding of either ligand would

alter the potential signalling of the other's receptor. As seen in biophysical experiments performed by Canals *et al.*, (2003), adding an A2A-R antagonist, prevented a canonical response to Ropinirole (D2-R agonist). In my study, both drugs were pre-applied simultaneously to allow equal binding opportunity. Although inhibiting A2A-Rs did not change the NMDA-R current on its own, it seemed to inhibit D2-R activation as no change in NMDA-R current was observed. Furthermore, when the results were compared to experiments where only D2-Rs were activated, there was no change in NMDA-R response. This suggests a different mechanism that drives D2-R response that will be discussed shortly. However, when the A2A-R antagonist was applied in the presence of a D2-R antagonist, there was a significant increase in NMDA-R current suggesting A2A-R ligand binding favours specific D2-R ligands. This is suggested by a study I carried out with the D2-R antagonist, Sulpiride. When introduced alone, it made no obvious difference on the overall mean NMDA-R current. However, when the A2A-R antagonist was introduced, the NMDA-R current increased by 75%. This may be due to further inhibiting the activation of $G\alpha_{i/o}$ protein coupled to D2-Rs. This then facilitates PKA-induced NMDA-R phosphorylation leading to enhanced NMDA current. This further suggests that A2A-Rs could have a potential role in D2-R modulation of NMDA-Rs in the dopaminergic neurons of the substantia nigra. Furthermore, it poses the question of whether a D2-R inhibitory mechanism is biologically present to allow such a phenomenon to occur or A2A-R tonic activation sufficient to balance known D2-R inhibitory effects?

When A2A-Rs were activated using 1 μM CGS21680, I observed a statistically significant increase in the mean NMDA-R current, however, not in the presence of 10 μM CGS21680. Effective D2-R ligand binding and subsequent activation of internal proteins was tested in the presence of an A2A-R agonist- 10 μM CGS21680. When D2-R agonist and antagonist were introduced in the presence of the A2A-R agonist, a significant increase in NMDA inward current was observed. Ferre *et al.*, (1991) showed that CGS21680, in addition to supressing D2-R affinity for a radio-labelled agonist, [^{3}H] N-propylnorapomorphine, it decreased (by nearly 3-fold) the low and high affinity

states of D2-Rs for dopamine (Ferré *et al.*, 1992). Inaddition, as seen by Borroto-Escuela *et al.*, (2018), dampening of D2-R effect by A2A-R is a known mechanism and is thus suggested in the research carried out in this thesis.

A2A-R agonist and antagonists were applied simultaneously at concentrations that allowed equal binding and effectiveness (% occupancy of 98% interchangeably). This resulted in an unexpected increase in inward NMDA-R current as Bruns, Lu and Pugsley, (1986) showed the CGS21680 effects were inhibited by A2A-R antagonist 8-phenyl-theophylline. The difference in results may be due to the slice preparation technique and long incubation period (30 mins) that Bruns et al., allowed for drugs to interact thus producing the stated results.

Understanding potential modulatory roles of D2-Rs on NMDA-Rs requires understanding the signalling cascades involved once receptors are either blocked or activated. As shown by Leonard and Hell, (1997) DA-Rs have different modulatory roles based on whether or not they are in physical contact with NMDA-Rs (Yang, *et al.*, 2014). This may occur via the activation of different secondary systems present in the cell; e.g, PKA versus PKC signalling cascades. Having said that, my results suggest that A2A-R and D2-R co-modualtion of NMDA-Rs is potentially via G-proteins and subsequently PKA-dependent. This is shown in experiments involving forskolin, a driver for cAMP production which in theory, should increase the phosphorylation and presence of NMDA-R on the surface membrane. When forskolin was introduced alone at both concentrations (0.5 μM and 2.5 μM), the NMDA-R current increased with a statisical significance relative to their corresponding controls. It was also evident that effects of forskolin are quite pronounced even after the drug has been washed off possibly because of the extent of accumulation of cAMP in a closed system. PKI (PKA inhibitor) was then introduced in the presence of forskolin. The increase in current observed was similar to the results in the presence of forskolin alone. This may be due to the shorter incubation period prior to recording and introducing forskolin. Aman *et al.*, (2014) showed that PKI decreased NMDA current after 10 mins of incubation prior to recordings by

increasing the channel closed time thus reducing receptor gating, but an effect on receptor trafficking is also possible.

To determine the signaling cascade triggered upon D2-R activation (whether inhibitory or excitatory), ropinirole was introduced after forskolin to determine whether it would reduce the NMDA-R effects caused by increasing cAMP production. The protocol included an initial control application of 20 μM NMDA. This was followed by an application of 0.5 μM Forskolin. This raised the NMDA-R current significantly (from 461 ± 80 pA, Control to 597 ± 74 pA, Forksolin; N=13, Paired T-Test, P=0.03). 200 nM Ropinirole was then preapplied as forskolin was washed off (as mentioned earlier, forskolin effects are irreversible with a simple washoff). This allowed the receptors to equilibrate prior to the application of NMDA. In the presence of the D2-R agonist- ropinirole, the mean NMDA-R current began to decrease. As the ropinirole application was maintained throughout the remainder of the protocol, a further decrease was observed. This suggests a decreased cAMP-PKA dependent effect on NMDA-Rs via D2-Rs. This effect of ropinirole was also seen at a higher concentration of forskolin (2.5 μM). The decrease in current observed in this experiment following application of ropinirole was much more pronounced than in previous experiments, where ropinirole was introduced alone. A similar reponse was seen in hippocampal CA1 neurons (see Appendix). It was therefore postulated that the endogenous levels of cAMP may not have been high enough in earlier experiments to establish a real effect of ropinirole on the NMDA-R current.

6.4 Non-receptor tyrosine kinase modulation of NMDA-Rs on P28 dopaminergic neurons of the SNc

6.4.1 Inhibiting Src and Fyn kinases decrease NMDA-R current

Alongside the Ser-Thr kinase activity involved in NMDA-R modulation, Src family protein kinases (SFK) were shown to play a substantial role in NMDA-R modulation. Both PP2 (src and fyn inhibitor) and Src-I1 (potent Src inhibitors) decreased NMDA-R currents rapidly and reversible by virtue of Src kinase's

ability to phosphorylate NMDA-Rs (figure 6). Lu *et al.*, (2018) showed that GluN2B at the Y1070 site is phosphorylated by Fyn (member of the SFK) *in vivo* and *in vitro*. This was shown by introducing a rabbit monoclonal antibody against phosphorylated Y1070 on GluN2B, which in turn produced a strong signal. However, the signal was eliminated upon phophatase treatment. Furthermore, when Fyn inhibitors PP2 and Su6656 were introduced to cultured neurons, the level of PY1070 was largely reduced but not in the presence of PP3 (an inactive PP2 analogue), further suggesting that Fyn is responsible for phosphorylating GluN2B.

Appreciating its phosphorylation potential, TAT-Fyn peptide (Transasctivator of Transcription) was introduced in my experiments to determine whether inhibiting Fyn would alter the NMDA-R current in the substantia nigra DAergic neurons. The results suggested that it had no effect on NMDA-Rs, as both the control and experimental Fyn peptides caused a significant increase in NMDA-R whole cell current. However, relative to its scrambled control- TAT-sSrc (producing a statistically significant increase), 10 μM TAT-Src did not change the NMDA-R current this suggests src modulation of NMDA-Rs is not limited to the direct interaction with NMDA-Rs. Both TAT-Fyn and TAT-Src were applied simultaneously to determine if there was a possible summation of effects, however, there was a similar response to the addition of the Src inhibitor peptide.

There is ample evidence in the literature related to Src phosphorylation of NMDA-Rs. But understanding the mechanisms that may control overactivation of NMDA-Rs is paramount as well. The effects of PP2 and Src-I1 on NMDA-R observed in my research suggests a potential role of Csk (an endogenous Src repressor) in regulating NMDA-R function through Src family kinase. Socodato *et al.*, (2017) showed that upon D1-R activation, there is an increase in PKA activity thus increasing phosphorylation of Ser^{364} at Csk kinase domain. The Csk induced inhibition of Src kinase was also observed in retinal neurons (Yaqub *et al.*, 2003; Socodato *et al.*, 2017). Considering the absense of D1-Rs in dopaminergic neurons of the substantia nigra, Csk activation must be driven by the transactivation of PDGF-Rs (Platelet derived growth factor- receptors) via

D2-R-βγ–coupled receptors. There is sufficient evidence to suggest the presence of PDGF-R on dopaminergic neurons (Valenzuela *et al.*, 1996; Kotecha *et al.*, 2002). MacDonald *et al.*, (2007) described the effect of PKA stimulation induced by PDGF-Rs where PKA accumulation leads to the subsequent phosphorylation of Csk tyrosine kinase. Specifically-induced, this phosphorylation would then inhibit Src kinase, supressing NMDA-R current. Kotecha *et al.* (2002) showed that the activation of D2-R-βγ, led to the phosphorylation of PDGF-R at Tyr330 and activation of the MAPK pathway in the CA1 region of the hippocampus (Caldwell *et al.*, 2012) All in all, they showed that Gβγ subunits are upstream of PDGF-R transactivation but downstream of D2/D4-Rs.

Another potential modulator of Src/Fyn kinase is the brain-specific striatal enriched protein phosphatase (STEP). It targets many synaptic substrates in neurons and its expression and activity are regulated by its ubiquitination and phosphorylation by PKA at Ser245 (Lombroso *et al.*, 1993; Valjent *et al.*, 2005; Won and Roche, 2020). The specific splice variant present in the striatum is the shorter form $STEP_{46}$. STEP activity can affect NMDA-Rs directly or indirectly via acting on other kinases. Primarily, STEP targets the GluN2B Y1472 residue within the endocytic motif and dephosphorylates it triggering internalisation (Lavezzari *et al.*, 2004; Won and Roche, 2020). Furthermore, they act indirectly on NMDA-Rs by dephosphorylating Y420 in the catalytic domain of Fyn kinase rendering it inactive (Nguyen, Liu and Lombroso, 2002; Won and Roche, 2020). Targeting STEP via potent inhibitors such as TC-2153 has been shown to increase tyrosine phosphorylation of STEP substrates such as GluN2B and ERK1/2 in neuronal cultures. Ultimately, overactivation and dysregulation can lead to cognitive deficits and may be age-related (Won and Roche, 2020). This suggests a future experiment worth performing which is testing the age-related effects of STEP phosphatase as well the overall modulation of Src/Fyn and ERK1/2 kinase on NMDA-Rs of the substantia nigra.

6.4.2 Inhibiting ERK and CaMKII decreased NMDA-R inward currrent

In this thesis, potential involvement of the MAPK cascade in modulating NMDA-Rs was studied using the ERK1/2 inhibitor, Ulixertinib. ERK1/2 is the final step in the phosphorylation cascade of the MAPK pathway therefore potentially allowing an easier understanding of its involvement in modulating NMDA-Rs in the substantia nigra. Upon application of the ERK1/2 inhibitor, the NMDA-R current showed a rapid significant decrease in NMDA-R current after which the effects were reversed causing the currents to return to baseline. This further suggests MAPK pathway's potential involvement in modulating SNc NMDA-R currents.

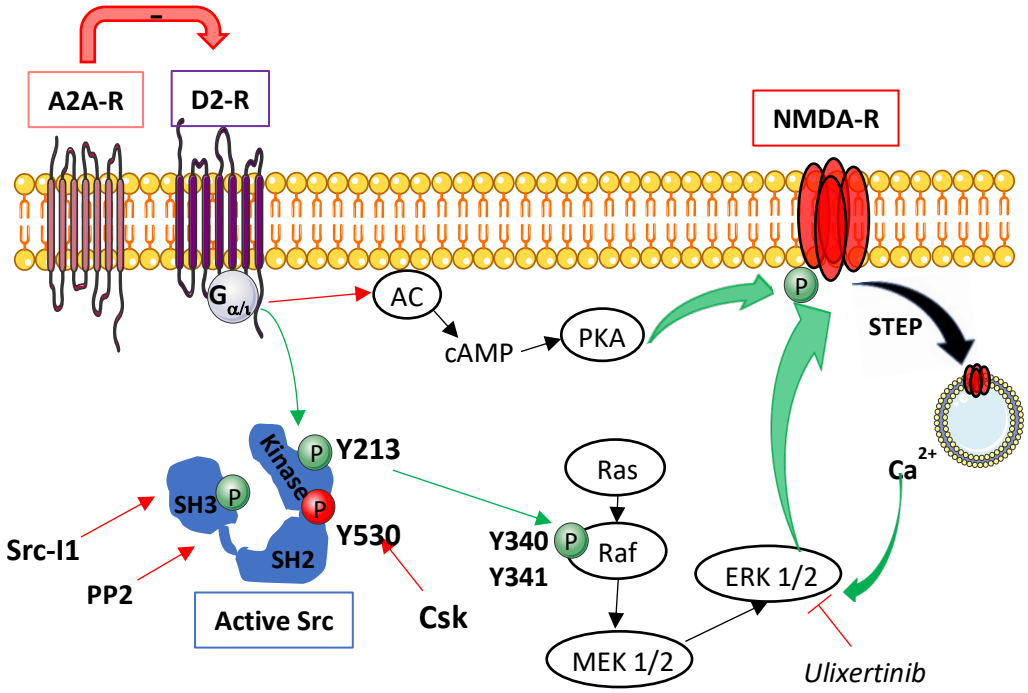

***Figure 6 A schematic diagram illustrating the postulated effects upon D2-R activation on NMDA-R response**, and the involvement of Src kinase the MAPK pathway. Also illustrated is A2A-R activation and its ability to occlude D2-R activation or inhibition.*

Lastly, the involvement of CaMKII in GluN2B containing NMDA-R modulation was studied. 20 μM TAT-CN21 peptide was used to inhibit CaMKII activity. Following the application of the scrambled control peptide, the steady-state NMDA-R current showed a statistically significant increase in current. However,

this increase was abolished in the presence of the active inhibitor. The resulting NMDA-R current was reduced relative to control (in the absence of CaMKII inhibitor) suggesting receptor modulation was encouraged.

The main aim of my research was to elucidate the modulative potential of D2-Rs on NMDA-Rs in dopaminergic neurons of the substantia nigra. It is evident that D2-Rs can decrease the overall NMDA-R current and this is a phenomenon observed in older animals in the presence of sufficient intracellular [cAMP]. This was made apparent upon the application of Forskolin and Ropinirole, a D2-R agonist. Furthermore, D2 and A2A-Rs can potentially modulate ligand binding to either receptor. Specifically, A2A-Rs inhibition allows for D2-R antagonist to exert it effects, and A2A-R agonist binding occludes D2-R ligand activity (whether inhibitory or excitatory). It was clear that dopaminergic neuron NMDA-Rs may be regulated via Src and Fyn kinase, however their effects may not involve direct interaction with NMDA-Rs. A potential postulate for the method of modulation via Src includes PKA phosphorylation of Ser^{364} of the Csk kinase domain, or the transactivation of PDGFR via D2- $G\alpha_{i/o}$ coupled receptor. PDGF-R activation has the ability to activate the MAPK pathway which my research suggested could affect NMDA-Rs upon the application of an ERK1/2 inhibitor, Ulixertinib. CaMKII phosphorylation of NMDA-R was previously shown in hippocampal slices (Barcomb *et al.*, 2016). Introducing a CaMKII inhibitor, TAT-CN21 decreased the NMDA-R current suggesting a similar regulatory role in dopaminergic neurons of the substantia nigra.

6.5 Future directions

Following experiments using Tat-CN21 and biocytin to label cells, it was evident that DA cell populations in different parts of the SNc (medial to lateral) show differential responses to any form of drug application. This was also observed in previous experiments done in my study where the array of data points formed visible distinct groups that responded differently to the same drug or combination of drugs. Furthermore, it has been shown that DAergic neurons found in ventrolateral and dorsal regions of the SNc project to different neurochemical compartments (Maurin *et al.*, 1999; Neuhoff *et al.*, 2002b). In addition, they differ in their neuroprotective nature based on their expression of the calcium-binding protein Calbindin (CB) D_{28}-k (Gerfen, 2000). In the SNc, DAergic neurons in the ventrolateral and caudal regions are prone to cellular degeneration which coincides with the absence of CB (German *et al.*, 1992; Dopeso-Reyes *et al.*, 2014). CB is essential in that it regulates Ca^{2+} ion availability in the cell by buffering Ca^{2+} overload thus protecting the cells from excitotoxicity (Reisner, *et al*., 1992; Dopeso-Reyes *et al.*, 2014). They are particularly vital in SNc DA neurons as Ca^{2+} receptors remain open for a longer period of time relative to other parts of the brain (C J Wilson and Callaway, 2000). This selective vulnerability seen in PD pathophysiology could be owed to the diverse differentiation routes during embryonic development. These in turn, produce disparity in the DA phenotypes (Smits, *et al*., 2006; Smidt and Burbach, 2007; Dopeso-Reyes *et al.*, 2014). Thus, future studies in elucidating the NMDA-R modulation and pharmacology could take cellular topography in the brain into consideration. This difference could be vital to understanding true effects of drugs that could potentially be exerting varied effects in different DA populations of the SNc. To perform these experiments, a combination of electrophysiology, to study the ionic electrical current and immunohistochemistry to visualise DA cells undergoing whole-cell patch clamp would be paramount.

Developing on the above experiments, would be to determine whether the results obtained in my experiments are D2-R specific or not. Thus, a D2-knockout (D2-KO) rat could be used. Studies on these rats would highlight any

effects that are not D2-R-specific and in addition, pronounce those that are. This would allow me to conclude the extent of modulation D2-R have on NMDA-Rs. Secondly, considering the potential heteromerization of D2-R and A2A-Rs in SNc DAergic neurons, A2A-KO could be examined as well. This will emphasize their importance in augmenting or dampening D2-R modulation. Making these leaps to better understand NMDA-R modulation will elucidate a lot of unknown knowledge with regards to cellular vulnerability in PD pathophysiology. Monitoring intracellular Ca^{2+} via imaging approaches, alongside other experiments, will further develop our understanding of the involvement of both calbindin and NMDA-Rs in protecting and degenerating cellular integrity as calcium is known to trigger versatile intracellular signals and changes.

Lastly, the use of a biased D2-R ligand (UNC9994) would help elucidate the true involvement of selectively activating β-arrestin upon D2-R activation. D2-Rs can signal through 2 transducers, either the $G_{\alpha/i}$- protein or β-arrestin. Selectively engaging either pathway to study their effects on NMDA-R current would help improve drugs targeting GPCRs in dopaminergic neurons of the substantia nigra. Another approach would be to use mutant mice that preferentially interact with either G-protein or β-arrestin (Pack *et al.*, 2018).

All in all, efforts towards elucidating NMDA-R modulation in SNc DAergic neurons will have implications in a number of neurodegenerative disorders, such as schizophrenia and PD and potentially bring about therapeutic targets with greater specificity and fewer side effects.

Chapter 7:

Appendix

P7 Experiments:

***Table 1*: Control 20μM NMDA (Dopamine neurones)**

Protocol: 20μM NMDA (120s) Peak 1 → Wash off (300s) Baseline 2→ 20μM NMDA (120s) Peak 2 → Wash off (300s) Baseline 3.

EDR File Name	Baseline 1(-pA)	Peak 1 (-pA)	Baseline 2 (-pA)	Peak 2 (-pA)	Baseline 3 (-pA)
30-7-2015_004.EDR	524	629.04	526	632.32	523
5-8-2015_003.EDR	26.1	890	41	724	23
6-8-2015_001.EDR	160	1023	130.6	907	96.5
6-8-2015_002.EDR	596	1069	220	685	320
7-8-2015_002.EDR	113	622	90.5	704	199
7-8-2015_003.EDR	50	1477	32.4	1882	162.5
7-8-2015_006.EDR	31.6	1078	118	917	162
10-8-2015_001.EDR	81	492	21	692	33
10-8-2015_004.EDR	114	892	83	799	5.7
10-8-2015_007.EDR	100	708	12	565	1
10-8-2015_010.EDR	90	1233	53	1185	58
	Mean	919		881	
	SEM	89.0		113	
	N=	11		11	
	Rats=	5			

Table 2: **20μM NMDA + 20μM Ropinirole**

Protocol: 20μM NMDA (120s) Peak 1 → Wash off + 20μM Ropinirole (300s) Baseline 2→ 20μM NMDA + 20μM Ropinirole (120s) Peak 2 → Wash off + 20μM Ropinirole (300s) Baseline 3.

EDR File Name	Baseline 1(-pA)	Peak 1 (-pA)	Baseline 2 (-pA)	Peak 2 (-pA)	Baseline 3 (-pA)
18-8-2015_001.EDR	80	370	9	406	Lost cell
18-8-2015_003.EDR	140	1048	44	1007	41
14-8-2015_002.EDR	230	1161	67	1202	71
19-8-2015_005.EDR	50	898	18	817	39
20-8-2015_003.EDR	340	1938	190	896	333
20-8-2015_004.EDR	350	1614	316	884	355
20-8-2015_006.EDR	220	944	202	957	182
20-8-2015_007.EDR	110	1288	98	535	152
21-8-2015_001.EDR	92	171	8	109	9
21-8-2015_002.EDR	330	794	291	766	313
24-8-2015_001.EDR	244	291	27	250	19
24-8-2015_004.EDR	300	740	85	839	190
24-8-2015_005.EDR	67	1090	3	1398	19
24-8-2015_006.EDR	320	1467	117	1061	132
24-8-2015_007.EDR	11.2	1288	7	1013	17
24-8-2015_008.EDR	40	555	3	958	51
24-8-2015_009.EDR	48	704	48	712	63
18-9-2015_002.EDR	50	1045.5	40	911.7	60
18-9-2015_004.EDR	20	858	10	764.31	12
21-9-2015_002.EDR	60	362.55	60	602.95	120

22-9-2015_002.EDR	22	739	350	1034.5	450
24-9-2015_002.EDR	148	1149	630	1558	580
25-9-2015_003.EDR	42	758	80	1120	170
25-9-2015_004.EDR	20	1425.2	200	1687.5	400
	Mean =	946		895	
	SEM =	88.8		75.0	
	N =	24		24	
	Rats=	11			

Table 3: **20μM NMDA + 10μM Compound-101**

Protocol: *Compound 101 in pipette solution, therefore present throughout recording*

20μM NMDA (120s) Peak 1 → Wash off (300s) Baseline 2→ 20μM NMDA (120s) Peak 2 → Wash off (300s) Baseline 3.

EDR File Name	Baseline 1 (-pA)	Peak 1 (-pA)	Baseline 2 (-pA)	Peak 2 (-pA)	Baseline 3 (-pA)
11-1-2017_001.EDR	56	454	78.5	724.5	110
11-1-2017_002.EDR	21.4	813.98	71	732.42	69
11-1-2017_005.EDR	12	1969.8	78	2066.6	175
12-1-2017-004.EDR	19.9	718.77	68.7	866.7	72
16-1-2017_002.EDR	33	860.67	175	849.15	231
16-1-2017_003.EDR	380	2169.2	449	1452.8	580
16-1-2017_004.EDR	69.5	907.21	145	977.1	182
16-1-2017_006.EDR	78	681.46	159	735.86	253
16-1-2017_007.EDR	143	589.22	260	851.44	343
17-1-2017_001.EDR	210	912.48	430	873.41	865
17-1-2017_005.EDR	146	700.99	87.9	639.11	36.1
	Mean	979		979	
	SEM	168		127	
	N=	11		11	
	Rats=	4			

Table 4: **20μM NMDA + 10μM Compound-101 + 20μM Ropinirole**

Protocol: *Compound 101 in pipette solution, therefore present throughout recording*

20μM NMDA (120s) Peak 1 → Wash off + 20μM Ropinirole (300s) Baseline 2→ 20μM NMDA + 20μM Ropinirole (120s) Peak 2 → Wash off + 20μM Ropinirole (300s) Baseline 3.

EDR File Name	Baseline 1(-pA)	Peak 1 (-pA)	Baseline 2 (-pA)	Peak 2 (-pA)	Baseline 3 (-pA)
8-3-2016_003.EDR	506	1182	1380	508.58	1525
8-3-2016_004.EDR	413	374.37	462	653.61	838
8-3-2016_006.EDR	120	669	260	684	Lost cell
7-3-2016_002.EDR	154	81	154	599.6	109.6
18-3-2016_004.EDR	187	193	113.2	649.8	164
22-3-2016_001.EDR	151.1	226.9	388	303	322
22-3-2016_002.EDR	158	344.09	54.9	583.88	88.4
22-3-2016_003.EDR	199	517.65	381	557.94	461
18-3-2016_001.EDR	404	179	294	1044	532
	Mean	419		620	
	SEM	113		65.0	
	N=	9		9	
	Rats=	5			

Table 5: **20μM NMDA+ 10μM Compound-101 + 200nM Ropinirole**

Protocol: *Compound 101 in pipette solution, therefore present throughout recording*

20μM NMDA (120s) Peak 1 → Wash off + 200nM Ropinirole (300s) Baseline 2→ 20μM NMDA + 200nM Ropinirole (120s) Peak 2 → Wash off + 200nM Ropinirole (300s) Baseline 3.

EDR File Name	Baseline 1 (-pA)	Peak 1 (-pA)	Baseline 2 (-pA)	Peak 2 (-pA)	Baseline 3 (-pA)
24-3-2016_004.EDR	143.3	223.7	222	631.79	256
24-3-2016_006.EDR	236	980.61	396	1143.5	468
18-4-2016_003.EDR	203	1553.6	165	1258.1	Lost cell
25-4-2016.004.EDR	31.5	334.73	94.1	747.07	175
27-4-2016_001.EDR	138	945.43	83.4	507.51	129.2
27-4-2016_002.EDR	216	398.56	463	640.26	Lost cell
27-4-2016_003.EDR	307	245.97	623	596.01	Lost cell
27-4-2016_005.EDR	112	493.32	156	514.83	171
3-5-2016_002.EDR	122.4	931.32	114	1480.8	96
6-5-2016_001.EDR	225	758	80.1	1521	104.1
6-5-2016_002.EDR	228	897.67	187	781.33	363
	Mean	706		893	
	SEM	123		116	
	N=	11		11	
	Rats=	6			

P21-23 Experiments:

***Table 6*: Control 20μM NMDA**

Protocol: 20μM NMDA (120s) Peak 1 → Wash off (300s) Baseline 2→ 20μM NMDA (120s) Peak 2 → Wash off (300s) Baseline 3 → 20μM NMDA (120s) Peak 3 → Wash off (300s) Baseline 4.

EDR File Name	Baseline 1 (-pA)	Peak 1 (-pA)	Baseline 2 (-pA)	Peak 2 (-pA)	Baseline 3 (-pA)	Peak 3 (-pA)	Baseline 4 (-pA)
1-12-2016_001.EDR	57	550.38	86.4	591.89	95.3	619.51	110
1-12-2016_003.EDR	35.3	400.24	123	372.62	147	413.97	83.4
1-12-2016_004.EDR	72.7	332.18	66.3	255.58	59	284.27	44.2
2-12-2016_001.EDR	68.4	49.5	135.5	505.37	78	729.52	107.9
2-12-2016_002.EDR	40	611.57	61.8	473.48	47.7	459.75	52.1
2-12-2016_003.EDR	81	148.62	102	190.12	128	369.72	189
2-12-2016_004.EDR	125	609.44	200	650.79	230	Lost cell	
2-12-2016_005.EDR	46.2	211.49	105	404.82	166	Lost cell	
2-12-2016_007.EDR	226	476.84	559	1043.1	757	1012.7	Lost cell
2-12-2016_008.EDR	80	458.68	90	665.89	77.7	569.15	65.3
2-12-2016_009.EDR	146	903.78	236	641.33	170	613.71	138
	Mean	432		526.82		563.59	
	SEM	73.19		70.55		72.99	
	N=	11		11		9	
	Rats=	2					

***Table 7*: 20μM NMDA + 200nM Ropinirole**

***Protocol*:** 20μM NMDA (120s) Peak 1 → Wash off + 200nM Ropinirole (300s) Baseline 2→ 20μM NMDA + 200nM Ropinirole (120s) Peak 2 → Wash off (300s) Baseline 3.

EDR File Name	Baseline 1 (-pA)	Peak 1 (-pA)	Baseline 2 (-pA)	Peak 2 (-pA)	Baseline 3 (-pA)
16-11-2016_001.EDR	120	115	125	366.52	150
16-11-2016_002.EDR	240	590.52	220	828.25	550
16-11-2016_003.EDR	55	352.94	82.3	511.78	97.2
16-11-2016_004.EDR	390	887.45	102	1094.7	309
16-11-2016_005.EDR	150	599.21	174	806.43	200
16-11-2016_006.EDR	88.4	773.77	235	1022.3	237
9-3-2017_001.EDR	220	643	398	943	393
9-3-2017_003.EDR	30	301	55	494	58
9-3-2017_005.EDR	32	702	87	860	131
9-3-2017_006.EDR	32	509.8	99	812.99	152
9-3-2017_007.EDR	78	1122.9	95	1306.2	128
9-3-2017_007.EDR	300	496.22	336	900.98	357
	Mean	591.15		828.93	
	SEM	77.95		76.99	
	N=	12		12	
	Rats=	2			

Table 8: **20μM NMDA + 10μM Compound-101 + 200nM Ropinirole**

Protocol: *Compound 101 in pipette solution, therefore present throughout recording*

20μM NMDA (120s) Peak 1 → Wash off + 200nM Ropinirole (300s) Baseline 2→ 20μM NMDA + 200nM Ropinirole (120s) Peak 2 → Wash off + 200nM Ropinirole (300s) Baseline 3.

EDR File Name	Baseline 1 (-pA)	Peak 1 (-pA)	Baseline 2 (-pA)	Peak 2 (-pA)	Baseline 3 (-pA)
28-11-2016_001.EDR	161	1024.2	148	1328.9	340
28-11-2016_002.EDR	53.7	479.13	108.4	534.36	160
28-11-2016_003.EDR	175	571.59	33.7	523.38	48.6
28-11-2016_004.EDR	190	508.73	197	453.49	269
28-11-2016_005.EDR	87.9	545.67	113.8	595.4	109.7
28-11-2016_007.EDR	76	486.45	125	590.06	126
28-11-2016_008.EDR	56	178.38	92.9	337.22	88
29-11-2016_001.EDR	75	339.36	66	670.78	62
29-11-2016_003.EDR	80.4	685.88	109.9	628.36	164
29-11-2016_004.EDR	118	574.19	66.7	650.18	84.1
29-11-2016_005.EDR	43.4	562.59	61.9	548.71	86.7
30-11-2016_003.EDR	40	778.81	15.1	654.45	27.7
30-11-2016_004.EDR	290	669.71	224	255.28	170
30-11-2016_005.EDR	30	675.81	31.9	523.99	46.2
	Mean	577.18		592.47	
	SEM	52.93		65.04	
	N=	14		14	
	Rats=	3			

P28 Experiments:

***Table 9*: Control 20μM NMDA**

***Protocol**:* 20μM NMDA (120s) Peak 1 → Wash off (300s) Baseline 2→ 20μM NMDA (120s) Peak 2 → Wash off (300s) Baseline 3 → 20μM NMDA (120s) Peak 3 → Wash off (300s) Baseline 4.

EDR File Name	Baseline 1 (-pA)	Peak 1 (-pA)	Baseline 2 (-pA)	Peak 2 (-pA)	Baseline 3 (-pA)	Peak 3 (-pA)	Baseline 4 (-pA)
22-11-2016_001.EDR	140	594.33	190	797.88	194	696.11	271
22-11-2016_004.EDR	380	494.84	652	737.46	682	834.5	844
22-11-2016_006.EDR	130	1003.4	103	1279.9	220	1512	200
22-11-2016_007.EDR	82.3	521.85	166	563.2	255	687.56	247
17-3-2017_002.EDR	67	1608.7	143	1309.4	201	1093.4	300
17-3-2017_003.EDR	180	788.12	356	635.83	377	600.28	346
17-3-2017_004.EDR	270	704.35	430	484.61	321	417.18	330
23-3-2017_001.EDR	19.6	397	58.8	482.75	89	472.75	62.3
23-3-2017_004.EDR	82	878.14	105.5	827.94	221	771.03	197
23-3-2017_005.EDR	71	910.8	80.6	886.23	147	850.37	135
8-8-2018_003.EDR	97	175	67	289	76	323	84
9-8-2018_005.EDR	157	165.71	124	353.7	181	455	310
	Mean	686.85		720.66		726.10	
	SEM	114.73		94.14		95.17	
	N=	12		12		12	
	Rats=	5					

Table 10: **20μM NMDA + 200nM Ropinirole**

Protocol: 20μM NMDA (120s) Peak 1 → Wash off + 200nM Ropinirole (300s) Baseline 2→ 20μM NMDA + 200nM Ropinirole (120s) Peak 2 → Wash off (300s) Baseline 3.

EDR File Name	Baseline 1 (-pA)	Peak 1 (-pA)	Baseline 2 (-pA)	Peak 2 (-pA)	Baseline 3 (-pA)
27-10-2016_003.EDR	214	490.42	380	536.65	353
27-10-2016_005.EDR	440	432.43	350	485.38	423
28-10-2016_004.EDR	61.1	283.9	84.9	250	100
10-11-2016_003.EDR	48.3	604.25	83.5	637	157
10-11-2016_004.EDR	61.3	306.55	118.9	410.61	151
10-11-2016_005.EDR	34.7	507.2	92.1	611.42	250
11-11-2016_002.EDR	220	477.6	303	693.21	240
11-11-2016_003.EDR	250	441.59	344	419.31	401
11-11-2016_004.EDR	62.9	204.32	97	235.6	136.5
11-11-2016_005.EDR	94.6	509.49	198	829.77	184
16-10-2017_001.EDR	90	220.83	118.4	163.21	130.2
16-10-2017_002.EDR	103	575.71	130	734.25	166
16-10-2017_004.EDR	100	1546.8	470	1204.5	381
16-10-2017_005.EDR	50	861.66	97	725.86	169
16-10-2017_006.EDR	89	2065.7	392	1231.7	275
	Mean	635.23		611.23	
	SEM	132.35		81.39	
	N=	15		15	
	Rats=	5			

Table 11: **20μM NMDA + 10μM Compound-101**

Protocol: *Compound 101 in pipette solution, therefore present throughout recording*

20μM NMDA (120s) Peak 1 → Wash off (300s) Baseline 2→ 20μM NMDA (120s) Peak 2 → Wash off (300s) Baseline 3 → 20μM NMDA (120s) Peak 3 → Wash off (300s) Baseline 4.

EDR File Name	Baseline 1 (-pA)	Peak 1 (-pA)	Baseline 2 (-pA)	Peak 2 (-pA)	Baseline 3 (-pA)	Peak 3 (-pA)	Baseline 4 (-pA)
31-3-2017_001.EDR	34.7	24.17	87.4	48.82	127	58.83	34.7
3-4-2017_001.EDR	76.2	742.19	79.7	787.2	133	812.84	76.2
3-4-2017_002.EDR	60.4	446.17	90.7	659.79	149	686.95	60.4
3-4-2017_003.EDR	40	565.8	160	711.82	739	Lost cell	
3-4-2017_004.EDR	129	727.39	235	831.76	Lost cell		
3-4-2017_005.EDR	107	1248.5	930	667.11	407	1069.8	107
5-4-2017_001.EDR	73.1	52	91.9	87.55	112	60.85	73.1
5-4-2017_002.EDR	110	84	100	120.7	119	182.34	110
5-4-2017_003.EDR	90	152.89	113	141.14	110	231.48	90
5-4-2017_004.EDR	32	352.78	105	304.87	160	321.66	32
5-4-2017_006.EDR	48.6	216.83	105	702.82	118	1109.2	48.6
	Mean	419.34		460.32		503.77	
	SEM	113.97		95.30		140.47	
	N=	11		11		9	
	Rats=	3					

Table 12: **20μM NMDA + 10μM Compound-101 + 200nM Ropinirole**

Protocol: *Compound 101 in pipette solution, therefore present throughout recording*

20μM NMDA (120s) Peak 1 → Wash off + 200nM Ropinirole (300s) Baseline 2→ 20μM NMDA + 200nM Ropinirole (120s) Peak 2 → Wash off + 200nM Ropinirole (300s) Baseline 3.

EDR File Name	Baseline 1 (-pA)	Peak 1 (-pA)	Baseline 2 (-pA)	Peak 2 (-pA)	Baseline 3 (-pA)
14-11-2016_001.EDR	230	488	320	865.33	310
24-3-2017_002.EDR	72	94.45	142	1015	139
28-3-2017_001.EDR	60.5	647.58	104	443.73	114.5
28-3-2017_002.EDR	75.2	561.73	150	474.24	Lost cell
28-3-2017_004.EDR	92	151.52	74.4	218.5	98
30-3-2017_002.EDR	155	1052.9	109.5	1135.6	128
30-3-2017_003.EDR	62.7	777.28	191	656.59	Lost cell
30-3-2017_005.EDR	34.4	715.94	32.7	695.65	48.2
30-3-2017_006.EDR	69.6	1834.4	325	2000	Lost cell
30-3-2017_007.EDR	48.7	332.49	26.6	338.59	42.7
	Mean	665.63		784.32	
	SEM	158.99		163.85	
	N=	10		10	
	Rats=	4			

Table 13: **20μM NMDA + 1μM Sulpiride**

Protocol: 20μM NMDA (120s) Peak 1 → Wash off + 1μM Sulpiride (300s) Baseline 2 → 20μM NMDA + 1μM Sulpiride (120s) Peak 2 → Wash off (300s) Baseline 3 → 20μM NMDA (120s) Peak 3 → Wash off (300s) Baseline 4.

EDR File Name	Baseline 1 (-pA)	Peak 1 (-pA)	Baseline 2 (-pA)	Peak 2 (-pA)	Baseline 3 (-pA)	Peak 3 (-pA)	Baseline 4 (-pA)
16-8-2017_001.EDR	330	51.88	450	96.588	558	209.29	679
16-8-2017_002.EDR	280	645.17	250	592.35	265	614.93	300
16-8-2017_004.EDR	107	275.42	244	540.47	305	637.82	434
16-8-2017_005.EDR	111	652.77	335	664.98	429	628.2	479
16-8-2017_006.EDR	97	343.63	127.8	511.32	62.6	Lost cell	
16-8-2017_007.EDR	124	900.57	409	1226.3	554	811	517
17-8-2017_002.EDR	270	1239.8	470	791.63	344	242	91
17-8-2017_003.EDR	200	292.21	303	562.59	300	648.35	
17-8-2017_004.EDR	73	1053.8	180	844.88	253	850.68	150
17-8-2017_005.EDR	36	113.22	70	203.7	151	543.37	169
17-8-2017_006.EDR	80	814.21	177	873.41	315	914.61	402
17-8-2017_007.EDR	70	661.93	118	878.3	287	626.37	290
	Mean	587.05		648.88		611.51	
	SEM	108.76		88.76		67.04	
	N=	12		12		11	
	Rats=	2					

***Table 14*: 20μM NMDA + 200nM SCH58621**

Protocol: 20μM NMDA (120s) Peak 1 → Wash off + 200nM SCH58621 (300s) Baseline 2 → 20μM NMDA + 200nM SCH58621(120s) Peak 2 → Wash off (300s) Baseline 3 → 20μM NMDA (120s) Peak 3 → Wash off (300s) Baseline 4.

EDR File Name	Baseline 1 (-pA)	Peak 1 (-pA)	Baseline 2 (-pA)	Peak 2 (-pA)	Baseline 3 (-pA)	Peak 3 (-pA)	Baseline 4 (-pA)
31-5-2017_002.EDR	176	680.54	146	610.96	178	562.44	183
31-5-2017_004.EDR	150	878.45	183	679.63	195	636.29	204
1-6-2017_002.EDR	66.4	717.32	91.5	753.17	109	721.44	294
1-6-2017_003.EDR	115	646.06	146	839.23	133	840.91	146
1-6-2017_004.EDR	108	379.94	84.5	623.32	Lost cell		
1-6-2017_005.EDR	38.3	292.66	199	471.34	81.1	458.68	92.4
1-6-2017_006.EDR	166	526.89	154	590.97	158	561.07	165
2-6-2017_001.EDR	38.2	699.77	146	671.54	136	704.96	153
2-6-2017_002.EDR	240	498.05	523	813.6	Lost cell		
2-6-2017_003.EDR	250	839.54	270	661.77	338	Lost cell	
2-6-2017_005.EDR	38	538.33	75.1	632.17	80.4	781.25	100
2-6-2017_007.EDR	80	377.35	106.2	489.2	72.2	565.16	83
2-6-2017_008.EDR	36.8	675.51	55.7	727.69	57.3	795.75	48.2
	Mean	596.18		658.81		795.90	
	SEM	49.66		30.33		39.58	
	N=	13		13		10	
	Rats=	3					

Table 15: **20μM NMDA + 1μM SCH58621**

Protocol: 20μM NMDA (120s) Peak 1 → Wash off + 1μM SCH58621 (300s) Baseline 2 → 20μM NMDA + 1μM SCH58621(120s) Peak 2 → Wash off (300s) Baseline 3 → 20μM NMDA (120s) Peak 3 → Wash off (300s) Baseline 4.

EDR File Name	Baseline 1 (-pA)	Peak 1 (-pA)	Baseline 2 (-pA)	Peak 2 (-pA)	Baseline 3 (-pA)	Peak 3 (-pA)	Baseline 4 (-pA)
25-10-2017_001.EDR	71	258.79	100	395.05	156	373.99	Lost cell
25-10-2017_002.EDR	149	463.87	140	676.27	199	797.58	Lost cell
25-10-2017_004.EDR	200	664.98	175	657.81	308	770.72	427
25-10-2017_005.EDR	74	386.96	114.4	334.01	202	446.78	271
31-10-2017_001.EDR	102	173.65	179	494.38	248	614.78	348
31-10-2017_002.EDR	77	296.48	213	861.97	311	1032.1	423
31-10-2017_003.EDR	110	661	194	821.38	372	824.13	445
31-10-2017_004.EDR	166	305.79	233	601.96	340	691.83	377
2-11-2017_002.EDR	108	1047.8	272	651.09	341	857.7	518
2-11-2017_003.EDR	170	813.45	224	853.58	249	962.22	308
2-11-2017_004.EDR	48	735.17	176	1095.6	282	1256.6	407
2-11-2017_005.EDR	89.9	367.28	155	405.88	241	463.41	274
2-11-2017_006.EDR	160	609.44	184	661.62	225	630	269
2-11-2017_007.EDR	66	710	278	626.37	Lost cell		
	Mean	535.33		652.64		747.83	
	SEM	67.16		55.80		69.45	
	N=	14		14		13	
	Rats=	3					

Table 16: **20μM NMDA + 1μM CGS21680**

Protocol: 20μM NMDA (120s) Peak 1 → Wash off + 1μM CGS21680 (300s) Baseline 2 → 20μM NMDA + 1μM CGS21680 (120s) Peak 2 → Wash off (300s) Baseline 3 → 20μM NMDA (120s) Peak 3 → Wash off (300s) Baseline 4.

EDR File Name	Baseline 1 (-pA)	Peak 1 (-pA)	Baseline 2 (-pA)	Peak 2 (-pA)	Baseline 3 (-pA)	Peak 3 (-pA)	Baseline 4 (-pA)
16-03-2017 _001.EDR	70	839.8	169	1967.**8**	226	1899.4	226
30-03-2017 _002.EDR	120	560	119	620	120	Lost cell	
05-04-2017_005.EDR	140	340	140	620	140	1200	145
07-04-2017 _004.EDR	60	251	86	339.4	99	490.7	144
07-04-2017 _005.EDR	70	424.8	92	1020	105	549	141
26-04-2017 _001.EDR	140	637.2	160	1196	145	1096	187
26-04-2017 _002.EDR	100	250.24	120	383.3	133	300	177
26-04-2017 _003.EDR	140	1176	140	1201	203	1145	311
26-04-2017 _004.EDR	80	449.2	173	646.97	210	522	220
27-04-2017 _002.EDR	36	605.5	87	664.1	126	747	168
27-04-2017 _005.EDR	190	560	210	530	212	580	210
28-04-2017 _001.EDR	100	920	111	625	96	1100	99
	Mean	584.48		817.79		875.37	
	SEM	80.65		132.63		133.54	
	N=	12		12		11	
	Rats=	7					

Table 17: **20μM NMDA + 10μM CGS21680**

Protocol: 20μM NMDA (120s) Peak 1 → Wash off + 10μM CGS21680 (300s) Baseline 2 → 20μM NMDA + 10μM CGS21680 (120s) Peak 2 → Wash off (300s) Baseline 3 → 20μM NMDA (120s) Peak 3 → Wash off (300s) Baseline 4.

EDR File Name	Baseline 1 (-pA)	Peak 1 (-pA)	Baseline 2 (-pA)	Peak 2 (-pA)	Baseline 3 (-pA)	Peak 3 (-pA)	Baseline 4 (-pA)
5-05-2017 _002.EDR	82	742.19	221	949.71	267	964	206
5-05-2017 _003.EDR	100	550	93	650	104	650	107
11-05-2017_003.EDR	80	332	80	351.56	81	380	80
11-05-2017_ 004.EDR	113	740	112	890	113	650	110
19-05-2017_001.EDR	220	860	240	658	211	528	215
19-05-2017_004.EDR	70	537	109	634	116	664	136
2-06-2017_001.EDR	60	947	86	1064	84	1050	97
18-8-2017_002.EDR	75	634.77	126.1	688.93	141.8	586.85	162
18-8-2017_003.EDR	170	204.77	198	405.27	221	451.97	294
18-8-2017_004.EDR	290	526.43	381	533.6	334	304.57	300
18-8-2017_005.EDR	185	884.4	199	1585.5	Lost cell		
18-8-2017_006.EDR	40.8	2108.6	160	1542.2	280	Lost cell	
18-8-2017_007.EDR	190	1283.4	408	1351.9	514	1286.3	498
	Mean	796.20		869.59		683.24	
	SEM	133.79		113.80		90.54	
	N=	13		13		11	
	Rats=	5					

***Table 18*: 20μM NMDA + 200nM Ropinirole + 10μM CGS21680**

Protocol: 20μM NMDA (120s) Peak 1 → Wash off + 200nM Ropinirole +10μM CGS21680 (300s) Baseline 2 → 20μM NMDA + 200nM Ropinirole+ 10μM CGS21680 (120s) Peak 2 → Wash off (300s) Baseline 3

EDR File Name	Baseline 1 (-pA)	Peak 1 (-pA)	Baseline 2 (-pA)	Peak 2 (-pA)	Baseline 3 (-pA)
7-4-2017_001.EDR	37.4	243.171	95.9	486.5	530
7-4-2017_002.EDR	137.8	332.79	76	532.07	230
7-4-2017_003.EDR	46.5	249.63	91.1	744.17	681
7-4-2017_004.EDR	25.6	374.6	95.9	589.45	108.5
26-4-2017_003.EDR	68.1	742.65	123	793.46	315
26-4-2017_001.EDR	88	497.59	173	462.8	207
27-4-2017_001.EDR	250	916.6	461	778.05	265
27-4-2017_002.EDR	218	660.55	391	658.42	196
27-4-2017_003.EDR	135	601.04	152	484.62	136.2
27-4-2017_004.EDR	57.1	399.63	154	468.44	104.3
28-4-2017_002.EDR	33.2	296.17	179	631.1	Lost cell
28-4-2017_004.EDR	125	213.62	162	524.75	162
28-4-2017_005.EDR	91.8	382.23	151	727.69	187
28-4-2017_006.EDR	98.2	306.55	118	440.98	107.6
28-4-2017_008.EDR	102.3	387.57	248	673.22	351
28-4-2017_009.EDR	127	405.58	190	702.67	282
	Mean	438.12		606.15	
	SEM	49.41		30.54	
	N=	16		16	
	Rats=	4			

***Table 19*: 20μM NMDA + 200nM Ropinirole + 200nM SCH58621**

Protocol: 20μM NMDA (120s) Peak 1 → Wash off + 200nm Ropinirole+ 200nM SCH58621 (300s) Baseline 2 → 20μM NMDA + 200nM Ropinirole + 200nM SCH58621(120s) Peak 2 → Wash off (300s) Baseline 3 → 20μM NMDA (120s) Peak 3 → Wash off (300s) Baseline 4.

EDR File Name	Baseline 1 (-pA)	Peak 1 (-pA)	Baseline 2 (-pA)	Peak 2 (-pA)	Baseline 3 (-pA)	Peak 3 (-pA)	Baseline 4 (-pA)
5-5-2017_001.EDR	350	1030	907	942.99	889	Lost cell	
10-5-2017_001.EDR	44.3	371.1	71.1	531.9	120.1	401.9	125.4
10-5-2017_003.EDR	171	226.29	173	570	185	559.08	278
10-5-2017_005.EDR	250	1114.7	526	1409.9	Lost cell		
12-5-2017_002.EDR	200	633.39	530	313.26	356	521.39	568
19-5-2017_002.EDR	50.2	252.99	124	675.81	277	470.58	217
19-5-2017_003.EDR	58.7	416.56	58.1	532.99	74	470.43	114
22-5-2017_001.EDR	68	1492.9	128.7	1052.2	133.7	1044.5	166
22-5-2017_002.EDR	37.7	628.81	55.7	624.85	80.6	623.02	109
22-5-2017_003.EDR	64.2	306.7	82.6	490.72	82.5	618.29	109.1
23-5-2017_004.EDR	152	524.9	208	604.1	238	733.18	156
	Mean	636.21		704.43		604.71	
	SEM	123.30		93.84		58.06	
	N=	11		11		11	
	Rats=	6					

Table 20: **20μM NMDA + 1μM Sulpiride + 10μM CGS21680**

Protocol: 20μM NMDA (120s) Peak 1 → Wash off + 1μM Sulpiride + 10μM CGS-21680 (300s) Baseline 2 → 20μM NMDA + 1μM Sulpiride + 10μM CGS-21680 (120s) Peak 2 → Wash off (300s) Baseline 3 → 20μM NMDA (120s) Peak 3 → Wash off (300s) Baseline 4.

EDR File Name	Baseline 1 (-pA)	Peak 1 (-pA)	Baseline 2 (-pA)	Peak 2 (-pA)	Baseline 3 (-pA)	Peak 3 (-pA)	Baseline 4 (-pA)
27-7-2017_001.EDR	64.2	360.11	158	434.88	149	591.43	220
27-7-2017_002.EDR	83.4	1079.6	154	1097.9	282	1164.1	414
27-7-2017_003.EDR	71.2	133.97	189	1051.6	207	907.14	108.7
28-7-2017_002.EDR	240	757.75	340	1186.5	515	1238.1	
28-7-2017_003.EDR	190	623.93	350	1058.7	483	1238.3	545
28-7-2017_004.EDR	280	1482.7	348	1279.3	437	1282.2	539
28-7-2017_005.EDR	80.9	441.74	148.3	544.43	480	Lost cell	
2-8-2017_001.EDR	80	628.66	174	886.99	256	842.59	380
2-8-2017_002.EDR	66	645.9	159	509.49	277	527.34	266
2-8-2017_003.EDR	146	561.83	343	438.54	320	Lost cell	
2-8-2017_004.EDR	160	1297.3	320	1498.3	367	1313	555
3-8-2017_001.EDR	87	783.32	108	581.36	109	638.43	143.7
3-8-2017_002.EDR	20	1067	52.4	981.6	Lost cell		
3-8-2017_003.EDR	60	295.56	187	632.93	294	724.95	
3-8-2017_004.EDR	137	831.55	198	1340.6	180	856.63	218
3-8-2017_005.EDR	113	1548.2	167	1311.5	377	1245.9	815
3-8-2017_006.EDR	110	1008.9	242	1227.1	396	1506.3	504
3-8-2017_007.EDR	130	1417.8	460	1765.3	680	1739.8	665
	Mean	831.43		990.39		1054.41	

	SEM	98.92		92.73		92.28	
	N=	18		18		15	
	Rats=	4					

Table 20: **20μM NMDA + 1μM Sulpiride + 200nM SCH-59621**

Protocol: 20μM NMDA (120s) Peak 1 → Wash off + 1μM Sulpiride + 200nM SCH-58621(300s) Baseline 2 → 20μM NMDA + 1μM Sulpiride + 200nM SCH-58621 (120s) Peak 2 → Wash off (300s) Baseline 3 → 20μM NMDA (120s) Peak 3 → Wash off (300s) Baseline 4.

EDR File Name	Baseline 1 (-pA)	Peak 1(-pA)	Baseline 2 (-pA)	Peak 2 (-pA)	Baseline 3 (-pA)	Peak 3 (-pA)	Baseline 4 (-pA)
9-8-2017_001.EDR	72	357.51	140.2	581.97	196	788.12	292
9-8-2017_002.EDR	120	726.78	258	665.74	307	640.72	314
9-8-2017_003.EDR	127	164.64	185	714.26	155	388.5	81.2
9-8-2017_004.EDR	159	250.85	288	448	303	771.18	445
9-8-2017_006.EDR	173	632.17	277	1138.5	389	1335.3	800
9-8-2017_007.EDR	130	501.86	244	878.91	450	999.76	564
14-8-2017_003.EDR	40	378.72	154	1124.1	645	1034.2	700
14-8-2017_005.EDR	250	1431.1	370	1396.3	566	1245.4	622
14-8-2017_006.EDR	59	634.16	218	1031.8	588	1008.6	480
14-8-2017_007.EDR	53	697.17	239	1174.5	492	956.12	500
15-8-2017_001.EDR	260	869.28	639	931.7	880	Lost cell	
15-8-2017_002.EDR	80	312.96	169	403.75	267	596.16	412
15-8-2017_003.EDR	50	319.52	176	500.03	319	781.1	390
15-8-2017_004.EDR	65	594.94	330	632.63	462	630.49	
	Mean	562.26		830.16		859.67	
	SEM	86.47		82.94		74.58	
	N=	14		14		13	
	Rats=	3					

***Table 22*: 20μM NMDA + 1μM SCH-58621 + 1μM CGS-21680**

Protocol: 20μM NMDA (120s) Peak 1 → Wash off + 1μM SCH58621 + 1μM CGS-21680 (300s) Baseline 2 → 20μM NMDA + 1μM SCH58621 + 1μM CGS-21680 (120s) Peak 2 → Wash off (300s) Baseline 3 → 20μM NMDA (120s) Peak 3 → Wash off (300s) Baseline 4.

EDR File Name	Baseline 1 (-pA)	Peak 1 (-pA)	Baseline 2 (-pA)	Peak 2 (-pA)	Baseline 3 (-pA)	Peak 3 (-pA)	Baseline 4 (-pA)
24-11-2017_001.EDR	106	875	312	675	289	675	358
24-11-2017_002.EDR	280	978.24	360	734.31	280	658.11	242
24-11-2017_003.EDR	268	853.27	227	811.46	300	696.26	300
24-11-2017_004.EDR	103	816.66	132	924.99	212	1006.6	336
24-11-2017_005.EDR	37.8	312.19	175	643.77	292	905.7	439
24-11-2017_006.EDR	50.1	541.38	110	904.69	153	1015.2	306
28-11-2017_003.EDR	120	227.9	85.5	363.01	92.6	428.47	73.7
28-11-2017_004.EDR	85.4	539.7	179	624.24	227	641.78	282
28-11-2017_005.EDR	90	355.53	170	580.9	Lost cell		
28-11-2017_006.EDR	60.3	346.98	99.1	425.87	130	413.82	169
29-11-2017_001.EDR	80	760.35	197	703.28	492	778.35	588
29-11-2017_002.EDR	114	266.57	92.5	197.14	116.7	343.17	171
29-11-2017_003.EDR	141	183.87	168	391.69	227	442.66	270
29-11-2017_004.EDR	82	501.68	205	837.55	297	Lost cell	
29-11-2017_005.EDR	191	122.07	280	359.04	357	397.49	462
29-11-2017_006.EDR	64	152.26	222	456.09	222	617.68	379
	Mean	489.60		602.06		644.31	
	SEM	71.75		54.30		59.84	
	N= 3 Rats	16		16		14	

Table 23: **20μM NMDA + 1μM PKI**

Protocol: **PKI was applied to the pipette solution, therefore present throughout the recording**

20μM NMDA (120s) Peak 1 → Wash off (300s) Baseline 2→ 20μM NMDA (120s) Peak 2 → Wash off (300s) Baseline 3 → 20μM NMDA (120s) Peak 3 → Wash off (300s) Baseline 4.

EDR File Name	Baseline 1	Peak 1	Baseline 2	Peak 2	Baseline 3	Peak 3	Baseline 4
19-6-2017_001.EDR	85	593.57	150	516.82	158	502.93	166
19-6-2017_002.EDR	58.9	836.49	85.8	689.7	149	652.16	180
19-6-2017_003.EDR	130	1244.7	219	1445.9	224	1426.1	240
19-6-2017_004.EDR	100	392.46	108	604.1	87.4	765.69	97.9
20-6-2017_001.EDR	83.4	530.7	118.4	409.55	620	801.54	150
20-6-2017_003.EDR	116	360.57	110	373.69	92	460.66	92
20-6-2017_004.EDR	33	380.86	107	590.52	104	765.84	74
20-6-2017_006.EDR	113	599.06	128	746.31	138	554.2	197
20-6-2017_008.EDR	59	1245.3	150	1024.2	163	1173.9	218
20-6-2017_009.EDR	72.8	663.15	113	500.64	98	570.37	138
21-6-2017_001.EDR	140	988.01	276	709.53	330	699.77	373
21-6-2017_002.EDR	109	450.9	139	596.77	266	619.35	207
21-6-2017_004.EDR	83.9	496.22	248	879.21	394	971.98	413
21-6-2017_005.EDR	230	923.61	503	690	486	704.04	437
	Mean	693.26		698.35		762.04	
	SEM	81.60		73.83		71.63	
	N=	14		14		14	
	Rats=	3					

Table 24: **20μM NMDA + 0.5μM Forskolin**

Protocol: 20μM NMDA (120s) Peak 1 → Wash off + 0.5μM Forskolin (300s) Baseline 2→ 20μM NMDA + 0.5μM Forskolin (120s) Peak 2 → Wash off (300s) Baseline 3 → 20μM NMDA (120s) Peak 3 → Wash off (300s) Baseline 4.

EDR File Name	Baseline 1 (-pA)	Peak 1 (-pA)	Baseline 2 (-pA)	Peak 2 (-pA)	Baseline 3 (-pA)	Peak 3 (-pA)	Baseline 4 (-pA)
8-2-2018_001.EDR	42	1396	141	1102.4	228	1519.6	352
8-2-2018_002.EDR	75	777.59	99	745.85	170	942.99	222
9-2-2018_001.EDR	230	397	260	525.51	270	679.17	383
9-2-2018_002.EDR	188	362.85	171	604.4	314	493.01	361
14-2-2018_001.EDR	161	525.82	244	375.82	219	634.31	230
14-2-2018_002.EDR	95	571.59	140	551.45	294	695.5	408
14-2-2018_004.EDR	49	117	82	278.47	172	329.44	302
14-2-2018_005.EDR	107	401	294	1061.9	434	1347.4	527
14-2-2018_006.EDR	120	632.48	202	959.93	362	978.7	397
19-2-2018_002.EDR	105	196	235	397	243	479.43	466
19-2-2018_003.EDR	160	399	766	635	229	808.56	269
19-2-2018_004.EDR	42.5	397.17	857	773	517	811.46	686
19-2-2018_005.EDR	100	266.72	191	531.62	271	587.62	367
19-2-2018_006.EDR	154	545.2	798	1099.2	466	1205	1168
	Mean	498.96		688.68		822.30	
	SEM	83.16		73.91		92.10	
	N=	14		14		14	
	Rats=	4					

***Table 25*: 20μM NMDA + 0.5μM Forskolin + 200nM Ropinirole**

Protocol: 20μM NMDA (120s) Peak 1 → Wash off + 0.5μM Forskolin (300s) Baseline 2→ 20μM NMDA + 0.5μM Forskolin (120s) Peak 2 → Wash off + 200nM Ropinirole (300s) Baseline 3 → 20μM NMDA + 200nM Ropinirole (120s) Peak 3 → Wash off (300s) Baseline 4 → 20μM NMDA (120s) Peak 4 → Wash off (300s) Baseline 5.

Values: -pA

EDR File Name	Baseline 1	Peak 1	Baseline 2	Peak 2	Baseline 3	Peak 3	Baseline 4	Peak 4	Baseline 5
20-2-2018_003.EDR	150	625.76	132	726.01	145	864.87	222	611.11	367
20-2-2018_005.EDR	83	688.93	87.7	556.95	87.8	488.43	104.4	391.85	130.5
20-2-2018_006.EDR	92.2	668.64	176	800.87	213	840.3	256	842.13	Lost cell
21-2-2018_004.EDR	48	177.46	100	261.69	189	656.28	258	846.1	283
28-2-2018_003.EDR	47	387.12	224	288.54	209	178.89	281	16	134
28-2-2018_004.EDR	67	599.82	117	636.44	131	607.15	149	497.74	162
1-3-2018_003.EDR	38	331	69	445.4	90	378.72	110	388.79	114
1-3-2018_004.EDR	60	169.98	41	416.87	164	419.92	149	551	409
6-3-2018_003.EDR	47	1136	138	1122.7	221	824.58	222	739.44	218
6-3-2018_004.EDR	151	226.75	160	528.87	184	511.17	171	501.71	186
6-3-2018_005.EDR	170	170.4	350	409.85	400	412.9	305	489.65	259
6-3-2018_006.EDR	48	355.99	146	976.26	403	778.05	414	270.39	505
6-3-2018_001.EDR	157	443.42	232	454.71	449	469	736	Lost	cell
	Mean	461.49		597.54		580.11		512.16	
	SEM	80.86		74.06		60.45		68.45	
	N=	13		13		13		12	
	Rats=	5							

Table 26: **20μM NMDA + 2.5μM Forskolin + 200nM Ropinirole**

Protocol: 20μM NMDA (120s) Peak 1 → Wash off + 2.5μM Forskolin (300s) Baseline 2→ 20μM NMDA + 2.5μM Forskolin (120s) Peak 2 → Wash off + 200nM Ropinirole (300s) Baseline 3 → 20μM NMDA + 200nM Ropinirole (120s) Peak 3 → Wash off (300s) Baseline 4 → 20μM NMDA (120s) Peak 4 → Wash off (300s) Baseline 5.

Values: -pA

EDR File Name	Baseline 1	Peak 1	Baseline 2	Peak 2	Baseline 3	Peak 3	Baseline 4	Peak 4	Baseline 5
19-1-2018_002.EDR	63	574.34	100	465.09	175	2	286	577.2	343
19-1-2018_004.EDR	92	147.09	534	152.04	341	38	528	248.23	640
22-1-2018_002.EDR	80	270	93.1	439.5	143	513.31	168	476.99	187
22-1-2018_004.EDR	38	193.33	60	325.66	110	306.25	150	Lost	cell
22-1-2018_005.EDR	170	248.11	197	505.83	260	609.59	387	523.22	413
26-1-2018_003.EDR	86	402.37	117	522.31	199	498.05	254	559.54	192
26-1-2018_002.EDR	47	906.37	127	799.71	298	844.12	463	985.11	566
29-1-2018_001.EDR	260	270.54	484	588.53	710	47.15	810	543.82	783
31-1-2018_001.EDR	43	324.1	141	363.32	181	538.18	294	623.63	300
31-1-2018_003.EDR	94	356.29	172	538.18	145	664.52	230	760.19	268
1-2-2018_001.EDR	44	656.43	120	687.26	222	804.29	426	833.59	470
1-2-2018_003.EDR	125	370.64	192	790.41	218	643.16	233	731.05	235
	Mean	393.30		514.82		459.05		623.87	
	SEM	63.00		54.46		85.11		59.55	
	N=	12		12		12		11	
	Rats=	6							

Table 27: **2.5μM Forskolin + 1μM CGS21680**

Protocol: 20μM NMDA (120s) Peak 1 → Wash off + 2.5μM Forskolin + 1μM CGS21680 (300s) Baseline 2→ 20μM NMDA + 2.5μM Forskolin + 1μM CGS21680 (120s) Peak 2 → Wash off (300s) Baseline 3 → 20μM NMDA (120s) Peak 3 → Wash off (300s) Baseline 4.

EDR File Name	**Baseline 1 (-pA)**	**Peak 1 (-pA)**	**Baseline 2 (-pA)**	**Peak 2 (-pA)**	**Baseline 3 (-pA)**	**Peak 3 (-pA)**	**Baseline 4 (-pA)**
8-12-2017_002.EDR	158	348.82	139	565.34	145	623.47	205
8-12-2017_003.EDR	121	943.76	194	875.09	270	1247.7	356
8-12-2017_004.EDR	84	878.45	215	1071.6	286	1090	
8-12-2017_006.EDR	120	365.45	145.9	771.48	192	856.48	315
13-12-2017_001.EDR	65	497.8	100.6	482.45	103.8	840.3	107.4
13-12-2017_002.EDR	120	373.23	167	637.97	174	948.64	222
13-12-2017_004.EDR	109	421.45	134	851.59	145.4	687.41	234
13-12-2017_005.EDR	250	771.9	645	499.73	526	Lost cell	
13-12-2017_006.EDR	250	435.18	360	554.05	403	646.67	461
14-12-2017_003.EDR	133	781.4	378	570.22	363	836.33	410
14-12-2017_004.EDR	68	719.3	224	664.7	313	438.69	343
14-12-2017_005.EDR	320	544.43	608	444	703	Lost cell	
14-12-2017_006.EDR	186	243.53	302	621.8	318	596.31	341
	Mean	563.44		662.31		801.09	
	SEM	63.26		50.56		65.17	
	N=	13		13		13	
	Rats=	3					

Table 28: **20μM NMDA + 2.5μM Forskolin + 1μM PKI**

Protocol: PKI was applied to the pipette solution, therefore present throughout the recording

20μM NMDA (120s) Peak 1 → Wash off + 2.5μM Forskolin (300s) Baseline 2→ 20μM NMDA + 2.5μM Forskolin (120s) Peak 2 → Wash off (300s) Baseline 3 → 20μM NMDA (120s) Peak 3 → Wash off (300s) Baseline 4.

EDR File Name	Baseline 1 (-pA)	Peak 1 (-pA)	Baseline 2 (-pA)	Peak 2 (-pA)	Baseline 3 (-pA)	Peak 3 (-pA)	Baseline 4 (-pA)
19-12-2017_001.EDR	160	563.81	270	266.57	314	314.94	373
19-12-2017_003.EDR	40	510.25	99	523.22	124	Lost cell	
19-12-2017_004.EDR	57.6	252.23	143	426.48	134	497.44	160
19-12-2017_005.EDR	94	510.1	170	665.74	171	724.33	200
19-12-2017_006.EDR	66.4	550.99	127	636.6	142.4	505.52	180
19-12-2017_007.EDR	183	518.49	352	693.05	490	Lost cell	
20-12-2017_002.EDR	124	366.52	245	538.79	Lost cell		
20-12-2017_003.EDR	160	524.44	235	743.56	236	941.77	313
20-12-2017_005.EDR	260	318.6	301	554.2	316	901.95	403
20-12-2017_006.EDR	76	496.83	171	643.77	365	641.94	288
20-12-2017_007.EDR	160	445.56	320	1060.5	432	1055.8	
21-12-2017_003.EDR	70	309.6	133.4	581.05	136	700.53	296
21-12-2017_004.EDR	122	250.05	196	791.17	250	816.5	300
21-12-2017_005.EDR	223	163.27	258	335	316	485.23	307
	Mean	412.91		604.26		689.63	
	SEM	35.46		52.87		68.45	
	N=	14		14		11	
	Rats=	3					

Table 29: **20μM NMDA + 10μM PP3**

Protocol: PP3 was applied to the pipette solution, therefore present throughout the recording

20μM NMDA (120s) Peak 1 → Wash off (300s) Baseline 2→ 20μM NMDA (120s) Peak 2 → Wash off (300s) Baseline 3 → 20μM NMDA (120s) Peak 3 → Wash off (300s) Baseline 4.

EDR File Name	Baseline 1 (-pA)	Peak 1 (-pA)	Baseline 2 (-pA)	Peak 2 (-pA)	Baseline 3 (-pA)	Peak 3 (-pA)	Baseline 4 (-pA)
9-4-2018_002.EDR	95	440	130	361	1022	Lost cell	
9-4-2018_004.EDR	97	207.5	89	431.13	81	420.23	88.1
10-4-2018_002.EDR	72	264	394	417	336	219	155
10-4-2018_004.EDR	108	103	167	225.37	196	285.49	244
10-4-2018_007.EDR	60	735	120	512	128	610.66	116
10-4-2018_009.EDR	54	318.6	82.9	645.22	124	769.27	142
11-4-2018_002.EDR	180	22.2	22.3	139.47	45.6	143.74	61
11-4-2018_004.EDR	58	42.7	65.9	50	63	101.78	74.3
11-4-2018_006.EDR	55	159.91	97	359.81	129.5	506.44	217
11-4-2018_008.EDR	59	216.52	82.7	314.64	44.7	333.4	38
11-4-2018_003.EDR	125	153.2	161	397.75	151	617.98	180
12-4-2018_002.EDR	87	272.98	62.5	515.75	65	511.78	105
12-4-2018_004.EDR	50	334.24	95	458.91	91	613.25	87.9
12-4-2018_006.EDR	115	596.16	80	680.39	99.5	636.6	192
12-4-2018_008.EDR	87	244.14	118	739.9	147	885.47	142
	Mean	274.01		416.56		475.36	
	SEM	50.33		49.38		62.68	
	N=	15		15		14	
	Rats=	4					

***Table 30*: 20μM NMDA + 10μM PP2**

Protocol: PP2 was applied to the pipette solution, therefore present throughout the recording

20μM NMDA (120s) Peak 1 → Wash off (300s) Baseline 2→ 20μM NMDA (120s) Peak 2 → Wash off (300s) Baseline 3 → 20μM NMDA (120s) Peak 3 → Wash off (300s) Baseline 4.

EDR File Name	Baseline 1 (-pA)	Peak 1 (-pA)	Baseline 2 (-pA)	Peak 2 (-pA)	Baseline 3 (-pA)	Peak 3 (-pA)	Baseline 4 (-pA)
23-3-2018_001.EDR	80	195.47	92	342.25	143	394.7	175
23-3-2018_002.EDR	130	318.76	252	610.35	392	749.97	488
23-3-2018_003.EDR	250	1155	718	984	654	989.23	563
23-3-2018_004.EDR	144	407.26	297	679.17	355	637.21	410
23-3-2018_005.EDR	80	455.78	109	677.34	138	529.33	138
23-3-2018_006.EDR	73.5	90.37	80.1	229	120	204	155
23-3-2018_007.EDR	165	67	84	110	100	268	162
26-3-2018_002.EDR	55	107.27	77	197.91	111	257.26	114
26-3-2018_003.EDR	97	361.48	94	557.25	100	509.49	140
26-3-2018_004.EDR	40	196.38	81	360.72	100	528.72	113
26-3-2018_005.EDR	15	463	46	584.41	97	599.67	113
26-3-2018_006.EDR	220	549.77	176	542.91	222	615.08	232
26-3-2018_007.EDR	70	278.48	61.5	267	52	223.24	53.4
9-4-2018_001.EDR	60	673.33	126	788.57	156	725.1	164
9-4-2018_003.EDR	111	185.55	81	321.96	110	361.33	136
9-4-2018_005.EDR	143	385.88	123	643.46	241	764.92	338
10-4-2018_001.EDR	140	95	89	255	339	363	246
10-4-2018_003.EDR	140	336	16	883	1	945	19.4

10-4-2018_005.EDR	105	208.7	56	290	75.1	349	Lost cell
10-4-2018_008.EDR	49	413.59	84	627.37	248	700.68	164
10-4-2018_010.EDR	80	468.9	58.4	831.22	79	1172.6	119
11-4-2018_001.EDR	34	125.05	46.3	207.12	73.19	258.79	128.5
11-4-2018_005.EDR	123	870	41	764	81.9	724	Lost cell
11-4-2018_007.EDR	123	189.82	83	455.32	133	915.99	Lost cell
12-4-2018_003.EDR	142	694.58	180	623.47	140	668.79	169
12-4-2018_007.EDR	179	339.1	180	354.77	154	411.38	160
12-4-2018_009.EDR	203	329.59	180	709.23	190	785.22	183
	Mean	368.93		514.69		579.69	
	SEM	48.74		45.94		49.69	
	N=	27		27		27	
	Rats=	6					

Table 31: **20μM NMDA + 10μM Src-1 Inhibitor**

Protocol: Src-1 Inhibitor was applied to the pipette solution, therefore present throughout the recording

20μM NMDA (120s) Peak 1 → Wash off (300s) Baseline 2→ 20μM NMDA (120s) Peak 2 → Wash off (300s) Baseline 3 → 20μM NMDA (120s) Peak 3 → Wash off (300s) Baseline 4.

EDR File Name	Baseline 1 (-pA)	Peak 1 (-pA)	Baseline 2 (-pA)	Peak 2 (-pA)	Baseline 3 (-pA)	Peak 3 (-pA)	Baseline 4 (-pA)
16-4-2018_001.EDR	85	155.79	68	612.49	111	506.59	90
16-4-2018_004.EDR	70	59.9	67	282.14	86	468.6	121
16-4-2018_005.EDR	10	226.9	37	186.31	71	169.3	43.8
16-4-2018_006.EDR	34	352.71	25	512.85	50.3	576.71	80
17-4-2018_001.EDR	60	107.35	67	253.14	120	315.04	123
17-4-2018_003.EDR	61	824.51	98.2	958.71	85	1111.2	180
17-4-2018_004.EDR	186	215	165	250	257	422	323
17-4-2018_005.EDR	93	365	55	436.86	70.9	630.57	123
17-4-2018_006.EDR	85	211.79	90.3	579.86	181	725.4	234
17-4-2018_007.EDR	60	167.54	46.2	711.52	45	729.52	Lost cell
17-4-2018_008.EDR	49	628.2	39	660.48	132	1061.9	133
17-4-2018_009.EDR	140	429.61	127	490.65	190	573.81	251
18-4-2018_001.EDR	76	564.35	104	698	66	497.59	46.5
18-4-2018_002.EDR	103	147.7	66	253.3	57.4	385.44	67
18-4-2018_003.EDR	64	396.58	75.5	493.47	84.4	760.5	99.3
18-4-2018_004.EDR	48.5	526.12	169	471.65	167	846.71	98.3
	Mean	312.03		494.58		607.55	
	SEM	65.04		65.89		79.44	

	N=	12		12		12	
	Rats=	3					

Table 32: **20μM NMDA + 100μM Src-1 Inhibitor**

Protocol: Src-1 Inhibitor was applied to the pipette solution, therefore present throughout the recording

20μM NMDA (120s) Peak 1 → Wash off (300s) Baseline 2→ 20μM NMDA (120s) Peak 2 → Wash off (300s) Baseline 3 → 20μM NMDA (120s) Peak 3 → Wash off (300s) Baseline 4.

EDR File Name	Baseline 1 (-pA)	Peak 1 (-pA)	Baseline 2 (-pA)	Peak 2 (-pA)	Baseline 3 (-pA)	Peak 3 (-pA)	Baseline 4 (-pA)
25-4-2018_001.EDR	219	470.58	339	609	490	770	730
25-4-2018_002.EDR	70	730	82	809.78	161	874.43	313
25-4-2018_003.EDR	70	868.84	90	1052.6	134	1117.8	438
26-4-2018_001.EDR	148	520.17	200	486.45	251	136.87	142
26-4-2018_002.EDR	50	125.27	114	310.52	138	485.53	184
26-4-2018_003.EDR	84	363.92	104	434.88	139	396.27	144
26-4-2018_004.EDR	150	159.76	100	301.97	110	438.39	131
26-4-2018_005.EDR	94	157	92.4	378.57	116	289.25	110
26-4-2018_006.EDR	72	639	50	616.61	73	672.91	154
26-4-2018_007.EDR	114	908.66	77	892.49	122	1153.9	170
26-4-2018_008.EDR	78	756.84	85	884.25	138	954.44	132
27-4-2018_002.EDR	87	224.46	92	540.16	99.4	645.9	166
27-4-2018_003.EDR	70	439.15	47	455.47	50	478.52	52
27-4-2018_004.EDR	34	549.62	240	448.61	106	559.23	120
27-4-2018_005.EDR	95	527.19	210	608.52	250	692.14	255
27-4-2018_006.EDR	78	257.11	154	412	482	48	229
	Mean	481.10		577.62		607.10	
	SEM	63.61		55.98		79.92	
	N= 3 Rats	16		16		16	

Table 33: **20μM NMDA + 10μM Tat-sSrc**

Protocol: Tat-sSrc was applied to the pipette solution, therefore present throughout the recording

20μM NMDA (120s) Peak 1 → Wash off (300s) Baseline 2→ 20μM NMDA (120s) Peak 2 → Wash off (300s) Baseline 3 → 20μM NMDA (120s) Peak 3 → Wash off (300s) Baseline 4.

EDR File Name	Baseline 1 (-pA)	Peak 1 (-pA)	Baseline 2 (-pA)	Peak 2 (-pA)	Baseline 3 (-pA)	Peak 3 (-pA)	Baseline 4 (-pA)
8-8-2018_001.EDR	70.1	288.24	77.2	258	78	625	90
8-8-2018_004.EDR	184	505	80	683	83	936	176
9-8-2018_006.EDR	140	573	217	958	183	1054.5	468
10-8-2018_001.EDR	90	332	151	454	105	466	
10-8-2018_003.EDR	104	610.5	174	952	764	659	320
10-8-2018_005.EDR	111	449	77.7	686	287	Lost cell	
10-8-2018_007.EDR	76	241	97	485.89	150	Lost cell	
15-8-2018_001.EDR	33	254.97	269	538	370	274	230
15-8-2018_003.EDR	62	70	57	201	76.7	210	120
16-8-2018_001.EDR	42	218	63	335	109.4	376	113
16-8-2018_003.EDR	140	109	97	251	100	252	227
16-8-2018_005.EDR	79	486	133	456.39	135	432	Lost cell
16-8-2018_007.EDR	93	250	74.8	165	67	167	170
20-8-2018_001.EDR	202	125	167	232.7	146	297.55	195
20-8-2018_003.EDR	123	332	269	482	180	652.77	147
20-8-2018_005.EDR	197	128	140	213	138	318.45	157
	Mean	310.73		459.44		480.02	
	SEM	42.55		63.41		72.59	

	N=	16		16		14	
	Rats=	5					

Table 34: **20μM NMDA + 10μM Tat-Src**

Protocol: Tat-Src was applied to the pipette solution, therefore present throughout the recording

20μM NMDA (120s) Peak 1 → Wash off (300s) Baseline 2→ 20μM NMDA (120s) Peak 2 → Wash off (300s) Baseline 3 → 20μM NMDA (120s) Peak 3 → Wash off (300s) Baseline 4.

EDR File Name	Baseline 1 (-pA)	Peak 1 (-pA)	Baseline 2 (-pA)	Peak 2 (-pA)	Baseline 3 (-pA)	Peak 3 (-pA)	Baseline 4 (-pA)
19-7-2018_001.EDR	157	1183	73.9	1035	105	1473	332
19-7-2018_002.EDR	143	1048	78	1270	242	410	
19-7-2018_004.EDR	95.9	1407	57	1389	102	1411.1	164
19-7-2018_005.EDR	160	1238.6	125	1195.8	Lost cell		
19-7-2018_006.EDR	130	579.99	140	596.47	116	690	181
19-7-2018_007.EDR	48	851	76	997	74	1068	87
19-7-2018_008.EDR	53	369	157	505	183	707.86	225
19-7-2018_009.EDR	90	730.44	94	921	107	1069	662
20-7-2018_001.EDR	47	354	50	470.89	45	675	200
20-7-2018_002.EDR	68	531	44	726	56	753	94
20-7-2018_003.EDR	132	252.38	75	604.55	102	865	140
20-7-2018_004.EDR	80	521.39	101	685.42	154	682.22	198
20-7-2018_005.EDR	62	1738	60	1138.2	41	898.74	116
20-7-2018_006.EDR	250	631	124	697	21	807	120
20-7-2018_007.EDR	61	604	180	1075.9	317	1017	308
	MEAN	802.59		887.15		894.78	
	SEM	111.40		76.03		78.11	
	N=	15		15		14	
	Rats=	2					

***Table 35*: 20μM NMDA + 10μM Tat-sFyn**
Protocol: Tat-sFyn was applied to the pipette solution, therefore present throughout the recording
20μM NMDA (120s) Peak 1 → Wash off (300s) Baseline 2→ 20μM NMDA (120s) Peak 2 → Wash off (300s) Baseline 3 → 20μM NMDA (120s) Peak 3 → Wash off (300s) Baseline 4.

EDR File Name	Baseline 1 (-pA)	Peak 1 (-pA)	Baseline 2 (-pA)	Peak 2 (-pA)	Baseline 3 (-pA)	Peak 3 (-pA)	Baseline 4 (-pA)
8-8-2018_002.EDR	133	466.61	84	437	91	437	159
10-8-2018_002.EDR	107	689	130	842	126	979	118
10-8-2018_004.EDR	270	261	400	465	349	487	219
10-8-2018_006.EDR	63	253	41	636	95	685	83.3
15-8-2018_005.EDR	114	271.76	86	219.27	72.9	410.92	122.7
16-8-2018_002.EDR	132	513.29	80	753.33	69	1004	44
16-8-2018_004.EDR	21	210.27	40	298	78	479	Lost cell
16-8-2018_006.EDR	70	286	30	404	27	429	72
20-8-2018_004.EDR	48	330.6	94	361.79	105	424.65	103
20-8-2018_006.EDR	48	230	43	325	91	359	81
20-8-2018_007.EDR	187	251.31	150	487	213	848	182
20-8-2018_008.EDR	77	167	54	283	72	318.6	87
	Mean	327.49		459.28		571.76	
	SEM	43.88		55.78		70.33	
	N=	12		12		12	
	Rats=	5					

Table 36: **20μM NMDA + 10μM Tat-Fyn**

Protocol: Tat-Fyn was applied to the pipette solution, therefore present throughout the recording

20μM NMDA (120s) Peak 1 → Wash off (300s) Baseline 2→ 20μM NMDA (120s) Peak 2 → Wash off (300s) Baseline 3 → 20μM NMDA (120s) Peak 3 → Wash off (300s) Baseline 4.

EDR File Name	Baseline 1 (-pA)	Peak 1 (-pA)	Baseline 2 (-pA)	Peak 2 (-pA)	Baseline 3 (-pA)	Peak 3 (-pA)	Baseline 4 (-pA)
13-7-2018_001.EDR	44	7	70.6	499	90.8	605	149
13-7-2018_002.EDR	187	285	187	1802	324	2459	
13-7-2018_003.EDR	173	867	234	1039	Lost cell		
13-7-2018_004.EDR	77	1185	80.4	964	135	Lost cell	
13-7-2018_005.EDR	212	1606	221	1199	334	1344	231
13-7-2018_006.EDR	110	561	77.9	691	Lost cell		
13-7-2018_007.EDR	83	818	115	900	116	1228	168
13-7-2018_008.EDR	70	591	91.1	570	112	807	204
13-7-2018_009.EDR	51	352	86.4	668	104	830	117
18-7-2018_001.EDR	43.9	1625	95	1874	208	2618	1380
18-7-2018_002.EDR	183	838.78	104	1263.9	67	1537.6	59
18-7-2018_003.EDR	100	222.93	55.4	457.31	64.4	503.69	132
18-7-2018_004.EDR	57	285	141	340	109	337	113
18-7-2018_005.EDR	60	652	73	677	Lost cell		
18-7-2018_006.EDR	111	526	81	823	72	971	25.6
18-7-2018_007.EDR	169	884	159	1761	1050	1822	1011
	Mean	706.61		970.51		1255.19	

	SEM	116.25		122.50		213.36	
	N=	16		16		12	
	Rats=	2					

***Table 37*: 20μM NMDA + 10μM Tat-Src + 10μM Tat-Fyn**
Protocol: Tat-Src and Tat-Fyn were applied to the pipette solution, therefore present throughout the recording
20μM NMDA (120s) Peak 1 → Wash off (300s) Baseline 2→ 20μM NMDA (120s) Peak 2 → Wash off (300s) Baseline 3 → 20μM NMDA (120s) Peak 3 → Wash off (300s) Baseline 4.

EDR File Name	Baseline 1 (-pA)	Peak 1 (-pA)	Baseline 2 (-pA)	Peak 2 (-pA)	Baseline 3 (-pA)	Peak 3 (-pA)	Baseline 4 (-pA)
6-7-2018_002.EDR	80	306	107	695	191	879.52	220
6-7-2018_003.EDR	94	1030	194	814.21	215	396	76.3
6-7-2018_004.EDR	120	496.22	107	852.36	138	903.93	250
9-7-2018_002.EDR	160	213	176	403.75	274	510.86	427
9-7-2018_003.EDR	30	737	113	996	180	1121	236
9-7-2018_004.EDR	29.8	768	49	967	213	1080	180
9-7-2018_005.EDR	130	812.99	335	547.99	296	534	299
10-7-2018_001.EDR	160	844.42	155	867	202	1007	169
10-7-2018_002.EDR	197	149	164	298.46	179	289.92	198
10-7-2018_003.EDR	107	611.72	81.7	848.24	192	803.07	425
11-7-2018_001.EDR	161	967.56	213	1646	293	1131.9	548
11-7-2018_002.EDR	62	448	58.9	174	Lost cell		
11-7-2018_003.EDR	98	413	116.5	784.76	99	1137	130

11-7-2018_004.EDR	30	861.21	71.7	811	139	903.22	158
11-7-2018_005.EDR	63	1300.5	71	1078.8	172	1144	167
11-7-2018_006.EDR	200	1173	189	561.88	157	745	123
	Mean	695.73		771.65		839.09	
	SEM	84.69		86.33		74.07	
	N=	16		16		15	
	Rats=	4					

Table 38: **20μM NMDA + 1μM Ulixertinib**

Protocol: Ulixertinib was applied to the pipette solution, therefore present throughout the recording

20μM NMDA (120s) Peak 1 → Wash off (300s) Baseline 2→ 20μM NMDA (120s) Peak 2 → Wash off (300s) Baseline 3 → 20μM NMDA (120s) Peak 3 → Wash off (300s) Baseline 4.

EDR File Name	Baseline 1 (-pA)	Peak 1 (-pA)	Baseline 2 (-pA)	Peak 2 (-pA)	Baseline 3 (-pA)	Peak 3 (-pA)	Baseline 4 (-pA)
1-6-2018_001.EDR	63	76	125	356	63	396	78
1-6-2018_002.EDR	132	231	111	690	120	728	166
1-6-2018_003.EDR	93	153.05	71	291.6	118	390.33	Lost cell
1-6-2018_004.EDR	34	361	104.7	706.02	218	724.95	277
1-6-2018_005.EDR	210	360	240	802.31	361	1279	795
1-6-2018_006.EDR	45	729	61	362	106	861	168
3-7-2018_001.EDR	67	674.13	66	728	153	884.09	66.2
3-7-2018_002.EDR	180	670	138	741	240	823.97	204
3-7-2018_003.EDR	80	410.77	69	955.56	88	853.88	190
4-7-2018_001.EDR	78	291	74	781	130	676	167
4-7-2018_002.EDR	144	542	156	979	243	1058	Lost cell
4-7-2018_003.EDR	50	853	54.7	742.8	98	1106	566
4-7-2018_004.EDR	90	992.58	115	1031.5	195	1063.8	Lost cell
4-7-2018_005.EDR	72	0	123	373	270	666.8	386
4-7-2018_006.EDR	104	459	96.3	1002.3	84	1083	164
	Mean	453.50		702.81		839.65	
	SEM	74.42		64.44		65.65	
	N=	15		15		15	
	Rats=	3					

Table 39: **20μM NMDA + 20μM Tat-sCN21**

Protocol: Tat-sCN21 was applied to the pipette solution, therefore present throughout the recording

20μM NMDA (120s) Peak 1 → Wash off (300s) Baseline 2→ 20μM NMDA (120s) Peak 2 → Wash off (300s) Baseline 3 → 20μM NMDA (120s) Peak 3 → Wash off (300s) Baseline 4.

EDR File Name	Baseline 1 (-pA)	Peak 1 (-pA)	Baseline 2 (-pA)	Peak 2 (-pA)	Baseline 3 (-pA)	Peak 3 (-pA)	Baseline 4 (-pA)
8-11-2018_002.EDR	170	201	382	388	241	315	489
9-11-2018_004.EDR	98	487	446	489	650	574	323
9-11-2018_006.EDR	82	27	114	505	139	627	147
22-11-2018_002.EDR	280	209	297	397	283	351	334
22-11-2018_004.EDR	113	377	249	647	350	681	410
27-11-2018_004.EDR	192	91	211	155	206	83	146
27-11-2018_006.EDR	223	178	378	475	382	330	280
	Mean	224.29		436.57		423.00	
	SEM	60.15		56.99		80.49	
	N=	7		7		7	
	Rats=	4					

Table 40: **20μM NMDA + 20μM Tat-CN21**
Protocol: Tat-CN21 was applied to the pipette solution, therefore present throughout the recording
20μM NMDA (120s) Peak 1 → Wash off (300s) Baseline 2→ 20μM NMDA (120s) Peak 2 → Wash off (300s) Baseline 3 → 20μM NMDA (120s) Peak 3 → Wash off (300s) Baseline 4.

EDR File Name	Baseline 1 (-pA)	Peak 1 (-pA)	Baseline 2 (-pA)	Peak 2 (-pA)	Baseline 3 (-pA)	Peak 3 (-pA)	Baseline 4 (-pA)
7-11-2018_002.EDR	114	202	267	74	292	246	300
7-11-2018_003.EDR	129	76	192	104	207	76	230
8-11-2018_003.EDR	53	378	161	428	178	569	313
8-11-2018_005.EDR	61	535	179	565	215	742	182
9-11-2018_001.EDR	200	185	108	256	102	217	173
9-11-2018_003.EDR	126	361	270	321	313	302	573
9-11-2018_005.EDR	85	534	191	742	216	634	224
9-11-2018_007.EDR	95	570	145	462	180	465.7	205
22-11-2018_003.EDR	175	327	191	452	263	409	300
23-11-2018_001.EDR	64	218	121	362	165	423	153
23-11-2018_005.EDR	290	381	396	192	370	259	329
27-11-2018_003.EDR	83	160	173	134	227	138	249
27-11-2018_005.EDR	33	55	170	56	135	68	162
27-11-2018_007.EDR	208	106	267	156	470	224	684
	Mean	292.00		307.43		340.91	
	SEM	46.65		54.76		55.36	
	N=	14		14		14	
	Rats=	5					

Table 41: NMDA dose response data (P28 DAergic neurons of the SNc)

EDR File Name	*Baseline 1 (-pA)*	*5μM NMDA (-pA)*	*Baseline 2 (-pA)*	*10 μM NMDA (-pA)*	*Baseline 3 (-pA)*	*20 μM NMDA (-pA)*	*Baseline 4 (-pA)*
28-1-2019_004.EDR	167	48	100	176	204	203	167
28-1-2019_005.EDR	90	103	145	59	176	92	220
1-2-2019_001.EDR	47	39	129	32	161	34	147
1-2-2019_003.EDR	280	104	396	12	425	17	443
1-2-2019_004.EDR	107	115	282	224	435	410	555
1-2-2019_005.EDR	150	62	229	70	280	239	385
1-2-2019_006.EDR	144	86	218	28	205	21	221
7-2-2019_001.EDR	56	52	96.6	16	128	42	159
7-2-2019_002.EDR	124	57	169	91	213	192	250
7-2-2019_003.EDR	105	26	142	12	146	82	182
7-2-2019_006.EDR	243	60	228	86	233	247	239
7-2-2019_007.EDR	100	41	180	205	222	386	246
7-2-2019_008.EDR	98	26	159	40	196	60	195
	Mean	63		80.85		155.77	
	SEM	8.28		20.60		37.58	
	N=	13		13		13	

Table 41: Continues

EDR File Name	*Baseline 4 (-pA)*	*50 μM NMDA (-pA)*	*Baseline 5 (-pA)*	*100 μM NMDA (-pA)*	*Baseline 6 (-pA)*	*200 μM NMDA (-pA)*	*Baseline 7 (-pA)*
28-1-2019_004.EDR	167	805	389	957	480	366	349
28-1-2019_005.EDR	220	370	306	1168	811	1049	1451
1-2-2019_001.EDR	147	511	270	308	237	376	328
1-2-2019_003.EDR	443	310	517	486	766	1015	797
1-2-2019_004.EDR	555	990	659	1274	910	921	898
1-2-2019_005.EDR	385	778	564	728	745	1237	1218
1-2-2019_006.EDR	221	162	279	752	601	348	461
7-2-2019_001.EDR	159	167	210	326	391	740	618
7-2-2019_002.EDR	250	829	360	1262	800	823	985
7-2-2019_003.EDR	182	374	371	1381	748	1664	1220
7-2-2019_006.EDR	239	873	314	3000	541	2732	668
7-2-2019_007.EDR	246	979	262	2123	345	2509	405
7-2-2019_008.EDR	195	119	198	1278	370	1524	475
	Mean	559		1157.153846		1177.230769	
	SEM	105.1848016		244.8334337		211.2908784	
	N=	13		13		13	
	Rats	**3**					

Hippocampal Data: Pilot experiments performed on CA1 hippocampal neurons in P28 rats.

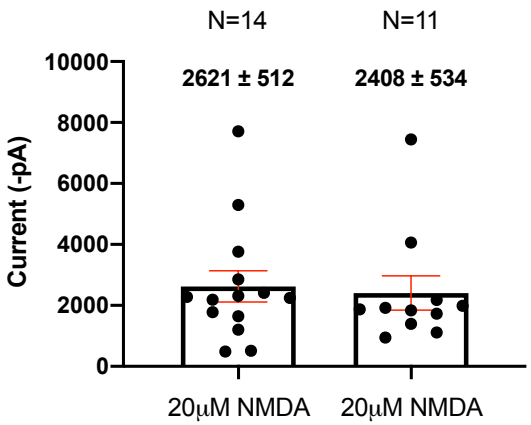

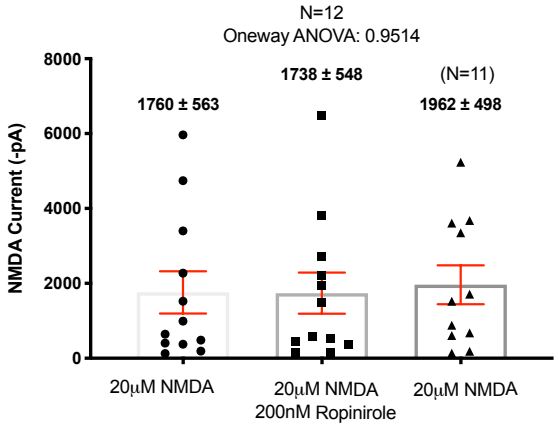

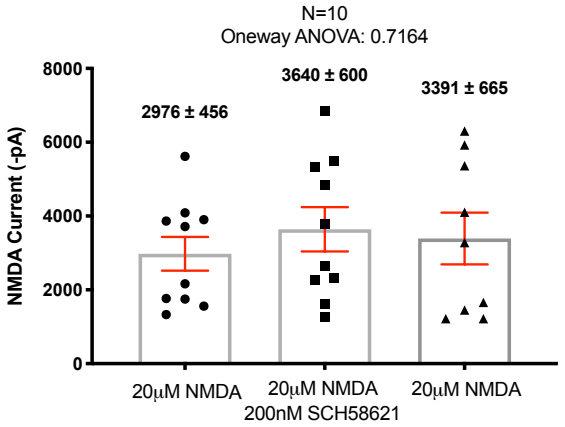

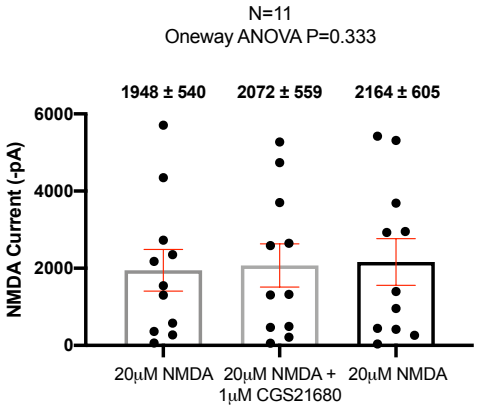

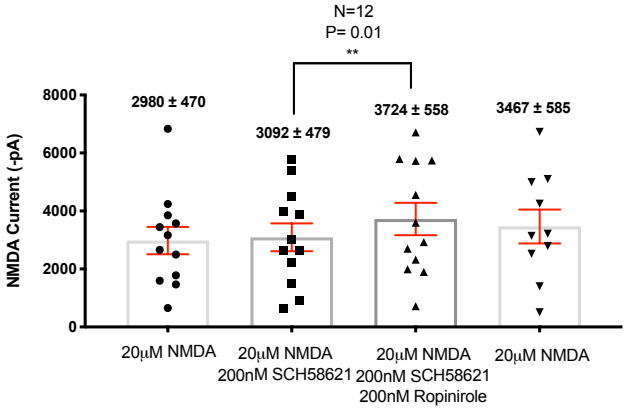

Chapter 8:

References

Akazawa, C. *et al.* (1994) 'Differential expression of five N-methyl-D-aspartate receptor subunit mRNAs in the cerebellum of developing and adult rats', *The Journal of Comparative Neurology*, 347(1), pp. 150–160. doi: 10.1002/cne.903470112.

Aman, T. K. *et al.* (2014) 'Separate intramolecular targets for protein kinase A control N-methyl-D-aspartate receptor gating and Ca2+ permeability.', *The Journal of biological chemistry*. American Society for Biochemistry and Molecular Biology, 289(27), pp. 18805–17. doi: 10.1074/jbc.M113.537282.

Ammari, R. *et al.* (2010) 'Subthalamic nucleus evokes similar long lasting glutamatergic excitations in pallidal, entopeduncular and nigral neurons in the basal ganglia slice', *Neuroscience*. Pergamon, 166(3), pp. 808–818. doi: 10.1016/J.NEUROSCIENCE.2010.01.011.

Andersen, P. H. *et al.* (1990) 'Dopamine receptor subtypes: beyond the D1/D2 classification.', *Trends in pharmacological sciences*. Elsevier, 11(6), pp. 231–6. doi: 10.1016/0165-6147(90)90249-8.

Armentero, M. T. *et al.* (2011) 'Past, present and future of A(2A) adenosine receptor antagonists in the therapy of Parkinson's disease.', *Pharmacology & therapeutics*. NIH Public Access, 132(3), pp. 280–99. doi: 10.1016/j.pharmthera.2011.07.004.

Ataman, Z. A. *et al.* (2007) 'The NMDA receptor NR1 C1 region bound to calmodulin: structural insights into functional differences between homologous domains.', *Structure (London, England : 1993)*. NIH Public Access, 15(12), pp. 1603–17. doi: 10.1016/j.str.2007.10.012.

Azdad, K. *et al.* (2009) 'Dopamine D2 and adenosine A2A receptors regulate NMDA-mediated excitation in accumbens neurons through A2A-D2 receptor heteromerization.', *Neuropsychopharmacology : official publication of the American College of Neuropsychopharmacology*. NIH Public Access, 34(4), pp. 972–86. doi: 10.1038/npp.2008.144.

Bain, J. *et al.* (2007) 'The selectivity of protein kinase inhibitors: a further update.', *The Biochemical journal*. Portland Press Ltd, 408(3), pp. 297–315. doi: 10.1042/BJ20070797.

Banks, P. J. *et al.* (2015) 'Disruption of hippocampal-prefrontal cortex activity by dopamine D2R-dependent LTD of NMDAR transmission.', *Proceedings of the National Academy of Sciences of the United States of America*. National Academy of Sciences, 112(35), pp. 11096–101. doi: 10.1073/pnas.1512064112.

Barcomb, K. *et al.* (2016) 'The CaMKII/GluN2B Protein Interaction Maintains Synaptic Strength.', *The Journal of biological chemistry*. American Society for Biochemistry and Molecular Biology, 291(31), pp. 16082–9. doi: 10.1074/jbc.M116.734822.

Bayer, K.-U. *et al.* (2001) 'Interaction with the NMDA receptor locks CaMKII in an active conformation', *Nature*. Nature Publishing Group, 411(6839), pp. 801–805. doi: 10.1038/35081080.

Bayer, K. U. and Schulman, H. (2019) 'CaM Kinase: Still Inspiring at 40', *Neuron*. Cell Press, 103(3), pp. 380–394. doi: 10.1016/J.NEURON.2019.05.033.

Beaulieu, J.-M. *et al.* (2011) 'Beyond cAMP: The Regulation of Akt and GSK3 by Dopamine Receptors.', *Frontiers in molecular neuroscience*. Frontiers Media SA, 4, p. 38. doi: 10.3389/fnmol.2011.00038.

Beaulieu, J.-M. and Gainetdinov, R. R. (2011) 'The Physiology, Signaling, and Pharmacology of Dopamine Receptors', *Pharmacological Reviews*, 63(1).

Bergman, M. *et al.* (1992) 'The human p50csk tyrosine kinase phosphorylates p56lck at Tyr-505 and down regulates its catalytic activity.', *The EMBO Journal*. European Molecular Biology Organization, 11(8), p. 2919.

Bhattacharya, S. and Traynelis, S. F. (2018) 'Unique Biology and Single-Channel Properties of GluN2A- and GluN2C-Containing Triheteromeric N-Methyl-D-Aspartate Receptors.', *Journal of experimental neuroscience*. SAGE Publications, 12, p. 1179069518810423. doi: 10.1177/1179069518810423.

Björklund, A. and Dunnett, S. B. (2007) 'Dopamine neuron systems in the brain: an update', *Trends in Neurosciences*. Elsevier Current Trends, 30(5), pp. 194–202. doi: 10.1016/J.TINS.2007.03.006.

Bliss, T. V and Collingridge, G. L. (1993) 'A synaptic model of memory: long-term potentiation in the hippocampus.', *Nature*, 361(6407), pp. 31–39. doi: 10.1038/361031a0.

Blythe, Sarah N *et al.* (2009) 'Cellular mechanisms underlying burst firing in substantia nigra dopamine neurons.', *The Journal of neuroscience : the official journal of the Society for Neuroscience*. NIH Public Access, 29(49), pp. 15531–41. doi: 10.1523/JNEUROSCI.2961-09.2009.

Bogerts, B., Häntsch, J. and Herzer, M. (1983) 'A morphometric study of the dopamine-containing cell groups in the mesencephalon of normals, Parkinson patients, and schizophrenics.', *Biological psychiatry*, 18(9), pp. 951–69.

Bolen, J. B. and Brugge, J. S. (1997) 'Leukocyte Protein Tyrosine Kinases:Potential Targets for Drug Discovery', *Annual Review of*

Immunology. Annual Reviews 4139 El Camino Way, P.O. Box 10139, Palo Alto, CA 94303-0139, USA , 15(1), pp. 371–404. doi: 10.1146/annurev.immunol.15.1.371.

Bonaventura, J. *et al.* (2015) 'Allosteric interactions between agonists and antagonists within the adenosine A2A receptor-dopamine D2 receptor heterotetramer.', *Proceedings of the National Academy of Sciences of the United States of America*. National Academy of Sciences, 112(27), pp. E3609-18. doi: 10.1073/pnas.1507704112.

Bonci, A. and Hopf, F. W. (2005) 'The dopamine D2 receptor: new surprises from an old friend.', *Neuron*. Elsevier, 47(3), pp. 335–8. doi: 10.1016/j.neuron.2005.07.015.

Bonifacino, J. S. and Traub, L. M. (2003) 'Signals for Sorting of Transmembrane Proteins to Endosomes and Lysosomes', *Annual Review of Biochemistry*. Annual Reviews 4139 El Camino Way, P.O. Box 10139, Palo Alto, CA 94303-0139, USA , 72(1), pp. 395–447. doi: 10.1146/annurev.biochem.72.121801.161800.

Borin, M. *et al.* (2014) 'Inward rectifier potassium (Kir) current in dopaminergic periglomerular neurons of the mouse olfactory bulb', *Frontiers in Cellular Neuroscience*. Frontiers, 8, p. 223. doi: 10.3389/fncel.2014.00223.

Borroto-Escuela, D. O. *et al.* (2018) 'A2AR-D2R Heteroreceptor Complexes in Cocaine Reward and Addiction', *Trends in Pharmacological Sciences*. Elsevier Current Trends, 39(12), pp. 1008–1020. doi: 10.1016/J.TIPS.2018.10.007.

Bourque, M.-J. and Trudeau, L.-E. (2000) 'GDNF enhances the synaptic efficacy of dopaminergic neurons in culture', *European Journal of Neuroscience*. John Wiley & Sons, Ltd (10.1111), 12(9), pp. 3172–3180. doi: 10.1046/j.1460-9568.2000.00219.x.

Braak, H. *et al.* (2004) 'Stages in the development of Parkinson's disease-related pathology', *Cell and Tissue Research*. Springer, 318(1), pp. 121–134. doi: 10.1007/s00441-004-0956-9.

Brdicka, T. *et al.* (2000) 'Phosphoprotein associated with glycosphingolipid-enriched microdomains (PAG), a novel ubiquitously expressed transmembrane adaptor protein, binds the protein tyrosine kinase csk and is involved in regulation of T cell activation.', *The Journal of experimental medicine*. The Rockefeller University Press, 191(9), pp. 1591–604. doi: 10.1084/jem.191.9.1591.

Breitenstein, C. *et al.* (2006) 'Tonic Dopaminergic Stimulation Impairs Associative Learning in Healthy Subjects', *Neuropsychopharmacology*. Nature Publishing Group, 31(11), pp. 2552–2564. doi: 10.1038/sj.npp.1301167.

Bromberg-Martin, E. S., Matsumoto, M. and Hikosaka, O. (2010) 'Dopamine in Motivational Control: Rewarding, Aversive, and Alerting', *Neuron*. Cell Press, 68(5), pp. 815–834. doi: 10.1016/J.NEURON.2010.11.022.

Brothwell, S. L. C. *et al.* (2008a) 'NR2B- and NR2D-containing synaptic NMDA receptors in developing rat substantia nigra pars compacta dopaminergic neurones.', *The Journal of physiology*. Wiley-Blackwell, 586(3), pp. 739–50. doi: 10.1113/jphysiol.2007.144618.

Bruns, R. F., Lu, G. H. and Pugsley, T. A. (1986) 'Characterization of the A2 adenosine receptor labeled by [3H]NECA in rat striatal membranes.', *Molecular Pharmacology*, 29(4).

Bunney, B. S., Aghajanian, G. K. and Roth, R. H. (1973) 'Comparison of Effects of L-Dopa, Amphetamine and Apomorphine on Firing Rate of Rat Dopaminergic Neurons', *Nature New Biology*, 245, pp. 123–125. doi: doi:10.1038/newbio245123a0.

Burris, K. D. *et al.* (1995) 'Lack of discrimination by agonists for D2 and D3 dopamine receptors', *Neuropsychopharmacology*. No longer published by Elsevier, 12(4), pp. 335–345. doi: 10.1016/0893-133X(94)00099-L.

Butini, S. *et al.* (2016) 'Polypharmacology of dopamine receptor ligands', *Progress in Neurobiology*. Pergamon, 142, pp. 68–103. doi: 10.1016/J.PNEUROBIO.2016.03.011.

Calabresi, P. *et al.* (2014) 'Direct and indirect pathways of basal ganglia: a critical reappraisal', *Nature Neuroscience*. Nature Publishing Group, 17(8), pp. 1022–1030. doi: 10.1038/nn.3743.

Caldwell, G. B. *et al.* (2012) 'Direct modulation of the protein kinase A catalytic subunit α by growth factor receptor tyrosine kinases.', *Journal of cellular biochemistry*. NIH Public Access, 113(1), pp. 39–48. doi: 10.1002/jcb.23325.

Canals, M. *et al.* (2003) 'Adenosine A2A-dopamine D2 receptor-receptor heteromerization: qualitative and quantitative assessment by fluorescence and bioluminescence energy transfer.', *The Journal of biological chemistry*. American Society for Biochemistry and Molecular Biology, 278(47), pp. 46741–9. doi: 10.1074/jbc.M306451200.

Carter, A. J. and Müller, R. E. (1991) 'Pramipexole, a dopamine D2 autoreceptor agonist, decreases the extracellular concentration of dopamine in vivo', *European Journal of Pharmacology*, 200(1), pp. 65–72. doi: 10.1016/0014-2999(91)90666-E.

Centonze, D. *et al.* (2002) 'Dopamine D2 receptor-mediated inhibition of dopaminergic neurons in mice lacking D2L receptors.', *Neuropsychopharmacology : official publication of the American College of Neuropsychopharmacology*, 27(5), pp. 723–6. doi: 10.1016/S0893-

133X(02)00367-6.

Cepeda, C. *et al.* (1998) 'Dopaminergic Modulation of NMDA-Induced Whole Cell Currents in Neostriatal Neurons in Slices: Contribution of Calcium Conductances', *Journal of Neurophysiology*, 79(1).

Chang, Y. H. *et al.* (1997) 'Activation of phosphodiesterase IV during desensitization of the A2A adenosine receptor-mediated cyclic AMP response in rat pheochromocytoma (PC12) cells.', *Journal of neurochemistry*, 69(3), pp. 1300–9.

Chazot, P. L. and Stephenson, F. A. (2002) 'Molecular Dissection of Native Mammalian Forebrain NMDA Receptors Containing the NR1 C2 Exon: Direct Demonstration of NMDA Receptors Comprising NR1, NR2A, and NR2B Subunits Within the Same Complex', *Journal of Neurochemistry*. John Wiley & Sons, Ltd (10.1111), 69(5), pp. 2138–2144. doi: 10.1046/j.1471-4159.1997.69052138.x.

Chen-Plotkin, A. S., Lee, V. M.-Y. and Trojanowski, J. Q. (2010) 'TAR DNA-binding protein 43 in neurodegenerative disease.', *Nature reviews. Neurology*. NIH Public Access, 6(4), pp. 211–20. doi: 10.1038/nrneurol.2010.18.

Chen, B.-S. and Roche, K. W. (2007) 'Regulation of NMDA receptors by phosphorylation.', *Neuropharmacology*. NIH Public Access, 53(3), pp. 362–8. doi: 10.1016/j.neuropharm.2007.05.018.

Chen, B.-S. and Roche, K. W. (2009) 'Growth factor-dependent trafficking of cerebellar NMDA receptors via protein kinase B/Akt phosphorylation of NR2C.', *Neuron*. NIH Public Access, 62(4), pp. 471–8. doi: 10.1016/j.neuron.2009.04.015.

Chen, H.-J. *et al.* (1998) 'A Synaptic Ras-GTPase Activating Protein (p135 SynGAP) Inhibited by CaM Kinase II', *Neuron*. Cell Press, 20(5), pp. 895–904. doi: 10.1016/S0896-6273(00)80471-7.

Chen, J.-F. *et al.* (2001) 'Neuroprotection by Caffeine and A 2A Adenosine Receptor Inactivation in a Model of Parkinson's Disease'. *Journal of Neuroscience*. 21 (10). DOI: https://doi.org/10.1523/JNEUROSCI.21-10-j0001.2001

Chen, J.-F., Lee, C. and Chern, Y. (2014) 'Adenosine Receptor Neurobiology: Overview', *International Review of Neurobiology*. Academic Press, 119, pp. 1–49. doi: 10.1016/B978-0-12-801022-8.00001-5.

Chen, L. and Mae Huang, L.-Y. (1992) 'Protein kinase C reduces Mg2+ block of NMDA-receptor channels as a mechanism of modulation', *Nature*, 356(6369), pp. 521–523. doi: 10.1038/356521a0.

Chen, R. H., Sarnecki, C. and Blenis, J. (1992) 'Nuclear localization and regulation of erk- and rsk-encoded protein kinases.', *Molecular and cellular biology*. American Society for Microbiology (ASM), 12(3), pp. 915–27. doi: 10.1128/mcb.12.3.915.

Cheung, H. H. and Gurd, J. W. (2001) 'Tyrosine phosphorylation of the *N* -methyl- d -aspartate receptor by exogenous and postsynaptic density-associated Src-family kinases', *Journal of Neurochemistry*. John Wiley & Sons, Ltd (10.1111), 78(3), pp. 524–534. doi: 10.1046/j.1471-4159.2001.00433.x.

Chinta, S. J. and Andersen, J. K. (2005a) 'Dopaminergic neurons', *The International Journal of Biochemistry & Cell Biology*, 37(5), pp. 942–946. doi: 10.1016/j.biocel.2004.09.009.

Choi, D. W., Koh, J. Y. and Peters, S. (1988) 'Pharmacology of glutamate neurotoxicity in cortical cell culture: attenuation by NMDA antagonists.', *The Journal of neuroscience : the official journal of the Society for Neuroscience*, 8(1), pp. 185–196.

Chong, H., Vikis, H. G. and Guan, K.-L. (2003) 'Mechanisms of regulating the Raf kinase family', *Cellular Signalling*. Pergamon, 15(5), pp. 463–469. doi: 10.1016/S0898-6568(02)00139-0.

Chu, H. and Zhen, X. (2010) 'Hyperpolarization-activated, cyclic nucleotide-gated (HCN) channels in the regulation of midbrain dopamine systems.', *Acta pharmacologica Sinica*. Nature Publishing Group, 31(9), pp. 1036–43. doi: 10.1038/aps.2010.105.

Di Ciano, P., Grandy, D. K. and Le Foll, B. (2014) 'Dopamine D4 receptors in psychostimulant addiction.', *Advances in pharmacology (San Diego, Calif.)*. NIH Public Access, 69, pp. 301–21. doi: 10.1016/B978-0-12-420118-7.00008-1.

Cieślak, M., Komoszyński, M. and Wojtczak, A. (2008) 'Adenosine A(2A) receptors in Parkinson's disease treatment.', *Purinergic signalling*. Springer, 4(4), pp. 305–12. doi: 10.1007/s11302-008-9100-8.

Constantinescu, R. (2008) 'Update on the use of pramipexole in the treatment of Parkinson's disease', *Neuropsychiatric Disease and Treatment*, pp. 337–352. doi: 10.2147/NDT.S2325.

Coultrap, S. J. *et al.* (2010) 'CaMKII autonomy is substrate-dependent and further stimulated by Ca2+/calmodulin.', *The Journal of biological chemistry*. American Society for Biochemistry and Molecular Biology, 285(23), pp. 17930–7. doi: 10.1074/jbc.M109.069351.

Coultrap, S. J. *et al.* (2014) 'Autonomous CaMKII Mediates Both LTP and LTD Using a Mechanism for Differential Substrate Site Selection', *Cell Reports*. Cell Press, 6(3), pp. 431–437. doi: 10.1016/J.CELREP.2014.01.005.

Coultrap, S. J. and Bayer, K. U. (2012) ‘CaMKII regulation in information processing and storage.’, *Trends in neurosciences*. NIH Public Access, 35(10), pp. 607–18. doi: 10.1016/j.tins.2012.05.003.

Cull-Candy, S., Brickley, S. and Farrant, M. (2001a) ‘NMDA receptor subunits: diversity, development and disease’, *Current Opinion in Neurobiology*, 11(3), pp. 327–335. doi: 10.1016/S0959-4388(00)00215-4.

Dickson, D. W. *et al.* (2009) ‘Neuropathological assessment of Parkinson’s disease: refining the diagnostic criteria’, *The Lancet Neurology*. Elsevier, 8(12), pp. 1150–1157. doi: 10.1016/S1474-4422(09)70238-8.

Dickson, D. W. (2012) ‘Parkinson’s disease and parkinsonism: neuropathology.’, *Cold Spring Harbor perspectives in medicine*. Cold Spring Harbor Laboratory Press, 2(8). doi: 10.1101/cshperspect.a009258.

Dodd, M. L. *et al.* (2005) ‘Pathological Gambling Caused by Drugs Used to Treat Parkinson Disease’, *Archives of Neurology*. American Medical Association, 62(9), p. 1377. doi: 10.1001/archneur.62.9.noc50009.

Dopeso-Reyes, I. G. *et al.* (2014) ‘Calbindin content and differential vulnerability of midbrain efferent dopaminergic neurons in macaques.’, *Frontiers in neuroanatomy*. Frontiers Media SA, 8, p. 146. doi: 10.3389/fnana.2014.00146.

Duda, J., Pötschke, C. and Liss, B. (2016) ‘Converging roles of ion channels, calcium, metabolic stress, and activity pattern of Substantia nigra dopaminergic neurons in health and Parkinson’s disease’, *Journal of Neurochemistry*. John Wiley & Sons, Ltd (10.1111), 139, pp. 156–178. doi: 10.1111/jnc.13572.

Dunah, A. W. *et al.* (1998) ‘Subunit composition of N-methyl-D-aspartate receptors in the central nervous system that contain the NR2D subunit.’, *Molecular pharmacology*. American Society for Pharmacology and Experimental Therapeutics, 53(3), pp. 429–37. doi: 10.1124/MOL.53.3.429.

Efremov, R. G. and Sazanov, L. A. (2011) ‘Structure of the membrane domain of respiratory complex I’, *Nature*. Nature Publishing Group, 476(7361), pp. 414–420. doi: 10.1038/nature10330.

Ehlers, M. D. *et al.* (1996) ‘Inactivation of NMDA Receptors by Direct Interaction of Calmodulin with the NR1 Subunit’, *Cell*. Cell Press, 84(5), pp. 745–755. doi: 10.1016/S0092-8674(00)81052-1.

Esmenjaud, J.-B. *et al.* (2018) ‘An inter-dimer allosteric switch controls NMDA receptor activity.’, *The EMBO journal*. EMBO Press, p. e99894. doi: 10.15252/embj.201899894.

Evron, T., Daigle, T. L. and Caron, M. G. (2012) 'GRK2: multiple roles beyond G protein-coupled receptor desensitization', *Trends in Pharmacological Sciences*. Elsevier, 33(3), pp. 154–164. doi: 10.1016/j.tips.2011.12.003.

Ferré, S. *et al.* (1991) 'Stimulation of high-affinity adenosine A2 receptors decreases the affinity of dopamine D2 receptors in rat striatal membranes.', *Proceedings of the National Academy of Sciences of the United States of America*. National Academy of Sciences, 88(16), pp. 7238–41. doi: 10.1073/pnas.88.16.7238.

Ferré, S. *et al.* (1992) 'Adenosine-dopamine interactions in the brain', *Neuroscience*. Pergamon, 51(3), pp. 501–512. doi: 10.1016/0306-4522(92)90291-9.

Ferré, S. *et al.* (1994) 'Antagonistic interaction between adenosine A2A receptors and dopamine D2 receptors in the ventral striopallidal system. Implications for the treatment of schizophrenia', *Neuroscience*. Pergamon, 63(3), pp. 765–773. doi: 10.1016/0306-4522(94)90521-5.

Ferré, S. *et al.* (2008) 'An update on adenosine A2A-dopamine D2 receptor interactions: implications for the function of G protein-coupled receptors.', *Current pharmaceutical design*. NIH Public Access, 14(15), pp. 1468–74.

Flint, A. C. *et al.* (1997) 'NR2A subunit expression shortens NMDA receptor synaptic currents in developing neocortex.', *The Journal of neuroscience : the official journal of the Society for Neuroscience*. Society for Neuroscience, 17(7), pp. 2469–76. doi: 10.1523/JNEUROSCI.17-07-02469.1997.

Ford, C. P. (2014) 'The role of D2-autoreceptors in regulating dopamine neuron activity and transmission.', *Neuroscience*. NIH Public Access, 282, pp. 13–22. doi: 10.1016/j.neuroscience.2014.01.025.

Forsythe, I. D. and Westbrook, G. L. (1988) 'Slow excitatory postsynaptic currents mediated by N-methyl-D-aspartate receptors on cultured mouse central neurones.', *The Journal of Physiology*. John Wiley & Sons, Ltd, 396(1), pp. 515–533. doi: 10.1113/jphysiol.1988.sp016975.

Forsythe, I. D., Westbrook, G. L. and Mayer, M. L. (1988) 'Modulation of excitatory synaptic transmission by glycine and zinc in cultures of mouse hippocampal neurons.', *The Journal of neuroscience : the official journal of the Society for Neuroscience*. Society for Neuroscience, 8(10), pp. 3733–41. doi: 10.1523/JNEUROSCI.08-10-03733.1988.

France, G. *et al.* (2017) 'Multiple roles of GluN2B-containing NMDA receptors in synaptic plasticity in juvenile hippocampus.', *Neuropharmacology*. Elsevier, 112(Pt A), pp. 76–83. doi: 10.1016/j.neuropharm.2016.08.010.

Fredholm, B. *et al.* (2001) 'Actions of Caffeine in the Brain with Special Reference to Factors That Contribute to Its Widespread Use',

Pharmacological Reviews. American Society for Pharmacology and Experimental Therapeutics, 51(1), pp. 83–133.

Fricker, M. *et al.* (2018) 'Neuronal Cell Death.', *Physiological reviews*. American Physiological Society, 98(2), pp. 813–880. doi: 10.1152/physrev.00011.2017.

Fukuzaki, K., Kamenosono, T. and Nagata, R. (2000) 'Effects of ropinirole on various parkinsonian models in mice, rats, and cynomolgus monkeys.', *Pharmacology, biochemistry, and behavior*, 65(3), pp. 503–8.

Fuxe, K. *et al.* (2010) 'Adenosine-Dopamine Interactions in the Pathophysiology and Treatment of CNS Disorders', *CNS Neuroscience & Therapeutics*, 16(3), pp. e18–e42. doi: 10.1111/j.1755-5949.2009.00126.x.

Gallo, E. F. (2019) 'Disentangling the diverse roles of dopamine D2 receptors in striatal function and behavior', *Neurochemistry International*. Pergamon, 125, pp. 35–46. doi: 10.1016/J.NEUINT.2019.01.022.

Gerfen, C. R. (2000) 'Molecular effects of dopamine on striatal-projection pathways', *Trends in Neurosciences*. Elsevier Current Trends, 23, pp. S64–S70. doi: 10.1016/S1471-1931(00)00019-7.

Gerfen, C. R. and Surmeier, D. J. (2011) 'Modulation of striatal projection systems by dopamine.', *Annual review of neuroscience*. NIH Public Access, 34, pp. 441–66. doi: 10.1146/annurev-neuro-061010-113641.

Gerlach, M. *et al.* (2003) 'Dopamine receptor agonists in current clinical use: comparative dopamine receptor binding profiles defined in the human striatum', *Journal of Neural Transmission*. Springer-Verlag, 110(10), pp. 1119–1127. doi: 10.1007/s00702-003-0027-5.

Gerlach, M. and Riederer, P. (1996) 'Animal models of Parkinson's disease: An empirical comparison with the phenomenology of the disease in man', *Journal of Neural Transmission*. Springer-Verlag, 103(8–9), pp. 987–1041. doi: 10.1007/BF01291788.

German, D. C. *et al.* (1992) 'Midbrain Dopaminergic Cell Loss in Parkinson's Disease and MPTP-Induced Parkinsonism: Sparing of Calbindin-D $_{25k}$?Containing Cells', *Annals of the New York Academy of Sciences*. John Wiley & Sons, Ltd (10.1111), 648(1 Neurotoxins a), pp. 42–62. doi: 10.1111/j.1749-6632.1992.tb24523.x.

German, D. C. and Manaye, K. F. (1993) 'Midbrain dopaminergic neurons (nuclei A8, A9, and A10): Three-dimensional reconstruction in the rat', *The Journal of Comparative Neurology*. John Wiley & Sons, Ltd, 331(3), pp. 297–309. doi: 10.1002/cne.903310302.

Germann, U. A. *et al.* (2017) 'Targeting the MAPK Signaling Pathway in

Cancer: Promising Preclinical Activity with the Novel Selective ERK1/2 Inhibitor BVD-523 (Ulixertinib).', *Molecular cancer therapeutics*. American Association for Cancer Research, 16(11), pp. 2351–2363. doi: 10.1158/1535-7163.MCT-17-0456.

Geyer, M. and Wittinghofer, A. (1997) 'GEFs, GAPs, GDIs and effectors: taking a closer (3D) look at the regulation of Ras-related GTP-binding proteins', *Current Opinion in Structural Biology*. Elsevier Current Trends, 7(6), pp. 786–792. doi: 10.1016/S0959-440X(97)80147-9.

Gibb, A. J. and Edwards, F. A. (1994) *Patch clamp recording from cells in sliced tissues*. Microelectrode Techniques. The Plymouth Workshop Handbook.

Giese, K. P. *et al.* (1998) 'Autophosphorylation at Thr286 of the α Calcium-Calmodulin Kinase II in LTP and Learning', *Science*. American Association for the Advancement of Science, 279(5352), pp. 870–873. doi: 10.1126/SCIENCE.279.5352.870.

Gingrich, J. R. *et al.* (2004) 'Unique domain anchoring of Src to synaptic NMDA receptors via the mitochondrial protein NADH dehydrogenase subunit 2.', *Proceedings of the National Academy of Sciences of the United States of America*. National Academy of Sciences, 101(16), pp. 6237–42. doi: 10.1073/pnas.0401413101.

Goldman-Rakic, P. *et al.* (2004) 'Targeting the dopamine D1 receptor in schizophrenia: insights for cognitive dysfunction', *Psychopharmacology*. Springer-Verlag, 174(1), pp. 3–16. doi: 10.1007/s00213-004-1793-y.

Gonon, F. G. (1988) 'Nonlinear relationship between impulse flow and dopamine released by rat midbrain dopaminergic neurons as studied by in vivo electrochemistry', *Neuroscience*. Pergamon, 24(1), pp. 19–28. doi: 10.1016/0306-4522(88)90307-7.

Goodell, D. J. *et al.* (2017) 'DAPK1 Mediates LTD by Making CaMKII/GluN2B Binding LTP Specific.', *Cell reports*. Elsevier, 19(11), pp. 2231–2243. doi: 10.1016/j.celrep.2017.05.068.

Grace, A. A. and Bunney, B. S. (1983) 'Intracellular and extracellular electrophysiology of nigral dopaminergic neurons—2. Action potential generating mechanisms and morphological correlates', *Neuroscience*. Pergamon, 10(2), pp. 317–331. doi: 10.1016/0306-4522(83)90136-7.

Grace, A. A. and Bunney, B. S. (1984) 'The control of firing pattern in nigral dopamine neurons: single spike firing.', *The Journal of neuroscience : the official journal of the Society for Neuroscience*. Society for Neuroscience, 4(11), pp. 2866–76. doi: 10.1523/JNEUROSCI.04-11-02866.1984.

Grant, S. G. *et al.* (1992) 'Impaired long-term potentiation, spatial learning, and hippocampal development in fyn mutant mice.', *Science (New York, N.Y.)*.

American Association for the Advancement of Science, 258(5090), pp. 1903–10. doi: 10.1126/science.1361685.

Green, D. R. and Kroemer, G. (2005) 'Pharmacological manipulation of cell death: clinical applications in sight?', *The Journal of clinical investigation*. American Society for Clinical Investigation, 115(10), pp. 2610–7. doi: 10.1172/JCI26321.

Grillner, P. and Mercuri, N. B. (2002) 'Intrinsic membrane properties and synaptic inputs regulating the firing activity of the dopamine neurons', *Behavioural Brain Research*. Elsevier, 130(1–2), pp. 149–169. doi: 10.1016/S0166-4328(01)00418-1.

Groc, L. *et al.* (2007) 'NMDA receptor surface trafficking and synaptic subunit composition are developmentally regulated by the extracellular matrix protein Reelin.', *The Journal of neuroscience : the official journal of the Society for Neuroscience*. Society for Neuroscience, 27(38), pp. 10165–75. doi: 10.1523/JNEUROSCI.1772-07.2007.

Groveman, B. R. *et al.* (2011) 'Roles of the SH2 and SH3 domains in the regulation of neuronal Src kinase functions.', *The FEBS journal*. NIH Public Access, 278(4), pp. 643–53. doi: 10.1111/j.1742-4658.2010.07985.x.

Guidolin, D. *et al.* (2015) 'G-protein-coupled receptor type A heteromers as an emerging therapeutic target', *Expert Opinion on Therapeutic Targets*. Informa Healthcare, 19(2), pp. 265–283. doi: 10.1517/14728222.2014.981155.

Guo, N. *et al.* (2010) 'Impact of D2 receptor internalization on binding affinity of neuroimaging radiotracers.', *Neuropsychopharmacology : official publication of the American College of Neuropsychopharmacology*. Nature Publishing Group, 35(3), pp. 806–17. doi: 10.1038/npp.2009.189.

Hackos, D. H. and Hanson, J. E. (2017) 'Diverse modes of NMDA receptor positive allosteric modulation: Mechanisms and consequences', *Neuropharmacology*. Pergamon, 112, pp. 34–45. doi: 10.1016/J.NEUROPHARM.2016.07.037.

Hallberg, B., Rayter, S. I. and Downward, J. (1994) 'Interaction of Ras and Raf in intact mammalian cells upon extracellular stimulation.', *The Journal of biological chemistry*, 269(6), pp. 3913–6.

Hammond, C. *et al.* (1978) 'Electrophysiological demonstration of an excitatory subthalamonigral pathway in the rat', *Brain Research*. Elsevier, 151(2), pp. 235–244. doi: 10.1016/0006-8993(78)90881-8.

Hanke, J. H. *et al.* (1996) 'Discovery of a novel, potent, and Src family-selective tyrosine kinase inhibitor. Study of Lck- and FynT-dependent T cell activation.', *The Journal of biological chemistry*. American Society for Biochemistry and Molecular Biology, 271(2), pp. 695–701. doi:

10.1074/jbc.271.2.695.

Hansen, K. B. *et al.* (2014) 'Distinct functional and pharmacological properties of Triheteromeric GluN1/GluN2A/GluN2B NMDA receptors.', *Neuron*. NIH Public Access, 81(5), pp. 1084–1096. doi: 10.1016/j.neuron.2014.01.035.

Hansen, K. B. *et al.* (2017) 'NMDA Receptors in the Central Nervous System', in. Humana Press, New York, NY, pp. 1–80. doi: 10.1007/978-1-4939-7321-7_1.

Hansen, K. B. *et al.* (2018) 'Structure, function, and allosteric modulation of NMDA receptors.', *The Journal of general physiology*. The Rockefeller University Press, 150(8), pp. 1081–1105. doi: 10.1085/jgp.201812032.

Hardingham, G. E., Arnold, F. J. L. and Bading, H. (2001) 'A calcium microdomain near NMDA receptors: on switch for ERK-dependent synapse-to-nucleus communication', *Nature Neuroscience*. Nature Publishing Group, 4(6), pp. 565–566. doi: 10.1038/88380.

Hardingham, G. E. and Bading, H. (2010) 'Synaptic versus extrasynaptic NMDA receptor signalling: implications for neurodegenerative disorders.', *Nature reviews. Neuroscience*. Europe PMC Funders, 11(10), pp. 682–96. doi: 10.1038/nrn2911.

Harney, S. C., Jane, D. E. and Anwyl, R. (2008) 'Extrasynaptic NR2D-Containing NMDARs Are Recruited to the Synapse during LTP of NMDAR-EPSCs', *Journal of Neuroscience*. Society for Neuroscience, 28(45), pp. 11685–11694. doi: 10.1523/JNEUROSCI.3035-08.2008.

Hell, J. W. (2014) 'CaMKII: Claiming Center Stage in Postsynaptic Function and Organization', *Neuron*. NIH Public Access, 81(2), p. 249. doi: 10.1016/J.NEURON.2013.12.024.

Hestrin, S., Sah, P. and Nicoll, R. A. (1990) 'Mechanisms generating the time course of dual component excitatory synaptic currents recorded in hippocampal slices', *Neuron*. Cell Press, 5(3), pp. 247–253. doi: 10.1016/0896-6273(90)90162-9.

Higley, M. J. and Sabatini, B. L. (2010) 'Competitive regulation of synaptic Ca2+ influx by D2 dopamine and A2A adenosine receptors.', *Nature neuroscience*. NIH Public Access, 13(8), pp. 958–66. doi: 10.1038/nn.2592.

Hillion, J. *et al.* (2002) 'Coaggregation, cointernalization, and codesensitization of adenosine A2A receptors and dopamine D2 receptors.', *The Journal of biological chemistry*. American Society for Biochemistry and Molecular Biology, 277(20), pp. 18091–7. doi: 10.1074/jbc.M107731200.

Hisahara, S. and Shimohama, S. (2011) 'Dopamine receptors and Parkinson's disease.', *International journal of medicinal chemistry*, 2011, p. 403039.

doi: 10.1155/2011/403039.

Hopf, F. W. *et al.* (2005) 'Atypical protein kinase C is a novel mediator of dopamine-enhanced firing in nucleus accumbens neurons.', *The Journal of neuroscience : the official journal of the Society for Neuroscience*. Society for Neuroscience, 25(4), pp. 985–9. doi: 10.1523/JNEUROSCI.3099-04.2005.

Hu, H. (2016) 'Reward and Aversion', *Annual Review of Neuroscience*. Annual Reviews , 39(1), pp. 297–324. doi: 10.1146/annurev-neuro-070815-014106.

Huang, L. *et al.* (2013) 'Modulation of A_2a receptor antagonist on D_2 receptor internalization and ERK phosphorylation.', *Acta pharmacologica Sinica*. Nature Publishing Group, 34(10), pp. 1292–300. doi: 10.1038/aps.2013.87.

Huang, Y.-Q. *et al.* (2001) 'CAKβ/Pyk2 Kinase Is a Signaling Link for Induction of Long-Term Potentiation in CA1 Hippocampus', *Neuron*. Cell Press, 29(2), pp. 485–496. doi: 10.1016/S0896-6273(01)00220-3.

Hutton, S. R. *et al.* (2017) 'ERK/MAPK Signaling Is Required for Pathway-Specific Striatal Motor Functions.', *The Journal of neuroscience : the official journal of the Society for Neuroscience*. Society for Neuroscience, 37(34), pp. 8102–8115. doi: 10.1523/JNEUROSCI.0473-17.2017.

Hyman, S. E., Malenka, R. C. and Nestler, E. J. (2006) 'Neural Mechanisms of Addiction: The Role of Reward-Related Learning and Memory', *Annual Review of Neuroscience*. Annual Reviews, 29(1), pp. 565–598. doi: 10.1146/annurev.neuro.29.051605.113009.

Iacobucci, G. J. and Popescu, G. K. (2017) 'Resident Calmodulin Primes NMDA Receptors for Ca2+-Dependent Inactivation', *Biophysical Journal*. Cell Press, 113(10), pp. 2236–2248. doi: 10.1016/J.BPJ.2017.06.035.

Iacobucci, G. J. and Popescu, G. K. (2018) 'Kinetic models for activation and modulation of NMDA receptor subtypes', *Current opinion in physiology*. NIH Public Access, 2, p. 114. doi: 10.1016/J.COPHYS.2018.02.002.

Iida, N. *et al.* (2001) 'Requirement of Ras for the activation of mitogen-activated protein kinase by calcium influx, cAMP, and neurotrophin in hippocampal neurons.', *The Journal of neuroscience : the official journal of the Society for Neuroscience*. Society for Neuroscience, 21(17), pp. 6459–66. doi: 10.1523/JNEUROSCI.21-17-06459.2001.

Imamoto, A. and Soriano, P. (1993) 'Disruption of the csk gene, encoding a negative regulator of Src family tyrosine kinases, leads to neural tube defects and embryonic lethality in mice', *Cell*. Cell Press, 73(6), pp. 1117–1124. doi: 10.1016/0092-8674(93)90641-3.

Jackson-Lewis, V. *et al.* (2000) 'Developmental cell death in dopaminergic neurons of the substantia nigra of mice', *The Journal of Comparative Neurology*. John Wiley & Sons, Ltd, 424(3), pp. 476–488. doi: 10.1002/1096-9861(20000828)424:3<476::AID-CNE6>3.0.CO;2-0.

Jellinger, K. A. (1991) *Changes Other than the Nigrostriatal Pathway*. *Molecular and Chemical Neuropathology. 14, pp.153-197.*

Jenner, P. (2003) 'Dopamine agonists, receptor selectivity and dyskinesia induction in Parkinson's disease.', *Current opinion in neurology*, 16 Suppl 1, pp. S3–S7. doi: 10.1097/00019052-200312001-00002.

Jiang, X. *et al.* (2008) 'Activated Src kinases interact with the *N* -methyl-D-aspartate receptor after neonatal brain ischemia', *Annals of Neurology*. John Wiley & Sons, Ltd, 63(5), pp. 632–641. doi: 10.1002/ana.21365.

Johnson, J. and Ascher, P. (1987) 'Glycine potentiates the NMDA response in cultured mouse neurons', *Nature* 325, 529-531.

Jones, S. and Gibb, A. J. (2005) 'Functional NR2B- and NR2D-containing NMDA receptor channels in rat substantia nigra dopaminergic neurones', *The Journal of Physiology*. John Wiley & Sons, Ltd (10.1111), 569(1), pp. 209–221. doi: 10.1113/jphysiol.2005.095554.

Joseph, J. . *et al.* (2002) 'Dopamine autoreceptor regulation of release and uptake in mouse brain slices in the absence of D3 receptors', *Neuroscience*. Pergamon, 112(1), pp. 39–49. doi: 10.1016/S0306-4522(02)00067-2.

Josselyn, S. A. and Nguyen, P. V (2005) 'CREB, synapses and memory disorders: past progress and future challenges.', *Current drug targets. CNS and neurological disorders*, 4(5), pp. 481–97. Available at: http://www.ncbi.nlm.nih.gov/pubmed/16266283 (Accessed: 25 March 2019).

Journal, E. *et al.* (1981) *Pfltigers Archiv Improved Patch-Clamp Techniques for High-Resolution Current Recording from Cells and Cell-Free Membrane Patches*.

Kalia, L. V. and Salter, M. W. (2003) 'Interactions between Src family protein tyrosine kinases and PSD-95', *Neuropharmacology*. Pergamon, 45(6), pp. 720–728. doi: 10.1016/S0028-3908(03)00313-7.

Karakas, E., Simorowski, N. and Furukawa, H. (2011) 'Subunit arrangement and phenylethanolamine binding in GluN1/GluN2B NMDA receptors', *Nature*. Nature Publishing Group, 475(7355), pp. 249–253. doi: 10.1038/nature10180.

Karschin, C. *et al.* (1996) 'IRK(1-3) and GIRK(1-4) inwardly rectifying K+ channel mRNAs are differentially expressed in the adult rat brain.', *The*

Journal of neuroscience : the official journal of the Society for Neuroscience. Society for Neuroscience, 16(11), pp. 3559–70.

Keck, T. M. *et al.* (2015) 'Identifying Medication Targets for Psychostimulant Addiction: Unraveling the Dopamine D3 Receptor Hypothesis.', *Journal of medicinal chemistry*. American Chemical Society, 58(14), pp. 5361–80. doi: 10.1021/jm501512b.

Kelly, E., Bailey, C. P. and Henderson, G. (2008) 'Agonist-selective mechanisms of GPCR desensitization.', *British journal of pharmacology*. Wiley-Blackwell, 153 Suppl 1(Suppl 1), pp. S379-88. doi: 10.1038/sj.bjp.0707604.

Khaliq, Z. M. and Bean, B. P. (2010) 'Pacemaking in dopaminergic ventral tegmental area neurons: depolarizing drive from background and voltage-dependent sodium conductances.', *The Journal of neuroscience : the official journal of the Society for Neuroscience*. NIH Public Access, 30(21), pp. 7401–13. doi: 10.1523/JNEUROSCI.0143-10.2010.

Kidger, A. M., Sipthorp, J. and Cook, S. J. (2018) 'ERK1/2 inhibitors: New weapons to inhibit the RAS-regulated RAF-MEK1/2-ERK1/2 pathway', *Pharmacology & Therapeutics*. Pergamon, 187, pp. 45–60. doi: 10.1016/J.PHARMTHERA.2018.02.007.

Kim, K. M. *et al.* (2001) 'Differential regulation of the dopamine D2 and D3 receptors by G protein-coupled receptor kinases and beta-arrestins.', *The Journal of biological chemistry*. American Society for Biochemistry and Molecular Biology, 276(40), pp. 37409–14. doi: 10.1074/jbc.M106728200.

Kim, S. J. *et al.* (2004) 'Distinct Regulation of Internalization and Mitogen-Activated Protein Kinase Activation by Two Isoforms of the Dopamine D2 Receptor', *Molecular Endocrinology*. Narnia, 18(3), pp. 640–652. doi: 10.1210/me.2003-0066.

Kotecha, S. A. *et al.* (2002) 'A D2 class dopamine receptor transactivates a receptor tyrosine kinase to inhibit NMDA receptor transmission', *Neuron*, 35(6), pp. 1111–1122. doi: 10.1016/S0896-6273(02)00859-0.

Kotecha, S. A. *et al.* (2003) 'Co-stimulation of mGluR5 and N-methyl-D-aspartate receptors is required for potentiation of excitatory synaptic transmission in hippocampal neurons.', *The Journal of biological chemistry*. American Society for Biochemistry and Molecular Biology, 278(30), pp. 27742–9. doi: 10.1074/jbc.M301946200.

Krapivinsky, G. *et al.* (2003) 'The NMDA Receptor Is Coupled to the ERK Pathway by a Direct Interaction between NR2B and RasGRF1', *Neuron*. Cell Press, 40(4), pp. 775–784. doi: 10.1016/S0896-6273(03)00645-7.

Krashia, P. *et al.* (2016) 'On the properties of identified dopaminergic neurons in the mouse substantia nigra and ventral tegmental area.', *The European*

journal of neuroscience. doi: 10.1111/ejn.13364.

Kravitz, A. V. *et al.* (2010) 'Regulation of parkinsonian motor behaviours by optogenetic control of basal ganglia circuitry', *Nature*. Nature Publishing Group, 466(7306), pp. 622–626. doi: 10.1038/nature09159.

Krupp, J. J. *et al.* (2002) 'Calcineurin acts via the C-terminus of NR2A to modulate desensitization of NMDA receptors', *Neuropharmacology*. Pergamon, 42(5), pp. 593–602. doi: 10.1016/S0028-3908(02)00031-X.

Kvernmo, T., Houben, J. and Sylte, I. (2008) 'Receptor-Binding and Pharmacokinetic Properties of Dopaminergic Agonists', *Current Topics in Medicinal Chemistry*, 8(12), pp. 1049–1067. doi: 10.2174/156802608785161457.

Lacey, M. G., Mercuri, N. B. and North, R. A. (1987) 'Dopamine acts on D2 receptors to increase potassium conductance in neurones of the rat substantia nigra zona compacta.', *The Journal of physiology*. Wiley-Blackwell, 392, pp. 397–416.

Lacey, M. G., Mercuri, N. B. and North, R. A. (1988) 'On the potassium conductance increase activated by GABAB and dopamine D2 receptors in rat substantia nigra neurones.', *The Journal of Physiology*. Wiley-Blackwell, 401, p. 437.

Lacey, M. G., Mercurit, N. B. and North, R. A. (1987) 'Dopamine acts of D2 Receptors to increase Potassium conductance in neurones of the rat substantia nigra zona compacta.', *J. Physiol*, 392, pp. 397–416.

Lai, C.-Y. *et al.* (2018) 'The D2 Dopamine Receptor Interferes With the Protective Effect of the A2A Adenosine Receptor on TDP-43 Mislocalization in Experimental Models of Motor Neuron Degeneration.', *Frontiers in neuroscience*. Frontiers Media SA, 12, p. 187. doi: 10.3389/fnins.2018.00187.

Lan, J. *et al.* (2001) 'Protein kinase C modulates NMDA receptor trafficking and gating', *Nature Neuroscience*. Nature Publishing Group, 4(4), pp. 382–390. doi: 10.1038/86028.

Lau, C. G. and Zukin, R. S. (2007) 'NMDA receptor trafficking in synaptic plasticity and neuropsychiatric disorders.', *Nature reviews. Neuroscience*, 8(6), pp. 413–26. doi: 10.1038/nrn2153.

Lavezzari, G. *et al.* (2004) 'Subunit-Specific Regulation of NMDA Receptor Endocytosis'. doi: 10.1523/JNEUROSCI.1890-04.2004.

Lee, C.-H. *et al.* (2014) 'NMDA receptor structures reveal subunit arrangement and pore architecture', *Nature*. Nature Publishing Group, 511(7508), pp. 191–197. doi: 10.1038/nature13548.

Lee, C. R. and Tepper, J. M. (2009) 'Basal Ganglia Control of Substantia Nigra Dopaminergic Neurons', in *Birth, Life and Death of Dopaminergic Neurons in the Substantia Nigra*. Vienna: Springer Vienna, pp. 71–90. doi: 10.1007/978-3-211-92660-4_6.

Lee, F. J. *et al.* (2002) 'Dual regulation of NMDA receptor functions by direct protein-protein interactions with the dopamine D1 receptor', *Cell*, 111(2), pp. 219–30.

Lee, S.-J. R. *et al.* (2009) 'Activation of CaMKII in single dendritic spines during long-term potentiation', *Nature*. Nature Publishing Group, 458(7236), pp. 299–304. doi: 10.1038/nature07842.

Lefkowitz, R. J. and Shenoy, S. K. (2005) 'Transduction of receptor signals by beta-arrestins.', *Science (New York, N.Y.)*. American Association for the Advancement of Science, 308(5721), pp. 512–7. doi: 10.1126/science.1109237.

Leonard, A. S. and Hell, J. W. (1997) 'Cyclic AMP-dependent protein kinase and protein kinase C phosphorylate N-methyl-D-aspartate receptors at different sites.', *The Journal of biological chemistry*. American Society for Biochemistry and Molecular Biology, 272(18), pp. 12107–15. doi: 10.1074/jbc.272.18.12107.

Liang, X. *et al.* (2004) 'The N-terminal SH4 region of the Src family kinase Fyn is modified by methylation and heterogeneous fatty acylation: role in membrane targeting, cell adhesion, and spreading.', *The Journal of biological chemistry*. American Society for Biochemistry and Molecular Biology, 279(9), pp. 8133–9. doi: 10.1074/jbc.M311180200.

Lisman, J., Yasuda, R. and Raghavachari, S. (2012) 'Mechanisms of CaMKII action in long-term potentiation', *Nature reviews. Neuroscience*. NIH Public Access, 13(3), p. 169. doi: 10.1038/NRN3192.

Liss, B. *et al.* (2005) 'K-ATP channels promote the differential degeneration of dopaminergic midbrain neurons', *Nature Neuroscience*. Nature Publishing Group, 8(12), pp. 1742–1751. doi: 10.1038/nn1570.

Liu, X. J. *et al.* (2008) 'Treatment of inflammatory and neuropathic pain by uncoupling Src from the NMDA receptor complex', *Nature Medicine*. Nature Publishing Group, 14(12), pp. 1325–1332. doi: 10.1038/nm.1883.

Liu, X. Y. *et al.* (2006) 'Modulation of D2R-NR2B Interactions in Response to Cocaine', *Neuron*, 52(5), pp. 897–909. doi: 10.1016/j.neuron.2006.10.011.

Liu, Y. *et al.* (1999) 'Structural basis for selective inhibition of Src family kinases by PP1', *Chemistry & Biology*. Cell Press, 6(9), pp. 671–678. doi: 10.1016/S1074-5521(99)80118-5.

Lombroso, P. J. *et al.* (1993) *A Protein Tyrosine Phosphatase Expressed*

within Dopaminoceptive Neurons of the Basal Ganglia and Related Structures, *The Journal of Neuroscience*.

Lopatin, A. N., Makhina, E. N. and Nichols, C. G. (1995) 'The mechanism of inward rectification of potassium channels: "long-pore plugging" by cytoplasmic polyamines.', *The Journal of general physiology*. The Rockefeller University Press, 106(5), pp. 923–55.

Lowe, J. D. *et al.* (2015) 'Role of G Protein-Coupled Receptor Kinases 2 and 3 in -Opioid Receptor Desensitization and Internalization', *Molecular Pharmacology*, 88(2), pp. 347–356. doi: 10.1124/mol.115.098293.

Lowry, W. E. *et al.* (2002) 'Csk, a Critical Link of G Protein Signals to Actin Cytoskeletal Reorganization', *Developmental Cell*. Cell Press, 2(6), pp. 733–744. doi: 10.1016/S1534-5807(02)00175-2.

Lu, W.-Y. *et al.* (1999) 'G-protein-coupled receptors act via protein kinase C and Src to regulate NMDA receptors', *Nature Neuroscience*. Nature Publishing Group, 2(4), pp. 331–338. doi: 10.1038/7243.

Lu, W. *et al.* (2018) 'Phosphorylation of tyrosine Y1070 at the GluN2B subunit is regulated by synaptic activity and critical for surface expression of NMDA receptors Running title: GluN2B Y1070 regulates surface expression of NMDARs', *at UCL Library Services on*. doi: 10.1074/jbc.M115.663450.

Lu, Y. M. *et al.* (1998) 'Src activation in the induction of long-term potentiation in CA1 hippocampal neurons.', *Science (New York, N.Y.)*. American Association for the Advancement of Science, 279(5355), pp. 1363–7. doi: 10.1126/science.279.5355.1363.

Luo, S. X. and Huang, E. J. (2016) 'Dopaminergic Neurons and Brain Reward Pathways: From Neurogenesis to Circuit Assembly.', *The American journal of pathology*. American Society for Investigative Pathology, 186(3), pp. 478–88. doi: 10.1016/j.ajpath.2015.09.023.

Luzardo-Alvarez, A., Delgado-Charro, M. B. and Blanco-Méndez, J. (2001) 'Iontophoretic Delivery of Ropinirole Hydrochloride: Effect of Current Density and Vehicle Formulation', *Pharmaceutical Research*. Kluwer Academic Publishers-Plenum Publishers, 18(12), pp. 1714–1720. doi: 10.1023/A:1013322613436.

Lynch, D. R. and Guttmann, R. P. (2002) 'Excitotoxicity: perspectives based on N-methyl-D-aspartate receptor subtypes.', *The Journal of pharmacology and experimental therapeutics*. American Society for Pharmacology and Experimental Therapeutics, 300(3), pp. 717–23. doi: 10.1124/JPET.300.3.717.

MacDermott, A. B. *et al.* (1986) 'NMDA-receptor activation increases cytoplasmic calcium concentration in cultured spinal cord neurones',

Nature. Nature Publishing Group, 321(6069), pp. 519–522. doi: 10.1038/321519a0.

Macdonald, D. S. *et al.* (2005) 'Modulation of NMDA Receptors by Pituitary Adenylate Cyclase Activating Peptide in CA1 Neurons Requires Gαq, Protein Kinase C, and Activation of Src', *Journal of Neuroscience*. Society for Neuroscience, 25(49), pp. 11374–11384. doi: 10.1523/JNEUROSCI.3871-05.2005.

MacDonald, J. F., Jackson, M. F. and Beazely, M. A. (2007) 'G protein-coupled receptors control NMDARs and metaplasticity in the hippocampus', *Biochimica et Biophysica Acta (BBA) - Biomembranes*. Elsevier, 1768(4), pp. 941–951. doi: 10.1016/J.BBAMEM.2006.12.006.

Mao, L.-M. and Wang, J. Q. (2015) 'Dopaminergic and cholinergic regulation of Fyn tyrosine kinase phosphorylation in the rat striatum in vivo', *Neuropharmacology*. Pergamon, 99, pp. 491–499. doi: 10.1016/J.NEUROPHARM.2015.08.017.

Mao, L.-M. and Wang, J. Q. (2016) 'Dopamine D2 receptors are involved in the regulation of Fyn and metabotropic glutamate receptor 5 phosphorylation in the rat striatum in vivo.', *Journal of neuroscience research*. NIH Public Access, 94(4), pp. 329–38. doi: 10.1002/jnr.23713.

Margolis, E. B., Lock, H., Chefer, V. I., *et al.* (2006) 'Kappa opioids selectively control dopaminergic neurons projecting to the prefrontal cortex.', *Proceedings of the National Academy of Sciences of the United States of America*. National Academy of Sciences, 103(8), pp. 2938–42. doi: 10.1073/pnas.0511159103.

Margolis, E. B., Lock, H., Hjelmstad, G. O., *et al.* (2006) 'The ventral tegmental area revisited: is there an electrophysiological marker for dopaminergic neurons?', *The Journal of physiology*. Wiley-Blackwell, 577(Pt 3), pp. 907–24. doi: 10.1113/jphysiol.2006.117069.

Martel, P. *et al.* (2011) 'Role of Kv1 Potassium Channels in Regulating Dopamine Release and Presynaptic D2 Receptor Function', *PLoS ONE*. Edited by C. Combs. Public Library of Science, 6(5), p. e20402. doi: 10.1371/journal.pone.0020402.

Massagué, J. and Chen, Y. G. (2000) 'Controlling TGF-beta signaling.', *Genes & development*. Cold Spring Harbor Laboratory Press, 14(6), pp. 627–44. doi: 10.1101/GAD.14.6.627.

Maurin, Y. *et al.* (1999) 'Three-dimensional distribution of nigrostriatal neurons in the rat: relation to the topography of striatonigral projections', *Neuroscience*. Pergamon, 91(3), pp. 891–909. doi: 10.1016/S0306-4522(98)00681-2.

Mavrikaki, M. *et al.* (2014) 'Ropinirole regulates emotionality and neuronal activity markers in the limbic forebrain.', *The international journal of neuropsychopharmacology / official scientific journal of the Collegium Internationale Neuropsychopharmacologicum (CINP)*, 17(12), pp. 1981–93. doi: 10.1017/S1461145714000728.

De Mei, C. *et al.* (2009) 'Getting specialized: presynaptic and postsynaptic dopamine D2 receptors', *Current Opinion in Pharmacology*. Elsevier, 9(1), pp. 53–58. doi: 10.1016/J.COPH.2008.12.002.

Mierau, J. *et al.* (1995) 'Pramipexole binding and activation of cloned and expressed dopamine D2, D3 and D4 receptors', *European Journal of Pharmacology: Molecular Pharmacology*. Elsevier, 290(1), pp. 29–36. doi: 10.1016/0922-4106(95)90013-6.

Millan, M. J. *et al.* (2002) 'Differential actions of antiparkinson agents at multiple classes of monoaminergic receptor. I. A multivariate analysis of the binding profiles of 14 drugs at 21 native and cloned human receptor subtypes.', *The Journal of pharmacology and experimental therapeutics*. American Society for Pharmacology and Experimental Therapeutics, 303(2), pp. 791–804. doi: 10.1124/jpet.102.039867.

Missale, C. *et al.* (1998) 'Dopamine Receptors: From Structure to Function', *Physiological Reviews*. American Physiological SocietyBethesda, MD , 78(1), pp. 189–225. doi: 10.1152/physrev.1998.78.1.189.

Monte-Silva, K. *et al.* (2009) 'Dose-Dependent Inverted U-Shaped Effect of Dopamine (D2 -Like) Receptor Activation on Focal and Nonfocal Plasticity in Humans'. *Journal of Neuroscience,* 29(19), p. 6124-6131 doi: 10.1523/JNEUROSCI.0728-09.2009.

Monyer, H. *et al.* (1994) 'Developmental and regional expression in the rat brain and functional properties of four NMDA receptors.', *Neuron*, 12(3), pp. 529–40.

Moran, M. F. *et al.* (1990) 'Src homology region 2 domains direct protein-protein interactions in signal transduction.', *Proceedings of the National Academy of Sciences of the United States of America*. National Academy of Sciences, 87(21), pp. 8622–6. doi: 10.1073/pnas.87.21.8622.

Morris, P. G., Mishina, M. and Jones, S. (2018) 'Altered Synaptic and Extrasynaptic NMDA Receptor Properties in Substantia Nigra Dopaminergic Neurons From Mice Lacking the GluN2D Subunit.', *Frontiers in cellular neuroscience*, 12, p. 354. doi: 10.3389/fncel.2018.00354.

Mulkey, R. M. *et al.* (1994) 'Involvement of a calcineurin/ inhibitor-1 phosphatase cascade in hippocampal long-term depression', *Nature*. Nature Publishing Group, 369(6480), pp. 486–488. doi: 10.1038/369486a0.

Murphy, J. A. *et al.* (2014) 'Phosphorylation of Ser1166 on GluN2B by PKA is critical to synaptic NMDA receptor function and Ca2+ signaling in spines.', *The Journal of neuroscience : the official journal of the Society for Neuroscience*. Society for Neuroscience, 34(3), pp. 869–79. doi: 10.1523/JNEUROSCI.4538-13.2014.

Nada, S. *et al.* (1991) 'Cloning of a complementary DNA for a protein-tyrosine kinase that specifically phosphorylates a negative regulatory site of p60c-src', *Nature*. Nature Publishing Group, 351(6321), pp. 69–72. doi: 10.1038/351069a0.

Nada, S. *et al.* (1993) 'Constitutive activation of Src family kinases in mouse embryos that lack Csk', *Cell*. Cell Press, 73(6), pp. 1125–1135. doi: 10.1016/0092-8674(93)90642-4.

Nakazawa, T. *et al.* (2001) 'Characterization of Fyn-mediated Tyrosine Phosphorylation Sites on GluRε2 (NR2B) Subunit of the *N* -Methyl-d-aspartate Receptor', *Journal of Biological Chemistry*, 276(1), pp. 693–699. doi: 10.1074/jbc.M008085200.

Nakazawa, T., Tezuka, T. and Yamamoto, T. (2002) 'Regulation of NMDA receptor function by Fyn-mediated tyrosine phosphorylation.', *Nihon shinkei seishin yakurigaku zasshi = Japanese journal of psychopharmacology*, 22(5), pp. 165–7.

Neet, K. and Hunter, T. (1996) 'Vertebrate non-receptor protein-tyrosine kinase families', *Genes to Cells*. John Wiley & Sons, Ltd (10.1111), 1(2), pp. 147–169. doi: 10.1046/j.1365-2443.1996.d01-234.x.

Neuhoff, H. *et al.* (2002a) 'I(h) channels contribute to the different functional properties of identified dopaminergic subpopulations in the midbrain.', *The Journal of neuroscience : the official journal of the Society for Neuroscience*, 22(4), pp. 1290–302.

Neuhoff, H. *et al.* (2002b) 'I(h) channels contribute to the different functional properties of identified dopaminergic subpopulations in the midbrain.', *The Journal of neuroscience : the official journal of the Society for Neuroscience*. Society for Neuroscience, 22(4), pp. 1290–302. doi: 10.1523/JNEUROSCI.22-04-01290.2002.

Neumann, M. *et al.* (2006) 'Ubiquitinated TDP-43 in frontotemporal lobar degeneration and amyotrophic lateral sclerosis.', *Science (New York, N.Y.)*. American Association for the Advancement of Science, 314(5796), pp. 130–3. doi: 10.1126/science.1134108.

Neve, Kim A, Seamans, J. K. and Trantham-Davidson, H. (2004) 'Dopamine receptor signaling.', *Journal of receptor and signal transduction research*, 24(3), pp. 165–205.

Newman-Tancredi, A. *et al.* (2002) 'Differential actions of antiparkinson agents at multiple classes of monoaminergic receptor. II. Agonist and antagonist properties at subtypes of dopamine D(2)-like receptor and alpha(1)/alpha(2)-adrenoceptor.', *The Journal of pharmacology and experimental therapeutics*. American Society for Pharmacology and Experimental Therapeutics, 303(2), pp. 805–14. doi: 10.1124/jpet.102.039875.

Neyton, J. and Paoletti, P. (2006) 'Relating NMDA receptor function to receptor subunit composition: limitations of the pharmacological approach.', *The Journal of neuroscience : the official journal of the Society for Neuroscience*. Society for Neuroscience, 26(5), pp. 1331–3. doi: 10.1523/JNEUROSCI.5242-05.2006.

Nguyen, T.-H., Liu, J. and Lombroso, P. J. (2002) 'Striatal enriched phosphatase 61 dephosphorylates Fyn at phosphotyrosine 420.', *The Journal of biological chemistry*. American Society for Biochemistry and Molecular Biology, 277(27), pp. 24274–9. doi: 10.1074/jbc.M111683200.

Nicola, S. M., Surmeier, D. J. and Malenka, R. C. (2000) 'Dopaminergic Modulation of Neuronal Excitability in the Striatum and Nucleus Accumbens', *Annual Review of Neuroscience*. Annual Reviews 4139 El Camino Way, P.O. Box 10139, Palo Alto, CA 94303-0139, USA , 23(1), pp. 185–215. doi: 10.1146/annurev.neuro.23.1.185.

Noh, H. *et al.* (2017) 'Modeling schizophrenia pathogenesis using patient-derived induced pluripotent stem cells (iPSCs).', *Biochimica et biophysica acta. Molecular basis of disease*. NIH Public Access, 1863(9), pp. 2382–2387. doi: 10.1016/j.bbadis.2017.06.019.

Ogawa, A. *et al.* (2002) 'Structure of the carboxyl-terminal Src kinase, Csk.', *The Journal of biological chemistry*. American Society for Biochemistry and Molecular Biology, 277(17), pp. 14351–4. doi: 10.1074/jbc.C200086200.

Okada, M. (2012) 'Regulation of the SRC family kinases by Csk.', *International journal of biological sciences*. Ivyspring International Publisher, 8(10), pp. 1385–97. doi: 10.7150/ijbs.5141.

Olanow, C. W. *et al.* (1994) 'A multicenter double-blind placebo-controlled trial of pergolide as an adjunct to sinemet® in Parkinson's disease', *Movement Disorders*. John Wiley & Sons, Ltd, 9(1), pp. 40–47. doi: 10.1002/mds.870090107.

Ongini, E. *et al.* (1997) 'Adenosine A $_{2A}$ Receptors and Neuroprotection', *Annals of the New York Academy of Sciences*. John Wiley & Sons, Ltd (10.1111), 825(1 Neuroprotecti), pp. 30–48. doi: 10.1111/j.1749-6632.1997.tb48412.x.

Onoda, T. *et al.* (1989) 'Isolation of a Novel Tyrosine Kinase Inhibitor,

Lavendustin A, from Streptomyces griseolavendus', *Journal of Natural Products*, 52(6), pp. 1252–1257. doi: 10.1021/np50066a009.

Oppenheim, R. W. (1991) 'Cell Death During Development of the Nervous System', *Annual Review of Neuroscience*. Annual Reviews 4139 El Camino Way, P.O. Box 10139, Palo Alto, CA 94303-0139, USA , 14(1), pp. 453–501. doi: 10.1146/annurev.ne.14.030191.002321.

Pack, T. F. *et al.* (2018) 'The dopamine D2 receptor can directly recruit and activate GRK2 without G protein activation.', *The Journal of biological chemistry*. American Society for Biochemistry and Molecular Biology, 293(16), pp. 6161–6171. doi: 10.1074/jbc.RA117.001300.

Panatier, A. *et al.* (2006) 'Glia-Derived d-Serine Controls NMDA Receptor Activity and Synaptic Memory', *Cell*. Cell Press, 125(4), pp. 775–784. doi: 10.1016/J.CELL.2006.02.051.

Paoletti, P., Bellone, C. and Zhou, Q. (2013) 'NMDA receptor subunit diversity: impact on receptor properties, synaptic plasticity and disease', *Nature Reviews Neuroscience*. Nature Research, 14(6), pp. 383–400. doi: 10.1038/nrn3504.

Parvez, S. *et al.* (2010) 'The dopamine-D2-receptor agonist ropinirole dose-dependently blocks the Ca2+-triggered permeability transition of mitochondria', *Biochimica et Biophysica Acta - Bioenergetics*, 1797(6–7), pp. 1245–1250. doi: 10.1016/j.bbabio.2010.02.001.

Paxinos, G and Franklin, K. B. J. (2012) *Paxinos and Franklin's the Mouse Brain in Stereotaxic Coordinates*, *São Paulo, Academic Press*. Available at: https://www.elsevier.com/books/paxinos-and-franklins-the-mouse-brain-in-stereotaxic-coordinates/paxinos/978-0-12-391057-8.

Paxinos, G. and Watson, C. (2013) *The Rat Brain in Stereotaxic Coordinates : Hard Cover Edition.* Elsevier Science.

Payne, D. M. *et al.* (1991) 'Identification of the regulatory phosphorylation sites in pp42/mitogen-activated protein kinase (MAP kinase).', *The EMBO journal*. European Molecular Biology Organization, 10(4), pp. 885–92.

Pearlstein, E. *et al.* (2015) 'Glutamatergic synaptic currents of nigral dopaminergic neurons follow a postnatal developmental sequence', *Frontiers in Cellular Neuroscience*. Frontiers, 9, p. 210. doi: 10.3389/fncel.2015.00210.

Pearlstein, E. *et al.* (2016) 'Abnormal Development of Glutamatergic Synapses Afferent to Dopaminergic Neurons of the Pink1(-/-) Mouse Model of Parkinson's Disease.', *Frontiers in cellular neuroscience*. Frontiers Media SA, 10, p. 168. doi: 10.3389/fncel.2016.00168.

Peng, J. *et al.* (2006) 'Nigrostriatal Dopaminergic Neurodegeneration in the

Weaver Mouse Is Mediated via Neuroinflammation and Alleviated by Minocycline Administration', *Journal of Neuroscience*, 26(45), pp. 11644–11651. doi: 10.1523/JNEUROSCI.3447-06.2006.

Perez-Otano, I. *et al.* (2001) 'Assembly with the NR1 subunit is required for surface expression of NR3A-containing NMDA receptors.', *The Journal of neuroscience : the official journal of the Society for Neuroscience*. Society for Neuroscience, 21(4), pp. 1228–37. doi: 10.1523/JNEUROSCI.21-04-01228.2001.

Pérez-Otaño, I., Larsen, R. S. and Wesseling, J. F. (2016) 'Emerging roles of GluN3-containing NMDA receptors in the CNS', *Nature Reviews Neuroscience*. Nature Publishing Group, 17(10), pp. 623–635. doi: 10.1038/nrn.2016.92.

Phillips, P. E. M. and Stamford, J. A. (2000) 'Differential recruitment of N-, P- and Q-type voltage-operated calcium channels in striatal dopamine release evoked by "regular" and "burst" firing', *Brain Research*, 884(1–2), pp. 139–146. doi: 10.1016/S0006-8993(00)02958-9.

Pilla, M. *et al.* (1999) 'Erratum: Selective inhibition of cocaine-seeking behaviour by a partial dopamine D3 receptor agonist', *Nature*. Nature Publishing Group, 400(6742), pp. 371–375. doi: 10.1038/22560.

Piña-Crespo, J. C. and Gibb, A. J. (2002) 'Subtypes of NMDA receptors in new-born rat hippocampal granule cells.', *The Journal of physiology*. Wiley-Blackwell, 541(Pt 1), pp. 41–64. doi: 10.1113/jphysiol.2001.014001.

Poetschke, C. *et al.* (2015) 'Compensatory T-type Ca2+ channel activity alters D2-autoreceptor responses of Substantia nigra dopamine neurons from Cav1.3 L-type Ca2+ channel KO mice', *Scientific Reports*. Nature Publishing Group, 5, p. 13688. doi: 10.1038/srep13688.

Raman, I. M., Tong, G. and Jahr, C. E. (1996) 'β-Adrenergic Regulation of Synaptic NMDA Receptors by cAMP-Dependent Protein Kinase', *Neuron*. Cell Press, 16(2), pp. 415–421. doi: 10.1016/S0896-6273(00)80059-8.

Rauner, C. and Köhr, G. (2011) 'Triheteromeric NR1/NR2A/NR2B receptors constitute the major N-methyl-D-aspartate receptor population in adult hippocampal synapses.', *The Journal of biological chemistry*. American Society for Biochemistry and Molecular Biology, 286(9), pp. 7558–66. doi: 10.1074/jbc.M110.182600.

Rebola, N. *et al.* (2008) 'Adenosine A2A Receptors Are Essential for Long-Term Potentiation of NMDA-EPSCs at Hippocampal Mossy Fiber Synapses', *Neuron*. Cell Press, 57(1), pp. 121–134. doi: 10.1016/J.NEURON.2007.11.023.

Reisner, P. D., Christakos, S. and Vanaman, T. C. (1992) 'In vitro enzyme activation with calbindin-D28k, the vitamin D-dependent 28 kDa calcium

binding protein', *FEBS Letters*. No longer published by Elsevier, 297(1–2), pp. 127–131. doi: 10.1016/0014-5793(92)80342-E.

Ren, R. *et al.* (1993) 'Identification of a ten-amino acid proline-rich SH3 binding site.', *Science (New York, N.Y.)*. American Association for the Advancement of Science, 259(5098), pp. 1157–61. doi: 10.1126/science.8438166.

Resh, M. D. (1993) 'Interaction of tyrosine kinase oncoproteins with cellular membranes', *Biochimica et Biophysica Acta (BBA) - Reviews on Cancer*. Elsevier, 1155(3), pp. 307–322. doi: 10.1016/0304-419X(93)90012-2.

Richard F. Heier, *et al.* (1997) 'Synthesis and Biological Activities of (R)-5,6-Dihydro-N,N-dimethyl-4H-imidazo[4,5,1-ij]quinolin-5-amine and Its Metabolites'. American Chemical Society . doi: 10.1021/JM960360Q.

Richardson, P. J., Kase, H. and Jenner, P. G. (1997) 'Adenosine A2A receptor antagonists as new agents for the treatment of Parkinson's disease', *Trends in Pharmacological Sciences*. Elsevier, 18(4), pp. 338–344. doi: 10.1016/S0165-6147(97)90660-X.

Riederer, P. and Laux, G. (2011) 'MAO-inhibitors in Parkinson's Disease.', *Experimental neurobiology*. Korean Society for Brain and Neural Science, 20(1), pp. 1–17. doi: 10.5607/en.2011.20.1.1.

Rondou, P., Haegeman, G. and Van Craenenbroeck, K. (2010) 'The dopamine D4 receptor: biochemical and signalling properties', *Cellular and Molecular Life Sciences*. SP Birkhäuser Verlag Basel, 67(12), pp. 1971–1986. doi: 10.1007/s00018-010-0293-y.

Rosenmund, C., Feltz, A. and Westbrook, G. L. (1995) 'Synaptic NMDA receptor channels have a low open probability.', *The Journal of neuroscience : the official journal of the Society for Neuroscience*. Society for Neuroscience, 15(4), pp. 2788–95. doi: 10.1523/JNEUROSCI.15-04-02788.1995.

Rosin, D. L. *et al.* (2003) 'Anatomy of adenosine A2A receptors in brain: morphological substrates for integration of striatal function.', *Neurology*. Wolters Kluwer Health, Inc. on behalf of the American Academy of Neurology, 61(11 Suppl 6), pp. S12-8. doi: 10.1212/01.WNL.0000095205.33940.99.

Roskoski, R. (2015) 'Src protein-tyrosine kinase structure, mechanism, and small molecule inhibitors', *Pharmacological Research*. Academic Press, 94, pp. 9–25. doi: 10.1016/J.PHRS.2015.01.003.

Ross, G. W. *et al.* (2000) 'Association of Coffee and Caffeine Intake With the Risk of Parkinson Disease', *JAMA*. American Medical Association, 283(20), p. 2674. doi: 10.1001/jama.283.20.2674.

Roux, P. P. and Blenis, J. (2004) 'ERK and p38 MAPK-activated protein kinases: a family of protein kinases with diverse biological functions.', *Microbiology and molecular biology reviews : MMBR*. American Society for Microbiology (ASM), 68(2), pp. 320–44. doi: 10.1128/MMBR.68.2.320-344.2004.

Rycroft, B. K. and Gibb, A. J. (2002) 'Direct effects of calmodulin on NMDA receptor single-channel gating in rat hippocampal granule cells.', *The Journal of neuroscience : the official journal of the Society for Neuroscience*. Society for Neuroscience, 22(20), pp. 8860–8. doi: 10.1523/JNEUROSCI.22-20-08860.2002.

Rycroft, B. K. and Gibb, A. J. (2004) 'Inhibitory interactions of calcineurin (phosphatase 2B) and calmodulin on rat hippocampal NMDA receptors', *Neuropharmacology*. Pergamon, 47(4), pp. 505–514. doi: 10.1016/J.NEUROPHARM.2004.06.001.

Sadowski, I., Stone, J. C. and Pawson, T. (1986) 'A noncatalytic domain conserved among cytoplasmic protein-tyrosine kinases modifies the kinase function and transforming activity of Fujinami sarcoma virus P130gag-fps.', *Molecular and cellular biology*. American Society for Microbiology (ASM), 6(12), pp. 4396–408. doi: 10.1128/mcb.6.12.4396.

Salter, M. W. and Kalia, L. V. (2004) 'Src kinases: a hub for NMDA receptor regulation', *Nature Reviews Neuroscience*. Nature Publishing Group, 5(4), pp. 317–328. doi: 10.1038/nrn1368.

Salter, M. W. and Pitcher, G. M. (2012) 'Dysregulated Src upregulation of NMDA receptor activity: a common link in chronic pain and schizophrenia.', *The FEBS journal*. PMC Canada manuscript submission, 279(1), pp. 2–11. doi: 10.1111/j.1742-4658.2011.08390.x.

Sans, N. *et al.* (2003) 'Aberrant formation of glutamate receptor complexes in hippocampal neurons of mice lacking the GluR2 AMPA receptor subunit.', *The Journal of neuroscience : the official journal of the Society for Neuroscience*. Society for Neuroscience, 23(28), pp. 9367–73. doi: 10.1523/JNEUROSCI.23-28-09367.2003.

Santoro, B. *et al.* (2000) 'Molecular and Functional Heterogeneity of Hyperpolarization-Activated Pacemaker Channels in the Mouse CNS', *Journal of Neuroscience*, 20(14).

Sanz-Clemente, A., Nicoll, R. A. and Roche, K. W. (2013) 'Diversity in NMDA Receptor Composition', *The Neuroscientist*. SAGE PublicationsSage CA: Los Angeles, CA, 19(1), pp. 62–75. doi: 10.1177/1073858411435129.

Scanlon, D. P. *et al.* (2017) 'An evolutionary switch in ND2 enables Src kinase regulation of NMDA receptors', *Nature Communications*. Nature Publishing Group, 8, p. 15220. doi: 10.1038/ncomms15220.

Schiemann, J. *et al.* (2012) 'K-ATP channels in dopamine substantia nigra neurons control bursting and novelty-induced exploration.', *Nature neuroscience*. Europe PMC Funders, 15(9), pp. 1272–80. doi: 10.1038/nn.3185.

Schiffmann, S. N. *et al.* (2007) 'Adenosine A2A receptors and basal ganglia physiology', *Progress in Neurobiology*, pp. 277–292. doi: 10.1016/j.pneurobio.2007.05.001.

Schmierer, B. and Hill, C. S. (2007) 'TGFβ–SMAD signal transduction: molecular specificity and functional flexibility', *Nature Reviews Molecular Cell Biology*. Nature Publishing Group, 8(12), pp. 970–982. doi: 10.1038/nrm2297.

Schmitz, Y., Schmauss, C. and Sulzer, D. (2002) 'Altered Dopamine Release and Uptake Kinetics in Mice Lacking D2 Receptors', *Journal of Neuroscience*. Society for Neuroscience, 22(18), pp. 8002–8009. doi: 10.1523/JNEUROSCI.22-18-08002.2002.

Seeman, P. (2006) 'Targeting the dopamine D_2 receptor in schizophrenia', *Expert Opinion on Therapeutic Targets*. Taylor & Francis, 10(4), pp. 515–531. doi: 10.1517/14728222.10.4.515.

Sesack, S. R., Aoki, C. and Pickel, V. M. (1994) 'Ultrastructural localization of D2 receptor-like immunoreactivity in midbrain dopamine neurons and their striatal targets.', *The Journal of neuroscience : the official journal of the Society for Neuroscience*. Society for Neuroscience, 14(1), pp. 88–106. doi: 10.1523/JNEUROSCI.14-01-00088.1994.

Sheng, M. *et al.* (1994) 'Changing subunit composition of heteromeric NMDA receptors during development of rat cortex', *Nature*. Nature Publishing Group, 368(6467), pp. 144–147. doi: 10.1038/368144a0.

Shill, H. A. and Stacy, M. (2009) 'Update on ropinirole in the treatment of Parkinson's disease.', *Neuropsychiatric disease and treatment*. Dove Press, 5, pp. 33–6.

Shuen, J. A. *et al.* (2008) 'Drd1a-tdTomato BAC transgenic mice for simultaneous visualization of medium spiny neurons in the direct and indirect pathways of the basal ganglia.', *The Journal of neuroscience : the official journal of the Society for Neuroscience*. Society for Neuroscience, 28(11), pp. 2681–5. doi: 10.1523/JNEUROSCI.5492-07.2008.

Sibley, D. R. (1999) 'New insights into Dopaminergic receptor function using antisence and genetically altered animals,' *Annual Review of Pharmacology and Toxicology*. Annual Reviews 4139 El Camino Way, P.O. Box 10139, Palo Alto, CA 94303-0139, USA , 39(1), pp. 313–341. doi: 10.1146/annurev.pharmtox.39.1.313.

Sicheri, F., Moarefi, I. and Kuriyan, J. (1997) 'Crystal structure of the Src family

tyrosine kinase Hck', *Nature*. Nature Publishing Group, 385(6617), pp. 602–609. doi: 10.1038/385602a0.

Simola, N. *et al.* (2006) 'Dopamine and adenosine receptor interaction as basis for the treatment of Parkinson's disease', *Journal of the Neurological Sciences*, 248(1), pp. 48–52. doi: 10.1016/j.jns.2006.05.038.

Singh, B. *et al.* (2006) 'Altered balance of glutamatergic/GABAergic synaptic input and associated changes in dendrite morphology after BDNF expression in BDNF-deficient hippocampal neurons.', *The Journal of neuroscience : the official journal of the Society for Neuroscience*. Society for Neuroscience, 26(27), pp. 7189–200. doi: 10.1523/JNEUROSCI.5474-05.2006.

Skeberdis, V. A. *et al.* (2006) 'Protein kinase A regulates calcium permeability of NMDA receptors', *Nature Neuroscience*. Nature Publishing Group, 9(4), pp. 501–510. doi: 10.1038/nn1664.

Skinbjerg, M. *et al.* (2009) 'Arrestin3 mediates D(2) dopamine receptor internalization.', *Synapse (New York, N.Y.)*. NIH Public Access, 63(7), pp. 621–4. doi: 10.1002/syn.20636.

Skinbjerg, M. *et al.* (2010) 'D2 dopamine receptor internalization prolongs the decrease of radioligand binding after amphetamine: a PET study in a receptor internalization-deficient mouse model.', *NeuroImage*. NIH Public Access, 50(4), pp. 1402–7. doi: 10.1016/j.neuroimage.2010.01.055.

Smidt, M. P. and Burbach, J. P. H. (2007) 'How to make a mesodiencephalic dopaminergic neuron', *Nature Reviews Neuroscience*. Nature Publishing Group, 8(1), pp. 21–32. doi: 10.1038/nrn2039.

Smits, S. M., Burbach, J. P. H. and Smidt, M. P. (2006) 'Developmental origin and fate of meso-diencephalic dopamine neurons', *Progress in Neurobiology*. Pergamon, 78(1), pp. 1–16. doi: 10.1016/J.PNEUROBIO.2005.12.003.

Sobolevsky, A. I., Rosconi, M. P. and Gouaux, E. (2009) 'X-ray structure, symmetry and mechanism of an AMPA-subtype glutamate receptor', *Nature*. Nature Publishing Group, 462(7274), pp. 745–756. doi: 10.1038/nature08624.

Socodato, R. *et al.* (2017) 'Dopamine promotes NMDA receptor hypofunction in the retina through D1 receptor-mediated Csk activation, Src inhibition and decrease of GluN2B phosphorylation', *Scientific Reports*. Nature Publishing Group, 7, p. 40912. doi: 10.1038/srep40912.

Sokoloff, P. *et al.* (2006) 'The dopamine D3 receptor: a therapeutic target for the treatment of neuropsychiatric disorders.', *CNS Neurological disorder Drug Targets*, 5(1), p. 25-43.

Standaert, D. G. *et al.* (1994) 'Organization of N-methyl-D-aspartate glutamate receptor gene expression in the basal ganglia of the rat', *The Journal of Comparative Neurology*. John Wiley & Sons, Ltd, 343(1), pp. 1–16. doi: 10.1002/cne.903430102.

Stocca, G. and Vicini, S. (1998) 'Increased contribution of NR2A subunit to synaptic NMDA receptors in developing rat cortical neurons', *The Journal of Physiology*. John Wiley & Sons, Ltd (10.1111), 507(1), pp. 13–24. doi: 10.1111/j.1469-7793.1998.013bu.x.

Stroebel, D., Casado, M. and Paoletti, P. (2018) 'Triheteromeric NMDA receptors: from structure to synaptic physiology.', *Current opinion in physiology*. Europe PMC Funders, 2, pp. 1–12. doi: 10.1016/j.cophys.2017.12.004.

Strömberg, I. *et al.* (2000) 'Electrophysiological and behavioural evidence for an antagonistic modulatory role of adenosine A_{2A} receptors in dopamine D_2 receptor regulation in the rat dopamine-denervated striatum', *European Journal of Neuroscience*. Blackwell Science Ltd, 12(11), pp. 4033–4037. doi: 10.1046/j.1460-9568.2000.00288.x.

Sturani, E. *et al.* (1997) 'The Ras Guanine Nucleotide Exchange Factor CDC25Mm Is Present at the Synaptic Junction', *Experimental Cell Research*. Academic Press, 235(1), pp. 117–123. doi: 10.1006/EXCR.1997.3660.

Suárez, F. *et al.* (2010) 'Functional heterogeneity of NMDA receptors in rat substantia nigra pars compacta and reticulata neurones.', *The European journal of neuroscience*. NIH Public Access, 32(3), pp. 359–67. doi: 10.1111/j.1460-9568.2010.07298.x.

Sulzer, D. and Surmeier, D. J. (2013) 'Neuronal vulnerability, pathogenesis, and Parkinson's disease', *Movement Disorders*, pp. 715–724. doi: 10.1002/mds.25187.

Sunahara, R. K. *et al.* (1991) 'Cloning of the gene for a human dopamine D5 receptor with higher affinity for dopamine than D1', *Nature*. Nature Publishing Group, 350(6319), pp. 614–619. doi: 10.1038/350614a0.

Svenningsson, P. *et al.* (1999) 'Opposite tonic modulation of dopamine and adenosine on c-fos gene expression in striatopallidal neurons', *Neuroscience*. Pergamon, 89(3), pp. 827–837. doi: 10.1016/S0306-4522(98)00403-5.

Sweatt, J. D. (2008) 'The neuronal MAP kinase cascade: a biochemical signal integration system subserving synaptic plasticity and memory', *Journal of Neurochemistry*. John Wiley & Sons, Ltd (10.1111), 76(1), pp. 1–10. doi: 10.1046/j.1471-4159.2001.00054.x.

Terman, G. W. *et al.* (2004) 'G-protein receptor kinase 3 (GRK3) influences

opioid analgesic tolerance but not opioid withdrawal', *British Journal of Pharmacology*. Wiley-Blackwell, 141(1), p. 55. doi: 10.1038/SJ.BJP.0705595.

Thal, D. M. *et al.* (2011) 'Molecular Mechanism of Selectivity among G Protein-Coupled Receptor Kinase 2 Inhibitors', *Molecular Pharmacology*, 80(2), pp. 294–303. doi: 10.1124/mol.111.071522.

Thomson, A. M., Girdlestone, D. and West, D. C. (1989) 'A local circuit neocortical synapse that operates via both NMDA and non-NMDA receptors', *British Journal of Pharmacology*. John Wiley & Sons, Ltd (10.1111), 96(2), pp. 406–408. doi: 10.1111/j.1476-5381.1989.tb11831.x.

Tiberi, M. *et al.* (1991) 'Cloning, molecular characterization, and chromosomal assignment of a gene encoding a second D1 dopamine receptor subtype: differential expression pattern in rat brain compared with the D1A receptor.', *Proceedings of the National Academy of Sciences of the United States of America*. National Academy of Sciences, 88(17), pp. 7491–5. doi: 10.1073/PNAS.88.17.7491.

Tiberis, M. *et al.* (1994) *High Agonist-independent Activity Is a Distinguishing Feature of the Dopamine DIB Receptor Subtype* Postdoctoral Fellow of the Medical Research Council of Canada and Research on Schizophrenia and Depression. recipient of a Young Investigator Award from the National Alliance for*.

Tiklová, K. *et al.* (2019) 'Single-cell RNA sequencing reveals midbrain dopamine neuron diversity emerging during mouse brain development', *Nature Communications*. Nature Publishing Group, 10(1), p. 581. doi: 10.1038/s41467-019-08453-1.

Tingley, W. G. *et al.* (1997) 'Characterization of Protein Kinase A and Protein Kinase C Phosphorylation of the N-Methyl-D-aspartate Receptor NR1 Subunit Using Phosphorylation Site-specific Antibodies', *Journal of Biological Chemistry*. American Society for Biochemistry and Molecular Biology, 272(8), pp. 5157–5166. doi: 10.1074/JBC.272.8.5157.

Van Tol, H. H. M. *et al.* (1991) 'Cloning of the gene for a human dopamine D4 receptor with high affinity for the antipsychotic clozapine', *Nature*. Nature Publishing Group, 350(6319), pp. 610–614. doi: 10.1038/350610a0.

Tong, H. and Gibb, A. J. (2008) 'Dopamine D1 receptor inhibition of NMDA receptor currents mediated by tyrosine kinase-dependent receptor trafficking in neonatal rat striatum.', *The Journal of physiology*, 586(19), pp. 4693–707. doi: 10.1113/jphysiol.2008.158931.

Tovar, K. R., McGinley, M. J. and Westbrook, G. L. (2013) 'Triheteromeric NMDA receptors at hippocampal synapses.', *The Journal of neuroscience : the official journal of the Society for Neuroscience*. NIH Public Access, 33(21), pp. 9150–60. doi: 10.1523/JNEUROSCI.0829-

13.2013.

Townsend, M., Liu, Y. and Constantine-Paton, M. (2004) 'Retina-Driven Dephosphorylation of the NR2A Subunit Correlates with Faster NMDA Receptor Kinetics at Developing Retinocollicular Synapses', *Journal of Neuroscience*. Society for Neuroscience, 24(49), pp. 11098–11107. doi: 10.1523/JNEUROSCI.1207-04.2004.

Traynelis, S. F. *et al.* (2010) 'Glutamate receptor ion channels: structure, regulation, and function.', *Pharmacological reviews*. American Society for Pharmacology and Experimental Therapeutics, 62(3), pp. 405–96. doi: 10.1124/pr.109.002451.

Trepanier, C. *et al.* (2013) 'Group II metabotropic glutamate receptors modify N-methyl-D-aspartate receptors via Src kinase.', *Scientific reports*. Nature Publishing Group, 3, p. 926. doi: 10.1038/srep00926.

Trepanier, C. H. *et al.* (2012) 'Regulation of NMDA receptors by the tyrosine kinase Fyn'. doi: 10.1111/j.1742-4658.2011.08391.x.

Tritsch, N. X. and Sabatini, B. L. (2012) 'Dopaminergic Modulation of Synaptic Transmission in Cortex and Striatum', *Neuron*, 76(1), pp. 33–50. doi: 10.1016/j.neuron.2012.09.023.

Uchida, S., Akaike, N. and Nabekura, J. (2000) 'Dopamine activates inward rectifier K+ channel in acutely dissociated rat substantia nigra neurones', *Neuropharmacology*. Pergamon, 39(2), pp. 191–201. doi: 10.1016/S0028-3908(99)00111-2.

Ungless, M. A. and Grace, A. A. (2012) 'Are you or aren't you? Challenges associated with physiologically identifying dopamine neurons.', *Trends in neurosciences*. NIH Public Access, 35(7), pp. 422–30. doi: 10.1016/j.tins.2012.02.003.

Usiello, A. *et al.* (2000) 'Distinct functions of the two isoforms of dopamine D2 receptors', *Nature*. Nature Publishing Group, 408(6809), pp. 199–203. doi: 10.1038/35041572.

Valenzuela, C. F. *et al.* (1996) 'Platelet-derived growth factor induces a long-term inhibition of N-methyl-D-aspartate receptor function.', *The Journal of biological chemistry*. American Society for Biochemistry and Molecular Biology, 271(27), pp. 16151–9. doi: 10.1074/jbc.271.27.16151.

Valjent, E. *et al.* (2005) 'Regulation of a protein phosphatase cascade allows convergent dopamine and glutamate signals to activate ERK in the striatum.', *Proceedings of the National Academy of Sciences of the United States of America*. National Academy of Sciences, 102(2), pp. 491–6. doi: 10.1073/pnas.0408305102.

Valjent, E. *et al.* (2009) 'Looking BAC at striatal signaling: cell-specific analysis

in new transgenic mice', *Trends in Neurosciences*. Elsevier Current Trends, 32(10), pp. 538–547. doi: 10.1016/J.TINS.2009.06.005.

Vang, T. *et al.* (2001) 'Activation of the COOH-terminal Src kinase (Csk) by cAMP-dependent protein kinase inhibits signaling through the T cell receptor.', *The Journal of experimental medicine*. The Rockefeller University Press, 193(4), pp. 497–507. doi: 10.1084/jem.193.4.497.

Wainger, B. J. *et al.* (2001) 'Molecular mechanism of cAMP modulation of HCN pacemaker channels', *Nature*, 411(6839), pp. 805–810. doi: 10.1038/35081088.

Wang, J., Chen, S. and Siegelbaum, S. A. (2001) 'Regulation of hyperpolarization-activated HCN channel gating and cAMP modulation due to interactions of COOH terminus and core transmembrane regions.', *The Journal of general physiology*. The Rockefeller University Press, 118(3), pp. 237–50.

Wang, L. P. *et al.* (2011) 'NMDA receptors in dopaminergic neurons are crucial for habit learning.', *Neuron*. NIH Public Access, 72(6), pp. 1055–66. doi: 10.1016/j.neuron.2011.10.019.

Wang, Y. T. and Salter, M. W. (1994) 'Regulation of NMDA receptors by tyrosine kinases and phosphatases', *Nature*. Nature Publishing Group, 369(6477), pp. 233–235. doi: 10.1038/369233a0.

Wang, Y T, Yu, X. M. and Salter, M. W. (1996) 'Ca(2+)-independent reduction of N-methyl-D-aspartate channel activity by protein tyrosine phosphatase.', *Proceedings of the National Academy of Sciences of the United States of America*. National Academy of Sciences, 93(4), pp. 1721–5. doi: 10.1073/pnas.93.4.1721.

Ward, R. A. *et al.* (2015) 'Structure-Guided Design of Highly Selective and Potent Covalent Inhibitors of ERK1/2', *Journal of Medicinal Chemistry*. American Chemical Society, 58(11), pp. 4790–4801. doi: 10.1021/acs.jmedchem.5b00466.

Watabe-Uchida, M. *et al.* (2012) 'Whole-Brain Mapping of Direct Inputs to Midbrain Dopamine Neurons', *Neuron*. Cell Press, 74(5), pp. 858–873. doi: 10.1016/J.NEURON.2012.03.017.

Watanabe, M. *et al.* (1992) 'Developmental changes in distribution of NMDA receptor channel subunit mRNAs', *NeuroReport*, 3(12), pp. 1138–1140. doi: 10.1097/00001756-199212000-00027.

Watanabe, M. *et al.* (1993) 'Distinct distributions of fiveN-methyl-D-aspartate receptor channel subunit mRNAs in the forebrain', *The Journal of Comparative Neurology*. John Wiley & Sons, Ltd, 338(3), pp. 377–390. doi: 10.1002/cne.903380305.

Webster, R. (2001) 'Dopamine (DA)', in *Neurotransmitters, Drugs and Brain Function*, pp. 137–161. doi: 10.1002/0470846577.ch7.

Wenzel, A. *et al.* (1984) *These properties underlie the neurophysiological functions of NMDA receptors*. Kullmann and Siegelbaum.

Westbrook, G. L., Mayer, M. L. and Forsythe, I. D. (1988) 'Conductance Mechanisms Activated by L-Glutamate', in *Neurobiology of Amino Acids, Peptides and Trophic Factors*. Boston, MA: Springer US, pp. 15–33. doi: 10.1007/978-1-4613-1721-0_2.

Wild, A. R., Jones, S. and Gibb, A. J. (2014) 'Activity-dependent regulation of NMDA receptors in substantia nigra dopaminergic neurones.', *The Journal of physiology*. Wiley-Blackwell, 592(4), pp. 653–68. doi: 10.1113/jphysiol.2013.267310.

Wilson, C J and Callaway, J. C. (2000) 'Coupled oscillator model of the dopaminergic neuron of the substantia nigra.', *Journal of neurophysiology*. American Physiological Society, 83(5), pp. 3084–100.

Wise, R. A. (2004) 'Dopamine, learning and motivation', *Nature Reviews Neuroscience*. Nature Publishing Group, 5(6), pp. 483–494. doi: 10.1038/nrn1406.

Wolf, M. et al. (1990) 'Autoreceptor Regulation of Dopamine Synthesis', *Annals of the New York Academy of Sciences*. John Wiley & Sons, Ltd (10.1111), 604(1 Presynaptic R), pp. 323–343. doi: 10.1111/j.1749-6632.1990.tb32003.x.

Won, S. and Roche, K. W. (2020) 'Regulation of glutamate receptors by striatal-enriched tyrosine phosphatase 61 (STEP 61)', *The Journal of Physiology*. John Wiley & Sons, Ltd, p. JP278703. doi: 10.1113/JP278703.

Xu, J. *et al.* (2008) 'Control of excitatory synaptic transmission by C-terminal Src kinase.', *The Journal of biological chemistry*. American Society for Biochemistry and Molecular Biology, 283(25), pp. 17503–14. doi: 10.1074/jbc.M800917200.

Xu, W., Harrison, S. C. and Eck, M. J. (1997) 'Three-dimensional structure of the tyrosine kinase c-Src', *Nature*. Nature Publishing Group, 385(6617), pp. 595–602. doi: 10.1038/385595a0.

Yaka, R. *et al.* (2002) 'NMDA receptor function is regulated by the inhibitory scaffolding protein, RACK1.', *Proceedings of the National Academy of Sciences of the United States of America*. National Academy of Sciences, 99(8), pp. 5710–5. doi: 10.1073/pnas.062046299.

Yaka, R. *et al.* (2003) 'Pituitary adenylate cyclase-activating polypeptide (PACAP(1-38)) enhances N-methyl-D-aspartate receptor function and brain-derived neurotrophic factor expression via RACK1.', *The Journal of*

biological chemistry. American Society for Biochemistry and Molecular Biology, 278(11), pp. 9630–8. doi: 10.1074/jbc.M209141200.

Yang, K. *et al.* (2012) 'Metaplasticity gated through differential regulation of GluN2A versus GluN2B receptors by Src family kinases.', *The EMBO journal*. European Molecular Biology Organization, 31(4), pp. 805–16. doi: 10.1038/emboj.2011.453.

Yang, K., Jackson, M. F. and MacDonald, J. F. (2014) 'Recent progress in understanding subtype specific regulation of NMDA receptors by G Protein Coupled Receptors (GPCRs).', *International journal of molecular sciences*. Multidisciplinary Digital Publishing Institute (MDPI), 15(2), pp. 3003–24. doi: 10.3390/ijms15023003.

Yaqub, S. *et al.* (2003) 'Activation of C-terminal Src kinase (Csk) by phosphorylation at serine-364 depends on the Csk-Src homology 3 domain.', *The Biochemical journal*. Portland Press Ltd, 372(Pt 1), pp. 271–8. doi: 10.1042/BJ20030021.

Yi, F. *et al.* (2018) 'Properties of Triheteromeric N-Methyl-d-Aspartate Receptors Containing Two Distinct GluN1 Isoforms', *Molecular Pharmacology*. American Society for Pharmacology and Experimental Therapeutics, 93(5), pp. 453–467. doi: 10.1124/MOL.117.111427.

Yi, F. *et al.* (2019) 'Functional and pharmacological properties of triheteromeric GluN1/2B/2D NMDA receptors', *The Journal of Physiology*, p. JP278168. doi: 10.1113/JP278168.

Yu, X. M. *et al.* (1997) 'NMDA channel regulation by channel-associated protein tyrosine kinase Src.', *Science (New York, N.Y.)*. American Association for the Advancement of Science, 275(5300), pp. 674–8. doi: 10.1126/science.275.5300.674.

Yu, X. M. and Salter, M. W. (1999) 'Src, a molecular switch governing gain control of synaptic transmission mediated by N-methyl-D-aspartate receptors.', *Proceedings of the National Academy of Sciences of the United States of America*. National Academy of Sciences, 96(14), pp. 7697–704. doi: 10.1073/PNAS.96.14.7697.

Zhao, M. M. *et al.* (1996) 'Identification of critical extracellular loop residues involved in alpha 1-adrenergic receptor subtype-selective antagonist binding.', *Molecular pharmacology*. American Society for Pharmacology and Experimental Therapeutics, 50(5), pp. 1118–26.

Zhu, H. *et al.* (2007) 'Expression and distribution of all dopamine receptor subtypes (D(1)-D(5)) in the mouse lumbar spinal cord: a real-time polymerase chain reaction and non-autoradiographic in situ hybridization study.', *Neuroscience*. NIH Public Access, 149(4), pp. 885–97. doi: 10.1016/j.neuroscience.2007.07.052.

Zhu, J. J. *et al.* (2002) 'Ras and Rap Control AMPA Receptor Trafficking during Synaptic Plasticity', *Cell*. Cell Press, 110(4), pp. 443–455. doi: 10.1016/S0092-8674(02)00897-8.